INFORMATION TO USERS

This manuscript has been reproduced from the microfilm master. UMI films the text directly from the original or copy submitted. Thus, some thesis and dissertation copies are in typewriter face, while others may be from any type of computer printer.

The quality of this reproduction is dependent upon the quality of the copy submitted. Broken or indistinct print, colored or poor quality illustrations and photographs, print bleedthrough, substandard margins, and improper alignment can adversely affect reproduction.

In the unlikely event that the author did not send UMI a complete manuscript and there are missing pages, these will be noted. Also, if unauthorized copyright material had to be removed, a note will indicate the deletion.

Oversize materials (e.g., maps, drawings, charts) are reproduced by sectioning the original, beginning at the upper left-hand corner and continuing from left to right in equal sections with small overlaps.

Photographs included in the original manuscript have been reproduced xerographically in this copy. Higher quality 6" x 9" black and white photographic prints are available for any photographs or illustrations appearing in this copy for an additional charge. Contact UMI directly to order.

Bell & Howell Information and Learning
300 North Zeeb Road, Ann Arbor, MI 48106-1346 USA
800-521-0600

UMI®

MECHANISM OF DRUG-INDUCED TORSADE DE POINTES POLYMORPHIC VENTRICULAR TACHYCARDIA

by

Sylvain Brunet

Submitted to
the Faculty of Graduate Studies and Research
in partial fulfillment of the requirements
for the degree of Doctor of Philosophy

Department of Pharmacology & Therapeutics
Faculty of Medicine
McGill University
Montreal, Quebec, Canada

June, 1998

National Library of Canada

Acquisitions and Bibliographic Services

395 Wellington Street
Ottawa ON K1A 0N4
Canada

Bibliothèque nationale du Canada

Acquisitions et services bibliographiques

395, rue Wellington
Ottawa ON K1A 0N4
Canada

Your file Votre référence

Our file Notre référence

0-612-44373-6

Canada

TABLE OF CONTENTS

page

CHAPTER I

PROARRHYTHMIC EFFECTS OF D-SOTALOL IN RABBIT VENTRICLE ASSOCIATED WITH DIFFERENTIAL EFFECTS ON REPOLARIZATION IN ENDOCARDIAL CELLS: AN IN VITRO STUDY

CHAPTER II

D-SOTALOL INDUCED VENTRICULAR ARRHYTHMIAS IN THE ISOLATED RABBIT HEART - MODEL AND MECHANISMS

PREFACE

In accordance with the "Guidelines Concerning Thesis Preparation" of the Faculty of Graduate Studies and Research of McGill University, the candidate has chosen the option of including, as part of the present thesis, the text of an original paper already published by a peer-reviewed journal, and original papers submitted, or suitable submission to learned journals. The text pertaining to this option is as follows:

"Candidates have the option of including, as part of the thesis, the text of one or more papers submitted or to be submitted for publication, or the clearly-duplicated text of one or more published papers. These texts must be bound as an integral part of the thesis. If this option is chosen, connecting texts that provide logical bridges between the different papers are mandatory. The thesis must be written in such a way that it is more than a mere collection of manuscripts; in other words, results of a series of papers must be integrated. The thesis must still conform to all other requirements of the "Guidelines for Thesis Preparation". The thesis must include: A Table of Contents, an abstract in English and French, an introduction which clearly states the rationale and objectives of the study, a review of the literature, a final conclusion and summary, and a thorough bibliography or reference list. Additional material must be provided where appropriate (e.g. in appendices) and in sufficient detail to allow a clear and precise judgment to be made of the importance and originality of the research reported in the thesis. In the case of manuscripts co-authored by the candidate and others, the candidate is required to make an explicit statement in the thesis as to who contributed to such work and to what extent. Supervisors must attest to the accuracy of such statements at the doctoral oral defense. Since the task of the examiners is made more difficult in these cases, it is in the candidate's interest to make perfectly clear the responsibilities of all the authors of the co-authored papers."

The "Results" section of this thesis consists of four manuscripts. The first two manuscripts and the fourth manuscript are to be submitted to the journal *Circulation*; The third manuscript will be submitted to the *Journal of Cardiovascular Electrophysiology*. The initial versions of the manuscripts were written by the candidate. These were all revised by the supervisor to make them suitable for publication.

ACKNOWLEDGEMENTS

I have enjoyed a lot of great times and many great interactions in the Department of Pharmacology and Therapeutics. I was also very fortunate to expand my knowledge with the group from the Centre de Recherche at the Sacré-Coeur hospital. I am proud to be a mixed product from these two very prestigious institutions. I am also very proud to have been able to represent both institutions at National and International scientific meetings.

Dr. B. I. Sasyniuk, my thesis supervisor, for her trust, support and criticism; her view of research will always stay with me. Chapeau!

Dr. Jacques Billette, for conversation and enthusiasm in research.

Dr. R. Capek, for his support in all my endeavors.

Dr. Y. Dekoninck, for all the times my computer crashed, and for your young research perspective.

Alan Foster, my personal photagrapher, for the good laughs, and crooked pictures!

Dr. D Varma, for his wise view of life.

Dr. B. Collier, for his sarcasm, it would not be safe to say more...

Dr. A. Padjen, my advisor, for keeping an eye on me (the other one being on his computer screen) and for all the celebration we assisted together (this before the phone rang).

Dr. R. Cardinal, to have allowed me to use his resources, and for his good research advice and support.

Dr A.C. Cuello, for being a strong and firm chairman.

Dr. R. Dasilva, for great support, enthusiasm, and for the good times we spend on the graduate committee.

Gaétan Tremblay, for is expert systems assistance and for cardiomap III

My parents and family, for their great support and for pretending that they knew what I was doing for the last 5 years... "Pills."

Vicky, for being a breath of fresh air in all our lives!

Burny, my best friend, for listening to me all the time even while sleeping. Even with your pour vision you can still meet me before anyone!
Murray sweet, for the laughs, and great mental support...

My girlfriend, without whom life would of been so boring..."I miss you like the desert miss the rain."
And last but not least

Dr. Selva Baltan, for the sun, and for believing in me when I may have sounded quite out of my mind. Most of the times, what counts is the end result!!! Yes!

ABSTRACT

Torsade de pointes (TdP) is a proarrhythmic side effect of antiarrhythmic drugs that prolong the QT interval. The exact electrophysiologic mechanism of TdP is under intense investigation. To study the mechanisms and characteristics of TdP requires an animal model in which the arrhythmia occurs at a high incidence, predictably, reproducibly and resembles the characteristics of the clinical arrhythmia. We have developed such a model in the isolated rabbit heart (chapter II). This model is based on our earlier work showing that in isolated ventricular preparations from the rabbit heart, class III drugs, such as *d*-sotalol induce a greater increase in action potential duration in Purkinje fibers than in ventricular muscle, resulting in generation of early afterdepolarization-dependent triggered activity in Purkinje fibers and their subsequent propagation to muscle as extra beats (chapter I). Studies in the whole heart suggested that the initiating beats of *d*-sotalol induced TdP have a subendocardial origin whereas later beats could be generated by reentry in muscle with disparate monophasic action potential durations (chapter II). The evidence presented in these studies was inconclusive because of the limited number of recording sites. To further clarify the relative contributions of impulse formation in the conducting system and reentry in muscle, we performed epicardial mapping using a sock electrode array to fit the rabbit heart. In addition plunge wires were used to record unipolar electrograms from the endocardial surface. The epicardial and endocardial electrograms were used to measure activation times as well as activation recovery intervals, a measure of local repolarization intervals. Using this technique in our TdP model, we were able to show that the generation of singlet beats and the first beats of couplets, triplets and TdP are due to the same mechanism - ie, a focal mechanism arising in the ventricular specialized conducting system in a context of increased dispersion of repolarization and probably due to the generation of triggered activity in the Purkinje system. The inhomogeneous prolongation of repolarization intervals, at slow heart rates, provides the functional dissociation, unidirectional block and delayed activation required to initiate reentry in the subsequent beats leading to TdP. The dispersion of repolarization is rapidly eliminated during a TdP episode which ultimately leads to its termination and explains why TdP is a self-limiting arrhythmia (chapters III and IV).

RÉSUMÉ

La torsade de pointes (TdP) est un effect proarythymique des antiarythmiques de classe III qui semble être causé par un allongement excessif de l'interval QT de l'electrocardiogramme. Le mécanisme exact de cette arythmie ventriculaire est sous intense investigations. Pour étudier le mecanisme et les charactéristiques de la TdP il faut un modèle animal dans lequelle cette arythmie peut être induite de façon élevée et sous des conditions similaires que l'arythmie clinique. Nous avons donc développé un modèle qui possède ces caractéristiques (chapitre II). Nous avons fondé ce modèle sur les mêmes conditions qui mènent a une plus grande prolongation des potentiels d'action des fibres de Purkinje que dans le muscle ventriculaire; ceci menant à l' apparition d' activitée déclenché de type prematuré ("early afterdepolarization, EAD") dans les fibres de Purkinje qui fût suivie par leurs propagation dans le muscle (chapitre I) Les études dans le coeur isolé suggèrent que le battement qui initie la TdP observée en présence du *d*-sotalol était d'origine subendocardique et que les battements subsequents étaient le resultat d'un mécanisme de réentrée dans le muscle où il y a une disparté de potentiel monophasique entre l'endocarde et l'épicarde (chapitre II). L'évidence présenté dans cette étude était inconclusif à cause du nombre restraint de sites d'enregistrements. Pour clarifier la contribution de l'activité déclenchée et de la réentrée pour les TdPs, nous avons fait la cartographie épicardique. Nous avons aussi fait des enresistrements endocardiques avec des fils localisés sur la paroie endocardique. Les enregistrements épicardiques et endocardiques ont été mesurés pour détecter les temps d'activation et les intervalles de repolarization active, une mesure de la repolarisation locale. Nous avons démontré que la generation de singulet, et le premier battement d'un couplet, triplet, et de la TdP était le resultat du même mécanisme; un mécanisme focal qui a pour origine le système de conduction spécialisée ventriculaire et probablement le resultat d'activité déclenché provenant du système de Purkinje. La prolongation inhomogène des intervalles de repolarisation donne la dissociation fonctionelle, le bloc

unidirectionel, et les delais d'activation necessaire pour l'initiation d'une réentrée qui mène à la TdP. La dispersion des intervalles de repolarisation est rapidement éliminée ce qui mène à la terminaison de la TdP. Ceci peut expliquer pourquoi cette arythmie se termine de façon spontanée (chapitres III et IV).

CONTRIBUTIONS OF AUTHORS

Studies in Chapters I and II were performed by the candidate in the laboratory of Dr. B. I. Sasyniuk at McGill University. Studies in Chapters III and IV were performed by the candidate in the laboratory of Dr. Cardinal at the Centre de recherche, Hôpital du Sacré-Coeur de Montréal, Québec, Canada. All these studies were done under the constant supervision of Dr. B. I. Sasyniuk of McGill University. The candidate was solely responsible for the experimental design, its execution, analysis and interpretation of all the studies. Katayoun Derakhchan, a PhD student supervised by both Dr. Cardinal and Dr. Sasyniuk, provided technical assistance in setting up some of the preparations (chapters III and IV) and was involved in some of the analysis in chapter III. Dr. Cardinal provided assistance in interpreting the data and in the writing of chapter III.

LIST OF ABBREVIATIONS

AP	Action Potential
APD	Action Potential Duration
4-AP	4-Amino-pyridine
ARI	Activation-recovery interval
ARI_{min}	Minimal activation-recovery interval
ARI_{max}	Maximal activation-recovery interval
ARID	Activation-recovery interval disparity
BCL	Basic cycle length
CL	Cycle length
CL-1	Immediately preceding cycle length
CI	Coupling interval
E	Embryonic day
DAD	Delayed afterdepolarization
EAD	Early afterdepolarization
ERG	Ether-a-go-go-related K^+ channel
IDV	Idioventricular depolarization
I_K	Delayed rectifier
I_{Kr}	Rapid component of the delayed rectifier
I_{Ks}	Slow component of the delayed rectifier
I_{K1}	Inward rectifier
I_{ti}	Transient inward current
I_{To}	Transient outward current
LAD	Left anterior descending artery
LQT	Long QT syndrome
MAP	Monophasic action potential
MAPD	Monophasic action potential duration
$MAPD_{90\%}$	Monophasic action potential duration at 90% repolarization

$MAPD_{apical}$	Monophasic action potential duration at 90% repolarization recorded from the epicardial apical surface
$MAPD_{basal}$	Monophasic action potential duration at 90% repolarization recorded from the epicardial basal surface
MAP_{endo}	Monophasic action potential duration at 90% repolarization recorded from the endocardial surface
MAP_{epi}	Monophasic action potential duration at 90% repolarization recorded from the epicardial surface
M cells	Midmyocardial ventricular cells
PDA	Posterior descending artery
PF	Purkinje fiber
PVT	Polymorphic ventricular tachycardia
SERCA	Sarcoplasmic reticulum Ca^{2+}-ATPase
TdP	Torsade de Pointes
T cell	Transitional cells
VM	Ventricular muscle
VSCS	Ventricular specialized conducting system
VT	Ventricular tachycardia

GENERAL INTRODUCTION

"Extreme remedies are very appropriate for extreme diseases"

-Hippocrates

1.1. Normal heart function

The heart's main function is to pump blood to the body. On average it pumps 5 L of blood per minute to supply the metabolic needs of the body. When the heart rate is either too slow or too fast, the cardiac output can be greatly compromised. At a very fast heart rate the pumping efficiency can be substantially reduced because of the shortening of the filling period. Abnormal electrical activity can either increase or decrease heart rate and therefore greatly impact on its main function.

1.1.1. Electrical activity of the Heart

1.1.1.1. Normal electrical activity of the heart

The human heart beats at an average rate of 72 beats per minute. Proper electrical activity is necessary for the heart to effectively pump blood to the entire body. This activity can be detected from the body surface in the form of an electrocardiogram. Impulses originate spontaneously and rhythmically within the sinoatrial node located near the junction of the superior vena cava and right atrium. Sinoatrial node generated action potentials (AP) almost simultaneously propagate to the right and left atrium giving rise to the P wave in the electrocardiogram. Three bundles of muscle fibers, internodal tract of Bachmann, Wenkebach, and Thorel, ensure simultaneous activation of both atria. The impulse then reaches the atrio-ventricular node, the gateway to the right and left ventricles, where it is slowed; this delay allows the ventricles to fill. Then the

impulse travels rapidly down the right and left bundle branches to the Purkinje system. Conduction velocity in Purkinje fibres is very fast and ensures that the impulses reach the ventricular muscle cells of both ventricles almost simultaneously; this gives rise to the QRS complex on the electrocardiogram.

Following full depolarization of the heart, the repolarization process can proceed. Cells located close to apical sites repolarize earlier than do the ones located closer to the base, therefore the repolarization wave front travels from the base to the apex of the heart. This gives rise to the T-wave of the electrocardiogram. The opposite direction in the movement of the depolarization and repolarization wave front explains why the QRS and T-wave have the same polarity on the electrocardiogram.

1.1.1.2. **Abnormal electrical activity and arrhythmias**

Any deviation from this previously described electrical activity can lead to cardiac arrhythmias. A bradycardia is an abnormal heart rate slower than 50 beats per minute, while a tachycardia is an abnormally rapid heart rate faster than 100 beats per minute. Since abnormal electrical activity may compromise the main function of the heart, which is to pump blood, it is imperative to understand the mechanisms leading to arrhythmias. Two main causes of arrhythmias have been recognized: 1) abnormal impulse initiation and 2) abnormal impulse propagation. The mechanism of both of these causes will be explored.

1.1.1.3. **Ion channels**

This section will describe the most important ion channels.

The activity of four different types of ion channels are responsible for the electrical activity of the heart. Ion channels are macromolecular pores across the membrane through which ions can flow. The cell actively pump Na^+ ions out of the cell and K^+ inside the cell, resulting in a gradient for both these ions. Since electrochemical gradients are created and maintained by the cell when channels' ionic gates open, ions will flow in or out of the cell; the direction of which will be dictated by the direction of the electrochemical gradient acting on particular ion. The potential which is associated with no net flux of a particular ion species can be calculated from the Nernst equation; the Nernst potential for the different ions is as follows: Na^+,+70 mV; K^+, -98 mV; Ca^{2+}, +150 mV; and Cl^-, -30 to -65 mV. For example, when only K^+ channels open, K^+ ions will flow out of the cardiac cell until the Nernst potential for K^+ ions is attained (-98 mV). These different ion channels are defined according to the type of ion that permeate through the channel; K^+ channels, Na^+ channels, Ca^{2+} channel, and Cl^- channels pass K^+, Na^+, Ca^{2+}, and Cl^- respectively. These channels have been targeted by antiarrhythmic drugs to regulate the electrical activity of the heart and also mutations specific to these same ion channels have been linked to the manifestation of the congenital long QT syndromes.

1.1.1.3.1. **Antiarrhythmic drugs**

Ventricular arrhythmias kill thousands of North-Americans every year. The American Heart Association reported that cardiovascular diseases claimed

954,720 lives in 1994; out of this number more than 250 000 are related to sudden cardiac deaths, of which ventricular arrhythmia is the major cause. Therefore preventing ventricular arrhythmias could reduce the number of death associated with sudden cardiac death and cardiovascular diseases. Prevention of life-threatening arrhythmias with drugs is a very promising research avenue that has been explored for many years. Over the years many drugs, with diverse efficacy and modes of action have been used.

Antiarrhythmic drugs have been classified into four different classes according to the Vaughan Williams's classification scheme; these are class I, II, III and IV.

1.1.1.3.1.1. **Class I**

Class I antiarrhythmic drugs block fast Na^+ channels, increase refractoriness and decrease conduction velocity. This class is subdivided into three subgroups, class Ia, Ib, and Ic, based on their efficacy at different heart rates. Class Ia (quinidine, procainamide, disopyramide) produce almost no block at normal heart rates and also cause AP prolongation. Class I b (e.g., lidocaine, phenytoin, tocainide, and mexiletine) produce more block at normal heart rates when compared to class I a and accelerate AP repolarization. Class I c (e.g., flecainide encainide, and propafenone) produce block at normal heart rates.

The results (review [1]) of the cardiac arrhythmia suppression trials (CAST) revealed an increase in mortality associated with the use of some class I antiarrhythmic drugs (encainide and flecainide). However, these same drugs are

still used in some patients with atrial fibrillation to alleviate their symptoms and to maintain them in sinus rhythm. Those are patients who have atrial fibrillation but not having the following heart diseases: myocardial infarction, ischemia, cardiac hypertrophy, etc. (review [2]).

1.1.1.3.1.2. **Class II**

All drugs belonging to this group block β-adrenergic receptor activation (e.g., propranolol). Their antiarrhythmic action is most likely the result of decreased automaticity of different pacemakers and increased fibrillation threshold. This is the only class of antiarrhythmic drug analyzed to decreased mortality in patients after a myocardial infarction (review [2]).

1.1.1.3.1.3. **Class III**

Drugs in this group prolong APD (e.g., sotalol, bretylium, amiodarone, azimilide) . Most class III drugs produce their clinical effect by selectively blocking the fast component of the delayed rectifier (I_{Kr}). The newer strategy which is exploited by the pharmaceutical industry is to develop a drug (e.g., amiodarone) which block multiple currents, including I_{kr}, and receptors. Beneficial effects of this group of drugs are still being evaluated.

1.1.1.3.1.4. **Class IV**

The antiarrhythmic agents belonging to class IV are Ca^{2+} channel blockers (e.g., verapamil, diltiazem). They are used clinically to depress Ca^{2+}-dependent AP s and to slow AV nodal conduction.

Other classification systems have been proposed because the presently used classification system has many limitations. 1) The present classification system is hybrid. Class I and IV include drugs which block channels, Class II include drugs which block receptors, and class III includes drugs which change an electrophysiological variable (APD). Furthermore the effect of one class can be achieved by many different mechanisms. 2) Some agents that have proven to have antiarrhythmic potential are not included: e.g., α-adrenergic blockers, cholinergic agonists, adenosine, and digitalis. 3) The classification is based on electrophysiological effect of drugs on isolated normal tissue, whereas the arrhythmias are observed in diseased tissue. 4) The effectiveness of multiple-action drugs is not addressed. For example, amiodarone may be placed in all four classes, I, II, III and IV.

The Sicilian Gambit classification system proposes that drugs be classified based on the cellular targets that drugs affect and the vulnerable parameters which may prevent the arrhythmias [3]. The vulnerable parameters will come from a knowledge of the mechanism that cause a particular arrhythmia; they include, for example, the increased phase 4 depolarization for enhanced automaticity or the APD prolongation for early after depolarization (EAD)-

dependent triggered activity, etc. . The cellular target are the ion channels, receptors, pumps, etc.., This approach may provide the flexibility and frame work for the rational use and development of antiarrhythmic drugs. There is a lot of controversy between this classification system and the Vaughan Williams classification system, but their combination or the knowledge of both, and their limitations, may prove useful. For now, the most commonly used and most predictive of the activity of a group of drugs is the Vaughan Williams classification system.

1.1.1.3.2. **Techniques to study arrhythmias**

Usually arrhythmia are observed clinically from a 12 lead ECG. The electrocardiogram reveals the activation sequence and sites with abnormal properties. In case arrhythmias cannot be observed in an acute recording session a holter monitoring may be taken. This is an electrogram recording that is recorded over a longer period of time (24 hours or more). Alternatively there are interventions to reproduce the arrhythmias and concomitantly test the effectiveness of different preventive interventions including antiarrhythmic drugs.

1.1.2. **Class III antiarrhythmic Drugs**

This thesis will focus on the action of a class III antiarrhythmic drug. Recently, drugs with class III action have been introduced clinically, and, although they appear to be very effective and offer new antiarrhythmic characteristics, they are associated with a proarrhythmic side effect that can often be life threatening, torsade de pointes (TdP). Excessive QT interval prolongation

is thought to be the likely culprit which leads to TdP. The risk of TdP has prevented clinical use of the newer class III antiarrhythmic drugs, and slowed further development of this class of drugs. Therefore elucidation of the proarrhythmic mechanism associated with class III drugs might provide ways to circumvent this life threatening arrhythmia, and allow exploit action of their positive antiarrhythmic profile which could prevent a number of deaths every year.

1.1.2.1. **History of Class III drugs**

The result of the CAST trials led to the search for compounds with a mode of action other than sodium channel blockade. In the early 1960s it was observed that hyperthyroidism is commonly associated with atrial fibrillation and that with myxoedema arrhythmias are rare [4]. These same authors found that when rabbits made hypothyroid (by surgery) or hyperthyroid (by thyroxine injections), repolarization is delayed in hypothyroidism and accelerated in hyperthyroidism [4]. They subsequently searched for compounds with a similar type of action (delayed repolarization) and identified two compounds, amiodarone and sotalol. This discovery introduced a new class of antiarrhythmic drugs, class III. It is worth mentioning that the increase QT interval prolongation which was associated with either drugs (quinidine) [5] or a congenital and familial syndrome [6], was associated with polymorphic ventricular tachycardias and sudden cardiac death; this led to the initial pursuit of class I drugs over class III drugs.

From then on, many drugs which possessed this specific effect have been synthesized. Sotalol's molecular structure, a racemic benzenesulfonamide, was exploited to derive more potent and specific compounds (*d*-sotalol, E-4031, dofetilide, clofilium, bretylium). Racemic sotalol possesses both class II and class III antiarrhythmic activity. The class II effect is absent in *d*-sotalol.

1.1.2.2. **Mechanism of action of Class III drugs**

Theoretically, the repolarization phase of an action potential could be delayed by multiple ways; by either increasing inward currents or decreasing outward currents. Blockade of a wide variety of outward currents identified in ventricular muscle (the transient outward current [7], the delayed rectifier [8], and the inward rectifier [9]) or enhancement of inward currents (L-type Ca^{2+} current, Ca^{2+} window current (BayK 8644), plateau current, Na^{+} window current [10]), can lead to delay of the repolarization phase of the AP. It is interesting that selective class III antiarrhythmic drugs, including those already clinically used, accomplish this effect by blocking I_{Kr}. Two component compose the delayed rectifier, a rapid and a slow activating component, I_{Kr} and I_{Ks} respectively. It is still not clear why modulation of one type of ion channel over other ones, which ultimately lead to a delayed repolarization, would be favored (review [11]).

Why was I_{Kr} chosen as target for antiarrhythmic drug over other channels? The following reasons were initially given [12]. "This current is targeted, initially, because of these drugs' profile, and the distribution and biophysical characteristics of this current system. Drugs that block this current are selective to

heart, and they show low affinity for other cardiac K^+ channels. Apparent homogeneous distribution of this channel throughout atria and ventricle would result in an uniform repolarization. It is an inward rectifier and its current flow will increase when extracellular K^+ is elevated as occurs during myocardial ischemia, and "based on its time- and voltage-dependence and its inward rectification characteristics, it is expected to play a specific and limited role in ventricle, namely to initiate termination of the AP plateau". Even though most of these assertions were not verified by cardiac electrophysiologists, the pharmaceutical companies directed most of their research programs in this direction.

1.2. **Antiarrhythmic and antifibrillatory efficacy of Class III drugs**

Over several years class III antiarrhythmic drugs have proven effective in some animal models for preventing death when compared to other antiarrhythmic drugs. Class III drugs are effective against induction of ventricular fibrillation by programmed electrical stimulation [13], they elevate ventricular fibrillation threshold [14], they can produce spontaneous defibrillation with restoration of normal sinus rhythm, and [14] they can either decrease or not change energy requirements of electrical defibrillation (review [15]).

These very positive initial animal studies warranted studies and clinical trials in human populations. Results with *d-l* sotalol were positive and the drug has been approved by the FDA and Health Protection Branch (Canada's agency) for treatment of life-threatening ventricular arrhythmias. This compound has both

class III and II antiarrhythmic properties. The results with other drugs possessing more selective class III antiarrhythmic effect (descendants of d-l-sotalol) are mixed. Some of these drugs were abandoned at various stages of clinical trials because of increased death and concern about risk of torsade de pointes arrhythmias as well as other adverse effects when compared to control groups: Drug (company, clinical trial stage), sematilide (Berlex, ?), almokalant (Hassle, II/III), E-4031 (Eisa, II) *d*-Sotalol (Bristol Myers Squibb, II/III), MK-499 (Merck, II). Only a few are still in clinical trial or marketed: d,l-sotalol (Berlex, marquetted), dofetilide (Pfizer, III), MS- 551 (Mitsui, ?), artilide (Upjohn, ?). The future will tell what will be their fate [12].

Of special interest *d*-sotalol was abandoned after the SWORD trial (Survival With Oral *D*-sotalol). *D*-sotalol was given to patients who had just suffered from a myocardial infarction. The trial was prematurely stopped by the monitoring committee, because the *d*-sotalol group showed a higher mortality rate when compared with the control group (4.6 versus 2.6 %) (review [16]). The patients supposedly died from the proarrhythmic side effect of the drug (TdP) but direct evidence was not established since no holter monitoring was taken in these patients. One major criticism of this study was the low mortality rate of the control group (2.6 %); usually the mortality rate is much higher in this patient population (5-15 %) (review [12]). This suggests that the patients in this group were not at a high risk of mortality. This served for the future patient selection for antiarrhythmic trials: for example, the ALIVE trial (AzimiLide post-Infarct

surVival Evaluation trial), which tests the effectiveness of azimilide, only enrolls patients who are at high risk.

1.3. Molecular target of selective class III Antiarrhymic drug

1.3.1. The rapid component of the delayed rectifier current

Most of the novel Class III antiarrhythmic drugs are selective blockers of the rapid component of the delayed rectifier current. The delayed rectifier has two components; a rapid component and a slow component, I_{Kr} and I_{Ks} respectively. I_{Kr}'s activation threshold is around -50 mV with a half point of -22 mV and a slope factor of 7.5 mV. Its inactivation half point is -9 mV with a slope factor of +22 mV. This current peaks at 0 mV, fully rectifies around +60 mV and inwardly rectifies at potentials ≥ -50 mV. The inward rectification mechanism is likely the result of fast channel inactivation [17,18].

On the other hand, I_{Ks} has very different biophysical properties. Its activation threshold is around -30 to -20 mV, half-point at +15.7 and a slope factor of +12.7 mV and it does not rectify. Conductance of I_{Ks} is much bigger than I_{Kr}, but at voltages between -20 to +20 mV for a duration of 225 msec (a pulse voltage and duration, which is similar to that observed at plateau potential of the AP and similar duration of guinea pig ventricular AP), the conductances of both currents are very similar [19]. A similar description has been obtained in different species [20,21] and systems [22,23], but different magnitudes of these two currents, I_{Kr} and I_{Ks}, may be observed in different species and different cell types within the same species.

1.3.1.1. **Molecular correlate of I_{Kr} and I_{Ks} channel**

The first *m*-RNA thought to be encoding for I_{Kr} was isolated from the rat brain hippocampus by *in situ* hybridization with a *c*-DNA isolated from fruit flies. The channel encoded from this *m*-RNA was termed ERG (ether-a-go-go-related K^+ channel) [22]. The term ether-a-go-go was used because fruit flies with a mutation in this channel dance when they are exposed to ether. It was subsequently recognized that there are two alternatively spliced *m*-RNA forms of this channel: HERG A, the originally isolated *m*-RNA, and HERG B (H is for human). These alternatively spliced *m*-RNA were first described in the mouse heart, MERG A and MERG B, (M is for mouse) [24]. ERG A *m*-RNA is expressed both in the brain and the heart while ERG B *m*-RNA is more abundantly expressed in the heart but relatively less in brain. When expressed in xenopus oocytes both *m*-RNA translate to express K^+ channels which are blocked by a class III drug (dofetilide) The major differences between these two channels are their activation and deactivation kinetics and their sizes. HERG A kinetics are slower than the native I_{Kr} current (4 to 5 times) and HERG B kinetics are faster than the native I_{Kr} current. The N-terminal of ERG B (M and H) is shorter and more basic than that of ERG A (M and H). This difference between these two proteins may have conferred them with the different electrophysiological properties previously described. It still remains to be determined what is the molecular determinant of the native I_{Kr} channel. It was proposed that the current could be formed by homomultimers or heteromultimers of either ERG A or ERG B [24].

I_{Ks} is thought to be the result of the co-assembly of two subunits which co-assemble to form a functional channel, KVLQT1 and minK [25]. KVLQT1 is a voltage-dependent K^+ channel protein linked to the first category of the congenital long-QT syndrome. MinK is a minimal K^+ channel protein; minimal because it is only made up of one transmembrane spanning domain as opposed to six membrane spanning domains for most K^+ channels.

1.3.2. **Blockade of I_{Kr} by class III antiarrhythmic agents**

I_{Kr} is selectively blocked by benzenesulfonamide (or methanesufonamide) class III antiarrhythmic agents (e.g., *d*-sotalol and E-4031) [22]. Blockade of I_{Kr} by these drugs has been described to be use-dependent [26,27], use independent, [28] voltage-dependent [29,30], tonic [26], and to vary with external K^+ concentration. Mechanisms of blockade and recovery from block of this current system has been widely investigated in a variety of experimental preparations. *In vitro* cardiac tissue (isolated myocytes) and channel expression of HERG construct in heterologous expression systems have been utilized (oocytes, AT-1 cells (mouse atrial tumor cell line)) using either patch clamping or ligand binding techniques.

Under specific conditions, almokalant, dofetilide, *d*-sotalol, and E-4031 exhibit use-dependent block (holding potentials ranged from -50 to +10 mV) [26]. This effect decreases over time owing to the long recovery time constant (10 sec at -50 mV) exhibited by these drugs. The expression "use-dependent" is commonly used when referring to currents and "rate dependent" when referring to

APs. Whereas others have not observed any use-dependent effect with E-4031 and dofetilide [28], the difference reported here is likely to be related to experimental differences.

As well, voltage-dependent block is different in different experimental systems and paradigms. Some authors observed a more potent block of tail current after a test potential to +60 then after those to < 0-10 mV [29]. However the steady state block of HERG expressed in xenopus oocytes did not exhibit voltage dependence (E-4031 and MK-499), and it was not affected by external K^+ concentration [27].

The following example shows use-dependent block and slow recovery from block of I_{Kr} which may be explained by the voltage dependency of block of these drugs. Almokalant, another selective I_{Kr} blocker, blocks this current in a use-dependent fashion, at 0 mV, and recovery from block is also voltage-dependent. The time constant for recovery from block is approximately 10 seconds at -50 mV and recovery is practically absent at more hyperpolarized potentials (-75mV). Therefore, under these experimental conditions, almokalant exhibits both use-dependent block and unblock of this channel [30].

It was also observed, in two different experimental systems, that the level of block was different at different external K^+ concentration. These observations have been made for tritriated dofetilide binding in both AT-1 cells and neonatal mouse cells. These cells have been described to express only the high affinity binding site which is believed to be the I_{Kr} channel [23,31]. When the external K^+ concentration is reduced there is more block or binding to I_{kr} [32,33].

It was recently shown from HERG chimeric channels results, that the site of block by dofetilide would be located to the H5 pore region of the HERG channel. More specifically a serine at position 620 in the S5-S6 linker region seems to be very important for the drug binding. The drug interaction seems to be dependent on the inactivation properties of the channel; if the channel does not have an intact C-terminal inactivation process, high affinity drug binding is greatly compromised [34,35]. This region is shared by both ERG isoforms.

1.3.3. **Reverse rate-dependence**

Most of the selective class III drugs prolong the APD more at slow than a fast stimulation rates; this effect is referred to as "reverse rate-dependence". This effect was observed in a variety of species (guinea pig[36] , dog[37] (review[38]), rabbit[39,40], and human[41,42]). On the other hand, almokalant in the pig heart has been reported not to have a reverse rate-dependent effect [43,44]. This difference may be related to a species difference, the low drug concentration used, or the fast stimulation rate used in this study. Ventricular APD is also reverse-rate dependent in most species (review [45]). For some unknown reason(s), selective class III drugs greatly accentuate this effect. The excessive prolongation of APD at slow stimulation rate is likely related to the main proarrhythmic side effect of this class of drugs, TdP. Three hypothesis have been proposed to explain the reverse rate-dependence effect.

The first hypothesis suggests that, because of the slow time constant of deactivation of I_{Ks}, incomplete deactivation of this current was observed at fast

stimulation rates. This results in a greater magnitude of I_{Ks} current at fast stimulation rates. It would therefore provide more repolarizing current at fast stimulation rates and explain the shorter APD observed at fast stimulation rates [28] when compared to a slow stimulation rate.

Two separate studies, based on measurement of faster recovery kinetics from deactivation of I_{Ks}, have challenged this hypothesis. They showed that the recovery kinetic from deactivation in the dog is more rapid than in the guinea pig (τ= 150 ms near -35 mV and decreasing to 30 ms near -85 mV vs 140 msec)[37], and therefore could not accumulate at fast stimulation rates. The second study, performed in guinea pig ventricular muscle cells, similar to the original study, reported much shorter time constant of recovery from deactivation for I_{Ks} (62 vs 140 msec) [46] . These differences may have been the result of using different voltage protocols and channel blockers in these two studies. These studies strongly question the ability of the recovery kinetics from deactivation of I_{Ks} to explain the phenomenon of reverse rate-dependence.

The second hypothesis suggests that reverse rate-dependence is related to the frequency dependent changes of the extracellular K^+ ions concentration and its modulation of the drug channel interaction [33]. It was observed that dofetilide blocks I_{Kr} current more at lower extracellular K^+ concentration than higher ones. It is also known that upon rapid pacing extracellular K^+ concentration increases[47]. The combination of these two observations suggests that this class of drugs block I_{Kr} channel less at a fast stimulation rate than at slow one. Therefore less blockade at a fast rate would likely mean less AP prolongation at that stimulation rate.

The third hypothesis suggests that drug molecules should bind more to the closed state of the channel, since at slow rate the delayed rectifier channels are mostly in the closed state. At slow pacing rates, cells spend a longer time at a resting membrane potential when compared to faster pacing rate [48].

1.4. Cellular target of selective class III antiarrhythmic drugs

1.4.1. Purkinje fibers being a preferred target

Similarly to other investigators, we have found that Purkinje cells are extremely sensitive to compounds which delay the repolarization phase (e.g., class III antiarrhythmic drugs [49,50], other drugs which block I_{Kr} [40,51-53], class Ib antiarrhythmic drugs [54,55], anthopleurin A [56]). The next section will elucidate possible origins and characteristics of Purkinje cells.

1.4.1.1. Purkinje fiber origin

The cellular origin of Purkinje cells is very controversial. There exist two major conflicting theories; myogenic and neurogenic developmental theories (review [57]). Specific protein markers have been associated with the Purkinje cell type, based on antibody immunoreactivity. Since some of these protein markers are normally expressed by either neuronal cells or striated muscle cells, these findings lead to the development of the opposing myogenic and neurogenic developmental theories.

1.4.1.1.1. **Cellular markers**

Overall, 11 specific cellular markers have been identified to Purkinje cells; of the 11 markers, seven are neuronal and only two are expressed in striated muscle cells. The remaining 2 markers are specific to the Purkinje cells.

Of the seven neuronal markers, five were immunologically detected and the remaining two were electrophysiologically detected. Immunoreactivity has been detected to 1) neurofilaments (embryonal avian polypeptide (EAP), 2) brain-associated glycoprotein, 3) NF-M (middle subunit of neurofilament), 4) neural crest cells protein marker (Natural Killer cell phenotype (HNK-1)), and to 5) acetylcholinesterase. Typical neuronal ion channels have also been detected: I_f (f: funny) and I_{ca}. It is believed that these ion channels, I_{ca} and I_f, are responsible for intrinsic rhythmic activity of Purkinje cells.

The striated muscle cell markers are the slow-type skeletal myosin heavy chain and the myosin binding protein H (MyBP-H) [58]. Detection of slow-type skeletal myosin heavy chain results from a crossreactivity between protein expressed in the anterior latissimus dorsi muscle (ALD58: 58 for antibody 58) and proteins expressed in Purkinje fibers. MyBP-H is expressed preferentially in the A band of Purkinje fibers myofibrils.

Like ventricular and atrial muscle cells, Purkinje cells are electrically coupled. This function is mediated by specialized regions of sarcolemmal interaction termed gap junctions. Gap junctions constitute a group of 6 connexins

on each cell that are in contact. Some investigators have shown that the Purkinje system expresses distinct connexins. Based on immunoreactivity results, some showed a preferential expression of connexin42 in the conduction system including the Purkinje system of avian hearts [59]. The pattern of expression in the Purkinje system is different than that of ventricular muscle cells. Unlike the ventricular muscle cells which make most of their contact at the Z-lines, end to end, the Purkinje cell make contact with other Purkinje cells both laterally and end to end, equally. These additional differences distinguishes them from surrounding myocardium [60].

In addition, Purkinje cells are shown to express more intracellular Ca^{2+} release channels sensitive to inositol 1,4,5-triphosphate (IP_3R) compared to atrial and ventricular myocytes [61] (review [62]). These are results from *in situ* hybridization studies and tritiated IP3 and immunofluorescence studies. Though there exists an heterogeneity in expression of IP_3R in adult heart within Purkinje cell population, Purkinje cells all express a different subtype of ryanodine receptors (RyR) when compared to ventricular muscle. They express RyR1 and RyR3 of which RyR1 is also expressed in skeletal muscle. Ventricular muscle cells express RyR2 based on *in situ* hybridization studies. They also express very low levels of sarcoplasmic reticulum Ca^{2+} ATPase (SERCA 2a *m*-RNA) when compared to ventricular muscle. Such a different composition appears to be related to a distinct functional role played by these two myocytes populations and

suggest that polymorphism of sarcoplasmic reticulum channel and pump genes may play a role in their modulation and control of cytosolic Ca^{2+} concentration.

1.4.1.1.2. **The myogenic theory**

In chick, the Purkinje fibers located deep in myocardium, transmural Purkinje fibers, are thought to arise from cardiomyocytes. Those cardiomyocytes in close proximity to coronary artery vessels have been shown to differentiate into Purkinje cells. It is postulated that a factor originating from the coronary artery leads to this differentiation process [63] (review [57]).

Retroviral cell-labelling techniques show that transmural Purkinje cells do not arise from neural crest cells. In this experiment, muscle cells are labeled with a retrovirus at a time when neural crest cells are absent from heart. Neural crest cells start their migration at E2-E3 (E: embryonic day) and enter the heart at E4. In this study, retroviral cell-labelling is performed at E3 when no neural crest cells are present in the heart (review [64]). The Purkinje cells are labelled. If the neural crest cells were the progenitors of Purkinje cells, Purkinje cells would not have been labelled.

1.4.1.1.3. **Neural crest cells and PF**

Some evidence implies that conduction system cells are derived from neural crest cells originating from the branchial arches which migrated and led to sequential formation of the sinoatrial node, atrioventricular node, atrioventricular junction and bundle branches. This evidence is based on immunoreactivity

evidence of NF-M and HNK-1 (a migrating neural crest and monocyte marker) together with double labelling to sarcomeric myosin heavy chains [65,66].

Contrary to this theory, it is also believed that cells that make up the coronary arteries are important in the genesis of Purkinje cells by an indirect mechanism (review [57]). Neural crest cells are important for generating a proper coronary artery system so that any perturbation of neural crest cell development may influence the development and differentiation process of Purkinje cells.

1.4.1.1.4. **The "four ring" theory**

This older theory suggests that the common bundle originates from the fusion of ventricular septation which produced an invagination in the bulboventricular ring and its fusion with the atrioventricular ring. The right bundle branch originates from bulboventricular ring tissue. The left bundle branch only secondarily appears by fanning out of cells from both atrioventricular and bulboventricular rings [67].

1.5. **Difference in conduction system of different species**

The specialized ventricular conduction system is anatomically different between mammalian species. There exist two types of anatomical distribution of Purkinje fibers. First, Purkinje fibers either, upon emergence from the His-bundle, travel on the endocardial surface, fan out and then make contact with ventricular muscle cells (dog, pig, rabbit, and human), or they travel on the endocardial surface, and then make their way transmurally, subsequently fan out, and then make contact with ventricular muscle cells (birds and ungulates) (review [68]). This

difference may be designed to decrease the activation time of bigger hearts to maintain efficient pumping.

It was shown in the rabbit heart that Purkinje cells make contact with a transitional cell layer before making contact with the ventricular muscle cell layer. Transitional cells extend thin ribbon-like projections which make contact with both Purkinje cell and ventricular muscle cellular layers [69]. Electrophysiological experimental evidence suggests that such a cellular organization exists in the dog heart as well [70,71].

1.6. **Endocardium and generation of arrhythmias**

The ventricular endocardial surface has been identified as part of the arrhythmic substrate in a variety of pathological arrhythmic heart conditions: myocardial infarction [72], ishemia/reperfusion [73-75], postdefibrillation [76], congenital and drug induced long QT syndrome associated arrhythmias, and ventricular fibrillation [77,78]. Why is the endocardium implicated in these various pathological conditions? In all of the previously mentioned arrhythmias, heterogeneous AP prolongation is present and is likely related to the arrhythmic substrate. More specifically, in most of these arrhythmias, PF are more prominently affected when compared with other ventricular muscle cells.

The subendocardial Purkinje fibers have been implicated in ischemia/reperfusion arrhythmias [75,77]. In ischemia, Janse et al. [77] have implicated the Purkinje system as being important for the presence of ventricular fibrillation. In their experiments ventricular fibrillation was eliminated after ablating a thin

layer of cells of the endocardial surface with Lugol's solution. Lugol's solution stains glycogen blue, and was therefore initially used to stain the ventricular specialized conduction system, because the VSCS contains more glycogen granules than the surrounding ventricular muscle. Others have shown, in normal heart, that the threshold for fibrillation is greatly elevated after ablating a thin layer of the endocardial surface with Lugol's solution [78]. This suggests that the endocardium and the Purkinje system are involved in ventricular fibrillation.

With respect to reperfusion arrhythmias, a combination of mediators have been implicated in the generation of their arrhythmic substrate: acidosis, hypoxia, free radical formation, and extracellular Ca^{2+} increases. It was clearly shown that there is a differential sensitivity to these mediators between different cell types on the endocardial surface which may be responsible for some of the arrhythmias observed in this condition [79,80].

Postdefibrillation arrhythmias are observed when electrical shocks are used to terminate ventricular fibrillation. A differential cellular response was introduced to explain the effect of applied electrical shock. *In vitro* experiments showed that electrical shocks delivered to the myocardium affect Purkinje fibers differently from ventricular muscle cells. Electrical shock induces repetitive activity in PF which, initially, does not propagate to surrounding cells, because ventricular muscle is rendered refractory by the electrical shock [76]. This latter effect may explain defibrillation effect of electrical shocks, while the former their proarrhythmic effect.

Compounds which have been shown to increase the APD have been associate with excessive QT interval prolongation and polymorphic ventricular tachycardia. Some of these compounds produce their effect by blocking a variety of currents, but the ones investigated either block the fast component of the delayed rectifier or delay the inactivation kinetics of the fast Na current (anthopleurin A). A differential drug effect has been proposed to explain the arrhythmia observed with these different compounds. The Purkinje fiber cells [40,49-53,56,81,82] and M-cells [83] have been shown to be more affected than other ventricular muscle cells. The M-cells are located in the subepicardial surface of the ventricle. The exact proarrhythmic mechanism of action of selective blockers of the fast component of the delayed rectifier is the subject of this thesis.

1.7. **Cellular mechanism of abnormal impulse formation**

Two major mechanisms have been proposed to lead to abnormal impulse formation, either triggered activity or focal-dependent re-excitation mechanisms. It is generally accepted that triggered activity arises from the result of active membrane properties. On the other hand, a focal dependent-re-excitation mechanism may implicate both active and passive membrane properties.

1.7.1. **Triggered Activity**

1.7.1.1. **EADs**

EADs are secondary membrane deflections which arise prior to the full repolarization of the AP. They usually arise on phase 2 or 3 of the AP. EADs have been observed in a variety of contexts. EADs are pause-dependent, in that they are usually observed at slow stimulation rates. They have been observed experimentally in a variety of conditions and in the presence of different mediators: ischemia/reperfusion [79] [80] (review [84]), platelet activating factor [85], endothelins [86-88], adrenergic stimulation (α-adrenergic agonist [56,89-91] and β-adrenergic agonist [93-96], intracellular oxygen-derived free radicals [97], Ca^{2+} channel agonist (BayK 8644), cardiac hypertrophy [98], Na^{+} channels inactivating compounds (toxins (anthopleurin A)) [56], hypokalemia [99,100], class III antiarrhythmic drugs [100], drugs which prolongs the APD [40,49,51,52,82], cesium [7], and direct voltage application [101] (table 1).

Table 1.

Experimental conditions in which EADs have been documented and studied

Ischemia/reperfusion [79,80,84]

- Platelet activating factor [85]
- Endothelin-1 [86-88]
- ATP [102]

α-Adrenergic stimulation [56,89-91]

β-Adrenergic stimulation [93-96]

Intracellular oxygen-derived free radicals [97]

Ca^{2+} overload [103]

Ca^{2+} channel agonist (BayK 8644) [104]

Cardiac hypertrophy [98]

Na^{+} Channel toxins (anthopleurin-A, see anemone toxin, Ibutalide) [10]

Class III antiarrhythmic drugs (d-sotalol, E-4031) [101]

Drugs which prolongs the APD (droperidol, astemizole, cisapride) [40,49,51,52,82]

Cs [9]

EDTA [105]

Hypokalemia [99,100]

Direct current injection [101]

As can be seen, a variety of interventions can lead to the generation of EADs. We will focus on the current(s) which is/are responsible for the generation of phase 2 type EADs (plateau type EADs).

Ca^{2+} ions flowing through the L-type Ca^{2+} channel are thought to be the charge carrier. This conclusion is based on the observation that that L-type Ca^{2+}

channel antagonists (dihydropyridines) prevent the generation of these EADs. These Ca^{2+} channels may be either activated directly by compounds or second messengers, or they are reactivated because of the more prolonged duration of the action potential's plateau phase. The latter hypothesis is believed to be the correct one (review [106]). Phase 3 type EADs are thought to be generated by a different mechanism. The Na^{+}/Ca^{2+} exchanger has been implicated in the induction of phase 3 type EADs [103].

1.7.1.1.1. **EADs and ventricular muscle**

This type of repolarization abnormality has been mostly reported for Purkinje cells. This may be because they are most commonly used for intracellular electrophysiologic experiments, mainly because they are easy preparations to work with. However, there have been a few reports of EADs in VM, the majority of these studies were performed on sliced and dissociated cells from myocardial preparations. In both experimental systems, cells are less well coupled than in the whole heart and may explain the EADs seen in these conditions [107,108].

A group of ventricular cells located in subepicardial layers has been associated with an increased sensitivity to slow rate and class III antiarrhythmic drugs when compared to epicardial and endocardial muscle layers: "M cells"[109]. Their sensitivity is said to be equivalent to that of Purkinje fibers. M cells have been identified in dog, guinea pig [98], and human [110] from ventricular slice preparations. However M-cells in guinea pig heart [98] have not been associated

with an increased sensitivity to class III drugs, an important defining characteristic of this cell type.

Existence of an M-cell layer *in vivo* has been recently debated; some investigators observed a slight M-cell layer [111] and others have failed to observe any, that is, both under control condition and in the presence of a compound with a class III effect [112,113]. These authors suggested that the M-cell layer observed *in vitro* may result from cellular electrical uncoupling [114].

1.7.1.1.2. **Concentration of class III antiarrhythmic drugs and EADs**

In studies in which EADs have been observed the concentration of drug was always very high. The concentration of drug in most of these studies would have mostly blocked I_{Kr}. For example, a rabbit model showing TdP *in vivo* and EAD in PF *in vitro* was exposed to drug concentrations (almokalant or cisapride) that blocked all of I_{Kr} tail current present in ventricular muscle cells [30,49,52,53,115]. EADs and triggered activity have also been observed with high concentrations erythromycin (50-100 μg/ml) in M-cell layer [116]. Similarly, these high concentrations of erythromycin blocked I_{Kr} completely. Even at these very high concentrations, EAD-dependent triggered activity was rarely observed in arterially perfused preparations. This may be explained by the blockade of other currents. It is important to note that the clinical serum levels of erythromycin associated with TdP are much lower (at most 30 μg/ml).

These extreme conditions (very high drug concentration, and slow heart rates) may have masked other phenomena that could have occurred at more clinically relevant conditions (lower drug concentration and faster heart rates). Does dispersion of repolarization play a more important role than do EADs at lower drug concentrations?

1.7.1.1.3. **EAD: mode of abolishment**

The ionic mechanism of EADs was studied by many investigators under different conditions. In summary, most interventions which abolish EAD's either lead to a decrease of a depolarizing current or an increase of a repolarizing current. In most experimental preparations the following compounds block an inward current causing abolishment of EADs: Ca^{2+} channel blockers (e.g., nisoldepine, nitrandipine) [40,87,95,101,117-119], magnesium [9,40,51,120-122] (review [123]), Na^{+} channel blockers [51,115,122,124] altering Ca^{2+} signal; IP3R antagonist (ryanodine) [95], other interventions that increase a repolarizing current; exposure to a higher external K^{+} concentration [40,51], K^{+} channel openers [125,126]. Also increase of pacing frequency has been effective in abolishing this phenomenon [122,124,127] (table 2).

Some other interventions reported here are controversial; for example, the inhibition of EADs by altering internal Ca^{2+} signal by blocking the ryanodine receptors [95,129]. Differences observed here may have been caused by a species, or methodological difference between the different studies.

In general all these interventions lead to a decrease of APD. Since these interventions are associated with a decrease in APD it is very hard to know if the

intervention is targeted to the current responsible for the EAD or that changing the ionic current balance impacts on the EAD formation. Only one intervention, Ca^{2+} channel blockers, have been shown, by Nattel et al. [119], to eliminate the EAD and not alter the APD. It suggested that Ca^{2+} channel blockers exert their action by blocking reactivated L-type Ca^{2+} current. Some investigators claim that interventions that lead to arrhythmia, for instance; toxins which alter Na^{+} inactivation kinetics (Anthopleurin A), will be abolished only by drugs that block Na^{+} channel [124]. This is not what is usually observed. There is a need to refine intervention conditions in order to reach clear conclusions.

Table 2.

Interventions that have been shown to abolish EADs

1-Increasing pacing frequency [122,124,127]

2- Ca^{2+} channel blockers (e.g., nisoldepine) [40,87,95,101,117-119]

3-Magnesium [9,40,51,120-122] *(review* [123]*)*

4- Na^{+} channel blockers [51,115,122,124]

5-IP3R antagonist (e.g., ryanodine) [95*]

6-Higher external K^{+} concentration [40,51]

7-K^{+} channel openers (e.g., pinacidil) [125,126]

**controversial*

1.7.1.1.4. **Mechanisms of action of magnesium**

Magnesium bolus injection is an effective intervention to prevent drug-induced TdP arrhythmias. The effect of magnesium to abolish EADs is a very complex one. There are many proposed modes of action to explain the antiarrhythmic efficacy of magnesium. It is more and more recognized that the intracellular source of magnesium is important. The blockade of L-type channel is the mode of action that is the most widely accepted [130] (review [131]). Another mechanism has been proposed by Zipes et al.[9] in which increased extracellular Mg^{2+} concentration would eventually lead to an increase in intracellular Mg^{2+} concentration and that this would activate the Na^{+}/K^{+} pump and increase intracellular K^{+} concentration [132]. This effect may increase a K^{+} conductance and lead to a faster repolarization of the APs and may then eliminate the EAD(s). Furthermore, magnesium may act like ryanodine on sarcoplasmic ryanodine

receptor and block these Ca^{2+} release channels. It was demonstrated that cytosolic magnesium can act to modulate the open probability of ryanodine receptor and attenuate responses to increases in cytosolic Ca^{2+} ions. Responses are reduced in amplitude and attenuation time constant is decreased which would effectively decrease Ca^{2+} ions released from the sarcoplasmic reticulum by this pathway [133]. A last mechanism suggested is that the effect of Mg^{2+} may be on ventricular muscle cells' refractory period. It has been documented that an increase in extracellular Mg^{2+} increases APD in ventricular muscle cells and also increases their relative refractory period beyond their AP's full repolarization [134]. Overall, the antiarrhythmic effect of magnesium may be the result of the combination of all the previously mentioned mechanisms.

1.7.1.2. **DAD mechanism**

The mechanism of DAD is much less controversial. DADs are secondary membrane depolarizations which arise after the full repolarization of the AP. DADs, as opposed to EADs, are observed at fast heart rates, and usually when the heart rate has just increased (review [135]). When they are generated by cardiac glycosides or catecholamines, DADs have been attributed to be the result of an intracellular Ca^{2+} overload. Cardiac glycosides block the Na^+-K^+ pump which increases the accumulation of internal Na^+. The Na^+ is extruded from the cell by the Na^+/Ca^{2+} exchanger. This leads to the entry of Ca^{2+} ions inside the cell, subsequently to the spontaneous release of Ca^{2+} from the endoplasmic reticulum and the activation of a transient inward current (I_{ti}) leading to DADs

Two possible mechanisms have been proposed to explain the genesis of I_{ti}. Either it is caused by the Na^+/Ca^{2+} exchanger's intrusion of Na^+ into the cells or Ca^{2+}-mediated activation of a membrane conductance. For example, a Ca^{2+} activated Cl^- has been demonstrated by some investigators [136]. It is not unlikely that they are the components of I_{ti}.

1.7.1.2.1. **EADs in relations to DAD**

Some theories tend to unify EADs and DADs [117]. The different charge carriers may just depend on the level of membrane repolarization. The appearance of DADs may facilitate the appearance of EADs. In some experimental conditions EADs and DADs seem to be closely related and have some association with the intracellular Ca^{2+} status of cells. When induced by isoproterenol [137] or cesium [95], there exist conflicting results which suggest that they, EADs and DADs, may or may not be related [93]. Intracellular Ca^{2+} overload may not be important in cesium induced EAD generation due to species differences.

Although EADs and DADs may be related initially by the intracellular Ca^{2+} concentration, different charge carriers may be responsible for their ultimate manifestation. For example, some investigators have found distinct Ca^{2+} transients during EADs and DADs when induced by isoproterenol or K^+ free Tyrode's solution [93,99]. They found that EADs lead to a synchronous Ca^{2+} signal throughout the cell which is very similar to the Ca^{2+} signal of a stimulated AP. On the other hand, DADs appear like focal Ca^{2+} transients propagating like a wave at a rate of 100μm/sec [93]. These authors believe that DADs result from intracellular

Ca^{2+} release from endoplasmic reticulum but that EADs result from Ca^{2+} entry through L-type Ca^{2+} channel, which would then lead to Ca^{2+} release from the sarcoplasmic reticulum [93].

1.7.1.3. **Passive membrane properties and electrotonic modulations**

Excitable cells may respond to the electrical influence of surrounding cells, electrotonic interactions. "A true electrotonic potential is a response whose characteristics are dictated by passive cable properties of the preparation and one in which active membrane properties play no role" [138].

Could electrotonic effect of surrounding cells be large enough to activate active membrane properties and/or modulate active membrane properties? The interactions may lead to similar "EAD and/or DAD like deflections". It is conceivable that under different experimental conditions different mechanism may be responsible for genesis of EADs and DAD like deflections.

1.8. **Reentry mechanism**

The second mechanism for arrhythmia formation is abnormal impulse conduction, reentry. Reentry has been investigated for many decades. It was first recognized by Mines [139] here at McGill University that an impulse could, under the appropriate conditions, reactivate a previously activated circuit. This could be maintained for many cycles. The understanding of this mechanism has been investigated in many different types of experimental system. The purpose of this section is to give the reader the working knowledge to understand the fundamental mechanism of reentry, and not to do an extensive review of the

phenomenon. It follows that the second important mechanism of arrhythmia formation is abnormal impulse conduction. The following elements are important to initiate a reentry mechanism: the substrate, trigger, facilitatory factors.

The classic reentrant substrate is a circuit where there is an area of slow conduction, giving time for tissue ahead of the wave front to electrically recover, and one area of unidirectional conduction block, to give a circulating orientation to the wave front. The sites of slow conduction and the area of unidirectional conduction block are usually at the same sites.

The presence of a substrate does not signify that there will be an arrhythmia; the presence of a trigger is critical. Very often this trigger is an ectopic beat which perturbs the normal electrical activation or unmasks slow conduction and unidirectional block area. Ectopic beats may arise at variable times in the diastolic interval thereby effectively scanning the pathways and eventually may trigger reentry ("window effect") (review [140]).

If substrate and trigger were enough to induce a reentry than electrically programmed electrical stimulation would be very reliable to induce reentrant type of arrhythmia in patients and therefore assess the potential arrhythmic risk of patients. Other elements are know as facilitators such as autonomic tone, electrolyte balance, metabolic activity, slow stimulation rate. Note that facilitators may be either substrate or trigger. There is no clear distinction between previously mentioned elements. These may create the substrate for the trigger and in some arrhythmias they can create the trigger.

1.8.1. **Short-long-short activation sequence**

TdP is usually initiated by a specific activation sequence, a sequence of a short followed by a long and another short coupling interval (short-long-short activation sequence). What is so special about this activation pattern? Is this activation sequence only characteristic of TdP?

This sequence of activation is very frequently observed before episodes of ventricular tachycardias. Electrical programmed stimulation utilizing this sequence facilitates induction of ventricular tachycardia [141] and macroreentry within the His-Purkinje system [142]. It has also been show that abrupt changes in cycle length results in differential changes in refractoriness between Purkinje and muscle fibers that could facilitate initiation of reentry [143].

1.9. **Torsade de pointes - History and definition**

The term torsade de pointes was coined by a French cardiologist named François Dessertenne in 1966 [144]. "What does this term mean *torsade* : twisted fringe, twist, coil, thick bullion (of epaulet); *pointes*: point (of pin, sword, etc.) tip, head (of arrow, lance)." Similar electrocardiographic features were first noted more then 40 years before [145,146].

Its importance was only recognized after Schwartz et al. reported a similar phenomena which they named "transient ventricular fibrillation"[147,148]. TdP has been described by a variety of descriptive terms "paroxysmal ventricular fibrillation"[149], "transient recurrent ventricular fibrillation"[150], "transient ventricular fibrillation"[147,148], "cardiac ballet" [151], "quinidine syncope" [5],

polymorphic ventricular tachycardia with QT interval prolongation, atypical ventricular tachycardia, ectopic ventricular tachycardia, multidirectional ventricular tachycardia, ventricular tachycardia-flutter, and ventricular fibrillo-flutter [152]. Since TdP can be associated with long runs of uniform QRS complexes and also conventional ventricular tachycardia can be bi-directional, criteria other than morphoiogical needed to be used [153] (review [154]).

Ever since the first American report which associated TdP with an arrhythmia that degenerates to ventricular fibrillation, we could clearly recognize that authors would have a problem identifying this arrhythmia. These reports described more the undulatory phase of ventricular fibrillation rather than that of TdP [155]. From then on the definition of TdP became more strict. Questions then arose as to whether TdP can be classified as a ventricular tachycardia or whether it is the earliest phase of ventricular fibrillation into which it often degenerates.

The definition that has become widely accepted originated from Dessertenne in an 1970 [156] paper and has been subsequently slightly modified by Weissenberger et al., [157] and Carlsson et al.[81] . A typical TdP has to include the following five characteristics: 1) it must be observed in context of prolonged QT interval, 2) it must occur spontaneously (not stimulated), 3) in the longer TdP, at least one of the ECG leads must show QRS complex that clearly undulates around the isoelectric line. 4) QRS complexes must be polymorphic, 5) the ventricular tachycardia must be composed of at least five consecutive beats, and 6) the tachycardia must be self-terminating. The twisting of the QRS complex may not be present in the shorter TdP [158] (table 3).

Table 3

Definition of TdP

-Long QT interval

-Spontaneous occurrence

-Polymorphous VT of more than 5 beats

-Self-terminating

1.9.1. **Models of Drug-Induced TdP arrhythmias**

Ever since TdP was identified by Dessertenne in 1966 [144], a number of models have been developed in order to study the mechanism of this arrhythmia. Early models were mainly concerned with mimicking the electrocardiographic features of TdP. Models were developed with toxic compounds which have been shown to lead to EAD in PF *in vitro* (cesium, and Anthopleurin A). Subsequently, attention was paid to conditions which are usually associated with the arrhythmia clinically. TdP is usually observed in the presence of a drug which prolongs the repolarization interval and to other facilitatory factors: hypokalemia, hypomagnesemia, and slow heart rates (table 4). These facilitatory factors were therefore introduced into these animal models.

Most early studies were more interested in reproducing the electrographic morphological appearance. This is achieved by a variety of interventions; by either stimulating at slighly varying frequencies the epicardium at two difference sites [159,160] or by applying locally aconitine at multiple epicardial sites [161].

Aconitine is a compound which delays inactivation of the fast Na^+ channel. Both of these interventions lead to electrocardiographic features very similar to TdP, and suggested that TdP is the result of two competing foci, as initially proposed by Dessertenne in 1966 [144]. The result from these studies did not tell us how the arrhythmia was initiated in patients.

Subsequently *in vivo* experiments were performed with compounds such as cesium [7,9] and Anthopleurin A [162] that had been shown to induce EADs in *in vitro* preparations. Cesium was often combined with other compounds which had been shown to prolong APD. Anthopleurin A delays the inactivation of the fast Na^+ channel. In both these models, electrocardiographic characteristics of TdP in the setting of prolonged QT intervals were evident, but the incidence of TdP was low. Based on *in vitro* investigations, it was suggested that the main effect of cesium and anthopleurin A induced TdP model was that EADs induced in PF were important in the generation of these arrhythmias *in vivo*. The major limitation of this model is that TdP was seldom observed, prolonged exposure with cesium is associated with hyperkalemia (hypertension) and the arrhythmia was sometimes resistant to overdrive suppression [163]. The major drawback of these models was that both these compounds used were not very selective; they can either block channels of heart and neurons. These models showed that delayed repolarization by either means can lead to TdP arrhythmias. They suggested that this was why TdP was seen with therapeutically used drugs.

In later models, investigators took advantage of the clinical reports which suggested that many facilitators were present when drug induced-TdP was

observed, therefore these facilitators were incorporated in the animal models of TdP. A very important characteristic of these models is the combination of clinically used class III drugs at a high concentration with chronic AV block (slow heart rate), hypokalemia induced by diuretics, and consciousness. In this model they were able to induce a polymorphic ventricular tachycardia which resembled that of TdP [157]. Interestingly the incidence of TdP was much higher when the animals were conscious than when they were anesthetized suggesting that an intact sympathetic system was needed for the induction of TdP. This model showed that TdP could be induced with class III antiarrhythmic drugs in animal models, and that many facilitatory factors were needed. Therefore, it was suggested that TdP was part of a syndrome and not just a specific arrhythmia [164].

Another model of drug-induced polymorphic VT is the *in vivo* rabbit [81]. Carlsson et al. suggested that a polymorphic tachycardia was observed in the presence of a prominent QT interval prolongation, and facilitatory factors. They similarly showed that TdP was more readily inducible in the conscious animal than the anesthetized one. Contrary to the dog model hypokalemia was not required, nor was atrioventricular block, however α-adrenergic stimulation was required. Akin to the previous models, they suggested that EAD-dependent triggered activity and dispersion of ventricular repolarization could be important for the initiation of TdP arrhythmia. They showed that a fast drug infusion rate was associated with a higher incidence of TdP than a slower one [49]. Interestingly sotalol failed to induce TdP in this model [165,166].

The major drawbacks of such models stem from the fact that this is an *in vivo* preparation. The heart's surface cannot be easily investigated with recording probes (contact monophasic action potential probes (MAP)). The animal needs to be maintained at basal physiological state. For example, the heart rate needs to be fast enough to maintain an adequate cardiac output. The plasma concentration of the drug needs to be measured. This particular preparation can go into heart failure and die before the experiment can even take place. Also another major limitation with one of these models is that TdP was sometimes observed under basal conditions [167]. Finally the cost of these preparations is very high.

From the use of *in vivo* models many questions about the mechanism of TdP remains unanswered. What is the importance of EAD-dependent triggered activity in the induction of TdP in the whole heart? Is the mechanism of initiation and perpetuation different or the same? Why does TdP self-terminate? What are the predisposing factors to TdP? Why are such extreme conditions (drug concentration, profound bradycardia, and facilitatory factors) needed in these animal models? What are the contributions of individual components in drug-induced TdP? What is the contribution of the drug in the induction of the arrhythmia? We could only answer these questions in a model in which TdP could be readily and frequently inducible.

Table 4

Causes and Conditions Leading to TdP

Congenital long QT syndrome
- Jervell and Lange-Nielsen syndrome
- Romano-Ward syndrome
- Sporadic, non-familial long QT syndrome

Drugs

Antiarrhythmic agents that prolong repolarization:
- class IA (quinidine, disopyremidine, procainamide) class III (d,l-sotalol, d-sotalol, amiodarone, *N*-acetylprocainamide, bretylium, dofetilide, semitelide, almokalant), others (encainide, ajmaline, aprindine, propafenone)

Cisapride
Cevoflurane
Prenylamine
Bepridil
Lidoflazine
Terodiline
Probucol
Tricyclic and tetracyclic antidepressant (e.g., amitriptyline, imipramine, doxepin, maprotiline)
Phenothiazines (thioridazine, chlorpromazine)
Haloperidol
Chloral hydrate
Antihistamine (astemizole, terfenadine)
Antibiotics (erythromycin, trimethoprim-sulfamethoxazole)
Chemotherapeutics (pentamidine)
Serotonin antagonists (ketanserin, zimeldine)
Arsenic poisoning, poisoning with organophosphorous insecticides

Electrolyte abnormalities
- Hypokalemia
- Hypomagnesemia

Bradyarrhythmia
- Sinus bradycardia
- Atrioventricular block

Ionic contrast media

Altered nutritional states
- Anorexia nervosa
- Diets, starvation

Cerebrovascular diseases
- Intracranial and subarachnoid hemorrhage, stroke, intracranial trauma

Hypothyroidism

Modified from reference (review [38])

1.10. Congenital long QT syndrome and torsade de pointes

Before it was suggested that prolonging the APD as an effective antiarrhythmic therapy, it was well known that some patients congenitally acquired excessive QT interval prolongation which was associated with sudden cardiac death and TdP [6]. There are two congenital long QT syndromes: the Jervell and Lange-Nielsen syndrome is autosomal recessive and associated with deafness [6], and the Romano-Ward syndrome is autosomal dominant and is not associated with deafness. In some cases it may present as *"forme fruste"* which only becomes apparent after exercise (review [154]).

Since 1995, great advances have occurred at the genetic level to link the Romano-Ward syndrome with specific channel mutations. Many genes have been linked to this syndrome. The candidate gene approach was used to identify mutations. At least five chromosomal defects have been identified to date: LQT1 through LQT5. LQT1 is on chromosome 11 (11p15.5), LQT2 is on chromosome 7 (7q35-36), LQT3 is on chromosome 3 (3p21-24), and LQT4 is on chromosome 4 (4q25-27). (review [154]). The chromosomal location of LQT5 has not yet been identified.

Some families are still excluded from linkage at all five regions, which suggests that more disease-causing genes are yet to be discovered. For example, KvLQT1 on chromosome 11, HERG on chromosome 7, SCN5A on chromosome 3, and KCNE1 have been linked to LQT1 [168], LQT2, LQT3 and LQT5 [169],

respectively (reviews [154,170]). KVLQT1 is believed to encode for a K^+ channel when combined with I_{sK} protein (minK gene on chromosome 21) [25]. Mutations in either protein subunits (IsK or KVLQT1) have been shown to lead to altered channel function [168,171].

Many mutations (at least 35) have been found in the *m*-RNA of these genes which when expressed in xenopus oocytes lead to either compromised or no channel function.

In KvLQT1 gene, point mutations in the S2-S3 loop and pore region yield no channel activity whereas a point mutation in the S5 transmembrane domain yields a channel with a reduced macrocospic current when expressed in *Xenopus laevis* oocytes [168]. Frameshift deletion-insertion events in the C-terminus have been observed in the Jervell and Lange-Nielsen long QT syndrome [172].

Seven mutations have been identified in the HERG gene. Six are missense mutations and one is an intragenic deletion. From studies of its kinetics and pharmacology it is believed that HERG encodes for the native rapid component of the delayed rectifier current [22,27] (review [173-175]).

Three mutations in SCN5A, a Na^+ channel, have been associated with LQT3 family. When their *m*-RNA is expressed in xenopus oocytes there is the expression of Na^+ channels that have different inactivation properties when compared to non-mutated channel. Two of the mutations are missense mutations and one is an intragenic deletion. This intragenic deletion is located close to domain III-IV linker that is believed to be important for channel inactivation.

Overall, these mutations in the genes of these channels - KvLQT1, minK, SCN5A, and HERG - would result in a net positive charge moving into cells in the course of a normal AP and, if unopposed, would lead to prolonged APD. This effect could lead to an increase in QT interval if enough cells were affected by this mutation. Some cells may be affected more by these mutations and this would lead to an increase in dispersion of repolarization in the heart. This opens the possibility that patients with the congenital long QT syndrome would be more affected by the use of drugs with selective class III actions. This would obviously depend on the type of mutations and site of action of these drugs.

Some cases of Jervell and Lange-Nielsen (JLN) and Romano Ward (RW) long QT syndrome are related at the molecular level. Their cardiac manifestation are caused by different mutations in KvLQT1 gene. Note that JLN syndrome is associated with deafness (autosomal recessive). KVLQT1 and minK have both been shown to be expressed in the inner ear [172,176]. They are thought to be involved in the control of endolymph homeostasis which is essential for normal hearing, and their mutation may explain the deafness associated with this syndrome [172]. It would not be surprising for the JLN syndrome to be shown to be multigenic similar to RW long QT syndrome.

1.11. Thesis objectives

Since the Cardiac Arrhythmia Suppression Trials demonstrating increased mortality with class I antiarrhythmic drugs in patients post myocardial infarction, attention has focused on drugs which selectively prolong repolarization without slowing conduction, in particular, the selective I_{Kr} blockers. The single greatest liability for future development of these drugs is the occasional and unpredictable development of exaggerated QT prolongation and torsade de pointes arrhythmias. Their proarrhythmic potential will, of course, depend upon the contribution of I_{Kr} to repolarization in the tissues and species being considered.

For many of the recently developed class III antiarrhythmic drugs, it has been shown that certain structures within the heart, such as Purkinje fibers or the midmyocardial (M) ventricular cells, respond with a much more marked prolongation of the action potential duration than other ventricular muscle cells, thus causing increased dispersion of repolarization. However, no clear relation between the proarrhythmic response seen *in vivo* and some critical prolongation of repolarization in either Purkinje fibers or M cells has yet been established. There is also wide agreement among investigators that drug induced TdP arrhythmias are somehow related to triggered activity brought about by EADs. However, whether EADs and triggered activity originating either in Purkinje

fibers or M cells are responsible for initiating TdP and/or maintaining its mechanism is still an unsettled question.

Our general hypothesis is that the beneficial antiarrhythmic effects of these drugs resides in their ability to prolong ventricular muscle repolarization in a homogeneous way while their proarrhythmic effect resides in an excessive prolongation of repolarization and/or development of EADs and triggered activity in the specialized ventricular conducting system on the endocardial surface of the ventricle under certain specific conditions.

To test this hypothesis, we chose the rabbit heart for several reasons, viz.; 1. Repolarization in the rabbit ventricle is predominantly due to the I_{Kr} current so these hearts may be more susceptible to the drugs than another species; it allowed us to use a multilevel approach in the same species since the mechanism of the arrhythmia could be studied, *in vitro, in situ, in vivo* as well as at the single cell level since procedures for obtaining isolated myocytes from the rabbit have been established, and 3. the rabbit heart has a preponderance of α receptors which may be involved in TdP. We chose *d*-sotalol as the prototypical drug as it has been recognized clinically as an effective antiarrhythmic drug and was initially proposed to be less arrhythmogenic and less prone to induce TdP arrhythmias than class 1A drugs but has recently been shown to increase mortality in postinfarct patients. This increased mortality was attributed to TdP arrhythmias. Perhaps such proarrhythmic effects could be prevented if the mechanism of this arrhythmia was known and the conditions leading to its induction were avoided.

Thus, the first objective of this thesis was to determine the conditions under which *d*-sotalol might prolong repolarization and induce EADs and triggered activity in rabbit ventricular endocardial preparations under *in vitro* conditions in order to determine its concentration and frequency dependent effects. Intracellular action potentials were used to measure the effects of *d*-sotalol on repolarization. We showed in this first study that d-sotalol, at high concentrations, selectively lengthened repolarization in Purkinje fibers versus ventricular muscle as a function of cycle length eventually leading to EADs and triggered activity selectively in Purkinje fibers which propagated to ventricular muscle as coupled action potentials. The generation of coupled rhythms was associated with critical disparities in repolarization on the endocardial surface.

The second objective was to apply this information to the isolated heart to determine if conditions which lead to triggered activity *in vitro* might result in ventricular arrhythmias *in situ*. In order to monitor action potential duration in specialized conducting cells on the endocardial surface compared with ventricular muscle we used monophasic action potential (MAP) recordings. The intent was to develop an isolated heart model of TdP arrhythmias which was predictable and reproducible and easily amenable to analysis in order that its mechanism of initiation and maintenance could be determined. We succeeded in developing a unique model in which we were able to define the entire spectrum of arrhythmias

leading up to TdP arrhythmias and to characterize the conditions responsible for its initiation using MAP recordings.

Having an ideal model to study TdP arrhythmias, our third objective was to characterize the arrhythmia more fully by investigating the mechanism of all beats of each TdP using a combination of epicardial activation mapping techniques together with unipolar recordings from the endocardial surface. Using these techniques we were able to show that the initiating beat of every TdP arrhythmia uniformly originated on the endocardial surface of the ventricles and was due to focal activity, thus confirming our previous data with MAP recordings in situ and microelectrodes in vitro that the mechanism of TdP was triggered activity originating in the specialized ventricular conducting system. The remaining beats of the TdP were either totally reentrant, totally focal or a combination of the two mechanisms.

Our fourth objective was not only to characterize more fully the entire sequence of arrhythmias leading up to TdP, as well as TdP itself, but to study the mechanism under conditions more clinically relevant in terms of drug concentrations and cycle lengths. Under more clinically relevant conditions, a typical sequence of arrhythmias occurred consisting of singlets, couplets, triplets, quadruplets and eventually TdP. This study combined epicardial activation mapping techniques together with MAP recordings from strategic sites on the epicardial surface. This study clearly showed that TdP was not a separate entity

but was part of a continuum in which the mechanism of the first coupled beat from singlets to TdP was focal originating from the endocardial surface, whereas all other beats were due to reentry. The results clearly showed the association of marked disparities in activation recovery intervals (an index of repolarization in the whole heart) with the initiation of TdP. Termination of the mechanism was due to elimination of this disparity.

The last objective of the thesis was to study which interventions would likely prevent initiation of TdP based on its mechanism of initiation, perpetuation and termination. Only a few preliminary results have been appended.

The above studies have greatly enhanced our understanding of the mechanism of TdP arrhythmias induced by class III antiarrhythmic drugs and provide a unique model which can now be used to assess the proarrhythmic potential of novel antiarrhythmic agents or of non cardiac drugs such as antihistaminic agents, antibacterials, and serotonin blocking drugs which have been associated with long QT intervals and TdP. Future studies will involve assessing the role of autonomic mediators in the initiation and perpetuation of this arrhythmia.

1.12. **References**

1. Singh BN: Do antiarrhythmic drugs work? Some reflections on the implications of the Cardiac Arrhythmia Suppression Trial. [Review]. *Clinical Cardiology* 1990;13:725-728

2. Singh BN: Controlling cardiac arrhythmias: an overview with a historical perspective. [Review] *American Journal of Cardiology* 1997;80:4G-15G

3. Rosen MR: Consequences of the Sicilian Gambit. *European Heart Journal* 1995;16 Suppl G:32-36

4. Vaughan Williams EM: Anti-dysrhythmic drugs - their mode of action, in Nayler WG (ed): *Contration and relaxation of the myocardium.* London, Academic Press, 1975, pp 293-323

5. Selzer A, Wray HW: Quinidine syncope: paroxysmal ventricular fibrillation occuring during treatment of chronic atrial arrhythmias. *Circulation* 1964;30:17-26

6. Jervell A, Lang-Nielsen L: Congenital deaf-mutism, functional heart disease with the prolongation of the QT interval, and sudden death. *American Heart Journal* 1957;54:59-68

7. Kaseda S, Gilmour RF, Jr., Zipes DP: Depressant effect of magnesium on early afterdepolarizations and triggered activity induced by cesium, quinidine, and 4-aminopyridine in canine cardiac Purkinje fibers. *American Heart Journal* 1989;118:458-466

8. Carmeliet E: Electrophysiologic and voltage clamp analysis of the effects of sotalol on isolated cardiac muscle and Purkinje fibers. *Journal of Pharmacology & Experimental Therapeutics* 1985;232:817-825

9. Bailie DS, Inoue H, Kaseda S, Ben-David J, Zipes DP: Magnesium suppression of early afterdepolarizations and ventricular tachyarrhythmias induced by cesium in dogs. *Circulation* 1988;77:1395-1402

10. el-Sherif N, Zeiler RH, Craelius W, Gough WB, Henkin R: QTU prolongation and polymorphic ventricular tachyarrhythmias due to bradycardia-dependent early afterdepolarizations. Afterdepolarizations and ventricular arrhythmias. *Circulation Research* 1988;63:286-305

11. Rees S, Curtis MJ: Which cardiac potassium channel subtype is the preferable target for suppression of ventricular arrhythmias [Review]. *Pharmacology & Therapeutics* 1996;69:199-217

12. Colatsky TJ: Antiarrhythmic drugs: where are we going? *Pharmaceutical news* 1995;2:17-23

13. Lynch JJ, Coskey LA, Montgomery DG, Lucchesi BR: Prevention of ventricular fibrillation by dextrorotatory sotalol in a conscious canine model of sudden coronary death. *American Heart Journal* 1985;109:949-958

14. Spinelli W, Parsons RW, Colatsky TJ: Effects of WAY-123,398, a new class III antiarrhythmic agent, on cardiac refractoriness and ventricular fibrillation threshold in anesthetized dogs: a comparison with UK-68798, E-4031, and dl-sotalol. *Journal of Cardiovascular Pharmacology* 1992;20:913-922

15. Colatsky TJ, Follmer CH, Starmer CF: Channel specificity in antiarrhythmic drug action. Mechanism of potassium channel block and its role in suppressing and aggravating cardiac arrhythmias. [Review] *Circulation* 1990;82:2235-2242

16. Advani SV, Singh BN: Pharmacodynamic, pharmacokinetic and antiarrhythmic properties of d-sotalol, the dextro-isomer of sotalol. [Review]. *Drugs* 1995;49:664-679

17. Yang T, Snyders DJ, Roden DM: Rapid inactivation determines the rectification and [K+]o dependence of the rapid component of the delayed rectifier K+ current in cardiac cells. *Circulation Research* 1997;80:782-789

18. Spector PS, Curran ME, Zou A, Keating MT, Sanguinetti MC: Fast inactivation causes rectification of the IKr channel. *Journal of General Physiology* 1996;107:611-619

19. Sanguinetti MC, Jurkiewicz NK: Two components of cardiac delayed rectifier K+ current. Differential sensitivity to block by class III antiarrhythmic agents. *Journal of General Physiology* 1990;96:195-215

20. Carmeliet E: Voltage- and time-dependent block of the delayed K+ current in cardiac myocytes by dofetilide. *Journal of Pharmacology & Experimental Therapeutics* 1992;262:809-817

21. Shibasaki T: Conductance and kinetics of delayed rectifier potassium channels in nodal cells of the rabbit heart. *Journal of Physiology* 1987;387:227-250

22. Sanguinetti MC, Jiang C, Curran ME, Keating MT: A mechanistic link between an inherited and an acquired cardiac arrhythmia: HERG encodes the IKr potassium channel. *Cell* 1995;81:299-307

23. Yang T, Wathen MS, Felipe A, Tamkun MM, Snyders DJ, Roden DM: K+ currents and K+ channel mRNA in cultured atrial cardiac myocytes (AT-1 cells). *Circulation Research* 1994;75:870-878

24. Lees-Miller JP, Kondo C, Wang L, Duff HJ: Electrophysiological characterization of an alternatively processed ERG K+ channel in mouse and human hearts. *Circulation Research* 1997;81:719-726

25. Sanguinetti MC, Curran ME, Zou A, Shen J, Spector PS, Atkinson DL, Keating MT: Coassembly of K(V)LQT1 and minK (IsK) proteins to form cardiac I(Ks) potassium channel [see comments]. *Nature* 1996;384:80-83

26. Carmeliet E: Use-dependent block of the delayed K+ current in rabbit ventricular myocytes. *Cardiovascular Drugs & Therapy* 1993;7 Suppl 3:599-604

27. Spector PS, Curran ME, Keating MT, Sanguinetti MC: Class III antiarrhythmic drugs block HERG, a human cardiac delayed rectifier K+ channel. Open-channel block by methanesulfonanilides. *Circulation Research* 1996;78:499-503

28. Jurkiewicz NK, Sanguinetti MC: Rate-dependent prolongation of cardiac action potentials by a methanesulfonanilide class III antiarrhythmic agent. Specific block of rapidly activating delayed rectifier K+ current by dofetilide. *Circulation Research* 1993;72:75-83

29. Krafte DS, Volberg WA: Voltage dependence of cardiac delayed rectifier block by methanesulfonamide class III antiarrhythmic agents. *Journal of Cardiovascular Pharmacology* 1994;23:37-41

30. Carmeliet E: Use-dependent block and use-dependent unblock of the delayed rectifier K+ current by almokalant in rabbit ventricular myocytes. *Circulation Research* 1993;73:857-868

31. Fiset C, Feng ZP, Wang L, Sheldon RS, Duff HJ: [3H]dofetilide binding: biological models that manifest solely the high or the low affinity binding site. *Journal of Molecular & Cellular Cardiology* 1996;28:1085-1096

32. Duff HJ, Feng ZP, Fiset C, Wang L, Lees-Miller J, Sheldon RS: [3H]dofetilide binding to cardiac myocytes: modulation by extracellular potassium. *Journal of Molecular & Cellular Cardiology* 1997;29:183-191

33. Yang T, Roden DM: Extracellular potassium modulation of drug block of IKr. Implications for torsade de pointes and reverse use-dependence. *Circulation* 1996;93:407-411

34. Ficker E, Jotolinek W, Kiehn J, Baumann A, Juelich F, Brown AM: Molecular determinant of dofetilide binding to HERG. *Biophysical Journal* 1997;72:A141

35. Ficker E, Jarolimek W, Kiehn J, Baumann A, Brown AM: Molecular determinants of dofetilide block of HERG K+ channels. *Circulation Research* 1998;82:386-395

36. Bjornstad H, Tande PM, Refsum H: Class III antiarrhythmic action of d-sotalol during hypothermia. *American Heart Journal* 1991;121:1429-1436

37. Gintant GA: Two components of delayed rectifier current in canine atrium and ventricle. Does IKs play a role in the reverse rate dependence of class III agents? *Circulation Research* 1996;78:26-37

38. Antzelevitch C, Sicouri S: Clinical relevance of cardiac arrhythmias generated by afterdepolarizations. Role of M cells in the generation of U waves, triggered activity and torsade de pointes. [Review]. *Journal of the American College of Cardiology* 1994;23:259-277

39. Nakaya H, Tohse N, Takeda Y, Kanno M: Effects of MS-551, a new class III antiarrhythmic drug, on action potential and membrane currents in rabbit ventricular myocytes. *British Journal of Pharmacology* 1993;109:157-163

40. Adamantidis MM, Kerram P, Caron JF, Dupuis BA: Droperidol exerts dual effects on repolarization and induces early afterdepolarizations and triggered activity in rabbit Purkinje fibers. *Journal of Pharmacology & Experimental Therapeutics* 1993;266:884-893

41. Okada Y, Ogawa S, Sadanaga T, Mitamura H: Assessment of reverse use-dependent blocking actions of class III antiarrhythmic drugs by 24-hour Holter electrocardiography. *Journal of the American College of Cardiology* 1996;27:84-89

42. Shimizu W, Kurita T, Suyama K, Aihara N, Kamakura S, Shimomura K: Reverse use dependence of human ventricular repolarization by chronic oral sotalol in monophasic action potential recordings. *American Journal of Cardiology* 1996;77:1004-1008

43. Tuininga YS, De Langen CD, Crijns HJ, Wiesfeld AC, Mook PH, Bel KJ, Lie KI: Electrophysiological, rate dependent, and autonomic effects of the class III antiarrhythmic almokalant after myocardial infarction in the pig. *Pacing & Clinical Electrophysiology* 1996;19:802-810

44. Wiesfeld AC, De Langen CD, Crijns HJ, Bel KJ, Hillege HL, Wesseling, H, Lie KI: Rate-dependent effects of the class III antiarrhythmic drug almokalant on refractoriness in the pig. *Journal of Cardiovascular Pharmacology* 1996;27:594-600

45. Surawicz B: Role of potassium channels in cycle length dependent regulation of action potential duration in mammalian cardiac Purkinje and ventricular muscle fibres. [Review]. *Cardiovascular Research* 1992;26:1021-1029

46. Groh JW, Gibson BA, Maylie JGM: Comparason of the rate-dependent properties of the class III antiarrhythmic agents azimalide (NE-10064) and E-4031: Consideration on the mechanism of reverse rate dependent action potential prolongation. *Journal of Cardiovascular Electrophysiology* 1997;8:529-536

47. Kline RP, Cohen I, Falk R, Kupersmith J: Activity-dependent extracellular K+ fluctuations in canine Purkinje fibres. *Nature* 1980;286:68-71

48. Weirich J: Frequency-dependent action of antiarrhythmic drugs: the useful concept of periodical ligand binding [editorial]. *Basic Research in Cardiology* 1992;87:205-214

49. Carlsson L, Abrahamsson C, Andersson B, Duker G, Schiller-Linhardt G: Proarrhythmic effects of the class III agent almokalant: importance of infusion rate, QT dispersion, and early afterdepolarisations [see comments]. *Cardiovascular Research* 1993;27:2186-2193

50. Sasyniuk BI, Brunet S: Proarrhythmic effects of *d*-sotalol in the rabbit ventricle associated with differential effects on endocardial cells at slow heart rates. *Circulation* 1994;90:I-146

51. Adamantidis MM, Lacroix DL, Caron JF, Dupuis BA: Electrophysiological and arrhythmogenic effects of the histamine type 1-receptor antagonist astemizole on rabbit Purkinje fibers: clinical relevance. *Journal of Cardiovascular Pharmacology* 1995;26:319-327

52. Carlsson L, Amos GJ, Andersson B, Drews L, Duker G, Wadstedt G: Electrophysiological characterization of the prokinetic agents cisapride and mosapride in vivo and in vitro: implications for proarrhythmic potential? *Journal of Pharmacology & Experimental Therapeutics* 1997;282:220-227

53. Puisieux FL, Adamantidis MM, Dumotier BM, Dupuis BA: Cisapride-induced prolongation of cardiac action potential and early afterdepolarizations in rabbit Purkinje fibres. *British Journal of Pharmacology* 1996;117:1377-1379

54. Sasyniuk BI, Valois M, Toy W: Recent advances in understanding the mechanisms of drug-induced torsades de pointes arrhythmias. *American Journal of Cardiology* 1989;64:29J-32J

55. Roden DM, Hoffman BF: Action potential prolongation and induction of abnormal automaticity by low quinidine concentrations in canine Purkinje fibers. Relationship to potassium and cycle length. *Circulation Research* 1985;56:857-867

56. el-Sherif N: Early afterdepolarizations and arrhythmogenesis. Experimental and clinical aspects. *Archives des Maladies du Coeur et des Vaisseaux* 1991;84:227-234

57. Mikawa T, Fischman DA: The polyclonal origin of myocyte lineages. [Review] *Annual Review of Physiology* 1996;58:509-521

58. Alyonycheva T, Cohen-Gould L, Siewert C, Fischman D, Mikawa T: Skeletal muscle-specific myosin binding protein-H is expressed in purkinje fibers of the cardiac conduction system. *Circulation Research* 1997;80:665-672

59. Gourdie RG, Green CR, Severs NJ, Anderson RH, Thompson RP: Evidence for a distinct gap-junctional phenotype in ventricular conduction tissues of the developing and mature avian heart. *Circulation Research* 1993;72:278-289

60. Pressler ML, Munster PN, Huang X: Gap junction disttribution in the heart: functional relevance, in Zipes PD, Jalife J (eds): *Cardiac electrophysiology -from cell to bedside-*. edsecond edition. Philadelphia, W.B. Saunders Company, 1995, pp 144-151

61. Gorza L, Schiaffino S, Volpe P: Inositol 1,4,5-trisphosphate receptor in heart: evidence for its concentration in Purkinje myocytes of the conduction system. *Journal of Cell Biology* 1993;121:345-353

62. Gorza L, Vettore S, Volpe P, Sorrentino V, Samuel JL, Anger M, Lompre AM: Cardiac myocytes differ in mRNA composition for sarcoplasmic reticulum Ca2+ channels and Ca2+ pumps. [Review] *Annals of the New York Academy of Sciences* 1995;752:141-148

63. Gourdie RG, Mima T, Thompson RP, Mikawa T: Terminal diversification of the myocyte lineage generates Purkinje fibers of the cardiac conduction system. *Development* 1995;121:1423-1431

64. Kirby ML: Role of extracardiac factors in heart development. [Review] *Experientia* 1988;44:944-951

65. Gorza L, Schiaffino S, Vitadello M: Heart conduction system: a neural crest derivative? *Brain Research* 1988;457:360-366

66. Gorza L, Vitadello M: Distribution of conduction system fibers in the developing and adult rabbit heart revealed by an antineurofilament antibody. *Circulation Research* 1989;65:360-369

67. Wenink ACG: Development of the human cardiac conducting system. *J Anat* 1997;121:617-631

68. Viragh S, Stoeckel ME, Porte A: Light and electron microscopic structure of the cardiac Purkinje fibers--review. [Review] *Physiologia Bohemoslovaca* 1987;36:233-242

69. Tranum-Jensen J, Wilde AA, Vermeulen JT, Janse MJ: Morphology of electrophysiologically identified junctions between Purkinje fibers and ventricular muscle in rabbit and pig hearts. *Circulation Research* 1991;69:429-437

70. Mendez C, Mueller WJ, Merideth J, Moe GK: Interaction of transmembrane potentials in canine Purkinje fibers and at Purkinje fiber-muscle junctions. *Circulation Research* 1969;24:361-372

71. Martinez-Palomo A, Alanis J, Benitez D: Transitional cardiac cells of the conductive system of the dog heart. Distinguishing morphological and electrophysiological features. *Journal of Cell Biology* 1970;47:1-17

72. Boutjdir M, el-Sherif N: Alpha 1-adrenoceptor regulation of delayed afterdepolarizations and triggered activity in subendocardial Purkinje fibers surviving 1 day of myocardial infarction. *Journal of Molecular & Cellular Cardiology* 1991;23:83-90

73. Lukas A, Antzelevitch C: Differences in the electrophysiological response of canine ventricular epicardium and endocardium to ischemia: Role of the transient outward current. *Circulation* 1993;88:2903-2915

74. Di Diego JM, Antzelevitch C: High [Ca2+]o-induced electrical heterogeneity and extrasystolic activity in isolated canine ventricular epicardium. Phase 2 reentry. *Circulation* 1994;89:1839-1850

75. Rozanski GJ, Witt RC: Alterations in repolarization of cardiac Purkinje fibers recovering from ischemic-like conditions: genesis of early afterdepolarizations. *Journal of Cardiovascular Electrophysiology* 1993;4:134-143

76. Li HG, Jones DL, Yee R, Klein GJ: Defibrillation shocks produce different effects on Purkinje fibers and ventricular muscle: implications for successful defibrillation, refibrillation and postshock arrhythmia. *Journal of the American College of Cardiology* 1993;22:607-614

77. Janse MJ, Kleber AG, Capucci A, Coronel R, Wilms-Schopman F: Electrophysiological basis for arrhythmias caused by acute ischemia. Role of the subendocardium. *Journal of Molecular & Cellular Cardiology* 1986;18:339-355

78. Damiano RJ, Jr., Smith PK, Tripp HF, Jr., Asano T, Small KW, Lowe JE, Ideker RE, Cox JL: The effect of chemical ablation of the endocardium on ventricular fibrillation threshold. *Circulation* 1986;74:645-652

79. Priori SG, Mantica M, Napolitano C, Schwartz PJ: Early afterdepolarizations induced in vivo by reperfusion of ischemic myocardium. A possible mechanism for reperfusion arrhythmias. *Circulation* 1990;81:1911-1920

80. Vera Z, Pride HP, Zipes DP: Reperfusion arrhythmias: role of early afterdepolarizations studied by monophasic action potential recordings in the intact canine heart during autonomically denervated and stimulated states. *Journal of Cardiovascular Electrophysiology* 1995;6:532-543

81. Carlsson L, Almgren O, Duker G: QTU-prolongation and torsades de pointes induced by putative class III antiarrhythmic agents in the rabbit: etiology and interventions. *Journal of Cardiovascular Pharmacology* 1990;16:276-285

82. Adamantidis MM, Lacroix DL, Caron JF, Dupuis BA: Electrophysiological and arrhythmogenic effects of the histamine type 1-receptor antagonist astemizole on rabbit Purkinje fibers: clinical relevance. *Journal of Cardiovascular Pharmacology* 1995;26:319-327

83. Sicouri S, Antzelevitch C: A subpopulation of cells with unique electrophysiological properties in the deep subepicardium of the canine ventricle. The M cell. *Circulation Research* 1991;68:1729-1741

84. Ducceschi V, Di Micco G, Sarubbi B, Russo B, Santangelo L, Iacono A: Ionic mechanisms of ischemia-related ventricular arrhythmias. [Review] *Clinical Cardiology* 1996;19:325-331

85. Hoffman BF, Guo SD, Feinmark SJ: Arrhythmias caused by platelet activating factor. *Journal of Cardiovascular Electrophysiology* 1996;7:120-133

86. Lu T, Huang Y, Jiang W: The electrophysiologic effects of endothelin. A patch clamp study in guinea pig ventricular myocytes. *Chinese Medical Journal* 1995;108:618-625

87. Yorikane R, Koike H, Miyake S: Electrophysiological effects of endothelin-1 on canine myocardial cells. *Journal of Cardiovascular Pharmacology* 1991;17 Suppl 7:S159-62

88. Yorikane R, Shiga H, Miyake S, Koike H: Evidence for direct arrhythmogenic action of endothelin. *Biochemical & Biophysical Research Communications* 1990;173:457-462

89. Lee JH, Rosen MR: Alpha 1-adrenergic receptor modulation of repolarization in canine Purkinje fibers. *Journal of Cardiovascular Electrophysiology* 1994;5:232-240

90. Moise NS, Gilmour RF, Jr., Riccio ML: An animal model of spontaneous arrhythmic death. *Journal of Cardiovascular Electrophysiology* 1997;8:98-103

91. Drouin E, Charpentier F, Gauthier C: alpha1-adrenergic stimulation induces early afterdepolarizations in ferret Purkinje fibers. *Journal of Cardiovascular Pharmacology* 1996;27:320-326

93. De Ferrari GM, Viola MC, D'Amato E, Antolini R, Forti S: Distinct patterns of calcium transients during early and delayed afterdepolarizations induced by isoproterenol in ventricular myocytes. *Circulation* 1995;91:2510-2515

94. Shimizu W, Ohe T, Kurita T, Takaki H, Aihara N, Kamakura S, Matsuhisa M, Shimomura K: Early afterdepolarizations induced by isoproterenol in patients with congenital long QT syndrome. *Circulation* 1991;84:1915-1923

95. Marban E, Robinson SW, Wier WG: Mechanisms of arrhythmogenic delayed and early afterdepolarizations in ferret ventricular muscle. *Journal of Clinical Investigation* 1986;78:1185-1192

96. Priori SG, Corr PB: Mechanisms underlying early and delayed afterdepolarizations induced by catecholamines. *American Journal of Physiology* 1990;258:H1796-805

97. Jabr RI, Cole WC: Alterations in electrical activity and membrane currents induced by intracellular oxygen-derived free radical stress in guinea pig ventricular myocytes. *Circulation Research* 1993;72:1229-1244

98. Sicouri S, Quist M, Antzelevitch C: Evidence for the presence of M cells in the guinea pig ventricle. *Journal of Cardiovascular Electrophysiology* 1996;7:503-511

99. Miura M, Ishide N, Oda H, Sakurai M, Shinozaki T, Takishima T: Spatial features of calcium transients during early and delayed afterdepolarizations. *American Journal of Physiology* 1993;265:H439-44

100. Roden DM: Current status of class III antiarrhythmic drug therapy. [Review]. *American Journal of Cardiology* 1993;72:44B-49B

101. Ming Z, Aronson R, Nordin C: Mechanism of current-induced early afterdepolarizations in guinea pig ventricular myocytes. *American Journal of Physiology* 1994;267:H1419-28

102. Song Y, Belardinelli L: ATP promotes development of afterdepolarizations and triggered activity in cardiac myocytes. *American Journal of Physiology* 1994;267:H2005-11

103. Szabo B, Sweidan R, Rajagopalan CV, Lazzara R: Role of Na+:Ca2+ exchange current in Cs(+)-induced early afterdepolarizations in Purkinje fibers. *Journal of Cardiovascular Electrophysiology* 1994;5:933-944

104. January CT, Riddle JM: Early afterdepolarizations: mechanism of induction and block. A role for L-type Ca2+ current. *Circulation Research* 1989;64:977-990

105. Li ZY, Wang YH, Maldonado C, Kupersmith J: Role of junctional zone cells between Purkinje fibres and ventricular muscle in arrhythmogenesis. *Cardiovascular Research* 1994;28:1277-1284

106. January CT, Chau V, Makielski JC: Triggered activity in the heart: cellular mechanisms of early after-depolarizations. [Review] *European Heart Journal* 1991;12 Suppl F:4-9

107. Liu TF, Chen XJ: Characteristics of early afterdepolarization in mouse atrial fibers. *Science in China - Series B, Chemistry, Life Sciences & Earth Sciences* 1994;37:29-36

108. Shen H, Liu TF: Generation of early afterdepolarization in mouse ventricular fibers at long cycle length [published erratum appears in Methods Find Exp Clin Pharmacol 1993 Jun;15(5):following 328]. *Methods & Findings in Experimental & Clinical Pharmacology* 1993;15:15-21

109. Sicouri S, Antzelevitch C: Afterdepolarizations and triggered activity develop in a select population of cells (M cells) in canine ventricular myocardium: the effects of acetylstrophanthidin and Bay K 8644. *Pacing & Clinical Electrophysiology* 1991;14:1714-1720

110. Drouin E, Charpentier F, Gauthier C, Laurent K, Le Marec H: Electrophysiologic characteristics of cells spanning the left ventricular wall of human heart: evidence for presence of M cells [see comments]. *Journal of the American College of Cardiology* 1995;26:185-192

111. el-Sherif N, Caref EB, Yin H, Restivo M: The electrophysiological mechanism of ventricular arrhythmias in the long QT syndrome. Tridimensional mapping of activation and recovery patterns. *Circulation Research* 1996;79:474-492

112. Sosunov EA, Anyukhovsky EP, Rosen MR: Effects of quinidine on repolarization in canine epicardium, midmyocardium, and endocardium: I. In vitro study. *Circulation* 1997;96:4011-4018

113. Anyukhovsky EP, Sosunov EA, Rosen MR: Regional differences in electrophysiological properties of epicardium, midmyocardium, and endocardium. In vitro and in vivo correlations. *Circulation* 1996;94:1981-1988

114. Anyukhovsky EP, Sosunov EA, Feinmark SJ, Rosen MR: Effects of quinidine on repolarization in canine epicardium, midmyocardium, and endocardium: II. In vivo study. *Circulation* 1997;96:4019-4026

115. Abrahamsson C, Carlsson L, Duker G: Lidocaine and nisoldipine attenuate almokalant-induced dispersion of repolarization and early afterdepolarizations in vitro. *Journal of Cardiovascular Electrophysiology* 1996;7:1074-1081

116. Antzelevitch C, Sun ZQ, Zhang ZQ, Yan GX: Cellular and ionic mechanisms underlying erythromycin-induced long QT intervals and torsade de pointes. *Journal of the American College of Cardiology* 1996;28:1836-1848

117. Ming Z, Nordin C, Aronson RS: Role of L-type calcium channel window current in generating current-induced early afterdepolarizations. *Journal of Cardiovascular Electrophysiology* 1994;5:323-334

118. Shimizu W, Ohe T, Kurita T, Tokuda T, Shimomura K: Epinephrine-induced ventricular premature complexes due to early afterdepolarizations and effects of verapamil and propranolol in a patient with congenital long QT syndrome. *Journal of Cardiovascular Electrophysiology* 1994;5:438-444

119. Nattel S, Quantz MA: Pharmacological response of quinidine induced early afterdepolarisations in canine cardiac Purkinje fibres: insights into underlying ionic mechanisms. *Cardiovascular Research* 1988;22:808-817

120. Adaniya H, Hayami H, Hiraoka M, Sawanobori T: Effects of magnesium on polymorphic ventricular tachycardias induced by aconitine. *Journal of Cardiovascular Pharmacology* 1994;24:721-729

121. Davidenko JM, Cohen L, Goodrow R, Antzelevitch C: Quinidine-induced action potential prolongation, early afterdepolarizations, and triggered activity in canine Purkinje fibers. Effects of stimulation rate, potassium, and magnesium. *Circulation* 1989;79:674-686

122. Kurita T, Ohe T, Shimizu W, Hotta D, Shimomura K: Early afterdepolarization in a patient with complete atrioventricular block and torsades de pointes [see comments]. *Pacing & Clinical Electrophysiology* 1993;16:33-38

123. Sawanobori T, Adaniya H, Hirano Y, Hiraoka M: Effects of antiarrhythmic agents and Mg2+ on aconitine-induced arrhythmias. [Review] *Japanese Heart Journal* 1996;37:709-718

124. Boutjdir M, Restivo M, Wei Y, Stergiopoulos K, el-Sherif N: Early afterdepolarization formation in cardiac myocytes: analysis of phase plane patterns, action potential, and membrane currents. *Journal of Cardiovascular Electrophysiology* 1994;5:609-620

125. Fish FA, Prakash C, Roden DM: Suppression of repolarization-related arrhythmias in vitro and in vivo by low-dose potassium channel activators. *Circulation* 1990;82:1362-1369

126. Carlsson L, Abrahamsson C, Drews L, Duker G: Antiarrhythmic effects of potassium channel openers in rhythm abnormalities related to delayed repolarization [see comments]. *Circulation* 1992;85:1491-1500

127. Damiano BP, Rosen MR: Effects of pacing on triggered activity induced by early afterdepolarizations. *Circulation* 1984;69:1013-1025

129. Verduyn SC, Vos MA, Gorgels AP, van der Zande J, Leunissen JD, Wellens HJ: The effect of flunarizine and ryanodine on acquired torsades de pointes arrhythmias in the intact canine heart. *Journal of Cardiovascular Electrophysiology* 1995;6:189-200

130. White RE, Hartzell HC: Effects of intracellular free magnesium on calcium current in isolated cardiac myocytes. *Science* 1988;239:778-780

131. Kelepouris E, Kasama R, Agus ZS: Effects of intracellular magnesium on calcium, potassium and chloride channels. [Review] *Mineral & Electrolyte Metabolism* 1993;19:277-281

132. Hexum T, Samson FE, Jr., Himes RH: Kinetic studies of membrane (Na+-K+-Mg2+)-ATPase. *Biochimica et Biophysica Acta* 1970;212:322-331

133. Valdivia HH, Kaplan JH, Ellis-Davies GC, Lederer WJ: Rapid adaptation of cardiac ryanodine receptors: modulation by Mg2+ and phosphorylation. *Science* 1995;267:1997-2000

134. Watanabe Y, Dreifus LS: Electrophysiological effects of magnesium and its interactions with potassium. *Cardiovascular Research* 1972;6:79-88

135. January CT, Fozzard HA: Delayed afterdepolarizations in heart muscle: mechanisms and relevance. [Review] *Pharmacological Reviews* 1988;40:219-227

136. Laflamme MA, Becker PL: Ca2+-induced current oscillations in rabbit ventricular myocytes. *Circulation Research* 1996;78:707-716

137. Priori SG, Yamada KA, Corr PB: Influence of hypoxia on adrenergic modulation of triggered activity in isolated adult canine myocytes. *Circulation* 1991;83:248-259

138. Antzelevitch C: Electrotonus and Reflection, in Rosen MR, Janse M, Wit A (eds): *Cardiac Electrophysiology: A Textbook.* New-York, Futura Publishing, 1990, 491-516

139. Mines GR: On dynamic equilibrium in the heart. *Journal of Physiology* 1913;46:349-382

140. Campbell RW: Predisposing factors for ventricular arrhythmias. [Review] *Journal of Cardiovascular Pharmacology* 1991;17 Suppl 6:S9-12

141. Denker S, Lehmann M, Mahmud R, Gilbert C, Akhtar M: Facilitation of ventricular tachycardia induction with abrupt changes in ventricular cycle length. *American Journal of Cardiology* 1984;53:508-515

142. Denker S, Lehmann MH, Mahmud R, Gilbert C, Akhtar M: Facilitation of macroreentry within the His-Purkinje system with abrupt changes in cycle length. *Circulation* 1984;69:26-32

143. Denker S, Lehmann MH, Mahmud R, Gilbert C, Akhtar M: Divergence between refractoriness of His-Purkinje system and ventricular muscle with abrupt changes in cycle length. *Circulation* 1983;68:1212-1221

144. Dessertenne F: [Ventricular tachycardia with 2 variable opposing foci]. [French]. *Archives des Maladies du Coeur et des Vaisseaux* 1966;59:263-272

145. MacWilliams JA: Some applications of physiology to medecine. II. Ventricular fibrillation and sudden death. *British Medical Journal* 1923;2:215

146. Wiggers CJ: Studies of ventricular fibrillation caused by electric shock. II. Cinematographic and electrocardiographic observations of the natural process in the dog's heart. Its inhibition by potassium and the revival of coordinated beats by calcium. *American Heart Journal* 1929;5:351

147. Schwartz SP, Hallinger LN: Transient ventricular fibrillation. VI. Observations on the peripheral arterial pulse pressure in the course of transient ventricular fibrillation during established auriculoventricular dissociation. *American Heart Journal* 1954;48:390

148. Schwartz SP, Orloff J, Fox C: Transient ventricular fibrillation. I. The prefibrillary period during established auriculoventricular dissociation with a note on the phonocardiograms obtained at such times. *American Heart Journal* 1949;21

149. Loeb HS, Pietras RJ, Gunnar RM, Tobin JRJ: Paroxysmal ventricular fibrillation in two patients with hypomagnesemia. Treatment by transvenous pacing. *Circulation* 1968;210

150. Tamura K, Tamura T, Yoshida S, Inui M, Fukuhara N: Transient recurrent ventricular fibrillation due to hypopotassemia with special note on the U wave. *Japanese Heart Journal* 1967;8:652

151. Smirk FH, Ng J: Cardiac ballet: repetitions of complex electrocardiographic patterns. *British Heart Journal* 1969;31:426

152. Haverkamp W, Shenasa M, Borggrefe M, Breithardt G: Torsade de Pointes, in Zipes PD, Jalife J (eds): *Cardiac electrophysiology -from cell to bedside-*. ed2nd Edition. Philadelphia, Saunder Company, 1995, pp 885-889

153. Slama R, Coumel Ph, Motte G, Gourgon R, Waynberger M, Touche S: Tachycardies ventriculaires et torsades de pointes: frontieres morphologiques entre les dysrythmies ventriculaires. *Archives des Maladies du Coeur et des Vaisseaux* 1973;1401

154. Krikler DM, Curry PV: Torsade De Pointes, an atypical ventricular tachycardia. *British Heart Journal* 1976;38:117-120

155. Singh BN, Gaarder TD, Kanegae T, Goldstein M, Montgomerie JZ, Mills H: Liquid protein diets and torsade de pointes. *JAMA* 1978;240:115-119

156. Motte G, Coumel P, Abitbol G, Dessertenne F, Slama R: [The long QT syndrome and syncope caused by spike torsades]. [French]. *Archives des Maladies du Coeur et des Vaisseaux* 1970;63:831-853

157. Weissenburger J, Davy JM, Chezalviel F, Ertzbischoff O, Poirier JM, Engel F, Lainee P, Penin E, Motte G, Cheymol G: Arrhythmogenic activities of antiarrhythmic drugs in conscious hypokalemic dogs with atrioventricular block: comparison between quinidine, lidocaine, flecainide, propranolol and sotalol. *Journal of Pharmacology & Experimental Therapeutics* 1991;259:871-883

158. el-Sherif N, Chinushi M, Caref EB, Restivo M: Electrophysiological mechanism of the characteristic electrocardiographic morphology of torsade de pointes tachyarrhythmias in the long-QT syndrome: detailed analysis of ventricular tridimensional activation patterns. *Circulation* 1997;96:4392-4399

159. D'Alnoncourt CN, Zierhut W, Bluderitz B: "Torsade de pointes" tachycardia. Re-entry or focal activity? *British Heart Journal* 1982;48:213-216

160. Bardy GH, Ungerleider RM, Smith WM, Ideker RE: A mechanism of torsades de pointes in a canine model. *Circulation* 1983;67:52-59

161. Leichter D, Danilo P, Jr., Boyden P, Rosen TS, Rosen MR: A canine model of torsades de pointes. *Pacing & Clinical Electrophysiology* 1988;11:2235-2245

162. Habbab MA, el-Sherif N: Drug-induced torsades de pointes: role of early afterdepolarizations and dispersion of repolarization. *American Journal of Medicine* 1990;89:241-246

163. Nayebpour M, Solymoss BC, Nattel S: Cardiovascular and metabolic effects of caesium chloride injection in dogs--limitations as a model for the long QT syndrome. *Cardiovascular Research* 1989;23:756-766

164. Curtis MJ: Torsades de pointes: arrhythmia, syndrome, or chimera? A perspective in the light of the Lambeth Conventions. [Review] *Cardiovascular Drugs & Therapy* 1991;5:191-200

165. Weissenburger J, Davy JM, Chezalviel F: Experimental models of torsades de pointes. [Review]. *Fundamental & Clinical Pharmacology* 1993;7:29-38

166. Davy JM, Weissenburger J, Chezalviel F, Ertzbischoff O: [Experimental models of torsades de pointes]. [French]. *Archives des Maladies du Coeur et des Vaisseaux* 1992;85 Spec No 4:15-21

167. Weissenburger J, Chezalviel F, Davy JM, Lainee P, Guhennec C, Penin, E, Engel F, Cynober L, Motte G, Cheymol G: Methods and limitations of an experimental model of long QT syndrome. *Journal of Pharmacological Methods* 1991;26:23-42

168. Shalaby YF, Levesque CP, Yang pw, Little AW, Conder LM, Jenkins-West T, Blanar AM: Dominant-Negative KvLQT1 Mutations Underlie the LQT1 form of Long QT Syndrome. *Circulation* 1997;96:1733-1736

169. Duggal P, Vesely MR, Wattanasirichaigoon D, Villafane J, Kaushik V, Beggs AH: Mutation of the gene for IsK associated with both Jervell and Lange-Nielsen and Romano-Ward forms of Long-QT syndrome. *Circulation* 1998;97:142-146

170. Ackerman MJ: The long QT syndrome: ion channel diseases of the heart. [Review]. *Mayo Clinic Proceedings* 1998;73:250-269

171. Splawski I, Tristani-Firouzi M, Lehmann MH, Sanguinetti MC, Keating, MT. Mutations in the hminK gene cause long QT syndrome and suppress IKs function. *Nature Genetics* 1997;17:338-340

172. Neyroud N, Tesson F, Denjoy I, Leibovici M, Donger C, Barhanin J, Faure S, Gary F, Coumel P, Petit C, Schwartz K, Guicheney P: A novel mutation in the potassium channel gene KVLQT1 causes the Jervell and Lange-Nielsen cardioauditory syndrome [see comments]. *Nature Genetics* 1997;15:186-189

173. Roden DM, Lazzara R, Rosen M, Schwartz PJ, Towbin J, Vincent GM: Multiple mechanisms in the long-QT syndrome. Current knowledge, gaps, and future directions. The SADS Foundation Task Force on LQTS. [Review] *Circulation* 1996;94:1996-2012

174. Keating MT, Sanguinetti MC: Pathophysiology of ion channel mutations. [Review] *Current Opinion in Genetics & Development* 1996;6:326-333

175. Keating MT, Sanguinetti MC: Molecular genetic insights into cardiovascular disease. [Review] *Science* 1996;272:681-685

176. Tesson F, Donger C, Denjoy I, Berthet M, Bennaceur M, Petit C, Coumel P, Schwarts K, Guicheney P: Exclusion of KCNE1 (IsK) as a candidate gene for Jervell and Lange-Nielsen syndrome. *Journal of Molecular & Cellular Cardiology* 1996;28:2051-2055

CHAPTER I

PROARRHYTHMIC EFFECTS OF *D*-SOTALOL IN RABBIT VENTRICLE ASSOCIATED WITH DIFFERENTIAL EFFECTS ON REPOLARIZATION IN ENDOCARDIAL CELLS: *IN VITRO* AND *IN SITU* CORRELATIONS

Current Status: Brunet S, Sasyniuk BI.

To be submitted to *Circulation*

Abstract

Using microelectrode techniques, we compared the effect of *d*-sotalol on action potential duration (APD) in Purkinje fibers (PF), ventricular muscle (VM) and "transitional" (T) cells in isolated superfused rabbit endocardial preparations. There was clearly heterogeneity of potentials on the endocardial surface which were variably modified by drug. PF action potentials (AP) had typically long durations and displayed spike and dome morphology. VM APs were typically short and lacked a notch. T cells had APs with or without a spike and dome configuration and intermediate durations. In the absence of drug, APs at these sites responded variably to abrupt changes in cycle length (CL). Both immediate and delayed time dependent changes were observed. The immediate change was a lengthening of duration in PF, and shortening in both T cells and VM. The delayed response was a CL dependent lengthening in all cells. *D*-sotalol affected mostly the delayed response. The drug lengthened the APD considerably in PF, much less in T cells and least in VM. The heterogeneity created by this selective action of the drug was accentuated at longer CLs. At CL $\geq$ 2.5 sec, concentrations of *d*-sotalol $\geq$ 20 μM induced early afterdepolarizations (EAD) in PF which propagated to VM producing coupled APs. Coupled APs were associated with critical disparities in repolarization between PF and muscle recording sites. Regardless of CL, the attainment of the critical disparity was the crucial factor for the generation of triggered activity in specialized conducting cells. Sustained triggered activity was only seen at very long CLs. . Multiple electrotonic

interactions between PF, T cells and VM apparently due to the creation of a functional refractory barrier in PF resulted in multiple triggered responses and sometimes sustained but self-limiting rapid chaotic rhythm which propagated to VM. Under the exact same conditions but at shorter CLs, *d*-sotalol induced coupled beats in the isolated Langendorff perfused rabbit heart. These coupled beats were associated with disparity in repolarization as a result of a selective CL dependent prolongation of endocardial monophasic action potentials (MAPs). Preparations which displayed coupled beats *in situ* showed triggered activity *in vitro* but at longer CLs than those required *in situ*. This study provides compelling evidence that the mechanism of initiation of coupled beats induced by *d*-sotalol in the intact isolated heart is triggered activity originating in PFs on the endocardial surface and provides the experimental basis for further evaluation of the proarrhythmic effect of *d*-sotalol in the isolated rabbit heart.

Introduction

For many of the recently developed class III antiarrhythmic drugs it has been shown that certain structures within the heart such as PFs or M cells, respond with a much more marked prolongation of the APD than the VM thus causing increased dispersion of repolarization. However, no clear relation between the proarrhythmic response and some critical prolongation of repolarization has yet been established. There is wide agreement among investigators that drug induced torsade de pointes (TdP) arrhythmias are somehow related to triggered activity brought about by EADs. However, whether EADs and triggered activity are responsible for initiating TdP and/or maintaining their mechanism is still an unsettled question.

Much of the evidence linking EAD induced triggered activity to TdP arrhythmias upon exposure to drugs with class III actions comes from *in vitro* studies of isolated PFs. [1-3] Both Hoffman and Roden [1] and Sicouri and Antzelevitch [2] demonstrated triggered activity in isolated canine PFs with no VM attached and perfused with quinidine. Such studies have shown that EADs and triggered activity readily occur when PFs are isolated from their attachment to muscle. Such activity is less readily induced in the canine heart in preparations in which PFs are attached to VM. [3,4] showed previously that quinidine produced EADs and triggered activity in PFs which propagated to muscle in preparations of isolated canine ventricular endocardial preparations. EAD induced triggered

activity occurred only when the preparations were paced at extremely slow rates under conditions of hypokalemia and acidosis. In such preparations it is difficult to control the rate because the automatic PF firing rate often overrides the pacing rate in the presence of a class III drug and hypokalemia and precludes a systematic study of the interaction of drug effects with either rate or tissue effects. It must also be remembered that a certain degree of cellular uncoupling results under such *in vitro* conditions.. With the exception of anecdotal data there are no systematic studies of antiarrhythmic drugs in syncytial preparations.

Carlsson et al [5-7] showed that the rabbit is exquisitely sensitive to the development of TdP when exposed to agents which prolong repolarization. However, these agents readily induced TdP in the conscious rabbit and rarely in the anesthetized rabbit unless α adrenergic stimulating agents were present. The reason for the exquisite sensitivity of the rabbit is not clear. Carlsson et al [7] attributed it to a high α_1 adrenergic receptor density in the rabbit and the effect of α_1-adrenergic stimulation on elevation of free cytosolic calcium levels. Thus, the rabbit seemed like an ideal species to use in order to assess the proarrhythmic effects of currently available class III agents and to determine the role of triggered activity in their induction.

D-Sotalol has been recognized as an effective antiarrhythmic drug [8-10] which was hypothesized to be less arrhythmogenic and less prone to induce TdP

arrhythmias than class 1A drugs [11-13]. This drug has pure class III actions but lacks the β-adrenergic blocking activity of the racemic mixture. However, recent studies have shown that there is increased mortality in patients postinfarct given *d*-sotalol than those on placebo. (Review) [14] This increased mortality was attributed to TdP arrhythmias. Perhaps such proarrhythmic effects could be prevented if the mechanism of this arrhythmia was known and the conditions leading to its induction were avoided.

The purpose of the present study was to determine the conditions under which *d*-sotalol might induce triggered activity in the rabbit ventricle under *in vitro* conditions and to apply this information to the *in situ* heart to determine if identical conditions might result in arrhythmias. Our results have implications for the generation of TdP arrhythmias in the isolated rabbit heart. The intent was to develop an isolated heart model of TdP arrhythmias in order that its mechanism may be determined. Preliminary reports of this work were published in abstract form. [15]

Methods

All procedures for animal care and experimentation followed the guidelines of the Canadian Council for Animal Care and were monitored by an institutional committee. Sixteen New Zealand White rabbits (body weight 2.0 - 2.5 Kg) were anaesthetized with xylazine (8 mg · Kg^{-1} i.m.) followed by ketamine hydrochloride (75 mg · Kg^{-1} i.m.). After intravenous administration of heparin (400 IU · Kg^{-1}), the hearts were rapidly excised and immediately immersed in a high K^+ Krebs-Henseleit solution for dissection (composition in mmol · $Liter^{-1}$: NaCl 122.0, KCl 25.8, $MgSO_4$ 0.5, $NaHCO_3$ 24.0, KH_2PO_4 1.2, $CaCl_2$ 1.8, Glucose 50). [16] A section of endocardium, either from the or right or left ventricle and including either a papillary muscle or trabeculae together with an attached network of PFs was dissected and pinned to the bottom of a tissue bath and superfused with high K^+ Krebs-Henseleit solution for one hour (12 ml · min^{-1}). The preparations were then continuously superfused with regular Krebs-Henseleit solution equilibrated with 95 % O_2 /5 % CO_2 (composition in mmol · $Liter^{-1}$: NaCl 122.0, KCl 2.8, $MgSO_4$ 0.5, $NaHCO_3$ 24.0, KH_2PO_4 1.2, $CaCl_2$ 1.8, Glucose 5.0, Pyruvate 2.0). The K^+ concentration was either 4.0 mM or 2.7 mM. No attempt was made to distinguish between the effects of either conc. Temperature was maintained at 36 ± 0.5 ° C. The preparations were stimulated at a CL of 0.5 sec during equilibration. Experiments were not started until the preparations had fully

recovered and displayed stable electrophysiological characteristics (usually about 2 hours).

The preparations were stimulated by a standard method with square wave pulses of 1- to 2 msec duration and twice threshold intensity via teflon-coated silver electrodes. [4] APs were recorded with 3 M KCl filled glass capillary microelectrodes (tip resistances, 20 to 40 ΩM) coupled by an Ag/AgCl junction to amplifiers with high input impedance and capacity neutralization (model 750 or KS-700, World Precision Instruments). All the signals were displayed on a storage oscilloscope (Tektronix 5113) and stored in digitized form on a personal computer (using a TL-125 A/D board and axotape^{tm} software, version 2 (Axon instruments). APDs at 90% repolarization were measured using Data-Pac II^{tm} software (Version 4.1, Run Technologies).

The preparations were superfused with varying concentrations (10-80μM) of *d*-sotalol while stimulating at a basic cycle length (BCL) of 0.5 sec. The stimulation CL was then increased from 0.5 to 5.5 seconds usually in one second steps. In some preparations the entire range of CLs was studied whereas in others only one or two CLs were assessed.

In 2 preparations, the hearts were equilibrated with 20μM *d*-sotalol on a non recirculating Langendorff apparatus (as described below), arrhythmias were

observed and then a similar endocardial preparation was excised and mounted in the tissue bath for further recording from PFs and VM.

In situ Preparations

Four New Zealand White rabbits of either sex (body weight 2.0 - 2.5 Kg) were anaesthetized with ketamine hydrochloride (75 mg × Kg^{-1} i.m.) followed by xylazine (8 mg × Kg^{-1} i.m.). Heparin (400 IU × Kg^{-1}) was administered through a marginal ear vein. The heart was rapidly excised and immediately immersed in 37 ° C modified Krebs-Henseleit solution previously bubbled with 95 % O2 and 5 % CO2 (composition in mmol × $Liter^{-1}$: NaCl 122.0, KCl 4.0, MgSO4 0.5, NaHCO3 24.0, KH2PO4 1.2, CaCl2 1.8, Glucose 50). It was then mounted on a non-recirculating Langendorff apparatus and perfused at a perfusion pressure of 65 cm H_20 with oxygenated Krebs-Henseleit's solution (composition in mmol × $Liter^{-1}$: NaCl 122.0, KCl 4.0, MgSO4 0.5, NaHCO3 24.0, KH_2PO_4 1.2, $CaCl_2$ 1.8, Glucose 5.0, Pyruvate 2.0).). The heart was immersed in a water-jacketed chamber filled with Krebs-Henseleit solution kept at a temperature of 37 ° C.

To pace the hearts at a fixed BCL, bipolar silver wire ring electrodes (diameter 1 mm) were sutured onto the mid wall of the left ventricle. To slow down the intrinsic heart rate, the atrioventricular node was destroyed by injecting 0.1- 0.2 ml of formaldehyde (37 %) directly into the node region. The hearts were paced at a BCL of 0.5 sec with a pulse width of 1 ms and twice diastolic threshold

intensity delivered by a pulse generator (Schema Versata) and a stimulation isolation unit (Digitimer Ltd. Model DS2).

MAP signals were simultaneously recorded from the left ventricular endocardial and right ventricular epicardial surfaces with two contact type Langendorff probes (4 French model number 225, EP Technologies, Inc). In order to monitor activity from the conducting system, a MAP probe was placed at a strategic location on the endocardial surface. Activity from VM cells was recorded from MAP probes placed either at strategic locations on the endocardial surface or on the right ventricular epicardial surface. Drug effect on VM was most easily monitored with a MAP probe located at the base of the right ventricular epicardial surface remote from any conducting system. An attempt was made to place the endocardial probe at sites which displayed the longest durations during pacing at slow cycle lengths while the epicardial probe was placed at sites of shortest durations. Since arrhythmias occurred when ever the hearts were paced at slow cycle lengths we assessed optimal placement of the endocardial probe by determining the sites which displayed the longest durations just prior to the occurrence of coupled beats.[15]. An ECG was recorded between an electrode on the left ventricular apex and a reference electrode on the root of the aorta.

The two MAP signals were amplified by DC amplifiers (Isodam, WPI) and the ECG was amplified by an AC amplifier (Dam50, WPI). All signals were simultaneously digitized at 1 kHz for storage on the hard disk of an IBM

compatible personal computer equipped with an A/D board (Tl-125 Axon Instrument) and Axotape software (Version 2, Axon Instrument). The data were temporarily stored on the hard disk of the computer and then permanently stored both on digital audio tapes using Tapedisk software version 6.4.0 and on recordable CDs for later retrieval and analysis.

The MAP signals were processed unfiltered by Data-Pac II Version 4.1 software with the selection criteria and advanced spreadsheet module (Run Technologies, Inc). Each of the MAP signals was analyzed for MAP duration at the 90% repolarization level ($MAPD_{90\%}$) [17]. The QT interval was measured unfiltered with axotape software using cursors. The end of the T-wave was taken at the point at which it reached the isoelectric line..

The hearts were equilibrated with 20 μM of *d*-sotalol for at least 25 minutes while pacing at the BCL. After the period of equilibration with drug the hearts were paced at a number of different longer CLs ranging from 1.5 to 5.5 sec. Each longer CL was maintained for 5 minutes and then the CL was changed back to the BCL of 0.5 sec. The protocols were done under control conditions and after equilibration with drug.

Drug solutions

A concentrated *d*-sotalol stock solution (4×10^{-2} M) was made from powder in double distilled water each week. The stock solution was diluted in

modified Krebs-Henseleit solution to the appropriate concentration of *d*-sotalol. *D*-sotalol was kindly supplied by Bristol-Myers Squibb Canada.

Data are presented as mean (± S.D). Unpaired student *t*-test analysis was used when comparing means obtained cell APD from different preparations. A probability $P \leq 0.05$ was considered statistically significant. Bonferroni's inequality was used when multiple student's *t*-test were needed.

Results

IN VITRO EXPERIMENTS

Heterogeneity of repolarization characteristics of cells on the rabbit ventricular endocardial surface under control conditions

Two characteristic layers of cells are present in the rabbit ventricular endocardial surface, viz., a superficial layer of PFs fanning out from free running Purkinje strands and the bulk of ventricular myocardial cells forming the ventricular myocardial mass. [18] A layer of transitional (T) cells provides close connections to overlying Purkinje cells and underlying muscle cells. PF and VM cells differ principally with respect to AP upstroke and repolarization characteristics. These cells were characterized with respect to APD before assessing drug effects.

APs were recorded from Purkinje cells present in free running Purkinje strands, from muscle cells recorded from the tip of the papillary muscle in which there are no superficial layers of Purkinje cells as shown previously by Sasyniuk and Mendez [19] and from T cells recorded at the termination of free running Purkinje strands in VM. Any APs recorded from free running strands were classed as PFs. Impalements anywhere near or peripheral to the insertion of a free running strand into muscle were classed as T cells. Thus, our definition of T cells was not restricted to cells present specifically at Purkinje-muscle junctions (as described

by Tranum -Jensen et al [18]) but rather to all Purkinje cells which were not located in the free running strands or in muscle areas devoid of Purkinje cells [19,20].

Rabbit Purkinje cell APs commonly displayed a prominent early repolarization phase (spike and dome morphology) that was absent in VM. Purkinje cell AP had the longest durations while VM cell APs had the shortest. T cells had features of both ventricular and Purkinje cells depending upon their proximity to either. These features of the three cell types are illustrated in fig. 1. The prominent spike and dome morphology is present in the record from the free running Purkinje strand and is absent in the VM cell recorded from the tip of the papillary muscle. T cells usually displayed attenuated spike and dome morphologies and durations intermediate between those in Purkinje strands and those in VM. The presence of a much reduced spike and dome but a short duration indicated proximity to VM.

Steady state CL dependent changes in APD under control conditions

The APDs in specialized conducting fibers and muscle fibers in the rabbit ventricular tissues responded differentially to steady state changes in CL. The steady state relationship between APD and CL in a typical Purkinje cell versus VM is illustrated in fig. 2. CL was changed sequentially from 0.3 sec to 5.0 sec. Successive increases in CL produced a gradual but progressive increase in APD in the Purkinje cell. In the VM cell there was initially an increase in APD up to a CL of 1.0 sec and then a progressive decline in APD as the CL was increased further.

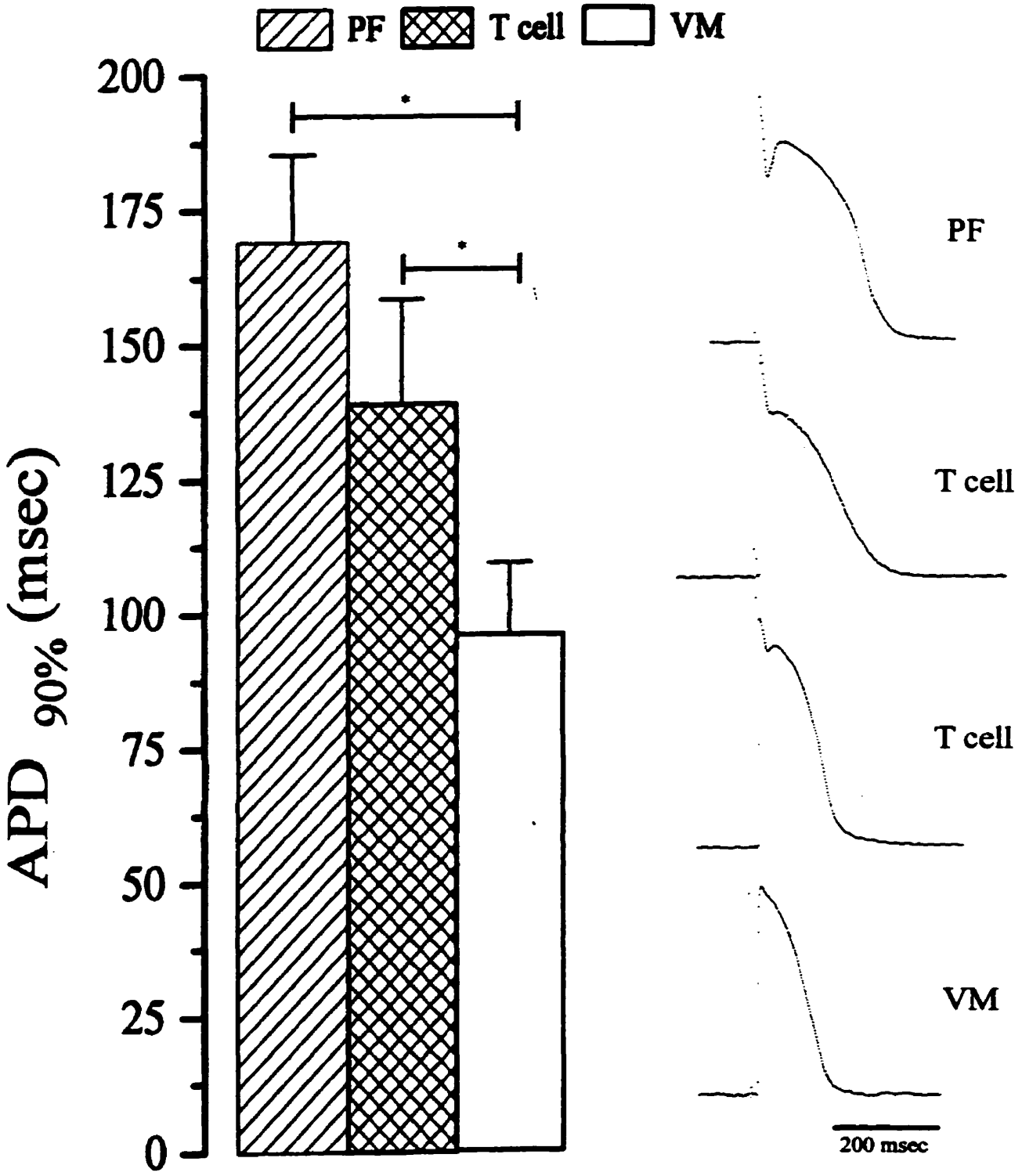
PF
T cell
VM
200
175
150
125
100
75
50
25
0
APD 90% (msec)
*
*
PF
T cell
T cell
VM
200 msec

Figure 1. Repolarization characteristics of 3 types of cells recorded from rabbit ventricular endocardial preparations under control conditions. Representative APs recorded from free running PF, VM cell from the tip of a papillary muscle and cells mostly at the termination of Purkinje strands in muscle (T cells). Bar graphs indicate the mean ± S.D. of $APD_{90\%}$ in the different cell types. All APs were recorded at a BCL of 0.5 sec. N= 17, 14, and 16 for PF, T, and VM cells, respectively. All means were significantly different from each other (* $P \leq 0.05$).

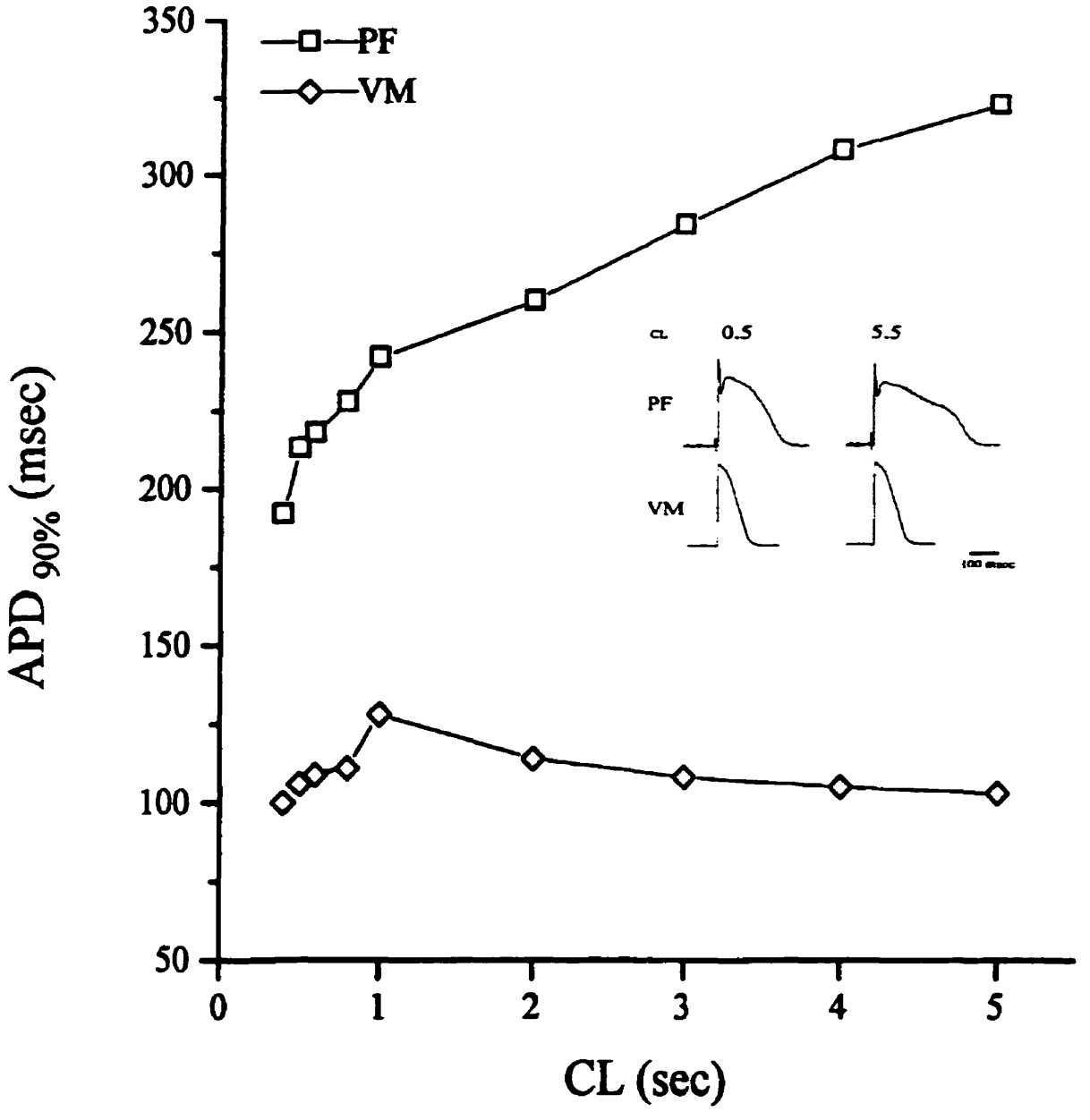

Figure 2. Typical example of the steady state dependence of $APD_{90\%}$ on CL in PF and VM cells. Recordings were obtained simultaneously and were maintained throughout the changes in CL. Each CL was maintained for 2 minutes. The CL was increased successively from 0.3 sec to 5 sec. Inset shows typical APs recorded from PF and VM sites at CL of 0.5 and 5 sec.

The resultant effect was a gradual CL dependent increase in the disparity between APDs in the VM cell and Purkinje cell. It was not possible to keep impalement in a T cell simultaneous with those in Purkinje and VM during the length of time required to do a steady state curve. Whenever such a relationship was determined for a T cell, the changes were intermediate showing qualitative changes similar to muscle but much more prolongation at long CLs. The average increase of APD at a long CL (2.5 or 3.5 sec) compared to a short CL (0.5 sec) was significantly prolonged in PF (196 ± 22 to 250 ± 35 msec; n= 8, $P \leq 0.05$) while it did not change significantly in VM (107 ± 21 to 103 ± 20 msec; n= 12) in 8 experiments.

Thus, the hallmark of PF APs to prolong dramatically with slowing of the stimulation rate observed in other species, particularly the dog, is also true in the rabbit. Similarly to the observation of Antzelevitch and Sicouri [21] in M cells, PF APs in the rabbit heart seldom if ever displayed phase 4 diastolic depolarization.

Instantaneous and time dependent changes in APD following abrupt changes in CL under control conditions

Although steady state changes in APD reveal important marked disparity in durations at long CLs, instantaneous and time dependent changes in duration during abrupt transitions in CL are more relevant to the generation of TdP arrhythmias. Slow adjustment of APDs to changes in CL may take several minutes to lengthen or shorten to a new steady state. Both qualitative and quantitative differences in the adjustment of APD to abrupt changes in CL occurred in the

three cell types as illustrated in fig. 3. The immediate effect after an increase in CL was an abrupt increase in APD in the Purkinje cell but a sharp decrease in both the T and VM cells. This was followed by a gradual increase in APD in all cells which continued to increase for the duration of the CL change. The gradual time dependent increase in APD was greatest in the specialized conducting cells and least in VM. Upon transition back to the shorter BCL there was an abrupt further increase in APD in all cells which peaked only after several seconds followed by an exponential decline back to the original values present before the CL change. It was difficult to hold impalement in VM cells throughout the transitions in CL but in all cases the changes in APD in these cells upon abrupt increases in CL was both qualitatively and quantitatively different from changes in free running Purkinje cells creating even larger disparities in APD between the cells at the two recording sites. The greatest disparities occurred after several minutes at the long CL and immediately after returning to a short BCL.

The quantitative changes in the T cells depended upon their proximity to either PF or VM cells. The APD of the T cell shown in fig. 3 which was recorded close to the free running strand followed more closely the changes in the Purkinje cells. Fig. 4 shows the CL dependent changes in two other T cells remote from the Purkinje strand and an adjacent VM cell recorded simultaneously. All of the changes in these T cells follow more closely those in the VM cell. Following abrupt transition to the longer CL the initial shortening of the APs is so marked (as occurs in VM) that the APD barely attains its value at 0.5 sec even after

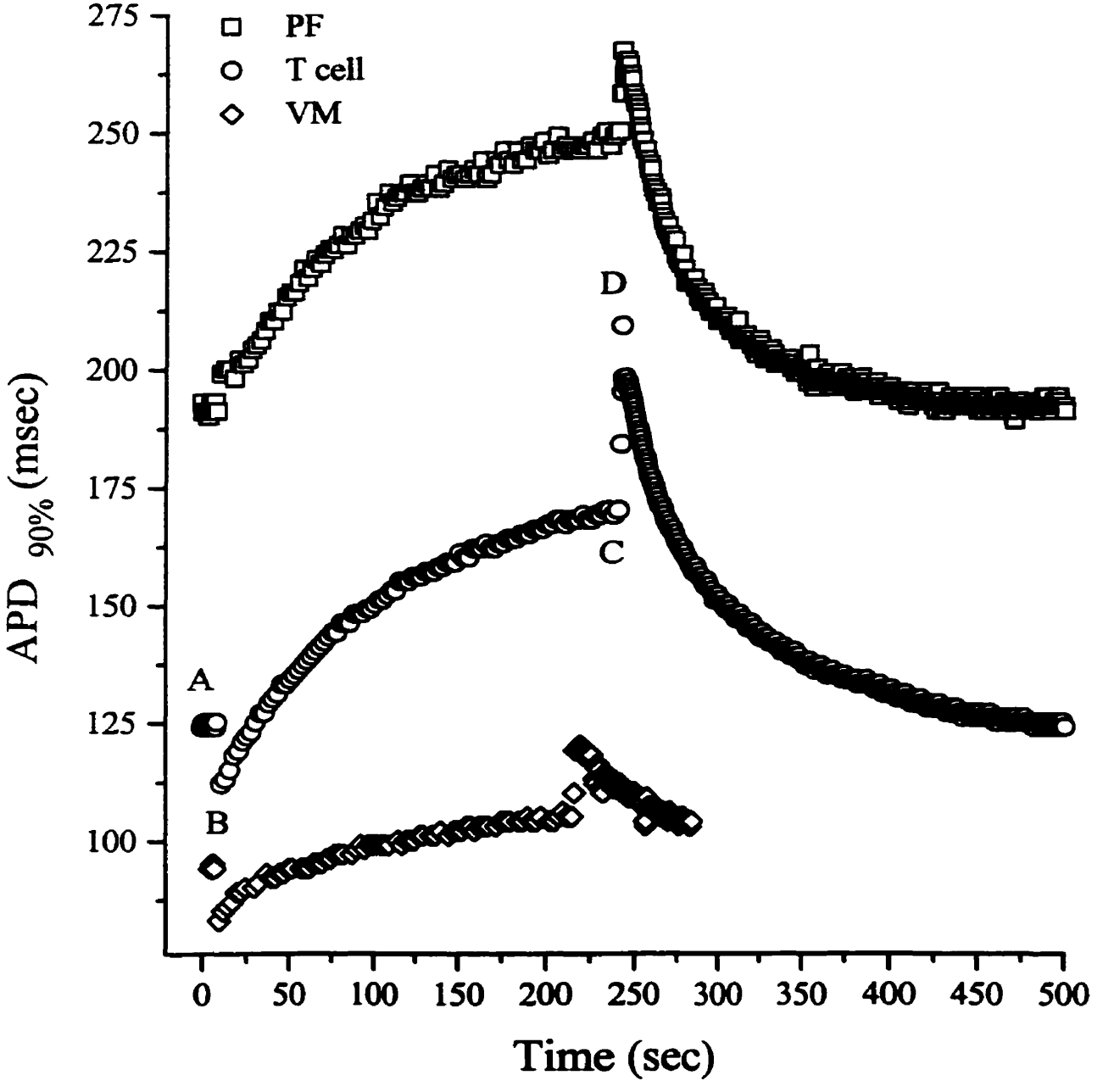
PF
T cell
VM
275
250
225
200
175
150
125
100
APD 90% (msec)
A
B
C
D
0
50
100
150
200
250
300
350
400
450
500
Time (sec)

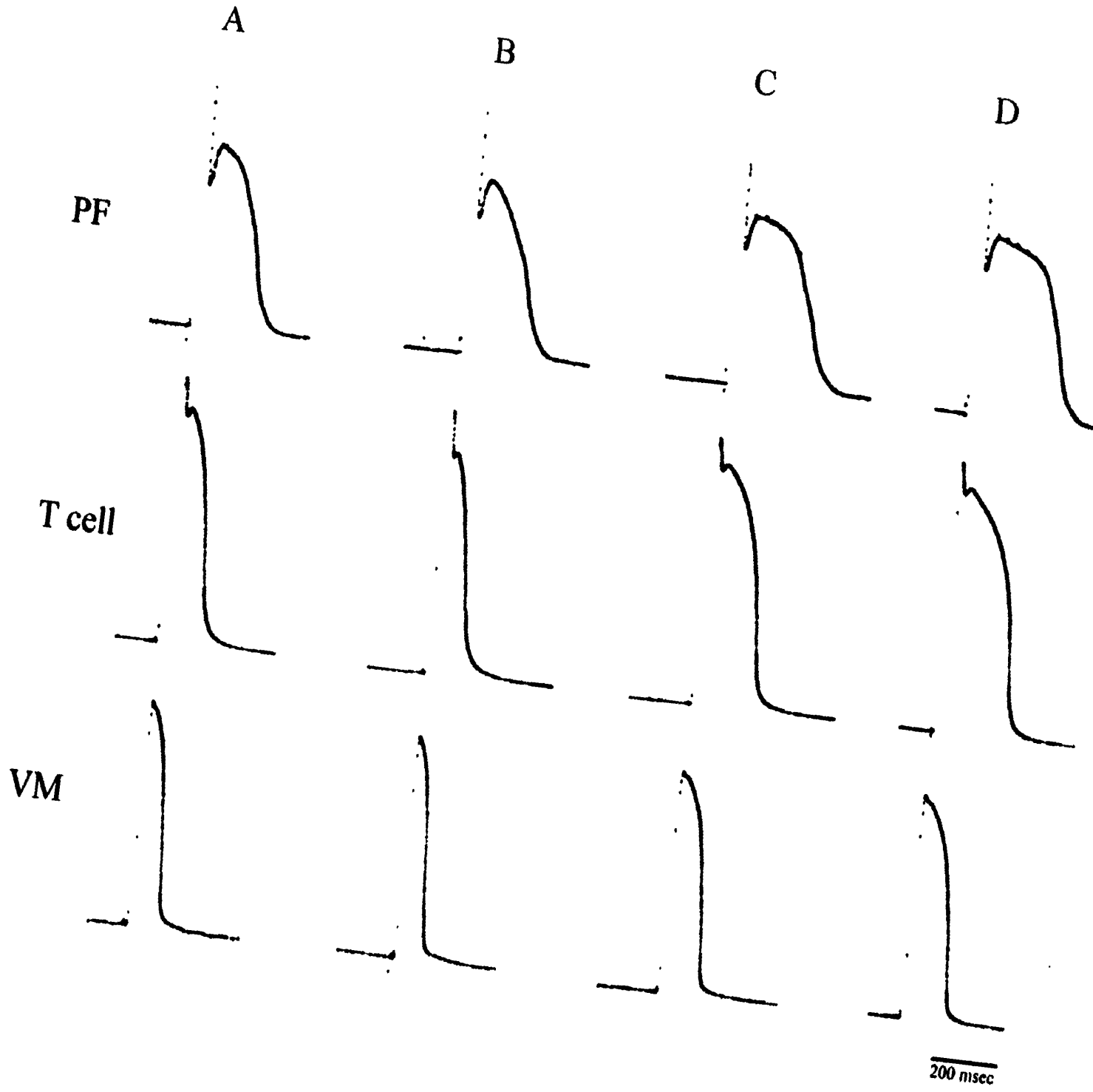
A
B
C
D
PF
T cell
VM
200 msec

Figure 3. Upper panel: Typical example of the time dependent changes in $APD_{90\%}$ in PF, T cell near the free running strand and VM at the tip of the papillary muscle following abrupt changes in CL from 0.5 to 2.5 sec and back to 0.5 sec. APs were recorded simultaneously from the PF and T cell recording sites. Time dependent changes in the VM cell was recorded in a subsequent run and the changes were followed for a slightly shorter time. Lower Panel: A, B, C and D indicate the APs recorded from the PF, T cell and VM recording sites at the following times: at a CL of 0.5 sec just prior to the abrupt increase in CL, the first AP upon switching to the longer CL, the last AP at the longer CL and the AP with the maximally recorded duration upon switching back to the shorter BCL. Scale bar: 200 msec.

several minutes of stimulation at the longer CL. Thus the CL dependent changes observed in the T cells are influenced by their electrotonic coupling to either the free running Purkinje cells or adjacent VM cells.

All time dependent changes in APD were CL dependent, being accentuated at longer CLs. However, the major change in APD in the Purkinje cell in response to a further increase in CL was an increase in the slope of the duration curve over time whereas in the VM cell it was a greater shortening of the first APD following the CL change with little or no change in the slope of the curve. Changes in the T cells depended upon their proximity to PF or VM but usually consisted of a further shortening of the initial APD (as in VM) followed by an increase in the slope (as in PF).

Effects of *d*-sotalol on the instantaneous and time dependent changes in APD after abrupt changes in CL

The effects of 20 to 40 μM of *d*-sotalol were assessed on APD in specialized conducting cells and VM. *D*-sotalol increased APD in all cells at all CL studied. In transitional cells, (fig. 4) *d*-sotalol did not alter the instantaneous changes in duration observed upon abrupt changes in CL but profoundly affected the slope of the time dependent increase in duration at the slow CL. There was also a larger CL dependent shortening of APD upon switching to a longer CL and a larger overshoot upon switching back to the shorter BCL as CL was lengthened.

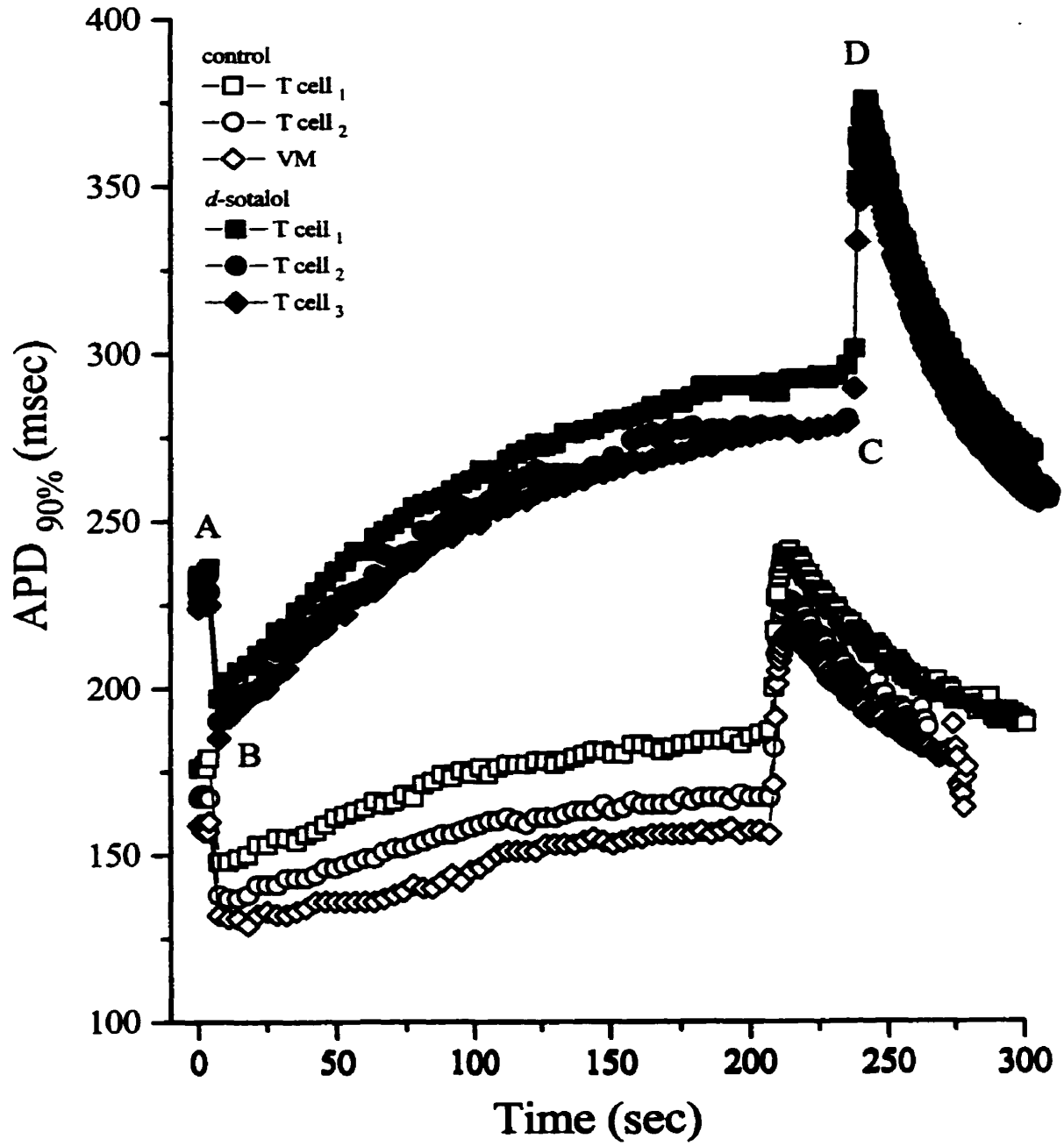
400
350
300
250
200
150
100
0
50
100
150
200
250
300
APD 90% (msec)
Time (sec)
control
T cell 1
T cell 2
VM
d-sotalol
T cell 1
T cell 2
T cell 3
A
B
C
D

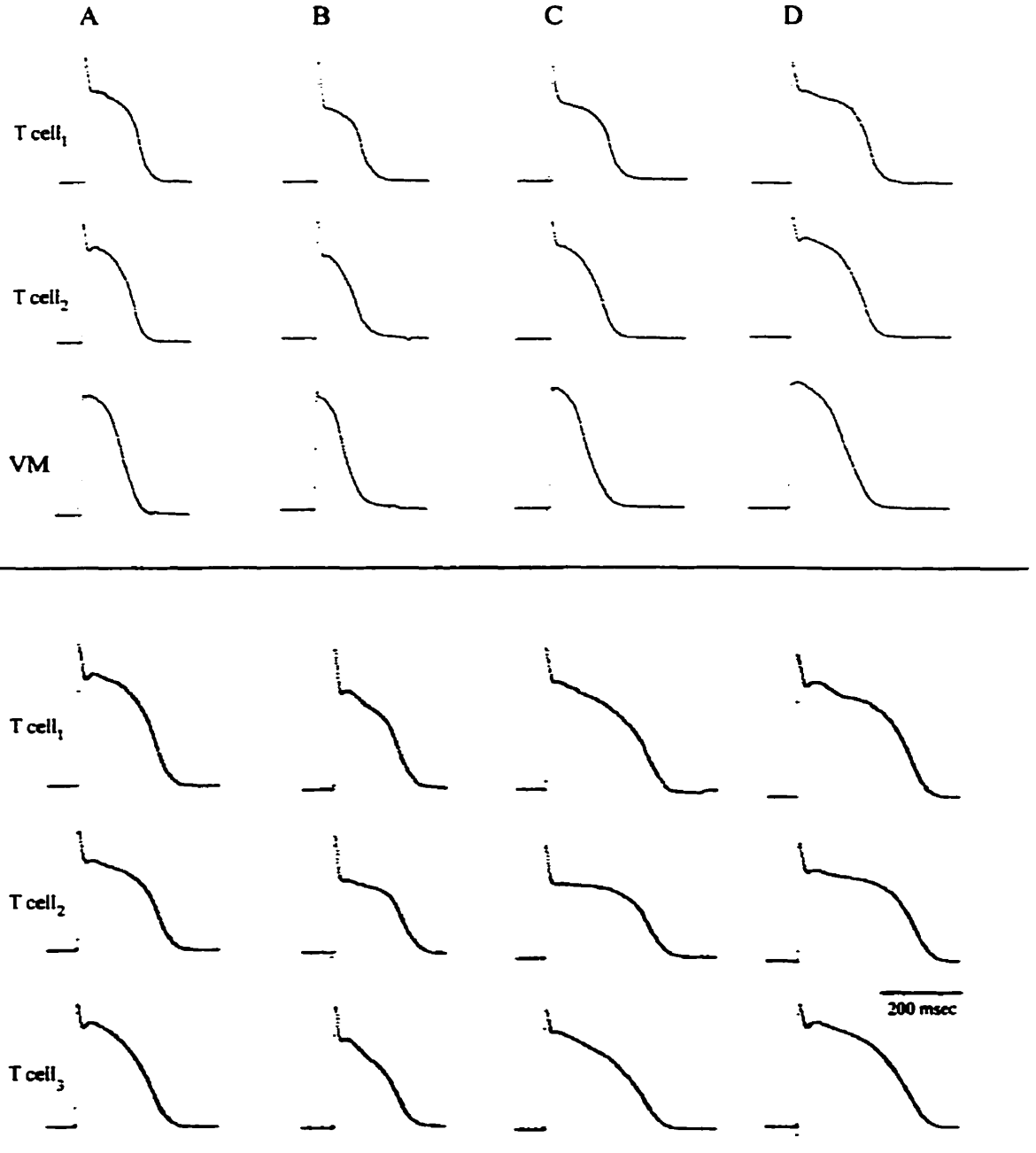
A
B
C
D
T cell1
T cell2
VM
T cell1
T cell2
T cell3
200 msec

Figure 4. Typical example of the time dependent changes in $APD_{90\%}$ in two T cells recorded more peripherally and an adjacent VM recorded simultaneously during abrupt changes in CL from 0.5 sec to 3.5 sec. A, B, C and D indicate the APs recorded at a CL of 0.5 sec, the first AP following the CL change, the last AP at the longer CL and the AP with the maximally recorded duration following an abrupt change in CL back to 0.5 sec. Note the two different configurations in the T cells. Scale bar: 200 msec. This figure also shows the effects of 20 μM *d*-sotalol on 3 T cells simultaneously recorded in the same preparation. T cell 2 was the same impalement as held under control conditions; the other two were in a similar area but different cells.

Fig. 5 illustrates a typical example of the effects of *d*-sotalol on the time dependent changes in APD in a PF recorded from a free running strand and a more peripheral T cell. At the BCL of 0.5 sec there was a greater lengthening of APD in the PF than in the T cell. Upon an abrupt increase in CL to 1.5 sec, the instantaneous increase in APD in the PF and decrease in APD in the T cell was similar to that seen under control conditions suggesting that the ionic mechanism of this effect was perhaps unrelated to the actions of *d*-sotalol. In both cells the gradual time dependent increase in APD at the longer CL was characterized by a greater slope when compared to control but much more pronounced in the PF. Thus the most marked increases in APD always occurred in the PF in the free running strand.

D-sotalol always produced marked lengthening of the APD in PFs with minimum lengthening of duration in VM. The drug produced a gradation of effect with maximal effect being observed in the free running PFs, a lessor effect in peripheral Purkinje and transitional fibers and least effect in VM.

This selective effect on duration in Purkinje cells was accentuated at progressively longer CLs as illustrated in fig. 6. At a CL of 1.5 sec there was a gradual increase in APD. At 2.5 sec the slope of the increase in APD was much steeper. Fig. 6 illustrates the marked disparity in APD between the Purkinje cell and the T cell under drug conditions versus control. This effect is further enhanced

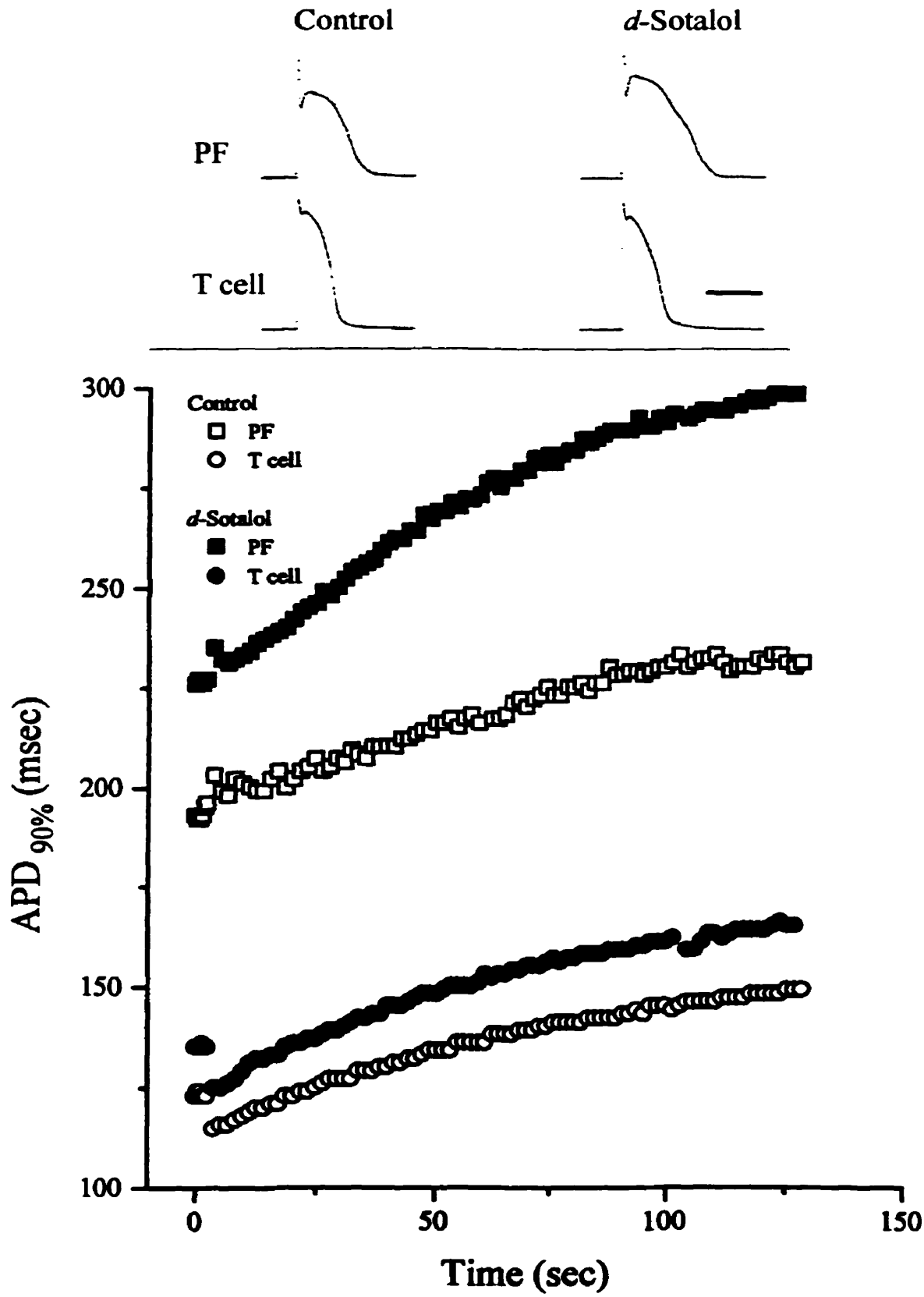
Control
d-Sotalol
PF
T cell
300
250
200
150
100
Control
PF
T cell
d-Sotalol
PF
T cell
APD 90% (msec)
0
50
100
150
Time (sec)

Figure 5. Typical example of the effects of *d*-sotalol (20μM) on the time dependent changes in $APD_{90\%}$ in PF compared with that in a T cell. CL was changed abruptly from 0.5 to 1.5 sec. Preparation was exposed to drug for 30 minutes. APs shown were recorded from the PF and T cell under control and drug conditions during maximal changes at the 1.5 sec CL. Scale bar: 200 msec.

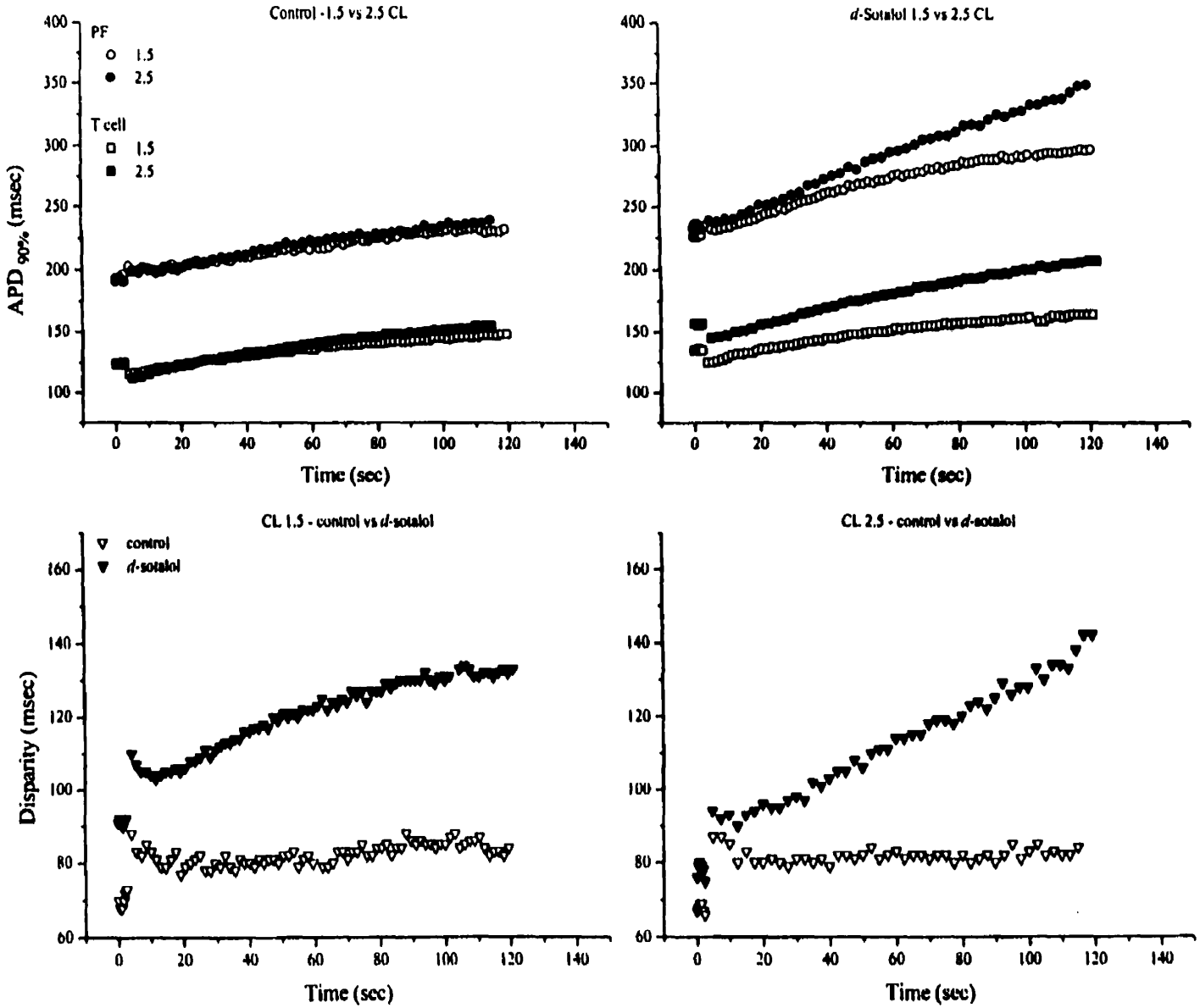
Control - 1.5 vs 2.5 CL
PF
1.5
2.5
T cell
1.5
2.5
APD 90% (msec)
Time (sec)
d-Sotalol 1.5 vs 2.5 CL
Time (sec)
CL 1.5 - control vs d-sotalol
control
d-sotalol
Disparity (msec)
Time (sec)
CL 2.5 - control vs d-sotalol
Time (sec)

Figure 6. Typical example of the CL dependent changes in APD in a PF compared to a T cell following superfusion with *d*-sotalol (20 μM). Note greater change in disparity in the PF in the presence of sotalol. Disparity is more pronounced at the longer CL.

at a 2.5 sec CL. Eventually triggered APs occurred in the presence of drug and further effects of CL could not be studied.

Initiation of triggered APs by *d*-sotalol at long CLs

In the presence of *d*-sotalol, 20-40 μM, unlike control conditions, triggered APs eventually occurred if the CL was sufficiently long and maintained for a sufficient length of time. Panel A of fig. 7 illustrates a typical example. Following an increase in CL there was a progressive lengthening of APD in both the PF and the T cell until coupled APs occurred. However, the effect in the PF was much more marked. Coupling was maintained if the long CL was maintained. Note the electrotonic interaction between the coupled response in the T cell and the PF with longer APD, thus causing a further prolongation of the APD in the PF cell. Thus, coupled responses in the T cell were accompanied by fused responses in the Purkinje cell. Panel B illustrates the marked differential effect of drug on $APD_{90\%}$ in the PF versus the T cell adjacent to muscle. There was approximately a 300 msec difference in duration between these two cells just prior to coupling. Once coupling occurred, coupled APs (singlets) in the T cell were accompanied by a fused response of greater than 900 msec in the Purkinje cell. APDs continued to increase until singlets became couplets.

Whether an abrupt increase in CL resulted in coupled APs appeared to depend upon the CL and the accompanying rate of increase in APD in the PF cell.

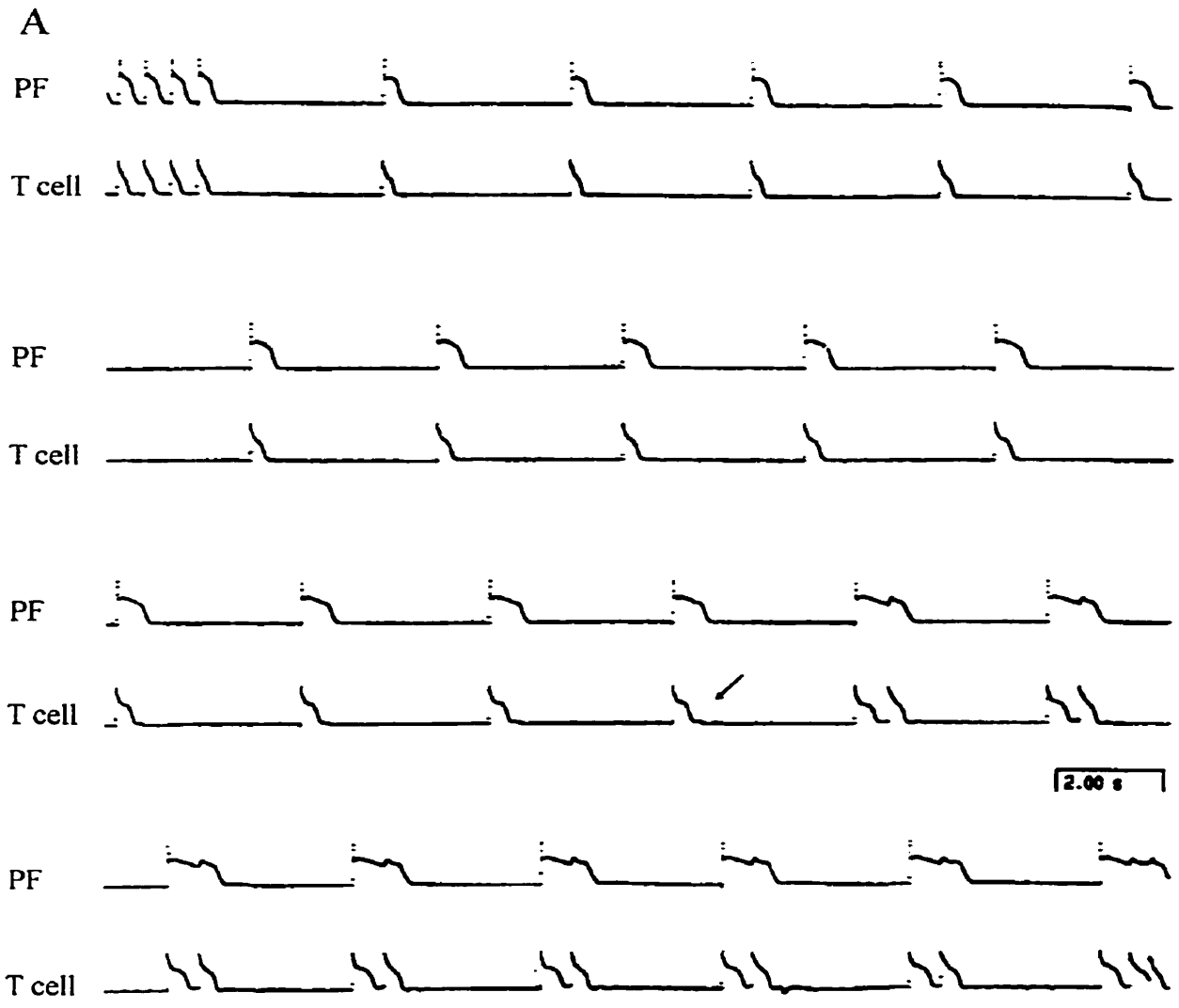
A
PF
T cell
PF
T cell
PF
T cell
2.00 s
PF
T cell

B

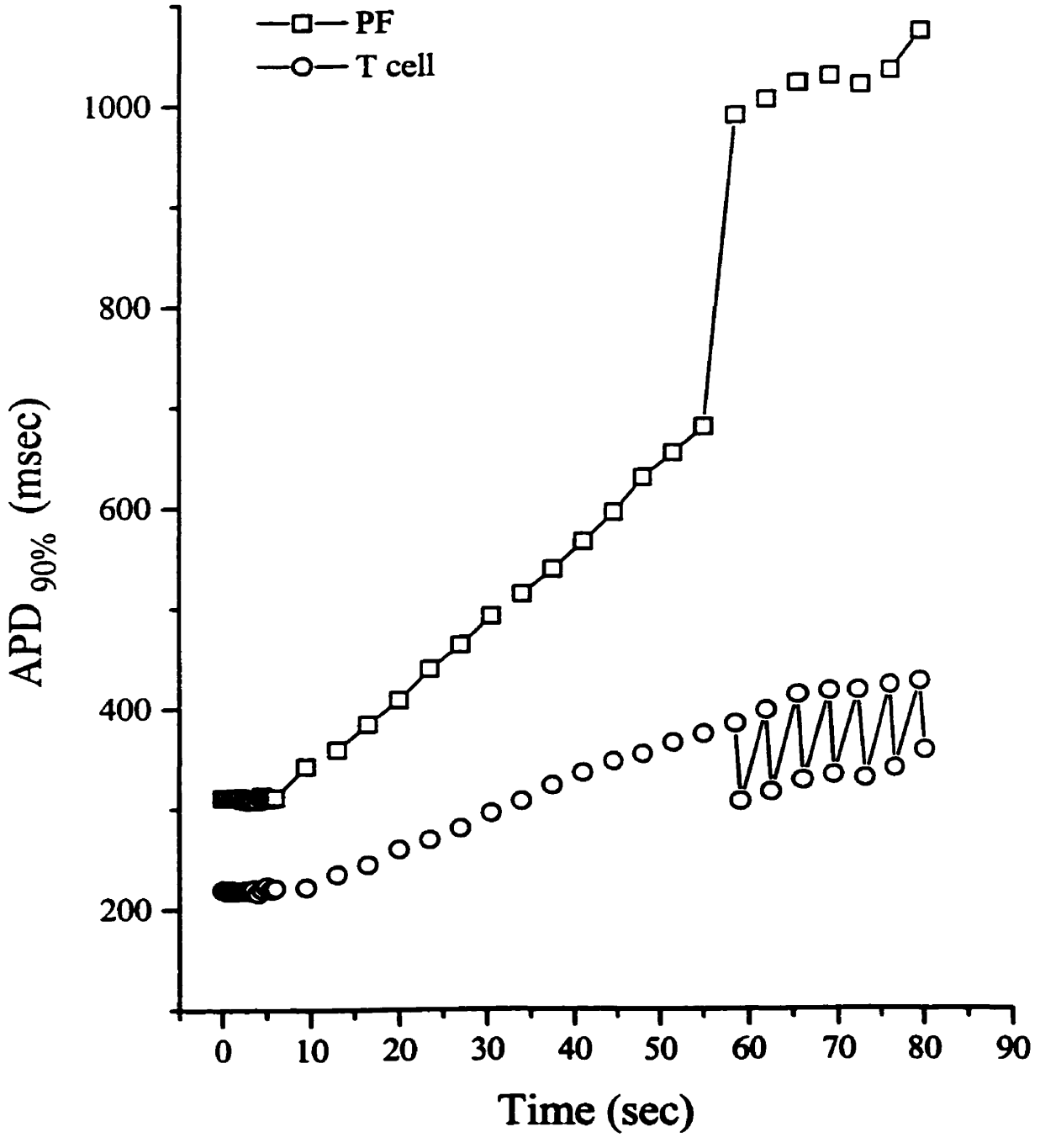
PF
T cell
1000
800
600
400
200
APD 90% (msec)
0
10
20
30
40
50
60
70
80
90
Time (sec)

Figure 7. Initiation of triggered activity in the presence of *d*-sotalol (40μM) following abrupt increases in the CL. A. Each panel shows APs recorded from a free running Purkinje strand and a T cell. All of the traces are continuous. CL was changed from 0.5 sec to 3.5 sec. B. Changes in $APD_{90\%}$ plotted versus time. Note more marked increase in APD in Purkinje cell than in the T cell prior to triggering. During triggering, coupled responses in the T cell were accompanied by an increase in duration of the fused response in the Purkinje cell to over 900 msec.

A

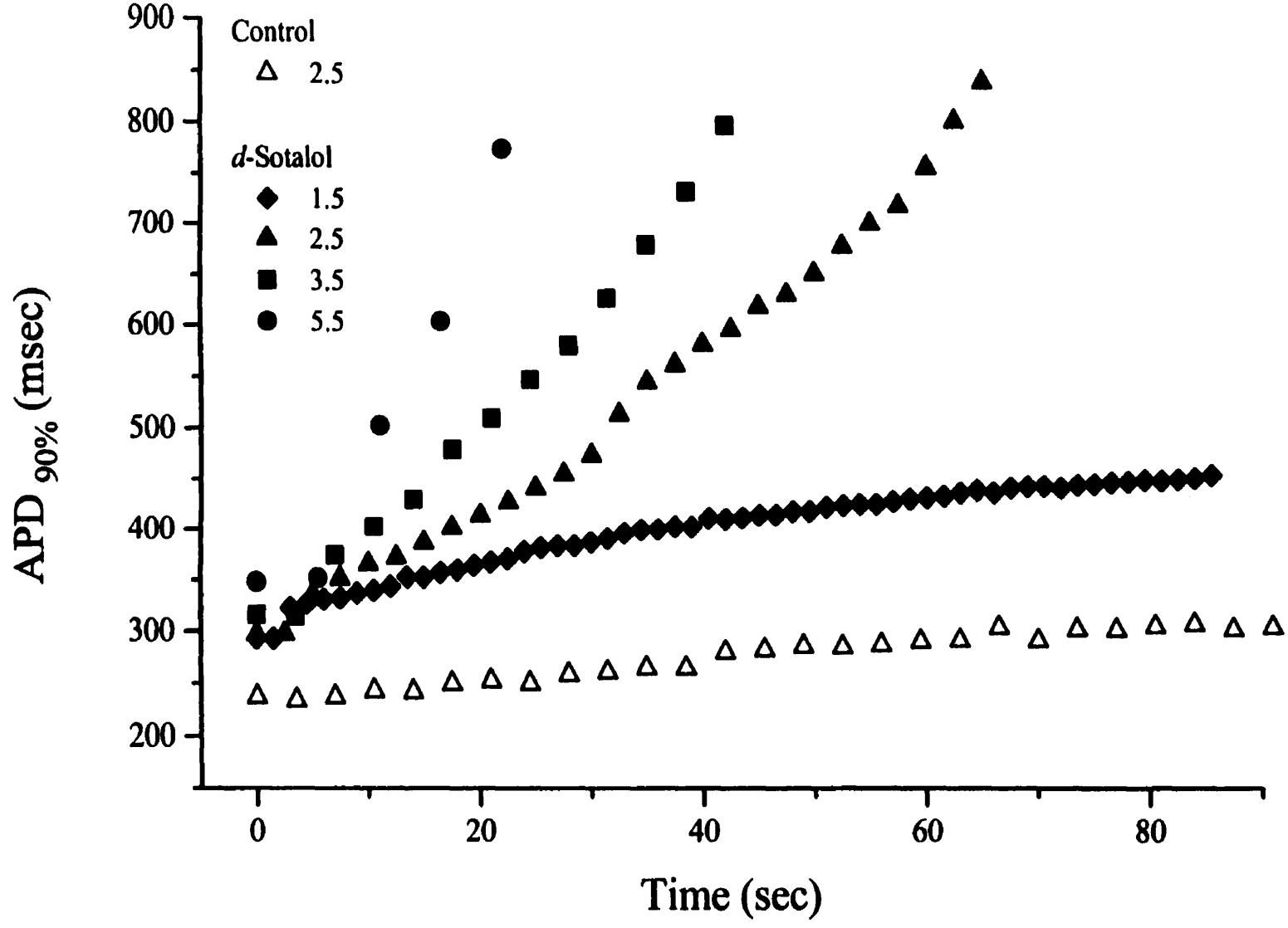
900
800
700
600
500
400
300
200
Control
2.5
d-Sotalol
1.5
2.5
3.5
5.5
APD 90% (msec)
0
20
40
60
80
Time (sec)

B

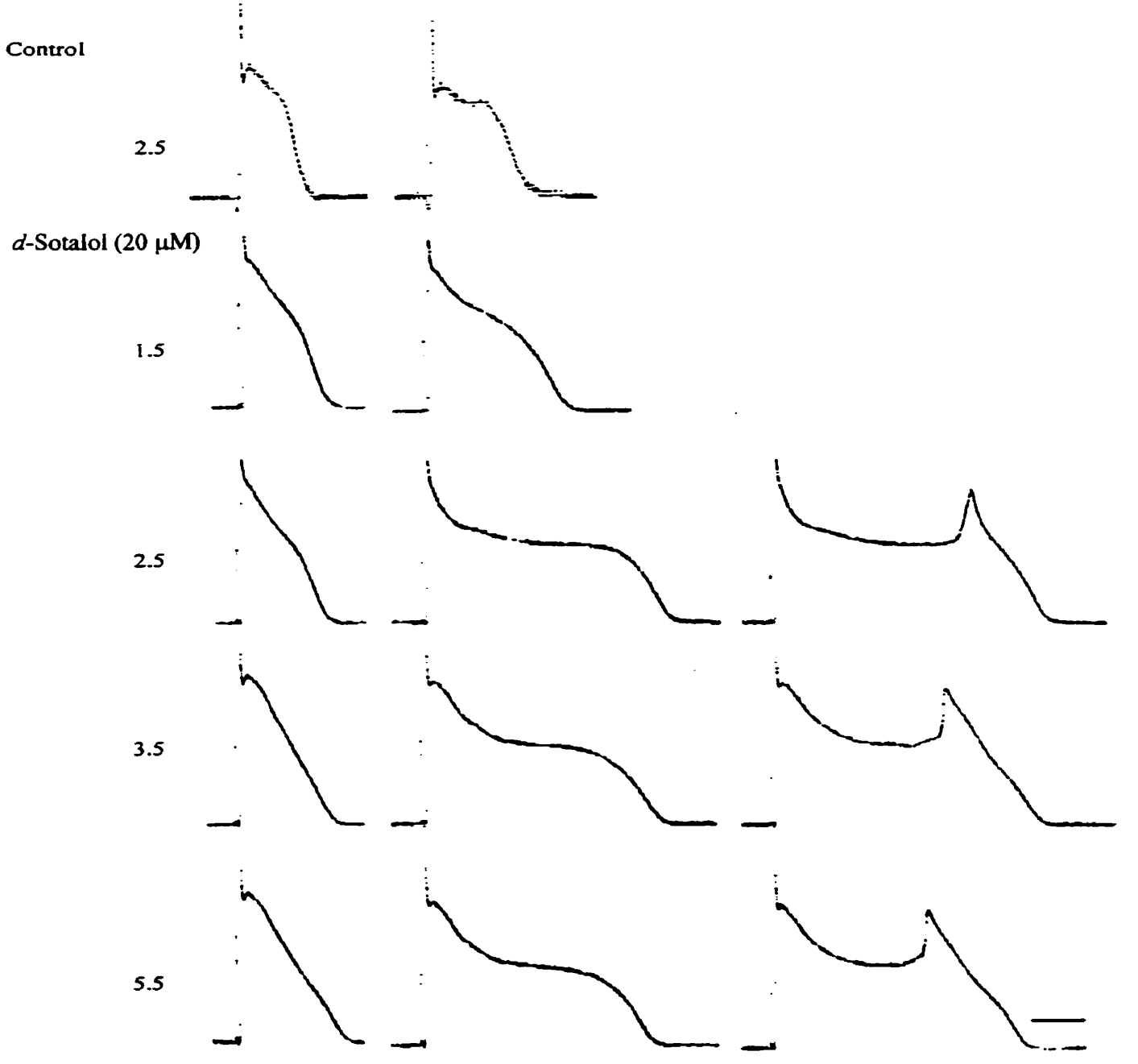

Figure 8. A. Effects of *d*-sotalol (20 μM) on the initiation of triggered activity is dependent on CL. The graph shows the changes in $APD_{90\%}$ following an abrupt increase in CL from 0.5 to 1.5, 2.5, 3.5 and 5.5 sec. Changes in APD are plotted up to the point of triggering in the presence of drug. B. First column of APs shows the last APs recorded at the basic CL of 0.5 sec under control and drug conditions. The second column shows the steady state control AP at a Cl of 2.5 sec, the steady state AP in the presence of drug at a CL of 1.5 sec and the last AP prior to triggering in the presence of drug and a CL of 2.5, 3.5 and 5.5 sec, respectively. The last column shows the first triggered AP in the presence of drug and a CL of 2,5, 3.5 and 5.5 sec, respectively. Note that a similar duration is reached prior to triggering regardless of CL. Also note that the triggered response occurs earlier at longer CLs. Scale bar: 200 msec.

A typical example is illustrated in fig. 8. In the presence of a CL of 1.5 sec the APD continued to increase for 5 minutes at a slow slope but no coupling occurred (curve truncated at 85 sec). However, at 2.5 sec CL, the rate of increase in APD was much more rapid. When APD reached a value exceeding 800 msec, triggered APs occurred. At 3.5 and 5.5 sec the slope of the APD/time relation was even steeper. Each time the APD in the PF cell reached a certain critical value (in this preparation approximately 800 msec) triggered APs occurred (fig. 8B). Thus, a similar value of APD was reached prior to triggering regardless of the CL. It was merely reached more quickly and with a lessor number of beats, suggesting that the crucial factor for triggering was not the CL but rather the absolute value of APD attained. There was, however, CL dependency in the coupling interval of the triggered AP. At each longer CL the triggered AP occurred earlier on the plateau of the AP. A similar effect was observed in 12 out 14 preparations in which similar protocols were applied. The critical APD of PF cells associated with coupling ranged from 400 to 928 msec (629 ± 205 msec, n=15).

Triggered APs occurred only in specialized conducting cells and never in VM cells but subsequently conducted to VM as coupled beats. Whether triggered activity originated only in PF cells in the free running strands or from T cells as well could not be confirmed but it was clear that the entire specialized conducting system played a role. Fig. 9 illustrates an example suggesting that perhaps the long APD in the PF cells electrotonically generates triggered APs in the adjacent T cells which are then conducted to VM. The upper panel shows APs obtained from

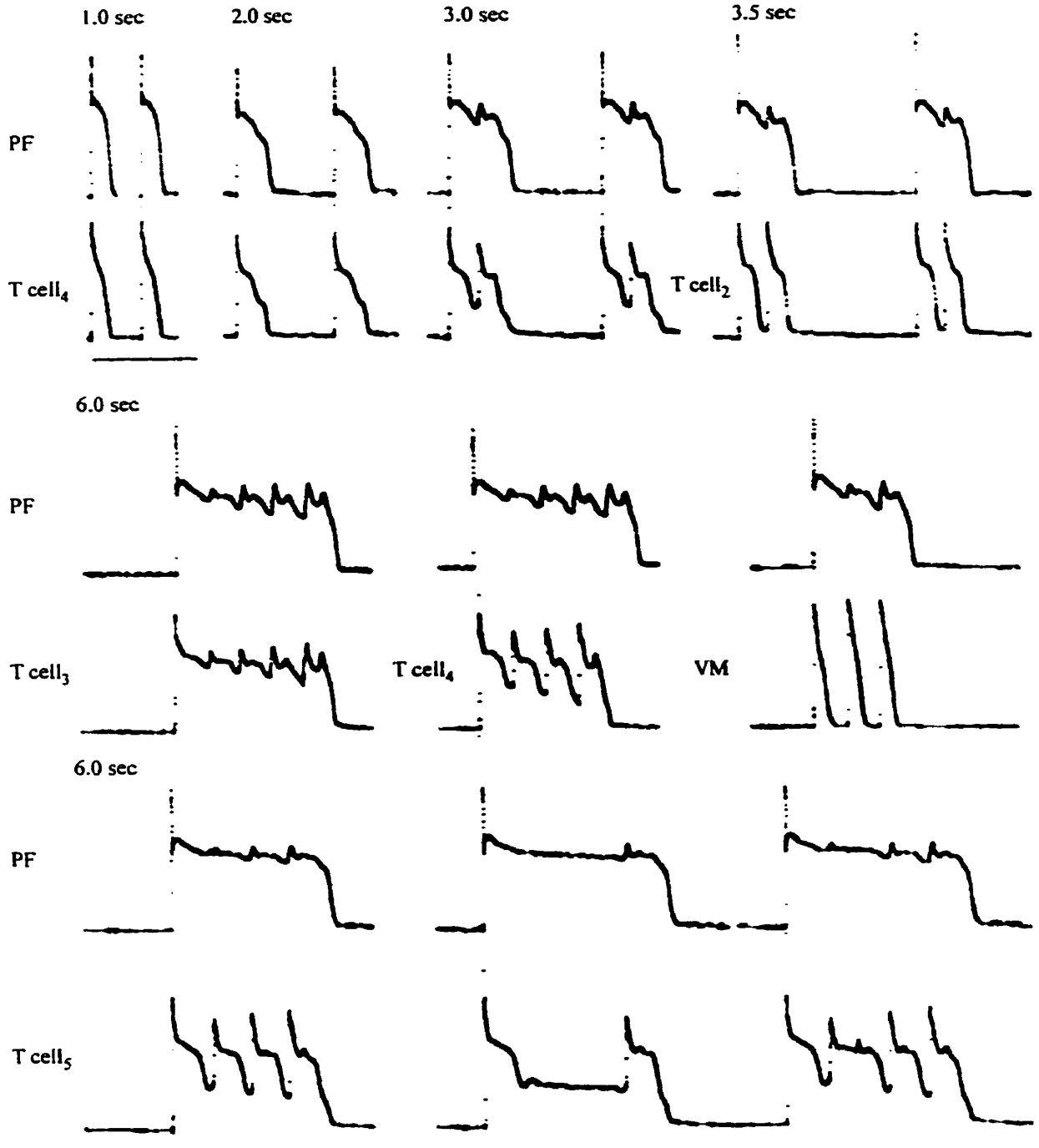

Figure 9. Multiple triggered activity at progressively longer CLs. In each panel the top trace is a record from a PF in a free running strand. The impalement was maintained in this cell throughout the experiment. The bottom traces shows APs obtained from a variety of T cells and from VM. The preparation was stimulated at a CL ranging from 1 sec to 6 sec as indicated. Scale bar: 2 sec.

a PF and an adjacent T cell during increases in CL from 1 to 1.5 to 2 seconds. As the CL was increased to 1 sec the AP lengthened in the PF. This was accompanied by a prominent electrotonic "hump" in the T cell. At a longer CL (2 sec) an AP was triggered off the electronic "hump" in the T cell which then appeared to be reflected back to the PF. When the T cell electrode was moved to a more peripheral site, full blown coupled APs were observed at that site. At an even longer CL (6 sec), multiple triggered activity occurred. While maintaining impalement in the PF, records were obtained from multiple peripheral sites including VM. The middle and bottom panels suggest that triggered activity occurs only in specialized cells and is conducted to VM cells which continue to have short APs. Since activity is observed in the free running PF only when there is activity in the T cells (bottom panels) it suggests that triggered activity is occurring in the T cells and propagating to VM while being reflected back to the long duration Purkinje cells. Propagation to VM results in coupled and multiple beats. Reflection to PF results in further prolongation of the AP which then acts either as a refractory barrier or as a source of depolarizing current to bring the T cells to threshold. This type of mechanism is suggested further in fig. 10 in which prolonged multiple activity is present in the T cell while the PF AP remains depolarized. This latter type of activity was observed only at extremely long CLs and was rarely seen in these preparations unless stimulation was stopped for a period of time and a single pulse was delivered to the preparations. Similar multiple triggered activity was observed in 5 preparations under similar conditions.

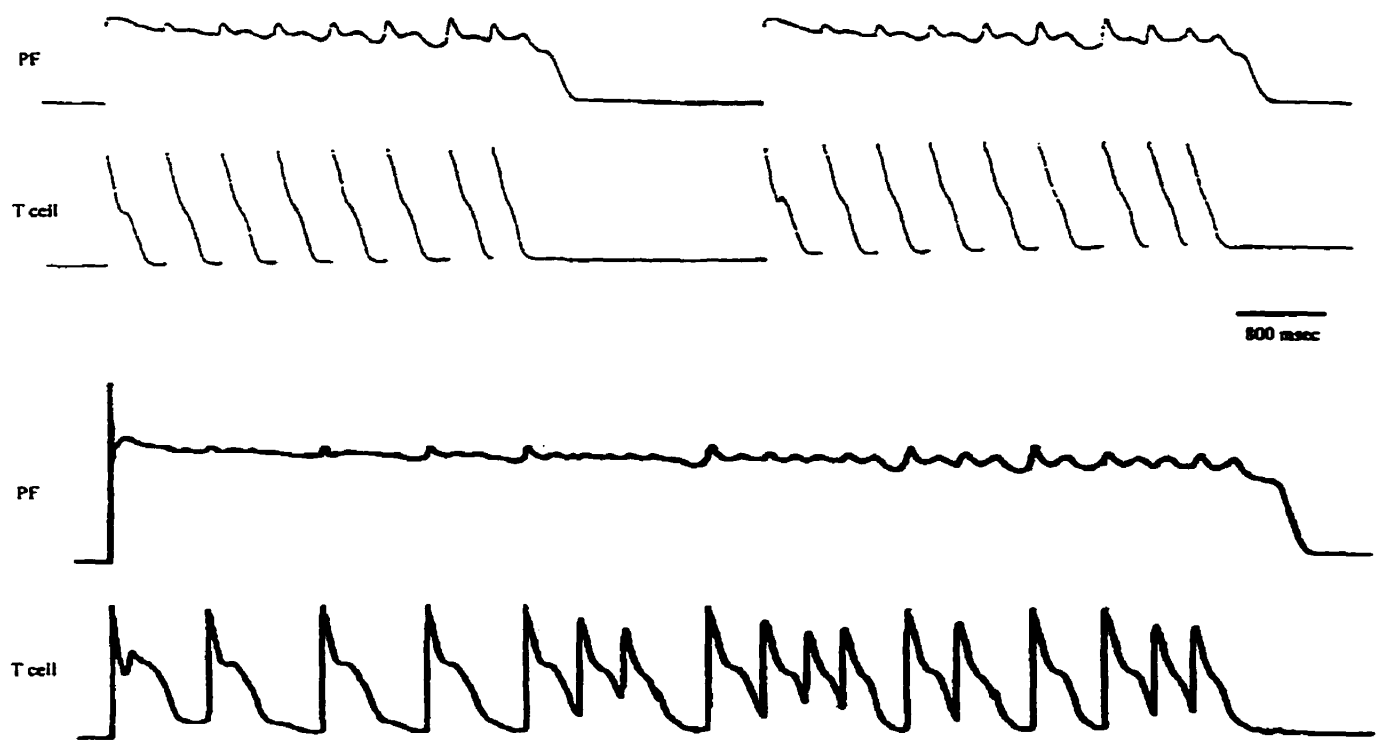

Figure 10. Multiple activity in a T cell reflected back to a PF cell suggesting that PF is acting as a refractory barrier. Preparation exposed to 40 μM *d*-sotalol. Top traces were recorded at a CL of 6 sec. In the bottom traces activity was recorded after a 35 sec pause in stimulation.

At very high doses (80μM) and after a period of termination of stimulation, recurrent triggered activity could be observed on rare occasions in both T cells and the free running Purkinje cells as shown in fig. 11. Again the Purkinje cell in the free running strand remained depolarized throughout the period of recurrent triggered activity in the T cell. There was clearly an interaction between activity at the two recording sites.

IN SITU EXPERIMENTS

In order to assess whether the changes that were observed *in vitro* corresponded to those occurring *in situ* we determined CL dependent changes in repolarization in the ventricles of Langendorff perfused rabbit hearts using MAP recordings. In order to assess repolarization changes in specialized conducting cells, MAPs were obtained from endocardial recording sites; to monitor changes in VM, MAPs were obtained from epicardial sites. Using the same protocols as under *in vitro* conditions we assessed CL and time dependent changes in MAPDs under control conditions. Fig. 12 shows a typical example. It is evident that the changes in MAPDs observed *in situ* reflect the changes in specialized conducting cells and VM observed *in vitro*. The changes observed on the endocardial MAPs reflect the changes observed in transitional cells adjacent to free running PFs in that the immediate response to a CL increase is a shortening of MAPD. The changes observed were CL dependent as under control conditions.

Figure 11. Spontaneous recurrent triggered activity in a T cell at very high doses of *d*-sotalol (80 μM) when stimulation was stopped for 2 min. Activity in PF indicates both independent triggered activity and interaction with activity in the T cell.

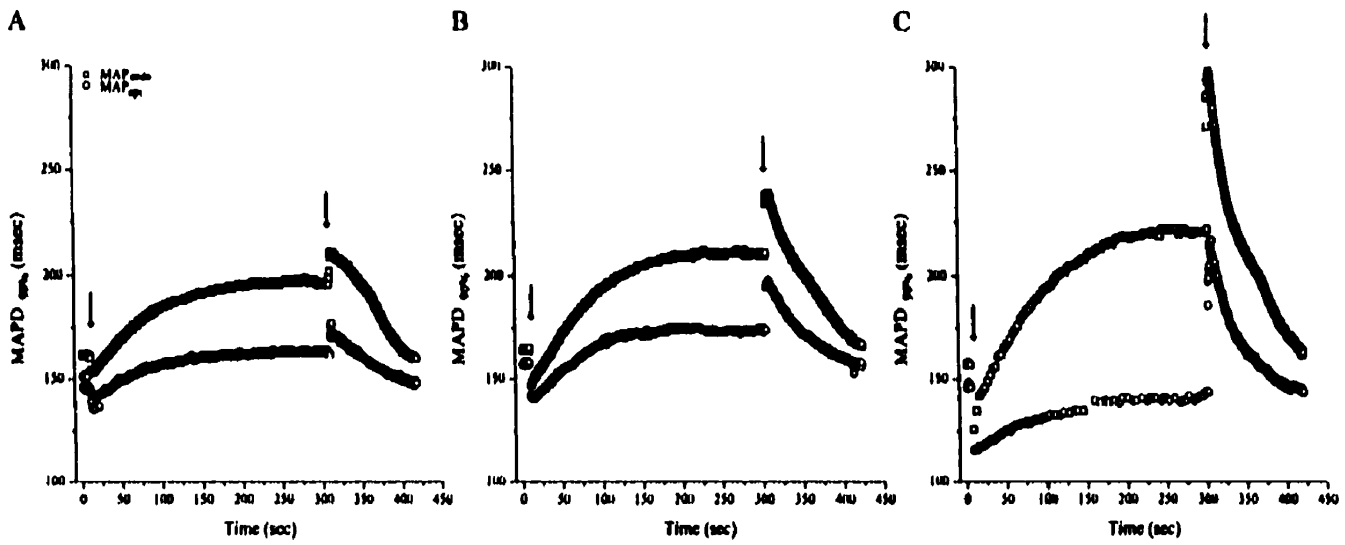

Figure 12. Time dependent changes in $MAPD_{endo}$ and $MAPD_{epi}$ following a change in CL from 0.5 to 0.8, 1.5 and 3.5 sec under control conditions.

We postulated that the same conditions which led to triggered APs *in vitro* should lead to coupled beats in the isolated Langendorff perfused heart. In 4 experiments, *d*-sotalol was administered to the *in situ* heart in which the AV node was blocked and the ventricles were paced. After equilibration with 20 μM of *d*-sotalol the pacing CL was increased to 1.5 sec while monitoring activity from the endocardium and epicardium. At a pacing CL of 1.5 sec coupled beats occurred which were eliminated each time the CL was switched back to 0.5 sec. Fig. 13 shows a typical example. The top panel shows a progressive increase in $MAPD_{endo}$ with minimal changes in MAP_{epi} following an abrupt increase in CL from 0.5 to 1.5 sec. When a critical disparity of over 200 msec is reached coupled beats occur (as indicated on both the ECG and the MAP_{epi}) accompanied by a fusion beat at the endocardial recording site. Changes in the QT interval paralleled the changes in the MAP_{endo}. This is essentially similar to what we observed *in vitro* (vide supra fig 7) and provides compelling evidence that the mechanism of initiation of the coupled beats *in situ* is triggered activity originating in PFs. The average increase in $MAPD_{endo}$ associated with coupling was 408 ± 74 msec, while the average increase in $MAPD_{epi}$ was 244 ± 35 msec at a CL of 1.5 sec.

The hearts which showed coupled rhythms *in situ* were then removed from the Langendorff set up, and a portion of the left ventricular endocardium was dissected and superfused under *in vitro* conditions in order to record intracellular

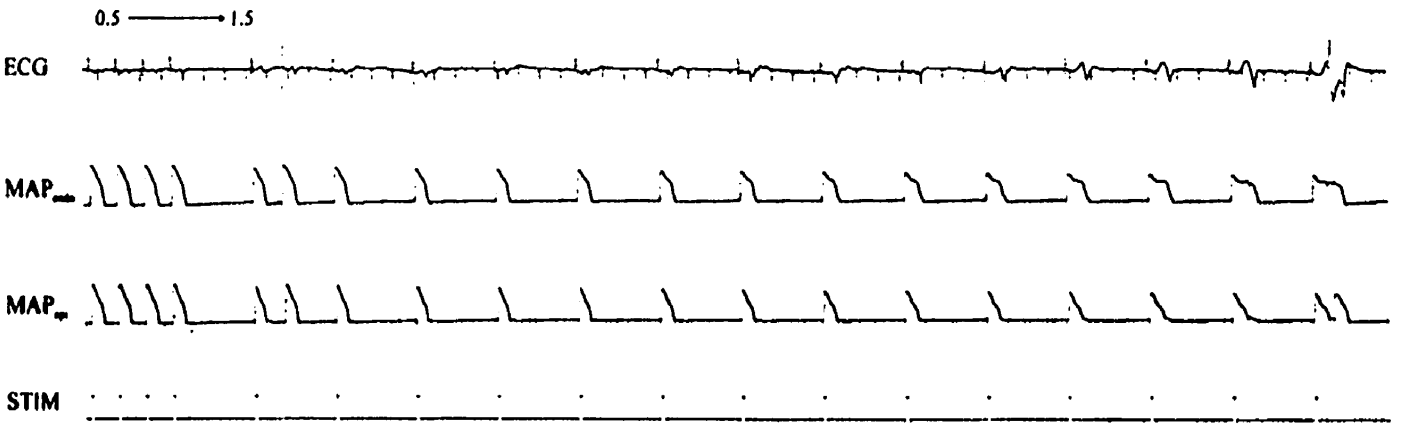
0.5
1.5
ECG
MAP
MAP
STIM

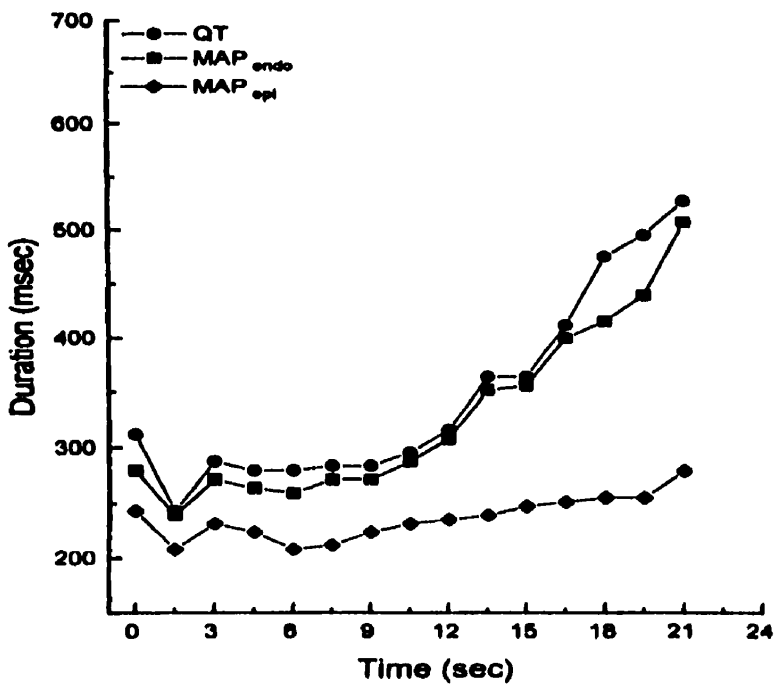
QT
MAP endo
MAP epi
700
600
500
400
300
200
Duration (msec)
0
3
6
9
12
15
18
21
24
Time (sec)

Figure 13. Generation of coupled beats in a Langendorff perfused rabbit heart following an abrupt increase in CL from 0.5 to 1.5 sec. Upper panel: shows an ECG trace together with MAP recordings obtained from the endocardial and epicardial surface and a stimulus artifact. Lower panel: graph showing the time dependent changes in QT interval and MAP_{endo} and MAP_{epi} following the CL increase and just prior to coupling.

activity from Purkinje cells and VM. When these preparations were subjected to the same protocols as *in situ*, triggered APs occurred in the recording from the PF with minimal effects seen in VM cells as illustrated in fig. 14. However, much longer CL were required to induce coupling under *in vitro* conditions (as observed above in hearts not Langendorff perfused).

In the *in situ* experiments we found that much smaller disparities in APD occurred in association with coupled beats than those observed in the vitro experiments. This is likely related to the fact that MAP recordings from endocardial sites reflect a composite of PF and VM APDs.

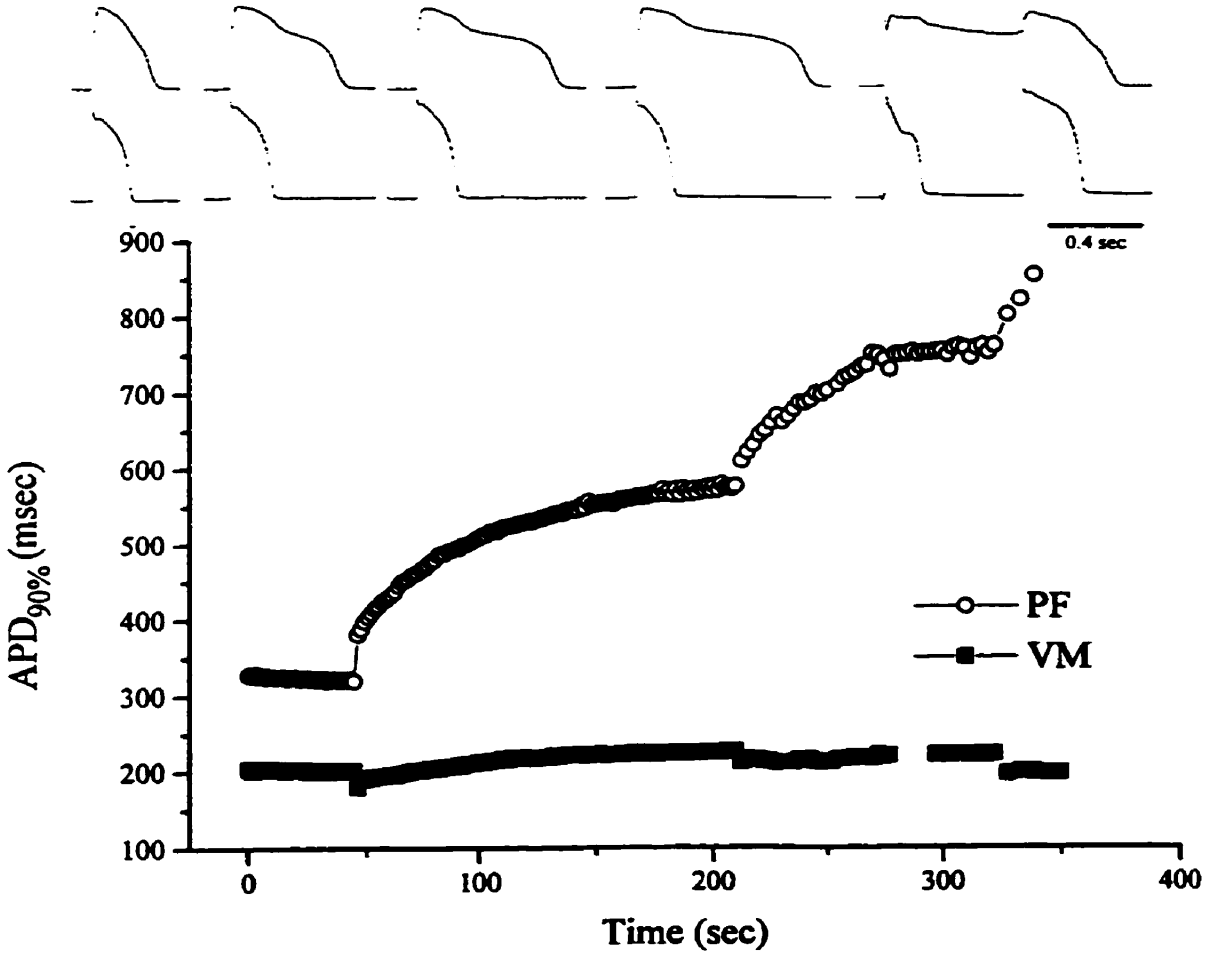

Figure 14. Differential time and CL dependent changes in $APD_{90\%}$ in a PF and VM cell recorded simultaneously. The CL was increased progressively from 0.5 sec to 1.5, 2.5, and 5.5 sec, respectively. Top traces show the last APs recorded at CLs of 0.5, 1.5, and 2.5 sec, the APs prior to coupling at 5.5 sec and the first coupled response. Preparation was taken from a heart in which 20 μM *d*-sotalol was administered during Langendorff perfusion. Under *in situ* conditions, the heart showed coupled beats at CL of 1.5 sec or greater.

Discussion

The most important finding in this study is the clear association between disparity in repolarization on the endocardial surface in the rabbit ventricle and the generation of triggered activity in PFs *in vitro* and coupled beats in the intact isolated heart. Only PFs uniquely displayed prolonged APDs and triggered activations. PFs (or transitional Purkinje cells) were thus the site of origin of triggered activations. Triggered activations occurred only after the attainment of certain critical APDs in the free running Purkinje strands *in vitro* and endocardial MAPs *in situ*. This study provides compelling evidence that the mechanism of initiation of coupled beats in the intact heart is triggered activity originating in PFs on the endocardial surface of the rabbit ventricle. Unlike previous studies, the conditions which led to coupled beats in the intact heart were identical to those which led to triggered activity in the *in vitro* preparations.

The results clearly show that *d*-sotalol produces a differential CL dependent prolongation of repolarization in the rabbit ventricle. *D*-sotalol produced marked lengthening of the APD and EADs in specialized conducting fibers with minimum lengthening of duration in VM. A gradation of effect was observed with maximal effect occurring in the free running PFs, a lessor effect in peripheral Purkinje and transitional fibers and least effect in VM.

The reason for the altered sensitivity of the specialized conducting cells to the actions of the drug is not known but likely related to differences in the contribution of a number of different ionic currents to repolarization in these cells versus VM cells. Paquette et al. [22] showed recently that a smaller I_{Kr} current density is present in Purkinje cells versus either endocardial or epicardial myocytes in the rabbit ventricle. Furthermore, Purkinje cells displayed a relatively flat steady state IV relationship compared to myocytes from endocardial and epicardial tissues indicating that only small changes in outward current can produce large changes in repolarization. On the other hand, there was no difference in the I_{To} current density in these cells. This may explain why PFs are more susceptible to prolongation of repolarization and generation of EADs and triggered activity.

Under control conditions at steady state, there was a biphasic CL dependent effect on APD in VM, an increase in APD occurring up to a CL of 1 sec and then a progressive decrease. This effect is likely related to the contribution of I_{To} to repolarization in these cells. As observed in fig. 3, the immediate shortening of APD following an increase in CL to 3.5 sec is so marked that even after more than 2 minutes at the long CL prolongation of repolarization in these cells does not even reach the value present at the BCL. This immediate shortening of APD is likely related to a recovery of the I_{To} current from inactivation in the rabbit ventricle at the longer CL. [23] This effect is not present in free running PFs as the major contribution of I_{To} in these cells is in the early repolarization phase

and not during phase 3 repolarization. (review) [24] Alteration of repolarization in VM and T cells is a complex interplay of at least two ionic currents, I_{Kr} and I_{To}. The relative contribution of these two currents to APD will depend on CL.

At the concentrations of *d*-sotalol used in this study only the I_{Kr} current would be inhibited by the drug. Thus, the greatest effect would be observed in those cells with the least I_{Kr} current to begin with and in which small changes in outward current would have the greatest effect on duration, ie., the PFs.

The relative importance of I_{Kr} to phase 3 repolarization in a specific tissue may thus be more important in determining the propensity toward exaggerated AP prolongation at slow heart rates than the mechanism of antiarrhythmic block of this channel. (review) [24] AP prolongation and proarrhythmia with *d*-sotalol exhibits concentration dependence in contrast to Class 1A drugs which exhibit reverse concentration dependence [25,26] Generation of triggered activity is more likely to occur at higher concentrations, longer CLs and lower K^+ concentrations. The larger the concentration of drug the less exposure time was required for generation of EADs. The effects of *d*-sotalol were concentration dependent, tissue dependent and CL dependent. The number of beats required to generate EADs in PFs were the least at high concentrations and long CLs under *in vitro* conditions. Much shorter CLs at similar concentrations were required to generate coupled beats in the *in situ* heart. This could be related to a long time constant for intracellular accumulation of drug under *in vitro* conditions. Our results agrees

with anecdotal reports with other drugs with class III actions [5,27-29] Demonstration of triggered activity in VM cells has only been made in isolated myocyte preparation with non therapeutic compounds such anthopleurin A. [30] and unphysiological conditions. Antzelevitch and Sicouri (review) [31] also showed that endocardial muscle cells in the dog never generate EADs and triggered activity in agreement with our results in the rabbit.

The term "reverse rate dependence" [32] was coined to account for greater prolongation of cardiac APs at low compared with high frequencies of stimulation. It seems clear from the present study that reverse use dependence is not equally manifest in all VM cells and this term should perhaps be reserved for the effects these drugs have in PFs as it is their effects in these fibers which are probably responsible for their proarrhythmic activity.

Two hypotheses have been proposed to explain the cellular mechanism responsible for the initiation of triggered activity in the presence of drugs which prolong repolarization, viz., the generation of EADs (review) [33] and/or prolonged repolarization-dependent reexcitation [34]. It has been hypothesized that fully repolarized tissue (VM) adjacent to still depolarized tissue (PFs) can result in a flow of current capable of initiating excitation in the cells already repolarized. Our results suggest that such a mechanism may be possible on the rabbit endocardial surface as a result of the unique connections between conducting cells and muscle cells.

In rabbit preparations, the superficial Purkinje layer covers only the basal half of the papillary muscles and only certain portions of the septum, usually the bottom half. [35] The activation sequence of the muscle layer occurs from the Purkinje layer only at specific junctional sites. These junctional sites become regions of high resistivity and low conduction as shown by Overholt et al [35] and Tranum-Jensen et al. [18]. Overholt et al [35] have shown that over most of the muscle surface in both canine and rabbit papillary muscles the Purkinje layer is incapable of directly activating the ventricular muscle layer whereas propagation can easily occur into the Purkinje layer at any region in which these cells are not refractory. Thus reentry can occur as a result of a low amplitude triggered response originating in the Purkinje layer blocking at most Purkinje-muscle junctions but propagating through others to either re-excite the Purkinje layer or extend the duration of its AP. It may also explain how a single triggered AP may lead to reentrant activity and thus TdP in the whole heart. Such a mechanism has shown previously to occur in normal Purkinje muscle preparations with the application of premature beats. [19,36]. It is conceivable that in *in vitro* preparations some of the junctional sites which may be located remote from the main Purkinje strand have been severed and may account for the necessity for more extreme conditions for the generation of coupled APs *in vitro*.

It is conceivable that current flow between cells with disparate APDs could give rise to secondary depolarizations which conduct to muscle and

subsequently to the rest of the heart. This hypothesis requires some degree of cellular uncoupling. Gibb et al. [37] showed in a theoretical model that phase 2 EADs are capable of triggering full APs in neighboring tissues only if the patches are separated by a relatively large resistive barrier. Such a resistive barrier is provided by the Purkinje muscle junction. Such a pronounced difference in the duration of the AP between different cell types within a given mass of tissue may set the stage for electrotonic interactions and prolonged repolarization-dependent re-excitation as suggested by Brugada and Wellens [34]. In the rabbit PF, the net current flowing during the plateau phase is very small as indicated by a steady state current voltage relationship in these cells being close to zero. [22] Thus in the presence of a drug prolonging repolarization a very small change in the current in the inward direction may easily induce EADs and triggered activity in these cells. Such electrotonic interactions between Purkinje and muscle cells were clearly demonstrated in the present study and provide support for prolonged repolarization-dependent reexcitation as a mechanism of arrhythmia generation.

Our results suggest that sustained triggered activity as a result of EADs in PFs requires uncoupling of these fibers from VM, very high concentrations of drug and extremely prolonged CLs. In syncytial preparations, usually only singlets or couplets were observed. In the present study, electrotonic interactions between transitional cells and their coupling to either the free running Purkinje cells or VM seemed to determine the induction of triggered activity in these cells and its subsequent propagation to VM as an extra response and reflection to the longer

duration more central fibers extending the duration of the APs in these cells even further. It is such a mechanism which would be expected to result in the generation of more than one extra beat in syncytial preparations. Such multiple activity was rare.

Conclusion

In vitro, there are significant differences of *d*-sotalol on Purkinje fibers versus VM that appear to reflect differences in the contribution of specific ion channels to APD in these cells as well as to electrotonic interactions between them across the Purkinje-muscle junctions. These differences influence the proarrhythmic actions of *d*-sotalol and result in the generation of coupled beats *in situ*. Our results suggest that the *in vitro* and *in situ* approaches used in the present study are mutually complimentary and provide the experimental basis for further evaluation of the proarrhythmic effects of *d*-sotalol, particularly TdP, in the isolated rabbit heart.

Acknowledgments

The authors wish to thank Ms. Kelly Harrison and Suzanne Seto for expert technical assistance, and Bristol-Myers Squibb Canada for supplying *d*-sotalol.

References

1. Roden DM, Hoffman BF: Action potential prolongation and induction of abnormal automaticity by low quinidine concentrations in canine Purkinje fibers. Relationship to potassium and cycle length. *Circulation Research* 1985;56:857-867

2. Davidenko JM, Cohen L, Goodrow R, Antzelevitch C: Quinidine-induced action potential prolongation, early afterdepolarizations, and triggered activity in canine Purkinje fibers. Effects of stimulation rate, potassium, and magnesium. *Circulation* 1989;79:674-686

3. Sasyniuk BI, Valois M, Toy W: Recent advances in understanding the mechanisms of drug-induced torsades de pointes arrhythmias. *American Journal of Cardiology* 1989;64:29J-32J

4. Valois M, Sasyniuk BI: Modification of the frequency- and voltage-dependent effects of quinidine when administered in combination with tocainide in canine Purkinje fibers. *Circulation* 1987;76:427-441

5. Carlsson L, Amos GJ, Andersson B, Drews L, Duker G, Wadstedt G: Electrophysiological characterization of the prokinetic agents cisapride and mosapride in vivo and in vitro: implications for proarrhythmic potential? *Journal of Pharmacology & Experimental Therapeutics* 1997;282:220-227

6. Abrahamsson C, Carlsson L, Duker G: Lidocaine and nisoldipine attenuate almokalant-induced dispersion of repolarization and early afterdepolarizations in vitro. *Journal of Cardiovascular Electrophysiology* 1996;7:1074-1081

7. Carlsson L, Almgren O, Duker G: QTU-prolongation and torsades de pointes induced by putative class III antiarrhythmic agents in the rabbit: etiology and interventions. *Journal of Cardiovascular Pharmacology* 1990;16:276-285

8. Brachmann J, Schols W, Beyer T, Montero M, Enders B, Kubler W: Acute and chronic antiarrhythmic efficacy of d-sotalol in patients with sustained ventricular tachyarrhythmias. *European Heart Journal* 1993;14 Suppl H:85-87

9. Brachmann J, Beyer T, Schmitt C, Schols W, Montero M, Hilbel T, Schweizer M, Kubler W: Electrophysiologic and antiarrhythmic effects of D-sotalol. *Journal of Cardiovascular Pharmacology* 1992;20 Suppl 2:S91-5

10. Lynch JJ, Coskey LA, Montgomery DG, Lucchesi BR: Prevention of ventricular fibrillation by dextrorotatory sotalol in a conscious canine model of sudden coronary death. *American Heart Journal* 1985;109:949-958

11. Waldo AL, Camm AJ, deRuyter H, Friedman PL, MacNeil DJ, Pauls JF, Pitt B, Pratt CM, Schwartz PJ, Veltri EP: Effect of d-sotalol on mortality in patients with left ventricular dysfunction after recent and remote myocardial infarction. The SWORD Investigators. Survival With Oral d-Sotalol [see comments] [published erratum appears in Lancet 1996 Aug 10; 348(9024):416]. *Lancet* 1996;348:7-12

12. Hohnloser SH, Singh BN: Proarrhythmia with class III antiarrhythmic drugs: definition, electrophysiologic mechanisms, incidence, predisposing factors, and clinical implications. [Review]. *Journal of Cardiovascular Electrophysiology* 1995;6:920-936

13. Hohnloser SH: Proarrhythmia with class III antiarrhythmic drugs: types, risks, and management. [Review]. *American Journal of Cardiology* 1997;80:82G-89G

14. Advani SV, Singh BN: Pharmacodynamic, pharmacokinetic and antiarrhythmic properties of d-sotalol, the dextro-isomer of sotalol. [Review]. *Drugs* 1995;49:664-679

15. Sasyniuk BI, Brunet S: Proarrhythmic effects of *d*-sotalol in the rabbit ventricle associated with differential effects on endocardial cells at slow heart rates. *Circulation* 1994;90:I-146(abstract)

16. Bielen F: Sodium-proton exchange in Cardiac Cells: Role in Modulation of Intracellular Sodium and Sodium-Dependent Processes. *Acta Biomedica Lovaniensia* 1991, 42

17. Franz MR, Kirchhof PF, Fabritz CL, Zabel M: Computer analysis of monophasic action potentials: manual validation and clinically pertinent applications. *Pacing & Clinical Electrophysiology* 1995;18:1666-1678

18. Tranum-Jensen J, Wilde AA, Vermeulen JT, Janse MJ: Morphology of electrophysiologically identified junctions between Purkinje fibers and ventricular muscle in rabbit and pig hearts. *Circulation Research* 1991;69:429-437

19. Sasyniuk BI, Mendez C: A mechanism for reentry in canine ventricular tissue. *Circulation Research* 1971;28:3-15

20. Mendez C, Mueller WJ, Merideth J, Moe GK: Interaction of transmembrane potentials in canine Purkinje fibers and at Purkinje fiber-muscle junctions. *Circulation Research* 1969;24:361-372

21. Sicouri S, Antzelevitch C: A subpopulation of cells with unique electrophysiological properties in the deep subepicardium of the canine ventricle. The M cell. *Circulation Research* 1991;68:1729-1741

22. Paquette T, Ogbaghebriel A, Shrier A, Sasyniuk BI: Regional distributions in K currents in myocytes isolated from rabbit ventricle. *Canadian Journal of Cardiology* 1996;12:85E(abstract)

23. Hiraoka M, Kawano S: Mechanism of increased amplitude and duration of the plateau with sudden shorthening of diastolic intervals in rabbit ventricular cells. *Circulation Research* 1987;60:14-26

24. Carmeliet E: K+ channels and control of ventricular repolarization in the heart. [Review]. *Fundamental & Clinical Pharmacology* 1993;7:19-28

25. Anyukhovsky EP, Sosunov EA, Feinmark SJ, Rosen MR: Effects of quinidine on repolarization in canine epicardium, midmyocardium, and endocardium: II. In vivo study. *Circulation* 1997;96:4019-4026

26. Weerapura M, Sasyniuk BI: Mechanism of induction of torsade de pointes arrhythmias by quinidine. *Canadian Journal of Cardiology* 1996;12:127E(abstract)

27. Carlsson L, Abrahamsson C, Andersson B, Duker G, Schiller-Linhardt G: Proarrhythmic effects of the class III agent almokalant: importance of infusion rate, QT dispersion, and early afterdepolarisations [see comments]. *Cardiovascular Research* 1993;27:2186-2193

28. Puisieux FL, Adamantidis MM, Dumotier BM, Dupuis BA: Cisapride-induced prolongation of cardiac action potential and early afterdepolarizations in rabbit Purkinje fibres. *British Journal of Pharmacology* 1996;117:1377-1379

29. Adamantidis MM, Kerram P, Caron JF, Dupuis BA: Droperidol exerts dual effects on repolarization and induces early afterdepolarizations and triggered activity in rabbit Purkinje fibers. *Journal of Pharmacology & Experimental Therapeutics* 1993;266:884-893

30. Boutjdir M, Restivo M, Wei Y, Stergiopoulos K, el-Sherif N: Early afterdepolarization formation in cardiac myocytes: analysis of phase plane patterns, action potential, and membrane currents. *Journal of Cardiovascular Electrophysiology* 1994;5:609-620

31. Antzelevitch C, Sicouri S: Clinical relevance of cardiac arrhythmias generated by afterdepolarizations. Role of M cells in the generation of U waves, triggered activity and torsade de pointes. [Review]. *Journal of the American College of Cardiology* 1994;23:259-277

32. Hondeghem LM, Snyders DJ: Class III antiarrhythmic agents have a lot of potential but a long way to go. Reduced effectiveness and dangers of reverse use dependence. *Circulation* 1990;81:686-690

33. Roden DM: Early after-depolarizations and torsade de pointes: implications for the control of cardiac arrhythmias by prolonging repolarization. [Review]. *European Heart Journal* 1993;14 Suppl H:56-61

34. Brugada P, Wellens HJ: Early afterdepolarizations: role in conduction block, "prolonged repolarization-dependent reexcitation," and tachyarrhythmias in the human heart. [Review]. *Pacing & Clinical Electrophysiology* 1985;8:889-896

35. Overholt ED, Joyner RW, Veenstra RD, Rawling D, Wiedmann R: Unidirectional block between Purkinje and ventricular layers of papillary muscles. *American Journal of Physiology* 1984;247:H584-95

36. Moe GK, Mendez C: Physiological basis of premature beats and sustained tachycardia. *New England Journal of Medicine* 1973;288:250-254

37. Wagner MB, Gibb WJ, Lesh MD: A model study of propagation of early afterdepolarizations. *IEEE Transactions on Biomedical Engineering* 1995;42:991-998

"We subsequently investigated if the same conditions which lead to triggered activity in endocardial preparations would lead to TdP in the whole heart. We used the isolated rabbit heart because it was previously shown that class III drugs in the *in vivo* model would lead to an arrhythmia resembling TdP arrhythmias in the presence of both a class III antiarrhythmic drug and α-adrenergic stimulation."

CHAPTER II

D-SOTALOL INDUCED VENTRICULAR ARRHYTHMIAS IN THE ISOLATED RABBIT HEART - MODEL AND MECHANISMS

Current Status: Brunet S, Sasyniuk BI.

To be submitted to *Circulation*

Abstract

A major limitation in the understanding of the proarrhythmic effects of drugs with class III actions, in particular, induction of Torsade de Pointes (TdP) is the lack of an adequate experimental model. We describe an isolated rabbit heart model in which arrhythmias were induced by clinically relevant concentrations of *d*-sotalol and bradycardia. This model is based on our previous in vitro experiments in rabbit ventricular preparations showing selective actions of *d*-sotalol on repolarization on cells in the ventricular specialized conducting system (VSCS). To compare drug effects on repolarization in the VSCS versus ventricular muscle (VM), monophasic action potentials (MAPs) were recorded from the left endocardial septum and compared with MAPs from the left endocardial free wall and right epicardial surface together with a volume conducted ECG. Drug administration produced a typical pattern of arrhythmias consisting of singlets which evolved into couplets, triplets and quadruplets and eventually TdP. There was a strong correlation between a critical threshold disparity in repolarization between MAP_{endo} and MAP_{epi} and induction of coupled beats. The disparity was the result of a drug induced cycle length (CL) dependent selective lengthening of MAP_{endo} potentials. This selective effect was associated with early afterdepolarizations (EADs) only on the endocardial surface. The time required for coupling to occur was a function of both drug concentration and CL (CL). Spontaneous episodes of TdP were almost always preceded by multiple rhythms and were initiated by a coupled beat. TdP occurred within a critical window of

CLs and its generation was highly reproducible. Termination of TdP was associated with elimination of disparity. The characteristics of TdP in our model bore a high resemblance to that of the clinical arrhythmia. The results parallel our in vitro data and suggest that triggered activity originating on the endocardial surface is the mechanism of initiation of *d*-sotalol induced arrhythmias including TdP. This new isolated heart model may be useful for the assessment of the proarrhythmic potential of novel class III drugs and offers several advantages to other models aimed at elucidating the mechanism of TdP *in situ*.

Introduction

Further efforts to develop a better antiarrhythmic agent have concentrated on drugs with the ability to prolong action potential duration (APD), as seen with the potassium channel blockers but with a better safety profile than amiodarone. The most widely studied of these agents is *d*-sotalol. *d*-sotalol blocks the rapid component of the delayed rectifier potassium current (I_{Kr}) and has no clinically meaningful β-blocking activity. (review) [1] The recent SWORD trial in which *d*-sotalol was evaluated in high risk post-MI patients found increased *d*-sotalol associated mortality as compared to placebo, the majority of which were presumed to be arrhythmic deaths due to TdPs. [2]

Understanding the mechanism of the possible proarrhythmic potential of the drug would help to identify patients at risk and prevent its occurrence and/or identify other drugs which lack this action. To gain further insight into its mechanisms and specific characteristics a model is required in which the arrhythmia can be obtained reliably, reproducibly and predictably and at the same time be easily amenable to analysis.

Previous models of *d*-sotalol induced TdP showed low incidence of proarrhythmia and have been difficult to study. (review) [3] Weissenburger et al. [4,5] describe a hypokalemic canine model with chronic AV block and hypertrophy studied in the conscious state. The major drawback of this model is that it requires

9-12 weeks of ventricular pacing to produce hypertrophy and spontaneous occurrence of arrhythmia was rare.. Vos et al. [6,7] describe a canine model with chronic AV block and hypertrophy studied in the anesthetized state and given IV bolus injections of *d*-sotalol combined with a pacing protocol. This model is tedious, also has a low incidence of spontaneous arrhythmia and requires programmed ventricular stimulation which under clinical conditions does not normally lead to TdP arrhythmias. In the anesthetized rabbit model of Carlsson et al. [8] high doses of Class III antiarrhythmic agents other than *d*-sotalol, reproducibly resulted in prolongation of the QT interval and self-terminating episodes of polymorphic arrhythmias resembling TdP, but only when combined with α-adrenergic stimulation with methoxamine. Similarly, Derakhchan et al. [9] found that high doses of *d*-sotalol induced polymorphic ventricular tachycardias (PVTs) more frequently in an anesthetized dog with acute AV block when combined with α-adrenergic stimulation with phenylephrine. Other models of TdP use compounds other than class III agents (cesium [10], Anthopleurin A [11], BAY K 8644 [12]). Thus, there is a need for a better model of this arrhythmia.

The exact electrophysiologic mechanism of TdP is still unclear. We showed previously that *d*-sotalol lengthened APD considerably in rabbit Purkinje fibers (PFs) and minimally in endocardial VM creating a large heterogeneity in durations between PFs and VM, particularly at long CLs (≥ 1.5 sec). Concentrations of *d*-sotalol ≥ 20 μM induced EADs in PFs which propagated to

VM resulting in coupled responses. We also showed that multiple electrotonic interactions between PFs and adjacent transitional cells apparently due to the creation of a functional refractory barrier in PFs resulted in a sustained but self limiting rapid chaotic rhythm which propagated to ventricular muscle. 13,14 We had determined previously the conditions under which these concentrations of *d*-sotalol produced EADs, triggered activity and arrhythmias *in vitro* and had shown that these same conditions led to coupled beats in the *in situ* isolated heart [15]. If EADs and triggered activity is the mechanism of initiation of TdP arrhythmias *in situ*, we hypothesized that conditions which result in triggered activity *in vitro* should cause TdP to develop in the whole heart. A corollary of this hypothesis is that differential effects of *d*-sotalol on PFs and VM would be reflected *in situ* as differences in disparity between durations of MAPs at endocardial and epicardial recording sites during stimulation at long CLs and that this differential effect is not only associated with generation of coupled beats but is also responsible for the generation of TdP arrhythmias. Thus, the purpose of the present investigation was to determine the conditions under which *d*-sotalol produces arrhythmias, to study their characteristics and to determine their mechanism of initiation.

Preliminary results have been published in abstract form [15]. Since we first reported our findings, a study was published by Zabel et al. [16] also in an isolated rabbit heart model showing generation of TdP arrhythmias following perfusion with very high concentrations (100 μM) of *d*-sotalol and requiring the lowering of potassium and magnesium concentrations in the perfusate to 50% of normal

levels. In their investigation, TdP was not maintained despite continued exposure to the low K^+ low Mg^{2+} solution. Thus, unlike previous investigators, we show that Ik_r blockade with *d*-sotalol alone can result in the spontaneous occurrence of TdP arrhythmias in the absence of either a synergistic effect of α-adrenergic stimulation or a necessity for facilitating interventions such as hypokalemia or hypomagnesemia. The probable mechanism of this arrhythmia is addressed.

Methods

All procedures for animal care and experimentation followed the guidelines of the Canadian Council for Animal Care and were monitored by an institutional committee.

Experimental Preparation

Nineteen New Zealand White rabbits of either sex (body weight 2.0 - 2.5 Kg) were anaesthetized with ketamine hydrochloride (75 mg × Kg^{-1} i.m.) followed by xylazine (8 mg × Kg^{-1} i.m.). Heparin (400 IU × Kg^{-1}) was administered through a marginal ear vein. The heart was rapidly excised and immediately immersed in 37 ° C modified Krebs-Henseleit solution previously bubbled with 95 % O_2 and 5 % CO_2 (composition in mmol × $Liter^{-1}$: NaCl 122.0, KCl 25.8, $MgSO_4$ 0.5, $NaHCO_3$ 24.0, KH_2PO_4 1.2, $CaCl_2$ 1.8, Glucose 50). It was then mounted on a non-recirculating Langendorff apparatus and perfused at a perfusion pressure of 65 cm H_20 with oxygenated Krebs-Henseleit's solution (composition in mmol × $Liter^{-1}$: NaCl 122.0, KCl 2.8, $MgSO_4$ 0.5, $NaHCO_3$ 24.0, KH_2PO_4 1.2, $CaCl_2$ 1.8, Glucose 5.0, Pyruvate 2.0).). The heart was immersed in a water-jacketed chamber filled with Krebs-Henseleit solution kept at a temperature of 37 ° C.

Stimulation and Recording Techniques

To pace the hearts at a fixed basic cycle length (BCL), bipolar silver wire ring electrodes (diameter 1 mm) were sutured onto the mid wall of the left ventricle. To slow down the intrinsic heart rate, the atrioventricular node was destroyed by injecting 0.1- 0.2 ml of formaldehyde (37 %) directly into the node region. The hearts were paced at a BCL of 0.5 sec with a pulse width of 1 ms and twice diastolic threshold intensity delivered by a pulse generator (Schema Versatae) and a stimulation isolation unit (Digitimer Ltd. Model DS2.

A volume conducted ECG was recorded by means of 4 Ag / AgCl pellet electrodes (In Vivo Metric) mounted on the walls and bottom of a circular cylinder of 9 cm diameter positioned to simulate "Einthoven" configuration with the "arm" electrodes fixed to the walls of the chamber and the "foot" and reference electrodes fixed beneath the heart. The circular cylinder was placed inside the water-jacketed chamber filled with Krebs'-Henseleit solution [17]. This permitted the recording of a volume-conducted ECG from the isolated heart closely resembling the surface ECG limb lead recordings. Usually a lead II ECG was recorded.

MAPs were simultaneously recorded from the left ventricular endocardial and right ventricular epicardial surfaces with two contact type Langendorff probes (4 French model number 225, EP Technologies). Since our previous results indicated that 20 to 40 μM of *d*-sotalol induced EADs and triggered activity only

in the ventricular conducting system and that the most marked increases in APD were observed in PFs, one way of monitoring activity from the conducting system is with a MAP probe placed at a strategic location on the endocardial surface. Since previous observations also indicated that VM cells on the endocardial surface of the rabbit heart have durations similar to those on the epicardial surface, (unpublished observations) drug effect on VM was most easily monitored with a MAP probe located at the base of the right ventricular epicardial surface remote from any conducting system. To determine the sites of optimal placement for the probes, we varied the location of the probes on the left ventricular endocardial and on the right ventricular epicardial surface in 3 experiments. An attempt was made to place the endocardial probe at sites which displayed the longest durations during pacing at long CLs while the epicardial probe was placed at sites of shortest durations. Since arrhythmias occurred when ever the hearts were paced at long CLs we assessed optimal placement of the endocardial probe by determining the sites which displayed the longest durations just prior to the occurrence of coupled beats.[13]. The protocol used was to stimulate the heart at a CL of 0.5 sec and then increase the CL to 1.5 sec until coupled beats occurred, as described previously. [13,14] This protocol was repeated with each site change. In each run a volume conducted ECG was recorded simultaneously with the endocardial and epicardial MAPs. Fig. 1 shows a typical example from one of the experiments. The top panel shows records from a left endocardial and a right epicardial site showing the maximal differences in disparity obtained just prior to coupling. The bottom panel shows minimal differences in disparity between endocardial and

epicardial sites just prior to coupling. The endocardial probe showing maximal changes in MAP duration (MAPD) was positioned in the lower third of the septum. (fig. 1 -upper panel) That showing minimal changes was positioned at a left endocardial apical wall site. (fig. 1 - lower panel) Both epicardial MAPs, obtained from the right ventricular base, as well as the QT intervals showed similar durations in both trials indicating that the differences observed at the endocardial sites were due to sites of placement of the probes and not due to differences in the response during two different stimulation sequences.. More importantly, the endocardial MAPD with the maximum change (upper panel) was similar to the change observed in the QT interval. In all of the experiments an attempt was made to place the endocardial probe at a left septal site which showed MAPD similar to the QT interval. Since the endocardial site with the least change in MAPD was similar to that obtained at the right ventricular base, records from these two sites also reflected maximal disparity at left endocardial sites as had been previously observed under *in vitro* conditions. Thus, the epicardial probe was always positioned at the right ventricular base which showed the least change in MAPD just prior to coupling since it was too difficult to position and maintain two endocardial probes in the left ventricle. Hence, any changes at these two recording sites would reflect near maximal disparity in each heart.

In all 3 experiments, the minimal $MAPD_{epi}$ was 211 ± 32 msec while that from the endocardium was 315 ± 83; the maximal $MAPD_{epi}$ was 299 ± 52 while

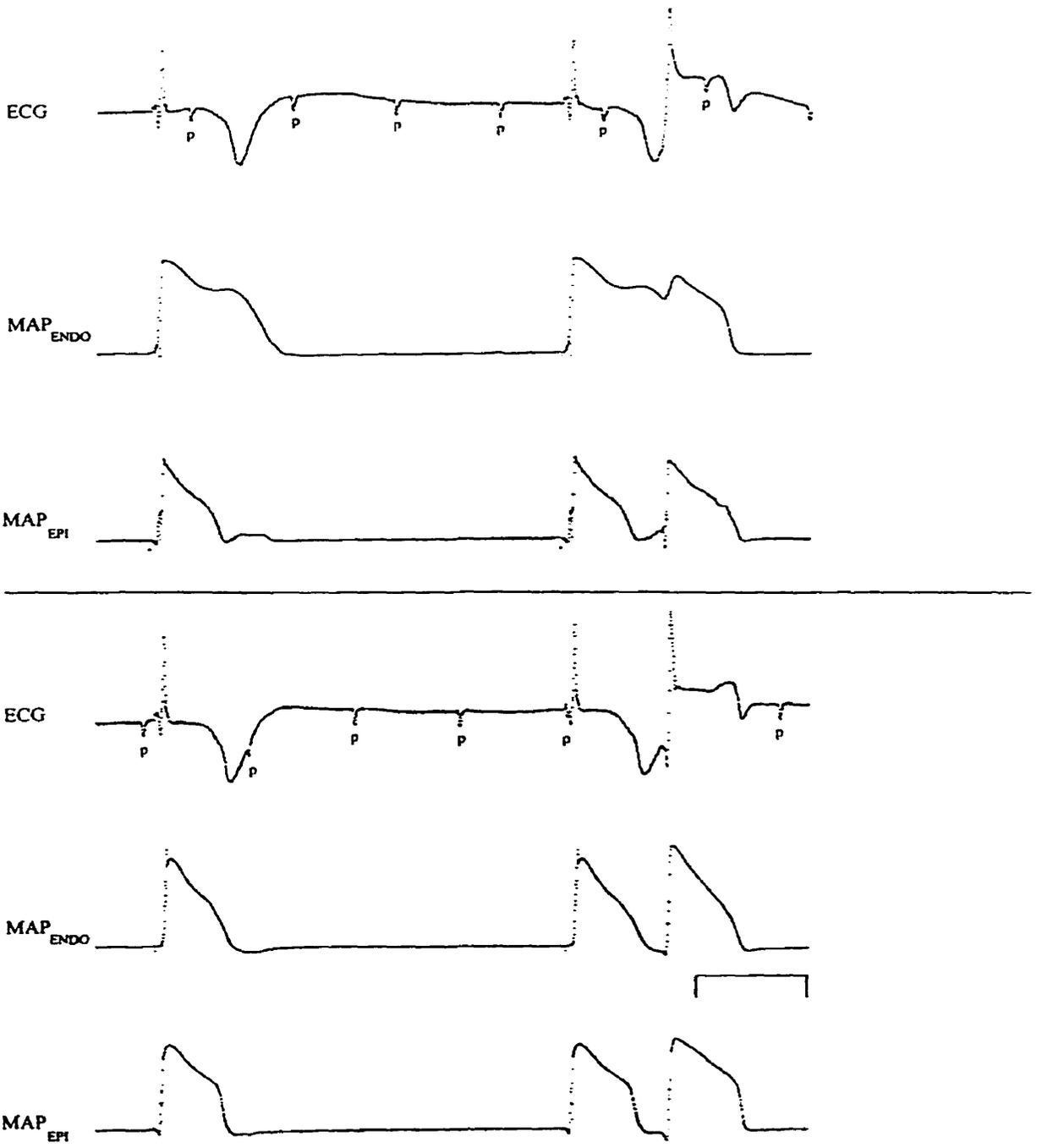
ECG
P
P
P
P
P
P
MAP ENDO
MAP EPI
ECG
P
P
P
P
P
P
MAP ENDO
MAP EPI

Figure 1. Typical example of the marked disparity in MAPD on the left ventricular endocardial surface as compared to epicardial recording sites prior to coupling. Each panel shows an ECG trace together with MAP recordings from an endocardial and epicardial site. In this and subsequent figures, "p" on the ECG record denotes the atrial potential. Each panel shows the last beat prior to coupling followed by the coupled beat. The upper panel shows the maximal MAPD obtained at a left ventricular endocardial recording site. The probe was positioned on the lower third of the left septum. The lower panel shows the MAP with the minimal MAPD obtained at an endocardial site from the left ventricular free wall. Both epicardial MAPs were obtained from a similar site on the right ventricular base. Note the marked disparity in MAPD between endocardial and epicardial sites in the upper panel versus that in the lower panel. In both cases the QT intervals are similar. Note that the maximal endocardial MAPD parallels the QT interval. Calibration bar is 400 msec.

that from the endocardium was 419 ± 69. The values for QT intervals were similar in all cases (437 ±44 versus 424 ± 42 and 427 ± 47 versus 435 ± 47) suggesting that any differences observed in MAPD at endocardial and epicardial sites were not related to major changes in the disparity associated with coupling and were thus attributed instead to the position of the MAP recording sites. Thus, in all experiments, the aim was to place the probes at sites reflecting this maximal disparity.

The values of MAPD obtained at endocardial sites reflects the fact that this probe is monitoring activity from both PFs and VM as shown by Ino et al. [18]. Thus the changes observed in disparity would be less than that observed between PFs and VM under *in vitro* conditions as was the case.

Data Acquisition and Analysis

The two MAPs were amplified by DC amplifiers (Isodam, WPI) and the volume conducted ECG was amplified by an AC amplifier (Dam50, WPI). All signals were simultaneously digitized at 1 kHz for storage on the hard disk of an IBM compatible personal computer equipped with an A/D board (TI-125 Axon Instrument) and Axotape software (Version 2, Axon Instrument). The data were temporarily stored on the hard disk of the computer and then permanently stored both on digital audio tapes using Tapedisk software version 6.4.0 and on recordable CDs for later retrieval and analysis.

The MAP signals were processed unfiltered by Data-Pac II Version 4.1 software with the selection criteria and advanced spreadsheet module (Run Technologies, Inc.). Each of the MAP signals was analyzed for MAPD at the 90% repolarization level ($MAPD_{90\%}$) [19]. The QT interval was measured unfiltered with axotape software using cursors. The end of the T-wave was taken at the point at which it reached the isoelectric line. If U waves were present, they were incorporated into the measurements since the end of the T-wave could not be differentiated in such situations. No distinction was made between T and U waves since we were interested in maximal changes in this interval.

Experimental protocols

The hearts were equilibrated with *d*-sotalol for at least 25 minutes while pacing at the BCL of 0.5 sec. After the period of equilibration with drug the hearts were paced at a number of different longer CLs ranging from 0.7 to 0.8, 1.0, 1.5 and 2.5 sec. Each longer CL was maintained for 5 minutes and then the CL was changed back to the BCL of 0.5 sec. The hearts were paced at the BCL for at least 2 minutes before another CL change was made. In some hearts the protocols were done under control conditions and prior to equilibration with drug.

Drug Solution

Stock solutions of *d*-sotalol of 10^{-2} M were freshly prepared from the powder every week.. The stock solution was added to the perfusate to obtain a final concentration of 10, 20 or 40 μM. These concentrations were chosen because they are within the range of serum levels associated with antiarrhythmic effectiveness and with TdP during clinical therapy with *d*-sotalol. The average free drug concentration present in human serum during oral administration and associated with antiarrhythmic effectiveness has been shown to be 13 μM while TdP was shown to occur at serum levels of 18 μM [20]. Similar concentrations induced EADs and triggered activity in PFs which resulted in coupled beats in endocardial preparations from rabbit hearts superfused with the drug. [13] *D*-sotalol was generously supplied by Bristol-Myers Squibb Canada

Definitions

Torsade de Pointes: was defined as a self-terminating PVT of at least 5 consecutive beats occurring in the context of a prolonged QT interval, longer episodes showing the typical twisting of the QRS complexes.

$MAPD_{epi}$: represents the monophasic action potential duration measured at 90% repolarization level of the epicardially recorded monophasic action potential signal. $MAPD_{endo}$: represents the monophasic action potential duration measured

at 90% repolarization level of the endocardially recorded monophasic action potential signal.

Disparity: is defined as the difference of the $MAPD_{endo}$ and the $MAPD_{epi}$ of the simultaneously recorded MAP signals.

A trial: is defined as the arrhythmias generated during an abrupt CL change from 0.5 sec to a longer CL and maintained for 5 minutes.

An arrhythmic cycle: is defined as the establishment of the conditions resulting in spontaneous generation of arrhythmia (either singlets, couplet, triplets, quadruplets, TdP or any combination thereof) followed by the spontaneous elimination of those conditions and a termination of the arrhythmia. Usually several arrhythmic cycles occurred during a single trial.

Statistical analysis

Data are presented as mean ± S.D. Where appropriate ANOVA analysis and paired and unpaired *t*-test was used to test for statistical significance. A *P* value of less then 0.05 was considered to be statistically significant.

Results

Concentration dependent effects of *d*-sotalol on QT interval, $MAPD_{endo}$ and $MAPD_{epi}$

Three hearts were perfused sequentially with 10, 20 and 40 μM concentrations of drug for one hour each while stimulating at the BCL of 0.5 sec. Effects on QT interval, $MAPD_{endo}$ and $MAPD_{epi}$ were determined after equilibration at each concentration and compared to control conditions. The results are summarized in fig. 2. All durations were significantly increased when compared to control. Values at 20 μM were greater than at 10 μM but not significantly so. Effects at 40 μM did not appear to be different from those at either 10 or 20 μM. MAP recordings were kept in a similar area but not necessarily the identical location throughout all concentration changes. It is possible that some of the lack of significant concentration dependent effects is related to this factor as drug effects are small at this rate of stimulation.

Pattern of arrhythmia induction by *d*-sotalol

In our previous *in vitro* study we showed that *d*-sotalol produced an interval dependent differential lengthening of APD in ventricular specialized

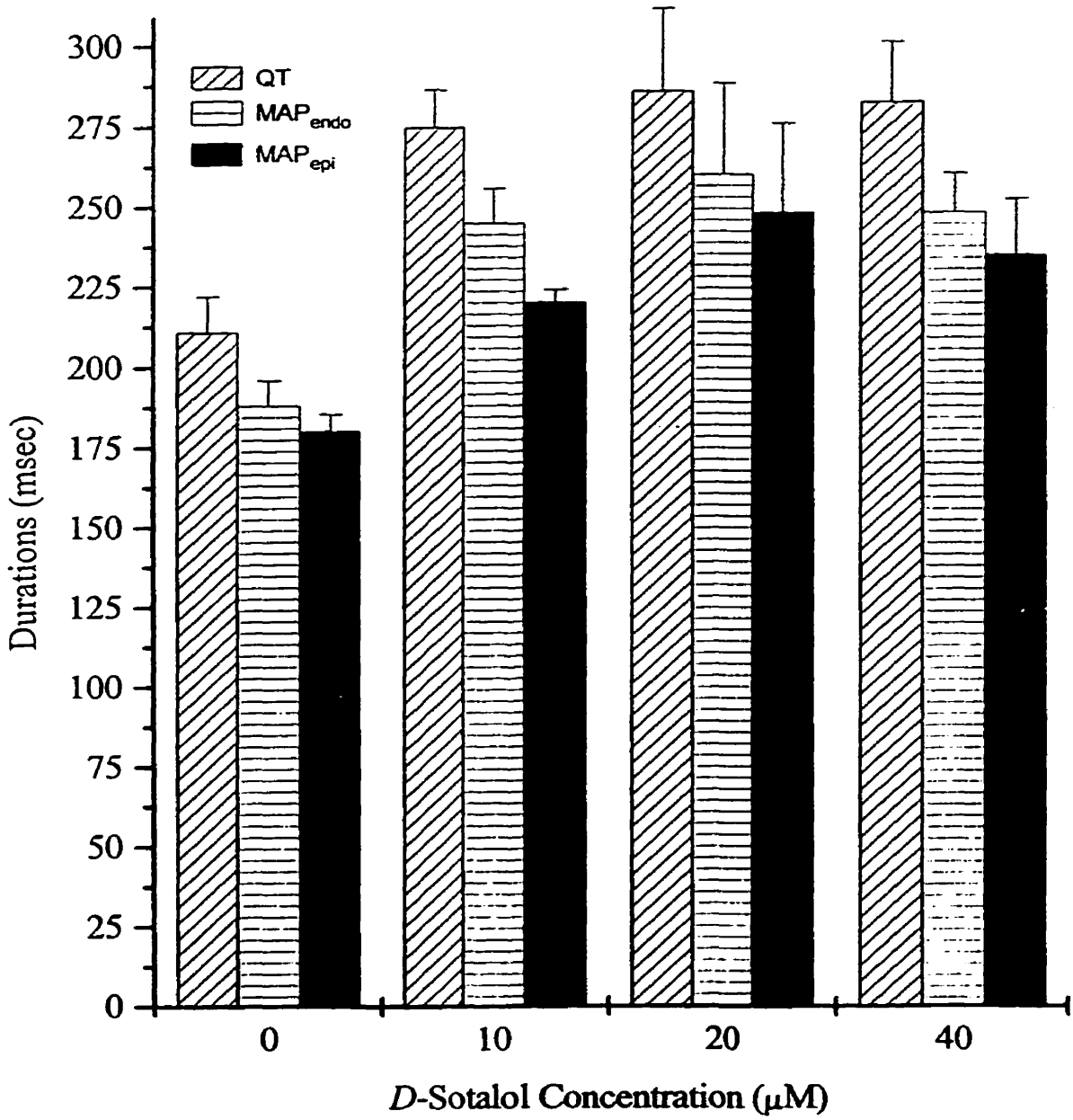

Figure 2. Concentration dependent effects of *d*-sotalol on QT interval , MAP_{endo} and, MAP_{epi} durations at BCL of 0.5 sec. Data obtained from 3 hearts in which drug was administered in progressively higher concentrations.

conducting cells versus VM cells on the endocardial surface which led to the generation of triggered action potentials (AP) in specialized cells with propagation to VM as coupled APs. We hypothesized that the same conditions which led to the generation of triggered activity under *in vitro* conditions would result in coupled beats under *in situ* conditions and would eventually lead to TdP arrhythmias. Thus, in the present study hearts were equilibrated with 10-40 μM of *d*-sotalol and subjected to the same protocol of CL changes as determined previously to result in the generation of triggered responses. Under these conditions, *d*-sotalol induced a typical sequence of arrhythmias in these preparations when the CL was increased to a critical value and kept at that value for several minutes. Fig. 3 A and B shows a typical example in which the first 80 sec of the CL change are shown in the presence of 40 μM of drug. In the absence of drug there were very small CL dependent changes in the intervals. In the presence of drug all of the intervals increased from the BCL. An abrupt increase in the CL was accompanied by an initial decrease followed by a progressive lengthening of both the QT interval and the MAPD from the endocardial recording site (MAP_{endo}) but an overall decrease in the MAP_{epi} duration resulting in a marked disparity in MAPDs between the two recording sites. The QT interval followed the changes in the MAP_{endo}. When the disparity had reached approximately 200 msec (QT interval - $MAPD_{epi}$; fig. 3B) a coupled beat (singlet) was generated. Following the first singlet, coupling continued to occur (as evidenced by double potentials at the epicardial recording site) and was accompanied by fused potentials at the endocardial site (as evidenced by a small hump on the plateau phase coincident with the coupled

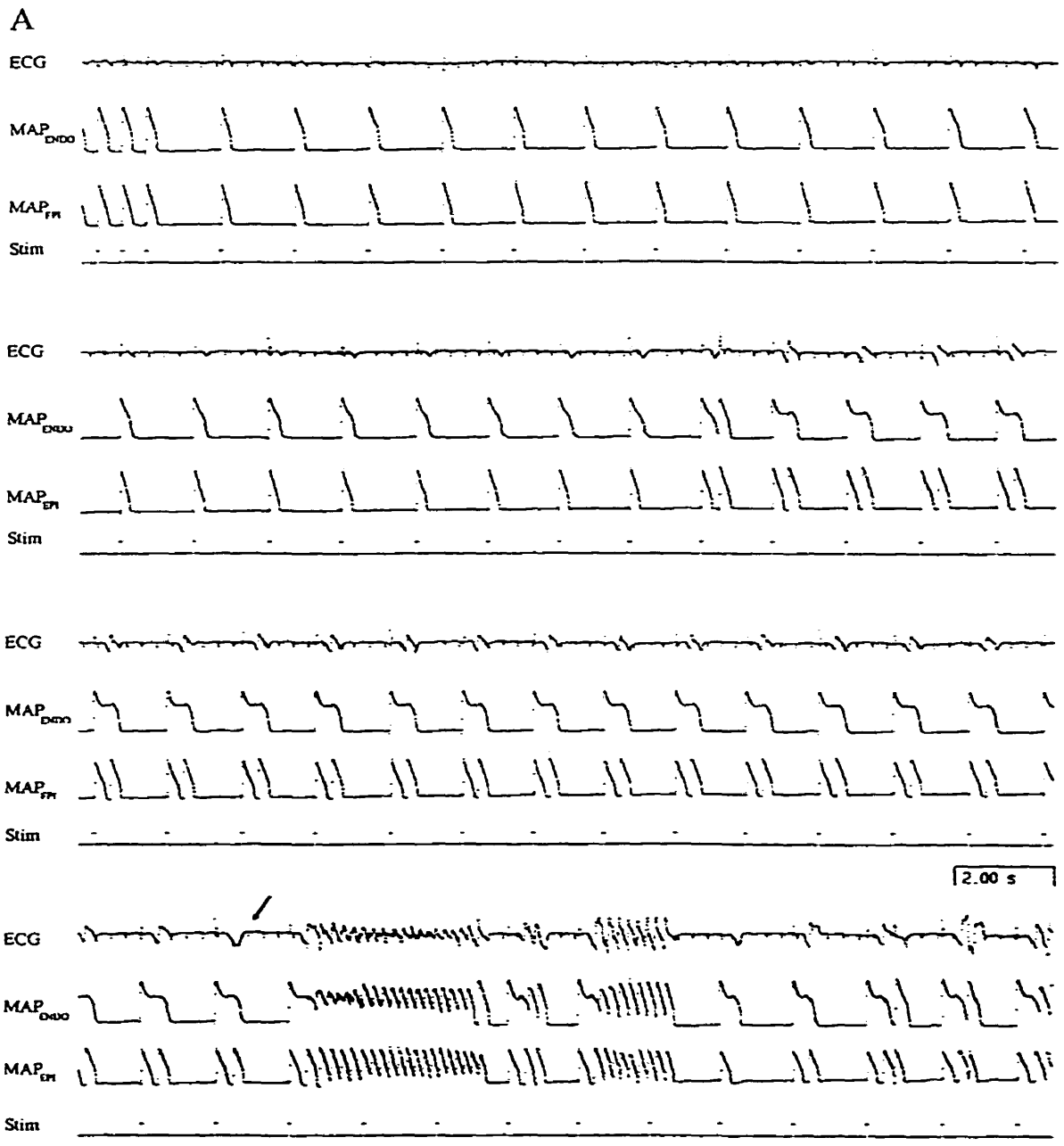
A
ECG
MAP
Stim
ECG
MAP
Stim
ECG
MAP
Stim
2.00 s
ECG
MAP
Stim

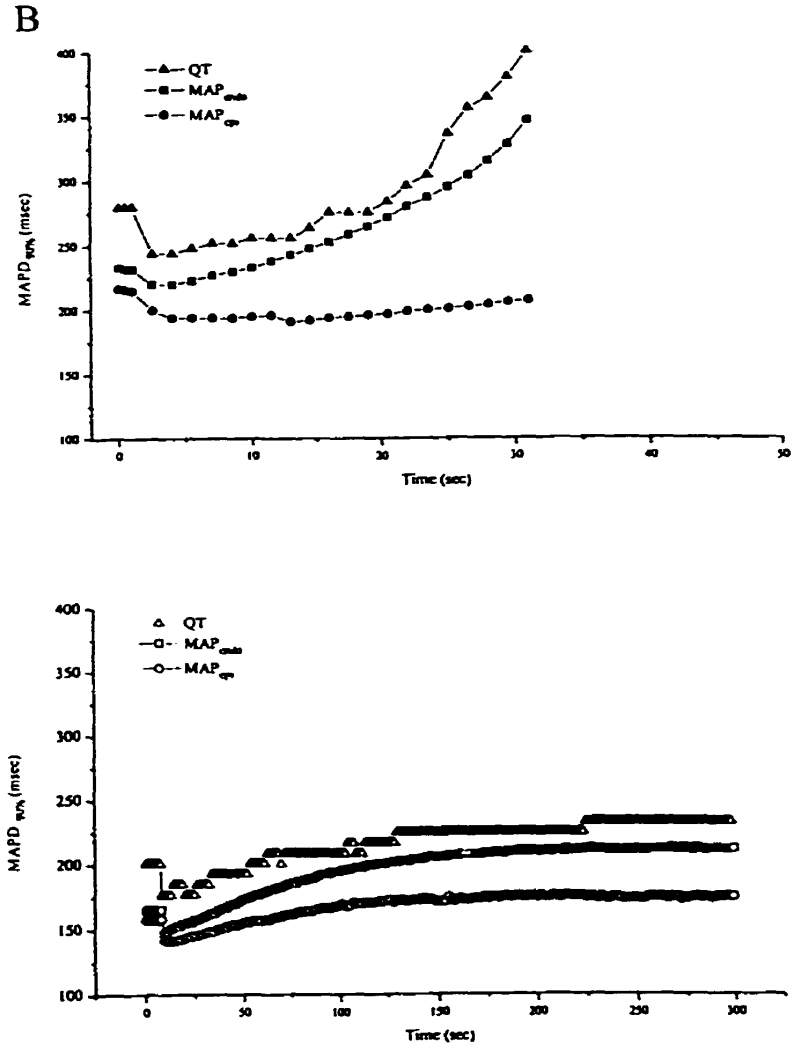

Figure 3. A. Typical sequence of arrhythmia induction by *d*-sotalol. Each panel shows an ECG, a MAP recorded from a left ventricular apical site (MAP_{endo}) and from a right ventricular epicardial basal site (MAP_{epi}) together with a stimulus artifact. The records are continuous. CL was changed abruptly from 0.5 to 1.5 sec. The first three APs in the first panel are the last 3 potentials recorded at the BCL of 0.5 sec. The heart was perfused with 40 μM *d*-sotalol. B. Plot of QT interval, MAP_{endo} and MAP_{epi} under control conditions and in the presence of *d*-sotalol up to the point of coupling.

response at the epicardial site). A long series of singlets was followed by several episodes of TdP after which singlets and couplets occurred and continued for the remainder of the trial. Generation of the first singlet was also accompanied by a progressive increase in the amplitude and width of the T wave. This first singlet occurred at the termination of the T wave. This result supports triggered activity as the mechanism of generation of the singlets. The first beat of the TdP is initiated by a singlet suggesting that this first beat is initiated by the same mechanism as that of the singlet. TdP is preceded by a singlet in which the MAP_{endo} is shorter in duration and the QT complex on the ECG is modified compared to the previous singlets (denoted by an arrow) suggesting that areas of functional conduction block may be occurring which may have affected propagation of the coupled beat and provided the conditions necessary for initiation of TdP.

At all CLs greater than 0.8 sec and at concentrations greater than 20 μM, CL dependent effects on electrophysiologic intervals could not be studied at steady state because coupled beats always ensued. Therefore, to assess CL dependent effects we determined drug effects on durations present just prior to coupling and thus associated with their generation. Fig. 4 shows the CL dependent effects of *d*-sotalol on the QT interval and MAP_{endo} and MAP_{epi} taken just prior to the generation of singlets in 20 trials in 6 experiments with 20 and 40 μM of *d*-sotalol. *d*-sotalol produced a significant CL dependent selective lengthening of $MAPD_{endo}$ and the QT interval. There was no concentration dependent effect.

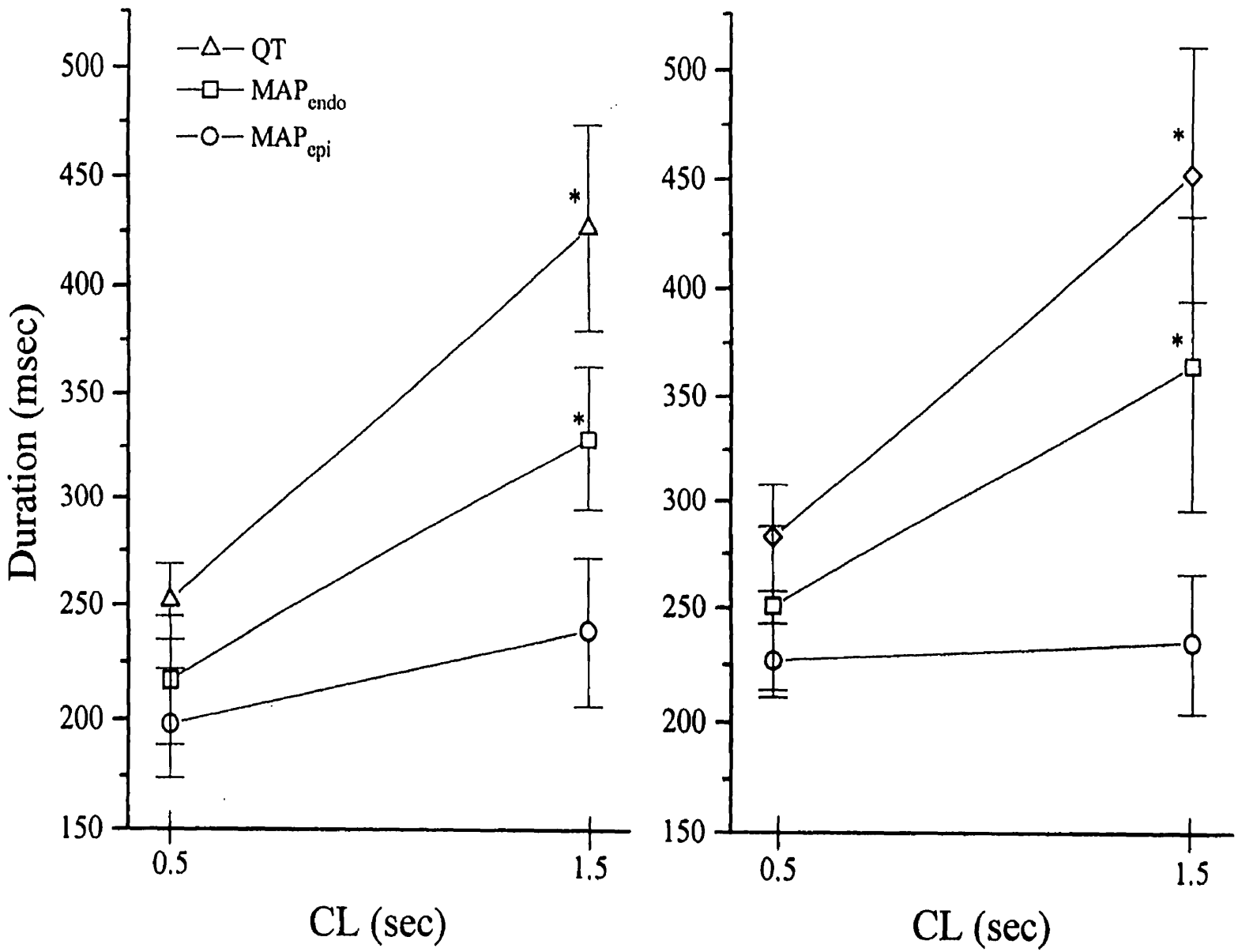
QT
MAP endo
MAP epi
Duration (msec)
500
450
400
350
300
250
200
150
0.5
1.5
CL (sec)
*
*
*
*
500
450
400
350
300
250
200
150
0.5
1.5
CL (sec)

Figure 4. Concentration and CL dependent effects of *d*-sotalol on QT interval, $MAPD_{endo}$ and $MAPD_{epi}$. Left hand graph shows effects at 20 μM; right at 40 μM.

Regardless of the concentration used whenever a certain disparity in durations occurred coupled beats were generated. The mean disparity associated with generation of singlets was 90 ± 34 and 130 ± 69 msec (mean ± SD; n= 20) in the presence of 20 and 40 μM, respectively. ($P \geq 0.05$)

The only significant concentration dependent effect was in the time required (number of beats) following the CL change to induce singlets. In the presence of 40 μM 13 ± 2 beats occurred prior to coupling while at 10 μM it took 69 ± 36 beats to induce coupling. This was due to an increase in the slope of the relation between duration and time at higher concentrations as indicated in fig. 5. At 10 μM it took nearly the entire trial to reach a similar disparity as was reached within a minute at 20 μM. In fact coupling did not occur at 10 μM. There was also a tendency for coupling to occur earlier if the preparations were exposed to drug for a greater length of time which may have been related simply to the amount of drug taken up by the tissues. In 6 preparations exposed to 20 μM of drug for 25-70 min the average time to the first singlet was 107 ± 65 sec whereas after 160-190 min on drug the average time was 53 ± 31 sec ($P \leq 0.05$) (stimulation CL 1.5 sec). The length of exposure to drug affected only the time required to attain coupling. The critical disparity required for coupling did not change. The time to reach coupling was also less at longer CL.

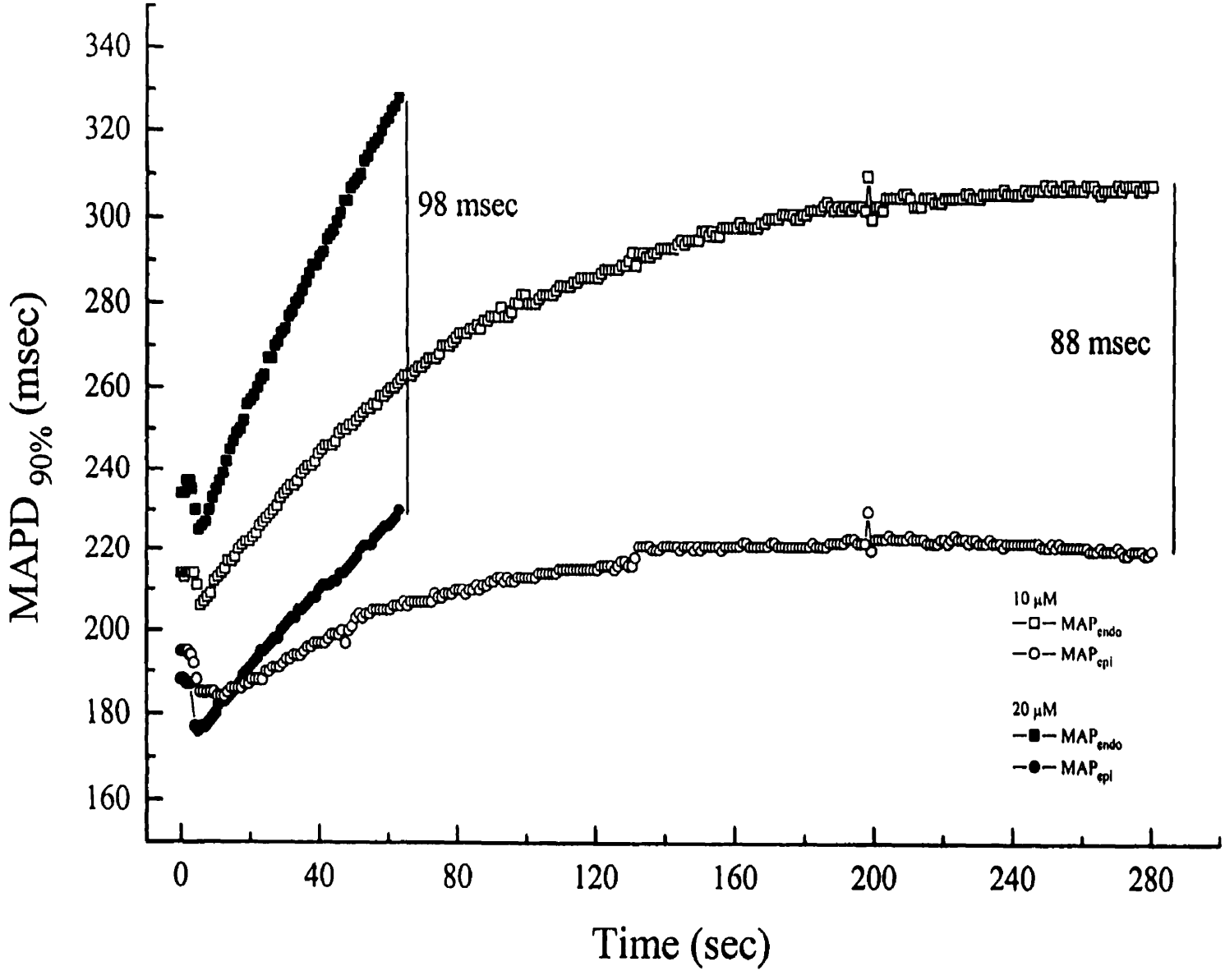
340
320
300
280
260
240
220
200
180
160
MAPD 90% (msec)
98 msec
88 msec
10 μM
MAPendo
MAPepi
20 μM
MAPendo
MAPepi
0
40
80
120
160
200
240
280
Time (sec)

Figure 5. Concentration dependent effects on the relationship between MAPD and time at slow CLs. CL was changed from 0.5 to 1.5 sec. Durations are plotted from the CL change to the last beat prior to coupling.

These effects were reproducible both within a given preparation and from one preparation to the next. In 12 trials in 5 hearts, the average coupling interval (CI) of the first coupled beat (419 ± 23 msec) was significantly longer than that of the second and subsequent coupled beats (377 ± 13 msec, $P \leq 0.05$).

Relationship of disparity to onset of arrhythmias and TdP

Since generation of arrhythmias in this model was highly reproducible it allowed us to consider further the mechanism responsible for the initiation of both singlets and TdP. Each protocol consisted of a period of stimulation at the BCL of 0.5 sec and a 5 min period of stimulation at a long CL ranging from 0.8 to 2.5 sec. followed by a return to the BCL. During each trial there were usually several spontaneous episodes of either singlets alone, a mixture of singlets, couplets, triplets and quadruplets and isolated or recurrent spontaneous episodes of TdP. Whether only singlets occurred or TdP usually depended on a combination of drug concentration and stimulating CL and/or time of exposure to drug. Fig. 6 shows a typical example of recurrent spontaneous episodes of a series of singlets in a preparation exposed to 20 μM of drug for 1.5 hrs in which the CL was increased from 0.5 to 1.0 sec. There were 4 spontaneous episodes of singlets in this 5 min trial. Following the CL change there was the typical decline in MAPDs followed by a progressive increase. The disparity in durations between MAP_{endo} and MAP_{epi}

I

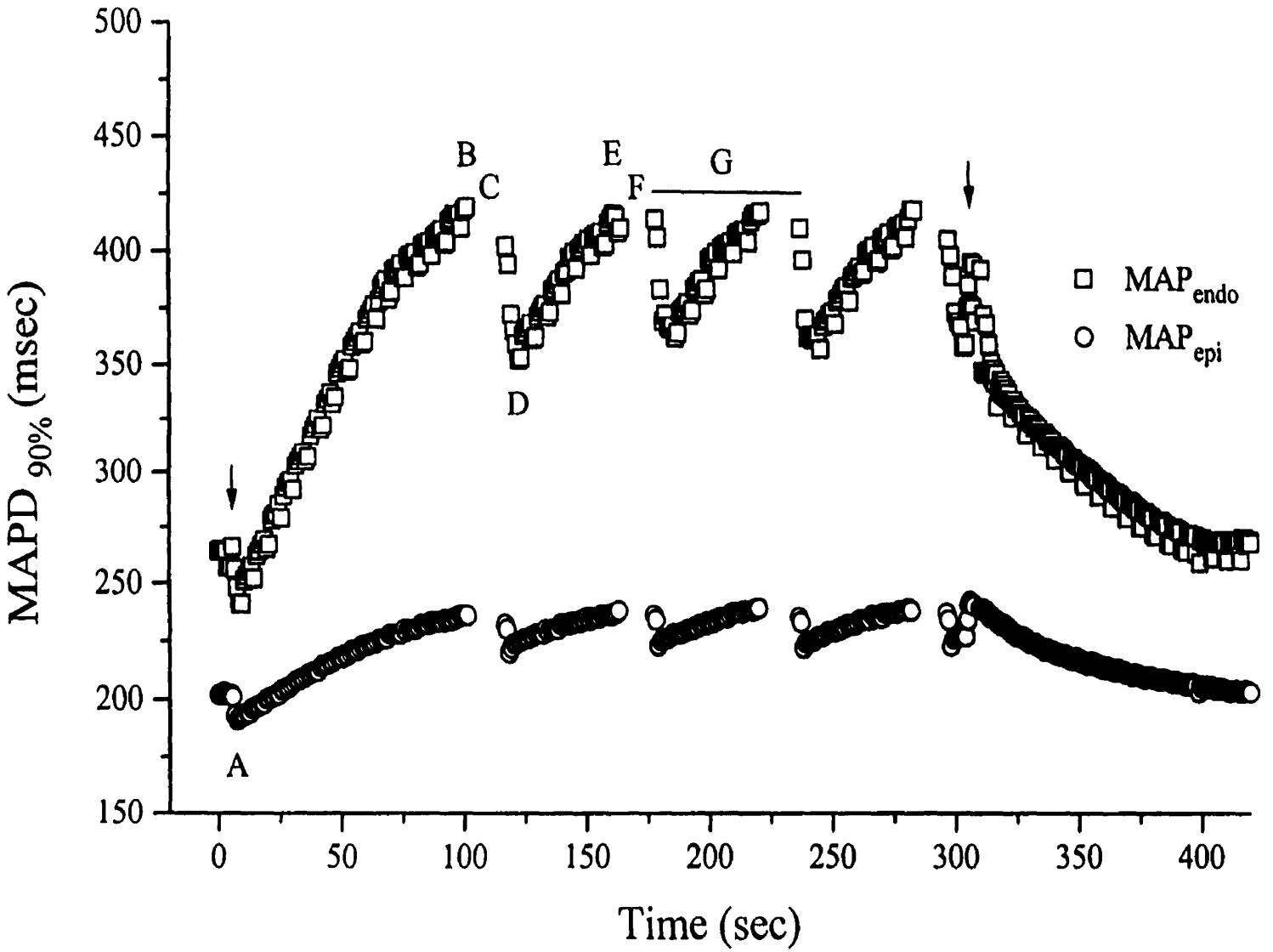
500
450
400
350
300
250
200
150
MAPD 90% (msec)
0
50
100
150
200
250
300
350
400
Time (sec)
A
B
C
D
E
F
G
MAP endo
MAP epi

II

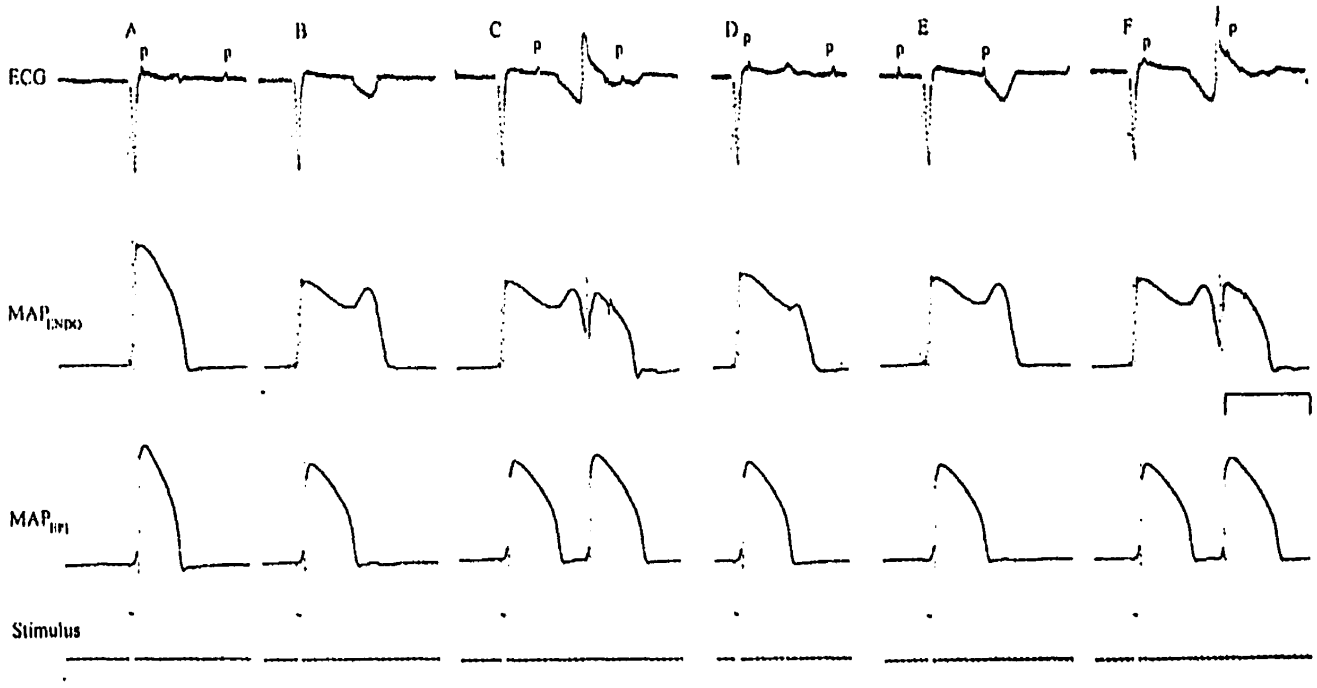

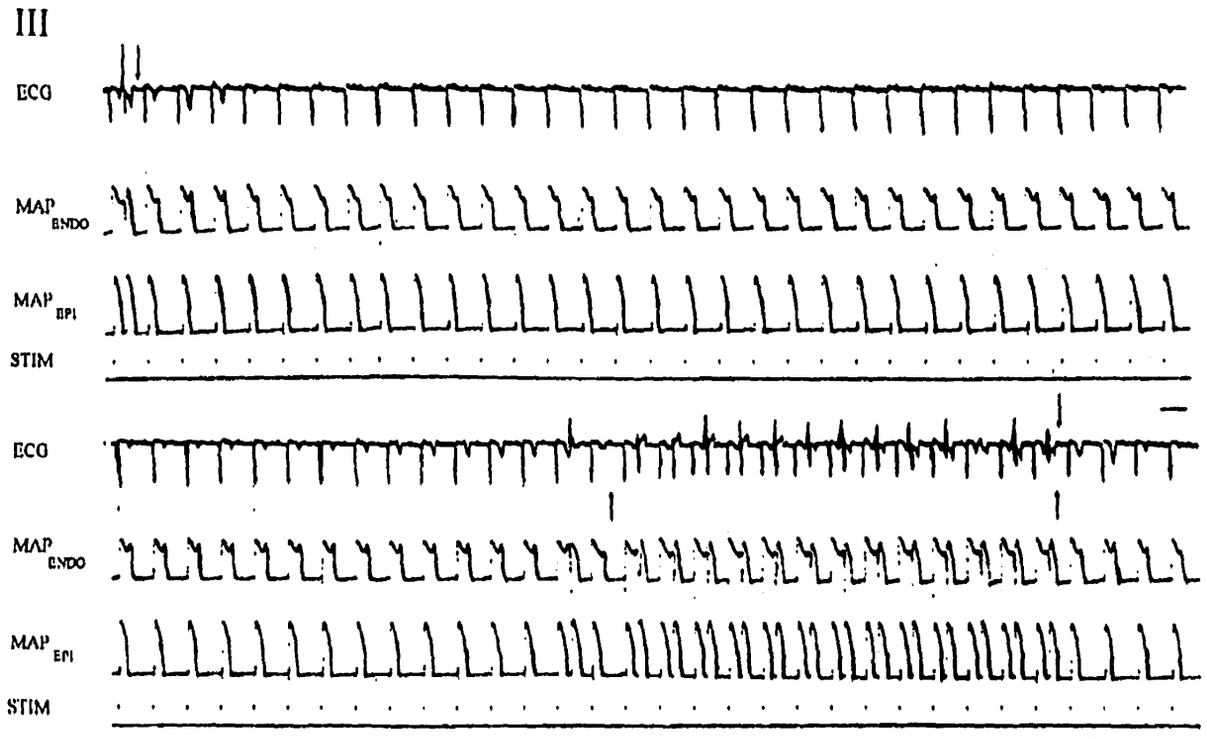
III
ECG
MAP ENDO
MAP EPI
STIM
ECG
MAP ENDO
MAP EPI
STIM

Figure 6. Typical example of spontaneous occurrence of repetitive arrhythmic cycles of multiple singlets in a 5 min trial of stimulation at a slow CL. Four consecutive arrhythmic cycles occurred during the 5 min trial. CL change from 0.5 to 1.0 sec. Preparation was exposed to 20 μM *d*-sotalol for 1.5 hours. I. Plot of MAP_{endo} and MAP_{epi} durations over time during the entire 5 min trial, beginning at the BCL and returning to the BCL (down arrows), showing the spontaneous changes in duration during 4 repetitive arrhythmic cycles. The gaps between the arrhythmic cycles indicate the presence of a series of singlets. II. A-F indicates first beat following CL change from 0.5 to 1.0 sec, last beat prior to initiation of singlets at the slow CL, first singlet, beat with shortest duration following spontaneous termination of singlets, last beat prior to second series of singlets and first singlet of second series, respectively. Calibration bar is 200 msec. The durations of these beats are indicated in the graph in I. III. Arrhythmic sequence showing a full arrhythmic cycle as indicated by G in the graph in I (interval between the down arrows). The arrhythmic cycle begins with elimination of singlets, followed by a progressive increase in the duration of the MAPs until their re-establishment and termination once again. The series of singlets (between up arrows) constitutes the gap in the second arrhythmic cycle. Also included are the last beat of the previous arrhythmic cycle and the first beat of the next one. Calibration bar is 400 msec.

occurring immediately prior to the generation of the first series of singlets was 183 msec. The endocardial recording site just prior to the generation of the first singlet had a prominent hump on its repolarization phase.(B in fig. 6, I and II) The size of this hump and the duration of the MAP_{endo} potential was shortened when coupled responses spontaneously terminated (D in fig. 6, I and II). This was followed by a another progressive lengthening of the MAP_{endo} duration until coupling occurred again (E and F in fig. 6, I and II). Coupled beats always occurred when the same level of disparity was attained between endocardial and epicardial recording sites. Return to the BCL resulted in a progressive exponential shortening of the durations back to the values at the BCL with termination of all episodes of singlets. Return to the shorter CL was always accompanied by a transient prolongation which preceded the gradual shortening.

This figure suggests a very strong association between a critical disparity in repolarization in the ventricles and induction of coupled beats. The conditions associated with coupling were very stable and reproducible. It is noteworthy that humps or "EADs" occurred only on the MAP recording from the endocardial site. These were never observed on the epicardial recording site. It is also worthy of note that a progressive increase in disparity was associated with a reversal in the polarity followed by a progressive increase in the amplitude and width of the T wave (fig. 6 III). Ninety six beats were required to attain the disparity associated with the first series of coupled beats whereas approximately half this number of beats (44-48) were required to achieve the exact same disparity in subsequent

episodes. This was due to the fact that durations did not shorten back to the baseline level after spontaneous termination of each series of coupled beats and thus a lessor number of beats were required to achieve the same disparity. The number of beats preceding initial coupling was an inverse function of the CL and a direct function of the drug concentrations as shown in fig. 7. Thus, a high drug concentration and a long CL were the most conducive to the early induction of coupled beats.

Singlets occurred reproducibly and reliably and consistently in every trial in every preparation in which the combination of drug concentration and CL was adequate to produce a certain critical degree of prolongation of MAPs at the endocardial recording site (128 ± 42 msec, n=13 trials in five hearts). Fig. 7 illustrates the CIs of each sequence of singlets in each arrhythmic cycle shown in fig. 6. This figure shows that the CI of the first singlet of each sequence of singlets is always longer than the second. The CI then progressively increases and becomes unstable for one or two beats before the sequence terminates. This kind of behaviour is in keeping with triggered activity as the mechanism of initiation of the coupled beats.

Usually singlets were followed by couplets, triplets or quadruplets the incidence of which was greater at higher drug concentrations and longer CLs. Of 123 TdP analyzed in 5 preparations, in 119 of them TdP was preceded by either a singlet or a combination of couplets, triplets and/or quadruplets. In only 4 of 123

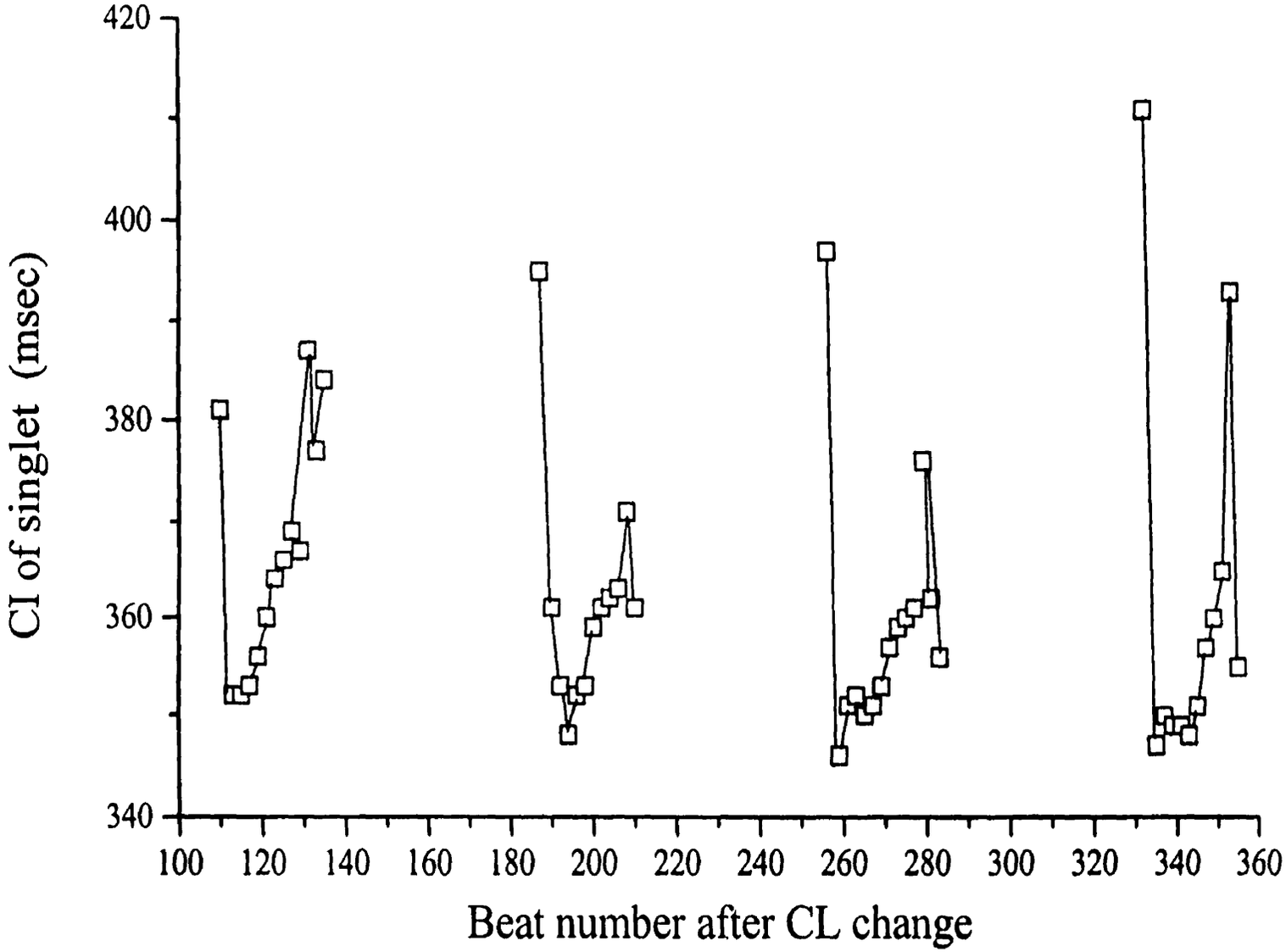
CI of singlet (msec)
420
400
380
360
340
100
120
140
160
180
200
220
240
260
280
300
320
340
360
Beat number after CL change

Figure 7. Changes in the beat to beat CI of each series of singlets during the four arrhythmic cycles illustrated in fig. 6.

instances did TdP occur after a certain critical disparity had been reached but not preceded by other arrhythmias.

Fig. 8 shows a typical example of the association of disparity in repolarization with spontaneous induction and termination of TdP. This trial shows an example of 5 spontaneous arrhythmic cycles 3 of which had episodes of TdP. In contrast to the example shown in fig. 6, the slope of the relationship between MAPD and time was very steep and the critical disparity was reached within approximately half the time. The first arrhythmic cycles resulted initially in an irregular arrhythmic sequence consisting of singlets, couplets, and triplets (A in fig. 8. I and II) followed by an episode of TdP (upper panel in B in fig. 8. III). The singlets generated showed irregular activation patterns as evidenced by various degrees of interruption of the repolarization phase of the endocardial MAP. Each episode of TdP was preceded by a singlet in a typical short-long-short sequence. Each TdP was initiated by a singlet arising late in the T wave. The MAP_{endo} configuration of both the singlet preceding TdP and the one initiating TdP were variable indicating different degrees of propagation of the premature beat. Each TdP displayed the typical twisting pattern on the ECG and was of variable duration. Spontaneous termination of TdP was followed by an abrupt shortening of duration of both the MAP_{endo} and MAP_{epi} potentials, especially of the MAP_{endo}. The degree of shortening of these potentials and the decrease in disparity in repolarization was correlated with the duration of the TdP as indicated in both the graph in fig. 8. I and the potentials in fig. 8. III. Neither the termination of TdP nor

I

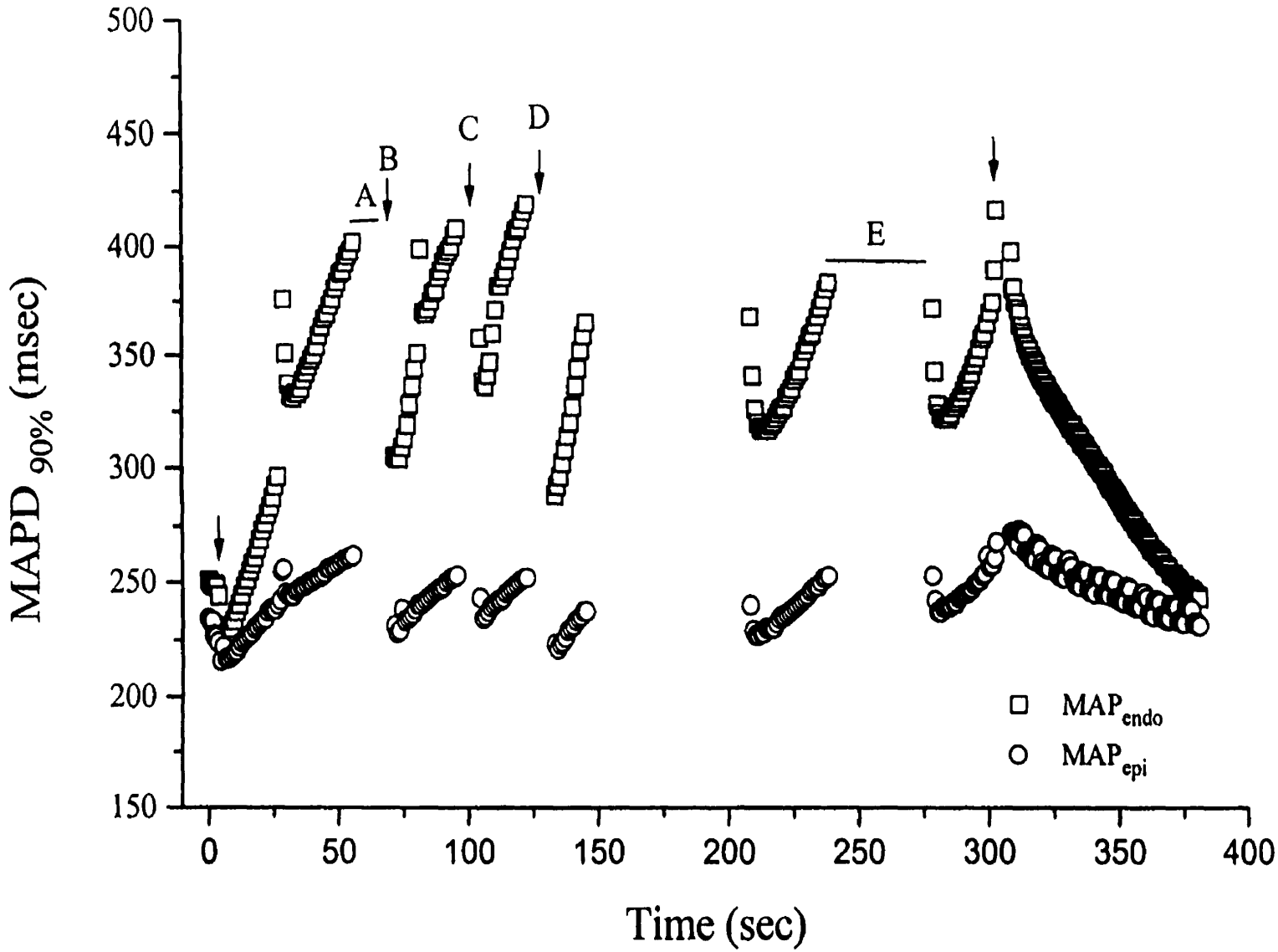
500
450
400
350
300
250
200
150
MAPD 90% (msec)
A
B
C
D
E
MAP endo
MAP epi
0
50
100
150
200
250
300
350
400
Time (sec)

II

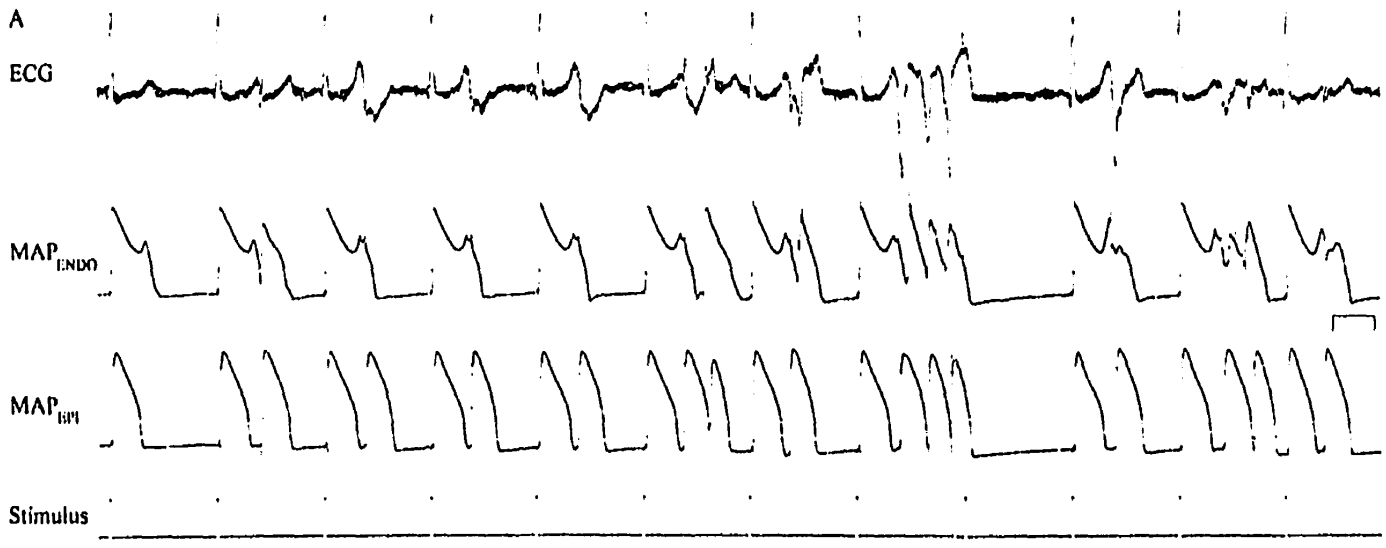

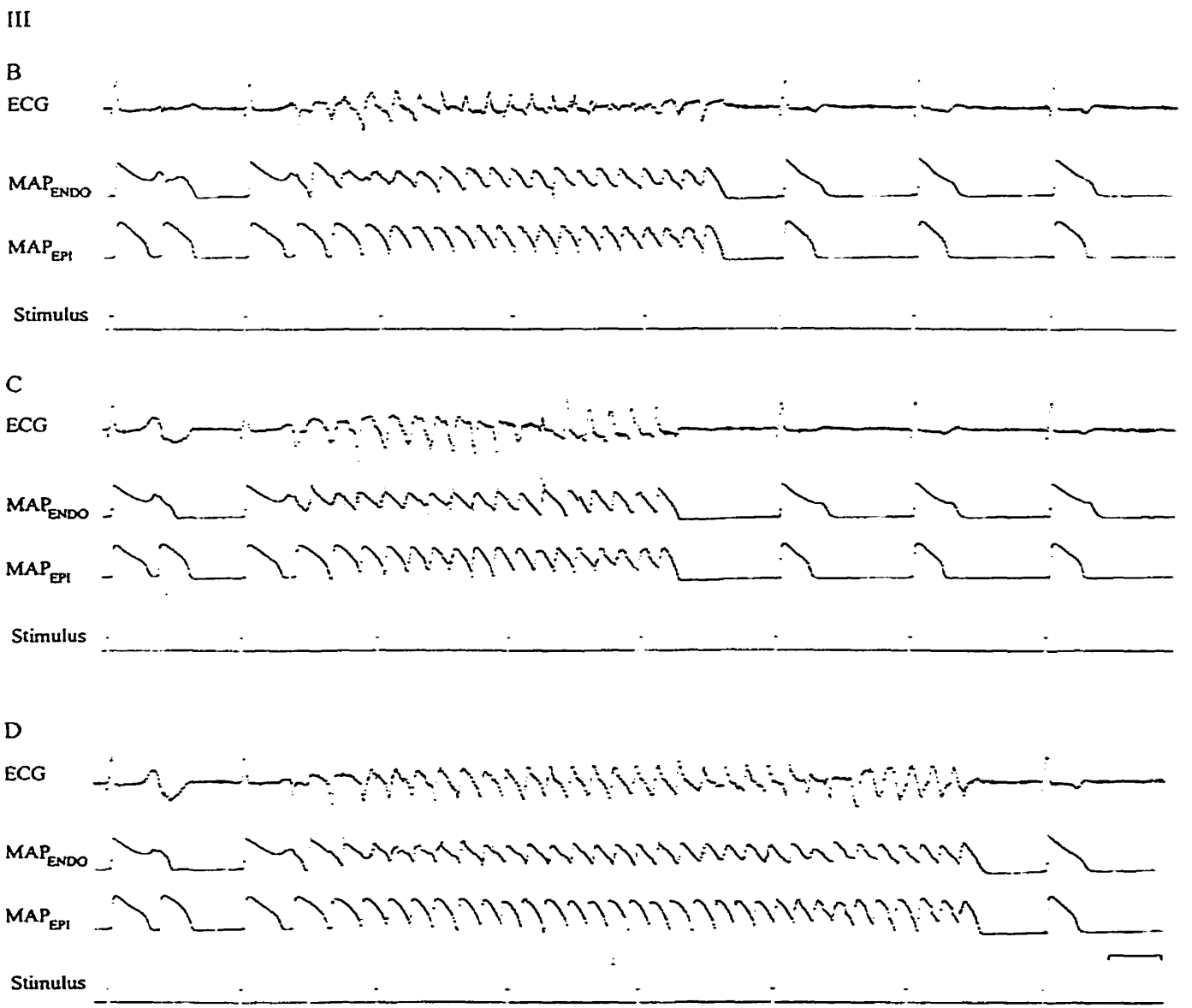
III
B
ECG
MAP ENDO
MAP EPI
Stimulus
C
ECG
MAP ENDO
MAP EPI
Stimulus
D
ECG
MAP ENDO
MAP EPI
Stimulus

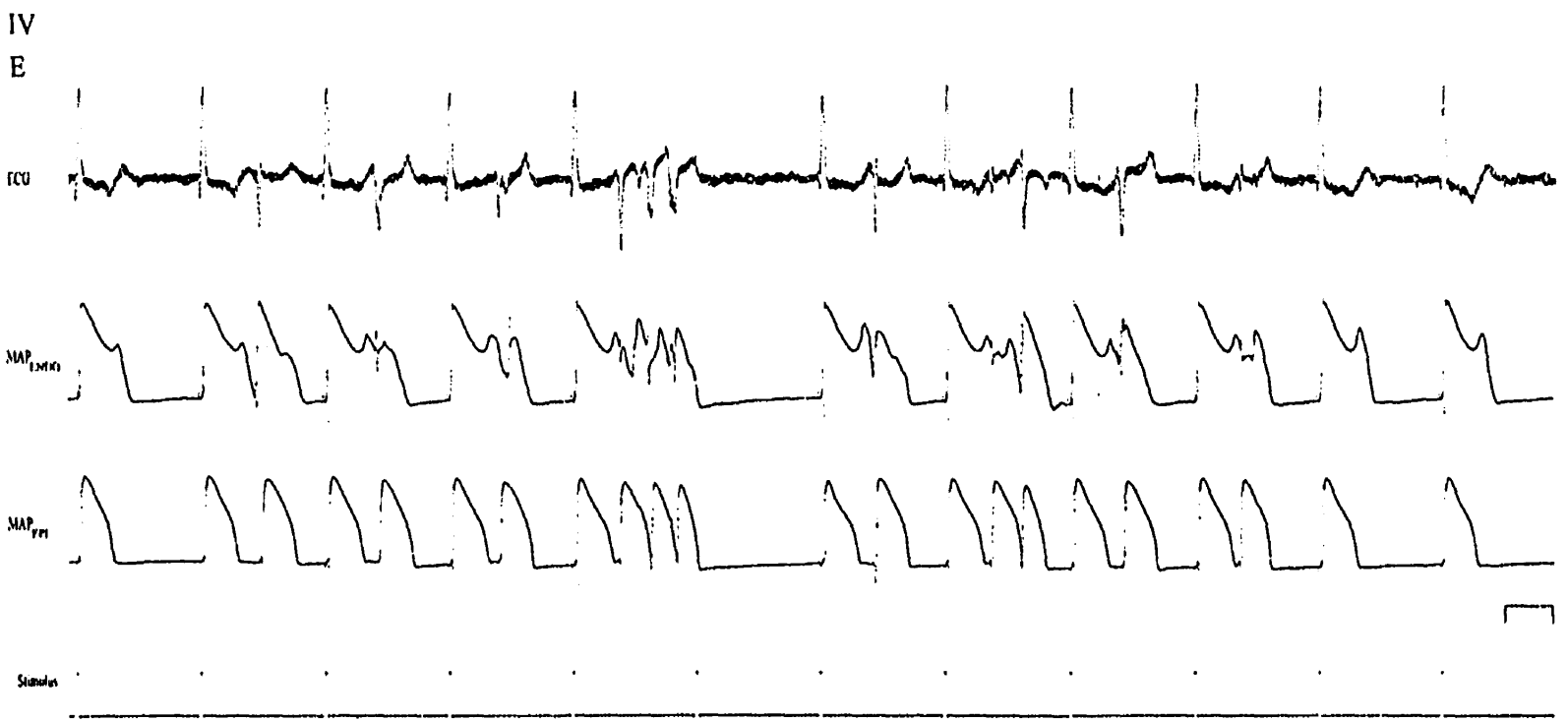
IV
E
ECG
MAP
MAP
Stimulus

Figure 8. Typical example of association of prominent disparity in repolarization with spontaneous induction of TdP and association of elimination of disparity with its termination in a typical 5 min trial of stimulation at a slow rate. CL was increased from 0.5 to 1.0 sec. I. Plot of MAP_{endo} and MAP_{epi} durations during the 5 min trial beginning at the BCL and returning to the BCL. This trial consisted of 5 spontaneous arrhythmic cycles 3 of which included episodes of TdP (B,C and D). The others consisted mainly of singlets, couplets, triplets and quadruplets. The gaps between arrhythmic cycles indicate periods of multiple arrhythmic activity. The arrows indicate the presence of TdP. II. Shows an arrhythmic sequence (A) prior to the initiation of the first TdP consisting of the last beat with maximally prolonged $MAPD_{endo}$ just prior to coupling followed by a number of singlets, two couplets and a triplet. III. Shows the 3 episodes of TdP (B,C and D) indicated in I. Note that each episode is preceded by a coupled beat in which the MAP_{endo} is fused. Each TdP begins with a long QT interval and a fused MAP_{endo} and shows typical twisting in the ECG trace. Each TdP is followed by regular beats with a reduced disparity. Durations of MAP_{endo} and MAP_{epi} in the beats following TdP are 304, 232 (disparity 72); 362, 240 (disparity 120); and 288, 224 (disparity 64) for TdP B, C, and D, respectively. IV. A complete arrhythmic cycle associated with less disparity than that associated with TdP and accompanied by singlets, couplets and triplets (indicated by E in the graph in I). Calibration bar is 400 msec.

the twisting pattern was related to the presence of the pacing stimulus as such stimuli were ineffective during each episode. Following spontaneous termination of each episode of TdP, the potentials again spontaneously increased in duration until a critical disparity was again reached and the cycle repeated itself. The remaining two arrhythmic cycles were highly arrhythmogenic but were not followed by TdP. Each showed variable sequences of singlets, couplets, and triplets. The last arrhythmic cycle was interrupted by a return to the BCL which was followed by a gradual shortening of potentials to the baseline values. Fig. 9 shows the intervals of a couplet, triplet, quadruplet and TdP in one of the sequences illustrated in fig. 8. As can be seen the first beat of each of these rhythms is within the range of the intervals of the singlet followed by a progressive decline in the interval going into TdP. Such behaviour is in keeping with triggered activity as the mechanism of the first beat of each of these rhythms followed by reentry.

Both the initiation of singlets and of TdP was associated with a critical disparity while its termination was associated with the elimination of this disparity. Fig. 10 summarizes the disparity present at the BCL, in beats preceding singlets and in the last beat of the TdP. The average endocardial/epicardial disparity was 128 ± 57 msec whereas the QT/epicardial disparity was even greater, 173 ± 57 msec. The greater latter disparity is likely related to the placement of the endocardial probe not always being located at a site of maximal duration. As TdP was almost always preceded by an arrhythmia it was not possible to measure

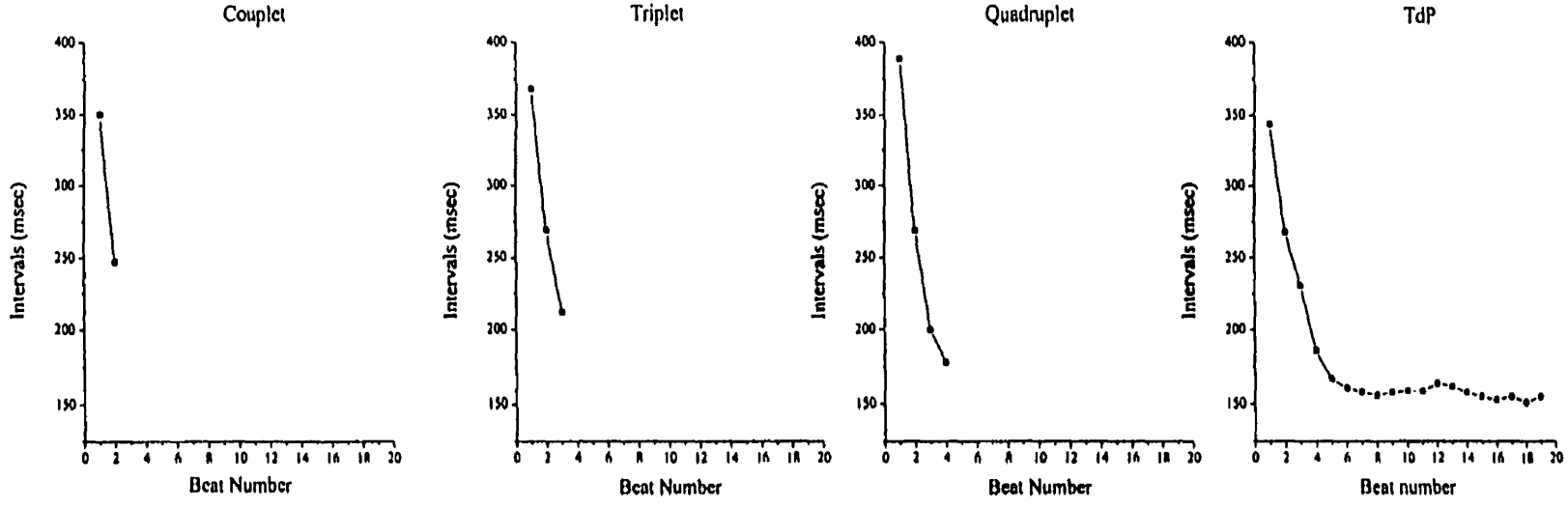

Figure 9. Comparison of the first CIs and the subsequent interval of a typical couplet, triplet and quadruplet with that of a TdP. The couplet and triplet preceded the TdP whereas the quadruplet followed it during one of the cycles illustrated in fig. 8.

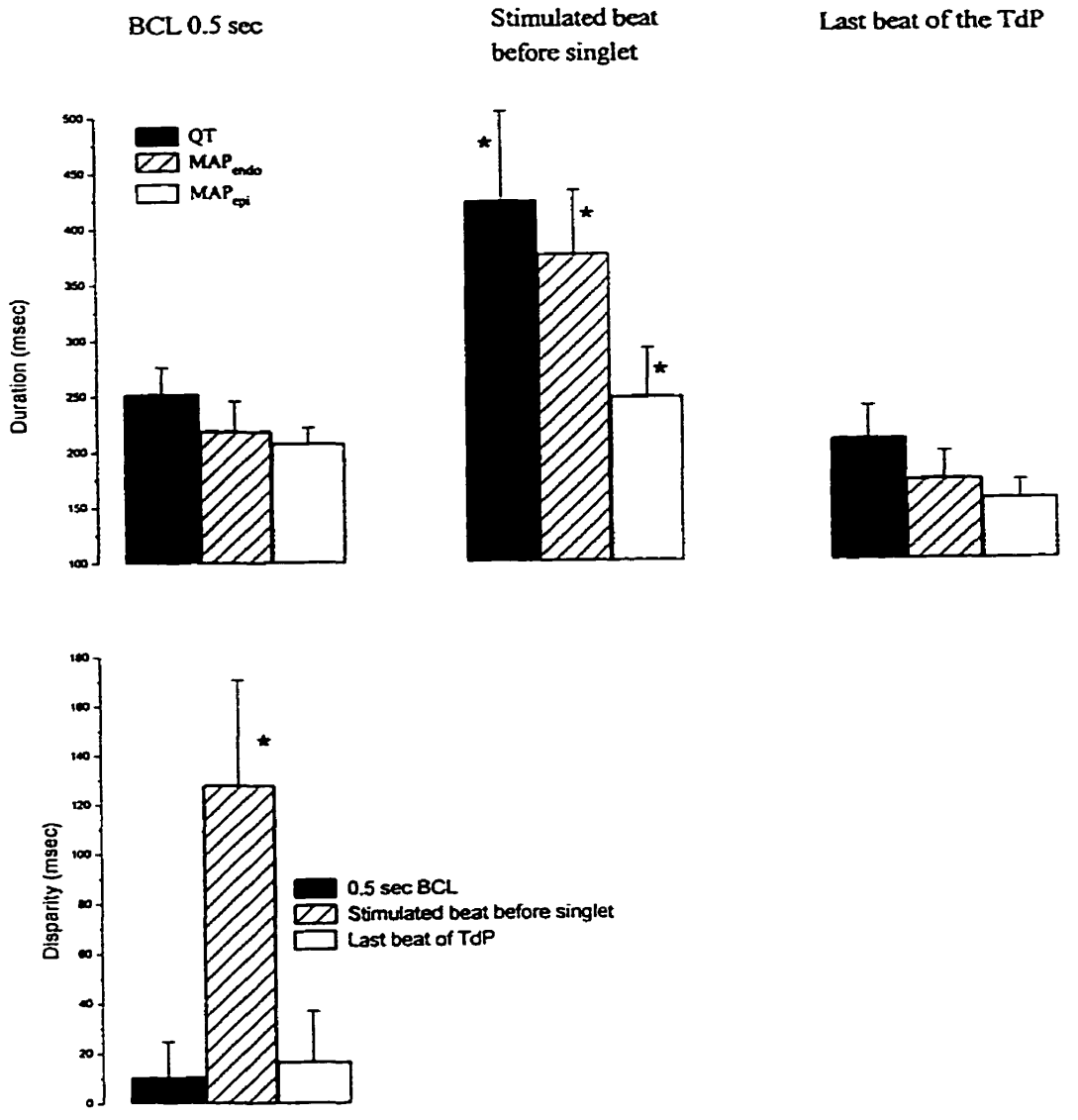

Figure 10. Comparison of the durations of QT, MAP_{endo}, and MAP_{epi} and the disparity in repolarization during the short BCL (0.5 sec) with the stimulated beat preceding the first singlet at along CL (1.0-1.5 sec) and the elimination of this disparity in the last beat of the TdP. All graphs show the mean ± SD. Data obtained from 13 trials in 5 hearts. All hearts exposed to 20 μM *d*-sotalol. Asterisk indicates significant difference from either the BCL or the last beat of the TdP.

directly the disparity preceding it. However, once the critical disparity for generation of singlets was reached any of the above rhythms including TdP could be generated.

Incidence of TdP - dependence on a critical CL window

In order to determine the optimum conditions for generation of TdP, we assessed the CL length dependence of this arrhythmia using an intermediate concentration of *d*-sotalol (20 μM). In 7 hearts the incidence of TdP was determined at 5 different CLs. In each heart, the CL was changed from the BCL of 0.5 sec to a longer CL for 5 min, returned to the BCL for at least 2 min and then switched to another longer CL. The CLs were studied in a sequentially increasing manner, a sequentially decreasing manner as well as at random. A total of 127 episodes of TdP were observed in these hearts. The results are summarized in fig. 11. Although TdP was observed at all CLs there appeared to be a critical range of CLs during which the incidence of this arrhythmia was higher. Within this critical window the number of arrhythmic cycles was greater. At short CLs the critical disparity associated with arrhythmia was usually not attained. At longer long CLs, even though the disparity obtained may have been greater, the preparations sometimes developed a stable arrhythmic pattern of coupled beats which remained throughout the trial. Fig. 12 shows a typical example in a preparation stimulated at a CL of 1.5 sec. As soon as coupling occurs the endocardial MAP shows a fused potential of long duration. This stable rhythm remained for 100 sec.

A

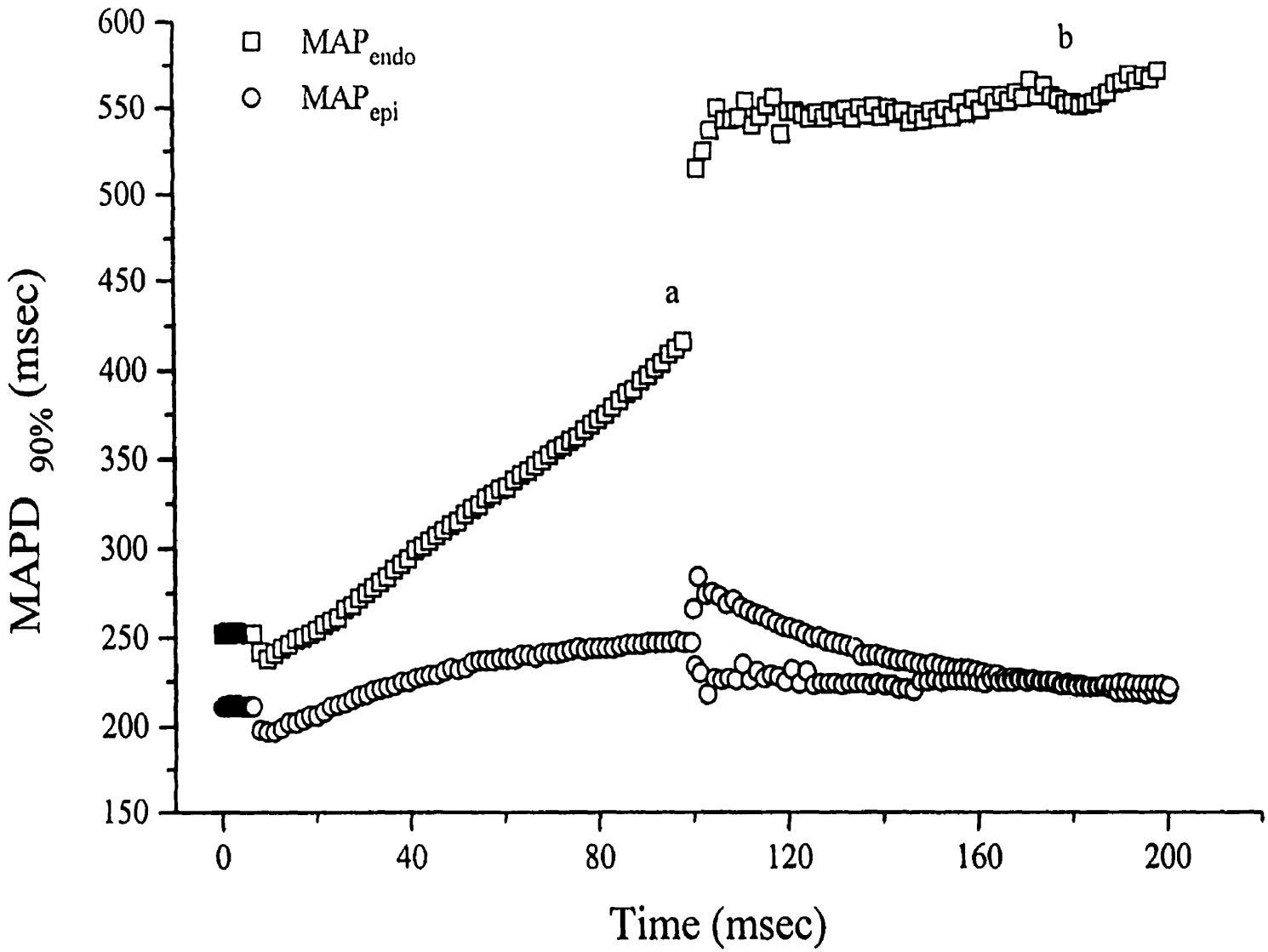
MAP endo
MAP epi
a
b
MAPD 90% (msec)
600
550
500
450
400
350
300
250
200
150
0
40
80
120
160
200
Time (msec)

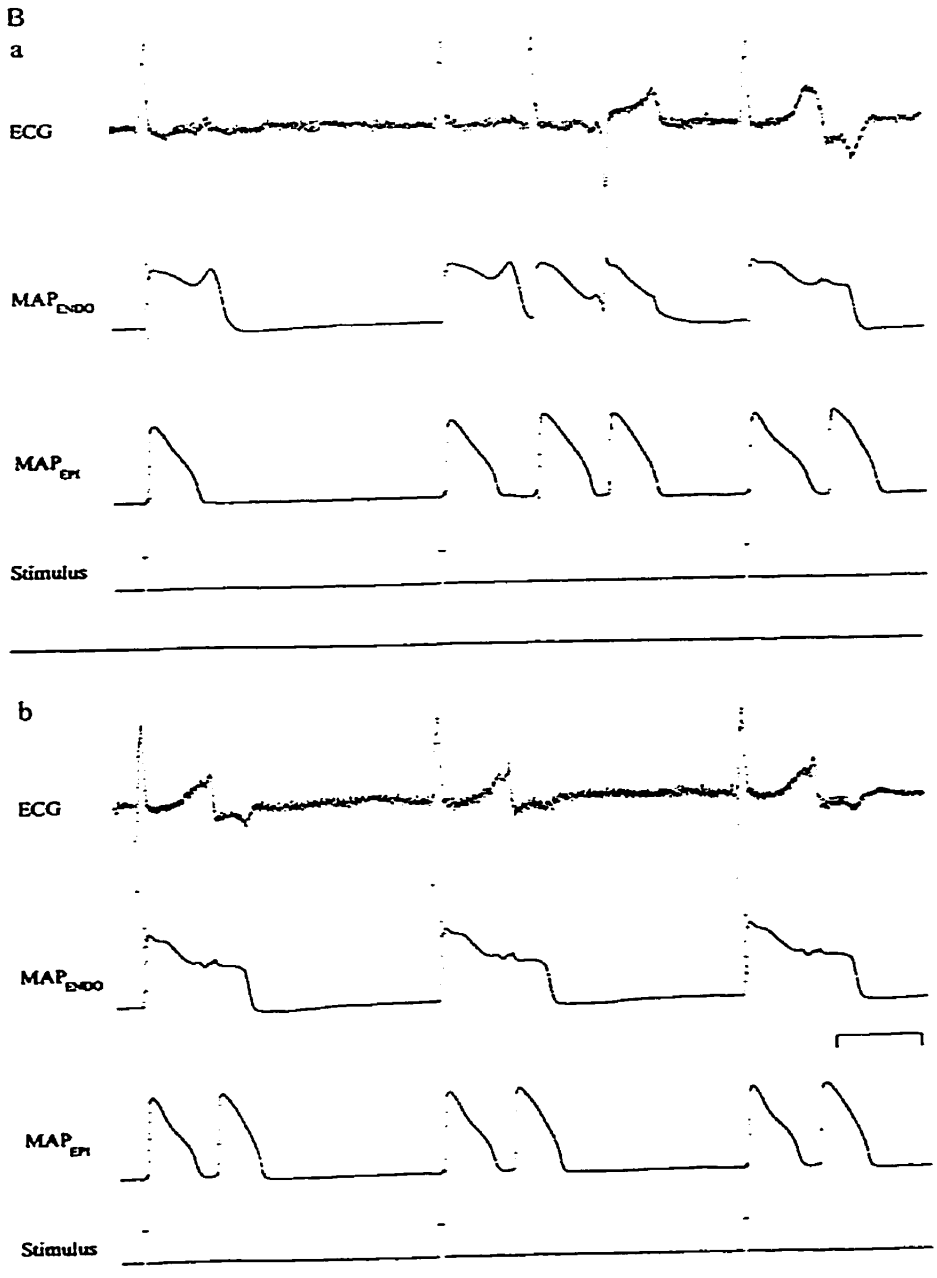

Figure 11. Association of fusion responses at the endocardial recording site with stable coupled responses at the epicardial site. Panel A shows the beat prior to coupling. First response is a couplet followed by a singlet. Panel B shows the stable pattern of singlets maintained for 100 sec. Preparation was exposed to 20 μM of *d*-sotalol; CL change from 0.5 to 1.5 sec.

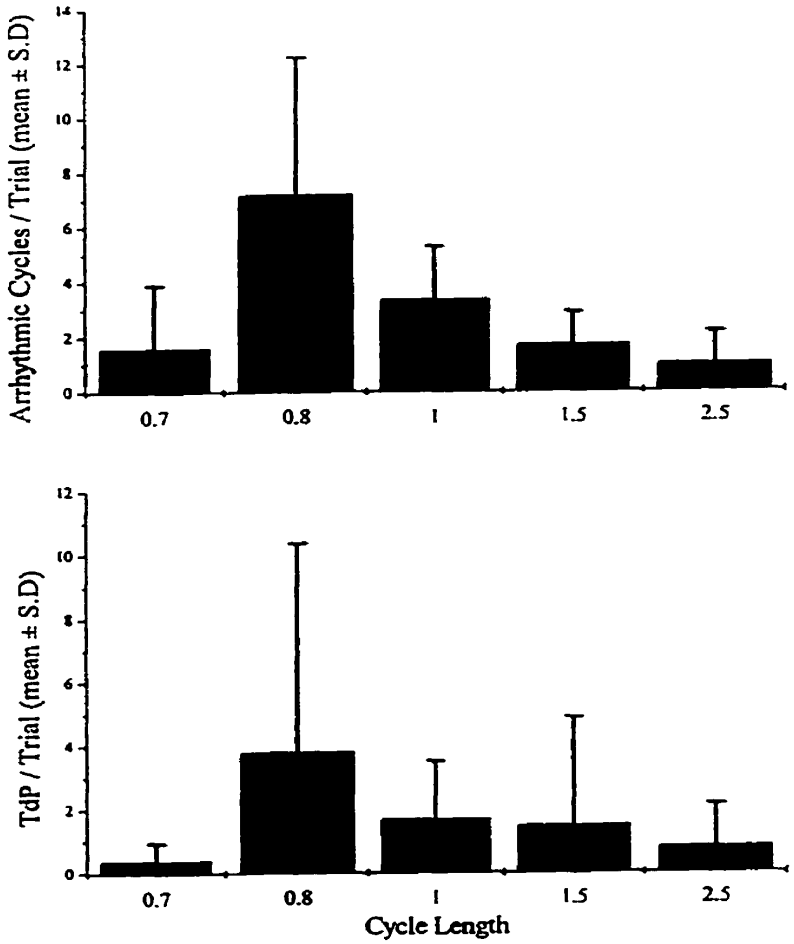

Figure 12. Dependence of TdP incidence and occurrence of arrhythmic cycles on a critical CL window. Data obtained from 7 hearts in which CL was changed from 0.5 sec to 0.7 - 2.5 sec either sequentially or at random.

In 5 additional hearts we determined the incidence of TdP during perfusion with 20 μM of *d*-sotalol over a course of 3 hr to assess its reproducibility. Beginning 25 min after the start of drug perfusion, the pacing CL was increased from the BCL of 0.5 sec to 1.5 sec for 5 min. The number of episodes of TdP during each 5 min trial was determined after which the CL was returned back to the BCL of 0.5 sec for 10 min and the trial was repeated over the course of 3 hr (a total of 13 trials). The results are plotted in fig. 13.

The incidence was more stable over the course of the first two hours of perfusion and appeared to increase during the last hour of perfusion which could be as high as 20 episodes per trial. In any one experiment the number of TdP generated ranged from 10 to 65 episodes. A total of 158 episodes of TdP were observed in these 5 hearts during 3 hr of drug perfusion.

TdP - Characteristics

To assess the characteristics of TdP in these hearts, a subset of 35 of these 158 TdP were further analyzed. The TdP were chosen at the beginning, middle and at the end of the experiments to make sure that the TdP characteristics did not change with time. All episodes of TdP were typically self limited.

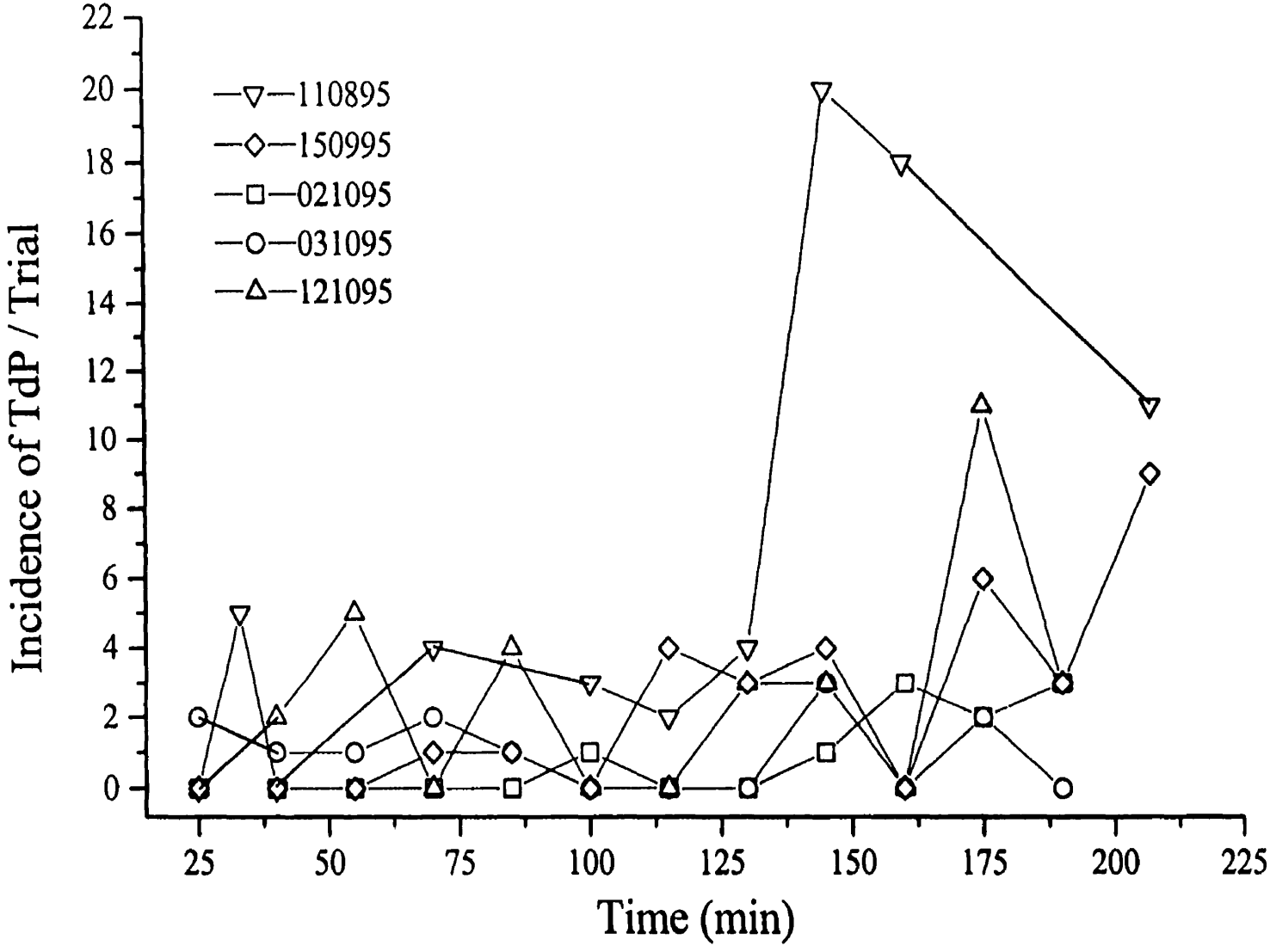
Incidence of TdP / Trial
Time (min)
110895
150995
021095
031095
121095
0
2
4
6
8
10
12
14
16
18
20
22
25
50
75
100
125
150
175
200
225

Figure 13. Incidence of TdP during 3 hr of perfusion with 20 μM *d*-sotalol in 5 hearts, beginning 25 min after the start of drug perfusion. Each symbol represents a different heart. Each point represents the number of episodes of TdP during a 5 min period of stimulation at a CL of 1.5 sec. Following each 5 min period the CL was switched back to the BCL of 0.5 sec for 10 min.

In all of the TdP analyzed, the CI of the first TdP beat to the stimulated beat was 367 ± 37 msec, the average CL was 196 ± 15 msec (307± 23 beats/min) and the average number of beats in each TdP episode was 10 ± 4 beats (mean ± S.D.) (range 5-31 beats). There were no differences between the characteristics of the TdP observed at the beginning of the experiment and those observed at the end.

Discussion

D-sotalol induced arrhythmias in the isolated rabbit heart

This study is the first to describe the proarrhythmic effects of *d*-sotalol, including the induction of TdP, in the presence of clinically relevant drug concentrations and bradycardia in an isolated Langendorff-perfused rabbit heart. In the presence of bradycardia, *d*-sotalol (10-40 μM) prolongs the QT interval and induces a typical pattern of arrhythmia generation beginning with singlets and progressing to couplets, triplets, quadruplets and eventually TdP. These arrhythmias occurred spontaneously in a predictable, reproducible manner. There was a progressive evolution of singlets into couplets, triplets, quadruplets and TdP. TdP was almost never observed in the absence of the lessor arrhythmias and was more likely to occur in the context of multiple rhythm disturbances rather than singlets alone. Thus, the presence of the lessor arrhythmias in the context of a prolonged QT interval and increased disparity could be considered a forerunner of TdP.

Electrophysiological mechanism of the initiation of arrhythmias

EADs leading to triggered activity or dispersion of repolarization leading to reentry have been the two hypotheses proposed to explain the mechanism of TdP. (review) [21] Dispersion of repolarization has been recognized as an important

electrophysiological alteration accompanying TdP [22,23]. However, precise evidence for either mechanism in the initiation and perpetuation of TdP has been lacking. The conditions chosen for the present study allowed us to determine the sequence of events leading up to the initiation of coupled beats and TdP *in situ* and allowed us to shed some light on their likely mechanism.

Initiation of coupled beats was correlated with a certain threshold of disparity of repolarization in the ventricles exceeding an average value of 128 msec. The results show for the first time a direct, selective, CL dependent, lengthening effect of *d*-sotalol on repolarization at sites on the endocardial surface of the rabbit ventricle where PFs would be expected to be located. It is this selective effect of the drug which creates the disparity in repolarization in ventricular tissue which was directly correlated with the generation of coupled beats and TdP.

Analysis of MAP recordings from the endocardial and epicardial surfaces provides compelling evidence that the coupled beats were the result of EAD induced triggered activity originating on the endocardial surface. Only recording sites on the endocardial surface showed secondary positive deflections on the plateau of the MAPs. Since these positive deflections always appeared on the plateau phase of endocardial MAPs and not during late phase 3 or 4 as observed by many other investigators [11,16,24] it is likely that they represent true EADs. Since in the rabbit ventricle PFs are only present on the endocardial surface [25] one would

expect such activity to be recorded only by an endocardial MAP electrode. This assessment is substantiated by our previous study using intracellular microelectrode recordings in rabbit ventricular endocardium in which we have shown that under identical conditions of drug concentration and pacing protocols, *d*-sotalol induces EADs and triggered activity only in PFs resulting in coupled responses in muscle. [14] Both the size of the "EAD like deflections" and durations of MAP_{endo} potentials changed in parallel as occurs in PFs under *in vitro* conditions prior to initiation of triggered activity. The durations recorded from the endocardial surface *in situ* are much shorter than those manifest in PFs. This is understandable since the MAP recording is a composite of PFs and VM and thus its duration would be in between that of either cell. [18]

One of the criticisms of triggered activity originating in PFs as a mechanism for TdP arrhythmias has been the fact that under *in vitro* conditions extremely long CLs are necessary to produce the phenomenon whereas *in situ* coupled beats occur at much shorter CLs. This is also understandable for a number of different reasons, viz., 1). PFs in preparations superfused under *in vitro* conditions are exposed to higher potassium concentrations in adjacent cells because of exposure to ischemic cells several layers below the surface cells. Class III drugs are known to produce less lengthening of APD in the presence of higher K^+ concentrations. Thus, longer CLs are necessary to produce the same effect [26] 2). depending on how the preparations are dissected the number of Purkinje muscle junctions and the opportunity for conduction of the triggered AP would be

considerably reduced (Valois and Sasyniuk, unpublished observations) and, 3). there would be less drug binding. Thus, triggered activity is only manifest under extreme conditions of CL and concentration under *in vitro* conditions.

The results clearly show that singlets and the first beats of couplets, triplets or quadruplets and TdP are initiated in the same way. Under *in vitro* conditions it was rare to see more than coupled APs unless the preparations were exposed to extreme conditions of dose and CL. Since the same sequence of events which led to initiation of triggered activity *in vitro* leads to initiation of singlets as well as the more complex rhythms *in situ* this is compelling evidence that the mechanism for initiation of singlets, couplets, triplets and quadruplets as well as TdP induced by *d*-sotalol is a triggered AP originating from PFs on the endocardial surface of the rabbit ventricle. Under the conditions of our experiments, the second and subsequent beats of couplets, triplets, quadruplets and TdP must be due to reentry since they exhibit a progressive decline in intervals, a characteristic not in keeping with triggered activity. Furthermore, the conditions which led to triggered activity in the first place is eliminated by the coupling itself and is only re-established after progressive lengthening of the endocardial potentials (as illustrated in figs. 6 and 8). A decrease in the CI of the singlet together with further prolongation of the endocardial potential was associated with conversion of singlets to multiple beats and TdP. Such beats would more likely be conducted with greater delay thus facilitating reentry. Multiple coupled beats preceding TdP result in variable diastolic intervals which would have variable effects on the duration of potentials

of subsequent beats, thus affecting conduction of coupled beats with greater likelihood of functional block developing and facilitating a reentry mechanism. Moe and Mendez [27] and Sasyniuk et al. [28] highlighted the importance of the immediately preceding CL on refractory period and its role in reentrant rhythms. If such disruption of the relationship between the immediately preceding CL and MAPD was not present then a stable bigeminal rhythm ensued as observed in fig. 12. Thus, the evolution of couplets into more complex rhythms and eventually TdP is really part of a continuum in which small changes in the coupling interval may determine whether or not TdP ensues.

Termination of TdP was associated with a CL dependent elimination of the disparity which led to its initiation. Thus, the arrhythmia itself eliminates the conditions which led to its initiation in the first place and explains why these episodes are self-terminating.

Although the endocardial MAP recordings (together with the *in vitro* data of the previous study) strongly suggests that the arrhythmias, including TdP originates in PFs on the endocardial surface there is the possibility that M cells are responsible for the lengthening of endocardial MAPs. However, this possibility is highly unlikely. Antzelevitch and Sicouri [29] have recently identified M cells in the deep subendocardial tissues of endocardial structures formed by invaginations of the free wall (papillary muscle, trabeculae and septum). They have also shown that M cells in these structures can generate EAD-induced triggered activity in

response to agents that induce triggered activity in PFs. Whether M cells are present in the rabbit heart is not known. However, in the dog heart these cells have been shown to occur deep within the septum and endocardium. If this is also the case in the rabbit, it is unlikely that the endocardial probe will pick up potentials several mm from the surface. Furthermore, a recent study by Rosen et al. [30] shows that M cells do not exhibit selective prolongation of their potentials under *in situ* conditions.

Comparison to TdP clinically

The spontaneous TdP arrhythmias generated in our model bare a high resemblance to the arrhythmias which occur clinically in that: 1. their generation is associated with prolonged QT intervals and broad large amplitude T waves; 2. their induction is highly CL dependent and associated with large disparities; 3. they are initiated by a coupled beat with a long CI in a typical short-long-short sequence; 4. the TdP of long duration display the typical gradual undulations and twisting of the QRS axis; 5. all of the TdPs are self terminating; 6. the volume conducted ECGs resemble those observed under clinical conditions. The frequencies of TdP occurring spontaneously in our rabbit model are faster than those occurring clinically. This would indeed be expected since the CL dependent shortening of APD in the rabbit heart is greater than in human ventricle. The frequency of TdP would define the limit of the rabbit refractory period in the

presence of *d*-sotalol which would be shorter than that present in the human ventricle.

Prolongation of the QT interval associated with the proarrhythmic effects of *d*-sotalol was due to greater dispersion of ventricular repolarization times within the ventricles due to the differential drug effects on endocardial versus epicardial tissue. Thus, the CL dependent nonuniform prolongation of MAPD by *d*-sotalol was responsible for the QT changes observed. A typical effect of *d*-sotalol was a reversal of the polarity of the T wave followed by a progressive increase in its amplitude and duration. The prolongation of the QT interval correlated with the disparity in repolarization between endocardial and epicardial potentials and was thus an indication of that disparity. U waves or split T waves were only present during multiple rhythms and were associated with very large differences in endo/epi disparity.

Advantages of model

This model is convenient for testing the potential proarrhythmic effects of cardioactive drugs and offers several major advantages to other models aimed at elucidating the basic mechanisms of TdP. As set out above, the characteristics of the arrhythmia resemble those in the clinical setting in several respects. In a previous study [15,31] we have shown that both quinidine and E-4031 induce TdP in our model (both drugs block the I_{Kr} current) whereas class I C drugs (flecainide)

which block mostly sodium channels do not (unpublished data), suggesting that this model is perhaps selective for the proarrhythmic effects of drugs with class III actions. Thus, this model can be used to assess the proarrhythmic effects of other pharmacological agents (such as antihistaminic drugs) for their propensity to develop TdP. The technique has advantages of simplicity and relatively low cost and permits the study of antiarrhythmic drugs free from the confounding effects of autonomic reflexes and variable hemodynamics. The stability and reproducibility of the arrhythmias provides an ideal model for activation mapping studies as we have done in a subsequent study. [32]

Comparison to other experimental models

A first important finding of the present study was that the spontaneous occurrence of PVT occurred with a high frequency in a reproducible, predictable manner without the necessity of alpha adrenergic stimulation as required in the model Carlsson et al. [33] nor the necessity of ionic interventions as in the model of Zabel et al. [16] In contrast to our model, *d*-sotalol and bradycardia alone were not sufficient to induce TdP arrhythmias in the isolated rabbit heart model of Zabel et al. [16]. Additional exposure to low potassium and magnesium concentrations was required to induce arrhythmias. Furthermore, arrhythmias subsided after only 2 minutes despite the continued presence of these interventions. Such a model does not permit a study of the mechanism of these arrhythmias. The dose of *d*-sotalol chosen by Zabel et al. [16] is extremely high. At such concentrations *d*-sotalol alters

not only the I_{Kr} current but many other currents as well including I_{K1} and I_{Na} [34]. They speculated that lack of autonomic innervation in their model was the reason for lack of arrhythmia generation. Since we obtained arrhythmias including a high incidence of TdP also in an isolated heart model, it seems that lack of autonomic innervation is unlikely the reason for lack of arrhythmias in their model . The requirement for α-adrenergic agonists in the model of Carlsson et al. [33,35] is likely related to a reflex slowing of the heart rate rather than to a facilitation of the proarrhythmic effects of class III drugs since exposure of our preparations to phenylephrine actually prevented the initiation of coupled beats (unpublished observations). Thus, autonomic effects are incidental to the class III effects of the drug. In the study by Asano et al. [36] PVT was induced in the isolated rabbit heart by both quinidine and E-4031. In their study arrhythmias were induced either by burst pacing or by a single pulse in the absence of idioventricular rhythms. Both induction modes are different from those in the present study and from the typical induction pattern observed clinically. In the model of Vos et al. [7] programmed electrical stimulation was used to induce TdP, a mode of initiation not usually associated with in TdP clinically.

Conclusion

Our model shows a high incidence of reproducible TdP arrhythmias allowing study of its mechanism. Occurrence of TdP is associated with an interval dependent disparity in repolarization in the ventricles and its initiation is

consistent with drug induced EAD-dependent triggered APs originating in the VSCS on the endocardial surface. Termination of TdP is associated with elimination of the disparity which was responsible for its initiation. Our model may be useful for the comparison of the proarrhythmic potential of novel class III drugs to initiate TdP.

Acknowledgments

The authors wish to thank Ms. Kelly Harrison and Suzanne Seto for expert technical assistance and Bristol-Myers Squibb Canada for supplying *d*-sotalol.

References

1. Singh BN, Ahmed R: Class III antiarrhythmic drugs. [Review]. *Current Opinion in Cardiology* 1994;9:12-22

2. Waldo AL, Camm AJ, deRuyter H, Friedman PL, MacNeil DJ, Pauls JF, Pitt B, Pratt CM, Schwartz PJ, Veltri EP: Effect of d-sotalol on mortality in patients with left ventricular dysfunction after recent and remote myocardial infarction. The SWORD Investigators. Survival With Oral d-Sotalol [see comments] [published erratum appears in Lancet 1996 Aug 10; 348(9024):416]. *Lancet* 1996;348:7-12

3. Weissenburger J, Davy JM, Chezalviel F: Experimental models of torsades de pointes. [Review]. *Fundamental & Clinical Pharmacology* 1993;7:29-38

4. Weissenburger J, Davy JM, Chezalviel F, Ertzbischoff O, Poirier JM, Engel F, Lainee P, Penin E, Motte G, Cheymol G: Arrhythmogenic activities of antiarrhythmic drugs in conscious hypokalemic dogs with atrioventricular block: comparison between quinidine, lidocaine, flecainide, propranolol and sotalol. *Journal of Pharmacology & Experimental Therapeutics* 1991;259:871-883

5. Weissenburger J, Chezalviel F, Davy JM, Lainee P, Guhennec C, Penin, E, Engel F, Cynober L, Motte G, Cheymol G: Methods and limitations of an experimental model of long QT syndrome. *Journal of Pharmacological Methods* 1991;26:23-42

6. Verduyn SC, Vos MA, Gorgels AP, van der Zande J, Leunissen JD, Wellens HJ: The effect of flunarizine and ryanodine on acquired torsades de pointes arrhythmias in the intact canine heart. *Journal of Cardiovascular Electrophysiology* 1995;6:189-200

7. Vos MA, Verduyn SC, Gorgels AP, Lipcsei GC, Wellens HJ: Reproducible induction of early afterdepolarizations and torsade de pointes arrhythmias by d-sotalol and pacing in dogs with chronic atrioventricular block. *Circulation* 1995;91:864-872

8. Abrahamsson C, Duker G, Lundberg C, Carlsson L: Electrophysiological and inotropic effects of H 234/09 (almokalant) in vitro: a comparison with two other novel IK blocking drugs, UK-68,798 (dofetilide) and E-4031. *Cardiovascular Research* 1993;27:861-867

9. Derakhchan K, Cardinal R, Brunet S, Klug D, Pharand C, Kus T, Sasyniuk BI: Polymorphic ventricular tachycardia induced by *d*-sotalol in canine preparations of atrio-ventricular block: initiation in the conduction system followed by spatially unstable reentry. *Cardiovascular Research* 1998;(in press)

10. Bailie DS, Inoue H, Kaseda S, Ben-David J, Zipes DP: Magnesium suppression of early afterdepolarizations and ventricular tachyarrhythmias induced by cesium in dogs. *Circulation* 1988;77:1395-1402

11. el-Sherif N: Early afterdepolarizations and arrhythmogenesis. Experimental and clinical aspects. *Archives des Maladies du Coeur et des Vaisseaux* 1991;84:227-234

12. January CT, Riddle JM, Salata JJ: A model for early afterdepolarizations: induction with the Ca2+ channel agonist Bay K 8644. *Circulation Research* 1988;62:563-571

13. Sasyniuk BI, Brunet S: Proarrhythmic effects of *d*-sotalol in the rabbit ventricle associated with differential effects on endocardial cells at slow heart rates. *Circulation* 1994;90:I-146(abstract)

14. Brunet S, Sasyniuk BI: Proarrhythmic effects of *d*-sotalol in rabbit ventricle associated with differential effects on repolarization in endocardial cells: *in vitro* and *in situ* correlations. Chapter I

15. Sasyniuk BI, Brunet S: Torsade de pointes induced by quinidine, *d*-sotalol & e-4031 in the isolated rabbit heart: importance of interval dependent dispersion of repolarization. *PACE* 1995;18:II-904(abstract)

16. Zabel M, Hohnloser SH, Behrens S, Li YG, Woosley RL, Franz MR: Electrophysiologic Features of Torsades de Pointes: Insight from a new isolated rabbit heart model. *Journal of Cardiovascular Electrophysiology* 1997;8:1148-1158

17. Zabel M, Portnoy S, Franz MR: Electrocardiographic indexes of dispersion of ventricular repolarization: an isolated heart validation study. *Journal of the American College of Cardiology* 1995;25:746-752

18. Ino T, Karagueuzian HS, Hong K, Meesmann M, Mandel WJ, Peter T: Relation of monophasic action potential recorded with contact electrode to underlying transmembrane action potential properties in isolated cardiac tissues: a systematic microelectrode validation study. *Cardiovascular Research* 1988;22:255-264

19. Franz MR, Kirchhof PF, Fabritz CL, Zabel M: Computer analysis of monophasic action potentials: manual validation and clinically pertinent applications. *Pacing & Clinical Electrophysiology* 1995;18:1666-1678

20. Link MS, Foote CB, Sloan SB, Homoud MK, Wang PJ, Estes NA, 3rd. Torsade de pointes and prolonged QT interval from surreptitious use of sotalol: use of drug levels in diagnosis. *Chest* 1997;112:556-557

21. Surawicz B: Electrophysiologic substrate of torsade de pointes: dispersion of repolarization or early afterdepolarizations?. [Review]. *Journal of the American College of Cardiology* 1989;14:172-184

22. Hohnloser SH, Singh BN: Proarrhythmia with class III antiarrhythmic drugs: definition, electrophysiologic mechanisms, incidence, predisposing factors, and clinical implications. [Review]. *Journal of Cardiovascular Electrophysiology* 1995;6:920-936

23. Habbab MA, el-Sherif N: TU alternans, long QTU, and torsade de pointes: clinical and experimental observations. *Pacing & Clinical Electrophysiology* 1992;15:916-931

24. Verduyn SC, Vos MA, van der Zande J, van der Hulst FF, Wellens HJ: Role of interventricular dispersion of repolarization in acquired torsade-de-pointes arrhythmias: reversal by magnesium. *Cardiovascular Research* 1997;34:453-463

25. Tranum-Jensen J, Wilde AA, Vermeulen JT, Janse MJ: Morphology of electrophysiologically identified junctions between Purkinje fibers and ventricular muscle in rabbit and pig hearts. *Circulation Research* 1991;69:429-437

26. Yang T, Roden DM: Extracellular potassium modulation of drug block of IKr. Implications for torsade de pointes and reverse use-dependence. *Circulation* 1996;93:407-411

27. Moe GK, Mendez C: Physiological basis of premature beats and sustained tachycardia. *New England Journal of Medicine* 1973;288:250-254

28. Sasyniuk BI, Mendez C: A mechanism for reentry in canine ventricular tissue. *Circulation Research* 1971;28:3-15

29. Sicouri S, Fish J, Antzelevitch C: Distribution of M cells in the canine ventricle. *Journal of Cardiovascular Electrophysiology* 1994;5:824-837

30. Sosunov EA, Anyukhovsky EP, Rosen MR: Effects of quinidine on repolarization in canine epicardium, midmyocardium, and endocardium: I. In vitro study. *Circulation* 1997;96:4011-4018

31. Weerapura M, Sasyniuk BI: Mechanism of induction of torsade de pointes arhhythmias by quinidine. *Canadian Journal of Cardiology* 1996;12:127E(abstract)

32. Brunet S, Derakhchan K, Cardinal R, Sasyniuk BI: Changes in activation-recovery interval disparity (ARID) accounts for initiation and termination of *d*-sotalol induced arrhythmias. *Canadian Journal of Cardiology* 1997;13:113C(abstract)

33. Carlsson L, Almgren O, Duker G: QTU-prolongation and torsades de pointes induced by putative class III antiarrhythmic agents in the rabbit: etiology and interventions. *Journal of Cardiovascular Pharmacology* 1990;16:276-285

34. Carmeliet E: Electrophysiologic and voltage clamp analysis of the effects of sotalol on isolated cardiac muscle and Purkinje fibers. *Journal of Pharmacology & Experimental Therapeutics* 1985;232:817-825

35. Carlsson L, Abrahamsson C, Andersson B, Duker G, Schiller-Linhardt G: Proarrhythmic effects of the class III agent almokalant: importance of infusion rate, QT dispersion, and early afterdepolarisations [see comments]. *Cardiovascular Research* 1993;27:2186-2193

36. Asano Y, Davidenko JM, Baxter WT, Gray RA, Jalife J: Optical mapping of drug-induced polymorphic arrhythmias and torsade de pointes in the isolated rabbit heart [see comments]. *Journal of the American College of Cardiology* 1997;29:831-842

"To further investigate the mechanism of initiation and perpetuation of TdP observed in this novel model of drug-induced TdP, we performed epicardial activation mapping. With this technique we could monitor globally both epicardial activation patterns and local repolarization."

CHAPTER III

MECHANISM OF *D*-SOTALOL INDUCED TORSADE DE POINTES IN AN ISOLATED RABBIT HEART MODEL - A MAPPING STUDY

Current Status: Brunet S., Derakhchan K., Cardinal R., Sasyniuk BI.

To be submitted to *Journal of Cardiovascular Electrophysiology*

Abstract

d-Sotalol induced torsade de pointes (TdPs) is a particular form of polymorphic ventricular tachycardia (PVT) which has been associated with acquired long QT syndrome. The mechanism of this arrhythmia is still unclear. In an isolated model of *d*-sotalol induced TdPs, a mapping approach was used to investigate all the beats of this arrhythmia. With a 63-contact sock electrode array epicardial mapping of 30 drug-induced TdP was performed. The site of origin of the first beat of the TdP was investigated with unipolar recordings from the endocardial surfaces. The hearts were paced at short (0.5sec) to long (5.5 sec) and back to short cycle length(CL). The initiating beats of some TdP displayed focal epicardial activation patterns similar to those of idioventricular (IDV) beats, which are known to originate from the ventricular specialized conduction system (VSCS). All TdP were divided into three categories on the basis of the activation sequences of the subsequent beats: 1) those in which all beats displayed a focal pattern, 2) those in which all beats displayed reentrant patterns, 3) those of the mixed type, in which some beats displayed a focal pattern and others displayed a reentrant pattern. We concluded that under the experimental condition the first beat of TdP was due to a triggered response likely originating from the VSCS, and that subsequent beats may be reentrant or focal.

Introduction

Most pharmacologic agents that prolong repolarization have been associated with the initiation of TdP. The mechanism that causes TdP has been extensively studied. Two main hypotheses have been proposed: early afterdepolarization (EAD) and dispersion of repolarization. [1] Although these two hypotheses are not mutually exclusive, evidence for either is lacking because of the limitations imposed by the available animal models and investigational methods. [2] Recent studies have used either toxins (anthropleurin A) or class III antiarrhythmic drugs in combination with alpha-adrenergic agonists to induce TdP arrhythmias. [3-5] We have shown previously that, in endocardial preparations excised from the rabbit ventricle, *d*-sotalol alone under conditions of extremely slow heart rates caused considerably more prolongation of the action potential duration in Purkinje fibers (PF) than in ventricular muscle (VM) at slow rates, thereby increasing the dispersion of repolarization. Moreover, the drug induced EADs in PF propagated to muscle as triggered responses. [6,7] From these *in vitro* results we hypothesized that TdP might be initiated by EAD-induced triggered APs originating in the VSCS. Based on our *in vitro* experiments, we developed a model of TdP in the isolated rabbit heart [8,9] in which we could induce TdP with therapeutic concentrations of *d*-sotalol at slow heart rates. Initiation of TdP was associated with drug induced interval dependent dispersion of repolarization due to the selectively greater prolongation of durations at endocardial recording sites,

which supported the hypothesis that both the disparity in repolarization and impulse formation in PF are involved in the initiation and maintenance of TdP arrhythmias.

The present study comprises a further analysis of the mechanism of this arrhythmia. Epicardial and endocardial unipolar potentials were recorded simultaneously during episodes of TdP induced by *d*-sotalol in isolated rabbit hearts with AV block. Epicardial activation sequences and timing of endocardial potentials were determined in individual beats of TdP episodes and compared to the activation sequences of IDV beats, for the possible involvement of the VSCS in these beats. Epicardial activation patterns were also investigated for the occurrence of circus movement reentry. Activation-recovery intervals (ARIs) were measured to determine the role of dispersion of repolarization in the generation of this arrhythmia. A similar approach was used in the mapping of in an *in vivo* canine model of TdP in which a combination of *d*-sotalol and an α_1-adrenergic agonist (phenylephrine) were necessary to induce spontaneous TdP. [5] A preliminary report of this study has been published in abstract form. [10]

Methods

All procedure for animal care and experimentation followed the guidelines of the Canadian Council for Animal Care and were monitored by an institutional committee. Seven New Zealand White rabbits (body weight, 2.0 - 2.5 Kg) were anaesthetized with xylazine (8 mg · Kg^{-1} i.m.) followed by ketamine hydrochloride (75 mg · Kg^{-1} i.m.). Heparin (400 IU · Kg^{-1}) was administered through a marginal ear vein. The rabbits were then exanguinated by severing one of the carotid arteries. The hearts were excised and immediately immersed in a modified Krebs-Henseleit solution previously bubbled with 95 % O_2 and 5 % CO_2 (composition in mmol · $Liter^{-1}$: NaCl 122.0, KCl 25.8, $MgSO_4$ 0.5, $NaHCO_3$ 24.0, KH_2PO_4 1.2, $CaCl_2$ 1.8, Glucose 50). They were quickly mounted in a non-recirculating Langendorf apparatus and perfused at a constant pressure of 65 cm H_20 with oxygenated hypokalemic Krebs-Henseleit's solution (2.7 mM K^+) (composition in mmol · $Liter^{-1}$: NaCl 122.0, KCl 1.5, $MgSO_4$ 0.5, $NaHCO_3$ 24.0, KH_2PO_4 1.2, $CaCl_2$ 1.8, Glucose 5.0, Pyruvate 2.0).

To slow down the intrinsic heart rate, the atrioventricular node was destroyed by injection of formaldehyde (37 %) into the AV nodal region. The resulting slow heart rate permitted us to stimulate the heart at variable CL. Bipolar stimulating electrodes were sutured onto the mid wall of the right or left ventricle

for pacing. The hearts were in a glass water-jacketed chamber filled with Krebs-Henseleit buffer solution to keep a constant temperature of approximately 37 °C.

The seven hearts were equilibrated for 25 minutes at 0.5 sec basic cycle length (BCL) with *d*-sotalol (40 μM) After this time they were paced alternatively at either the BCL of 0.5 or CL of 5.5sec when ever possible. The longer CL was maintained for approximately 5 minutes and then changed back to 0.5 sec . The hearts were equilibrated between rate changes at 0.5 sec CL for at least 2 minutes. The hearts were also left to beat spontaneously for a maximum of 1 min for mapping of the slow IDV rhythm. Such rhythm did not always develop.

Epicardial activation mapping was performed as described previously. 5,11 Briefly, unipolar recording contacts (63 sites) of the sock electrode array were connected to a multi-channel recording system and computer. Activation times were detected at the point of maximum slope deflections with dV/dt_{max} in excess of -0.5 $mV \cdot ms^{-1}$. All computer-selected events were verified by the operator on a videoscreen with an interactive program. Activation times were measured with reference to the earliest epicardial activation (zero time reference). Isochronal maps were computed automatically by linear interpolation and drawn at 10 or 20 ms intervals for selected IDV beats and each individual beat of the ventricular tachycardias (VT). ARI, an index of local repolarization interval which is highly correlated with the refractory period measurements, were measured from

dV/dt_{max} in the activation complex up to the maximum positive slope of the T wave of each of the 63 unipolar electrograms.

In four different experiments we inserted plunge wires for recording unipolar potentials from the endocardial surfaces of both ventricles. A total of 10 plunge wires were inserted in the area of earliest epicardial breakthrough of the IDV beats.

Isochronal activation maps and ARI maps were determined for sinus beats, IDV beats, and ventricular beats stimulated at short (0,5 sec) or long CL (5.5 sec), both before and after perfusion with *d*-sotalol, 40μM. Multiple episode of TdP were acquired for further analysis.

Drug

A concentrated drug stock solution (4×10^{-2} M) was made from powder in double distilled water each week. The stock solution was diluted in modified Krebs-Henseleit solution to the appropriate concentration of *d*-sotalol. *d*-Sotalol was kindly supplied by Bristol-Myers Squibb Canada.

Definition

TdP was defined as a self-terminating PVT of at least 5 consecutive extrasystoles occurring in the context of a prolonged QT interval. [12,13]

Statistical analysis

Student's paired and unpaired *t*-test was used as an indicator of statistical significance ($p \leq 0.05$). Bonferroni's inequality was used when multiple student's *t*-test were needed. Data are presented as mean $\pm$ SD.

Results

Epicardial activation mapping of sinus beats and idioventricular beats

In the canine heart, IDV rhythms developing after complete atrioventricular block, originate from the specialized conduction system and display typical activation patterns with the following two characteristics: 1) wide early epicardial breakthrough areas overlying the endocardial terminations of the conduction system, and 2) short total activation time. [5,11] Epicardial mapping of IDV rhythms showed three typical epicardial activation patterns. Similarly, we observed in the rabbit heart three typical isochronal epicardial patterns (fig. 1, lower panels) in which the early breakthrough area was localized either in the anterior RV, posteroapical LV or anteroapical LV, respectively. In all cases, the total epicardial activation time was short (28 ± 10 msec, n=18). When unipolar electrograms were recorded from the endocardial sites underlying the earliest epicardial breakthrough (4 experiments), endocardial activation was found to precede epicardial activation by 2-4 msec or to occur simultaneously. No significant difference was observed between IDV beats observed in the absence and presence of *d*-sotalol.

Sinus beats recorded prior to induction of atrio-ventricular block (fig. 1, upper right hand map) displayed wide epicardial breakthrough areas extending over the anterior RV and anterior apical LV, and had significantly shorter total

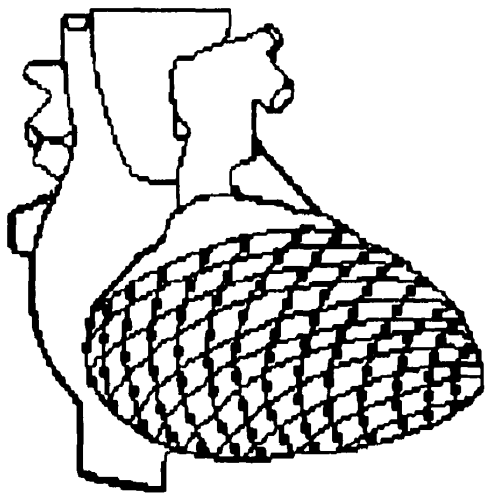

Electrode grid

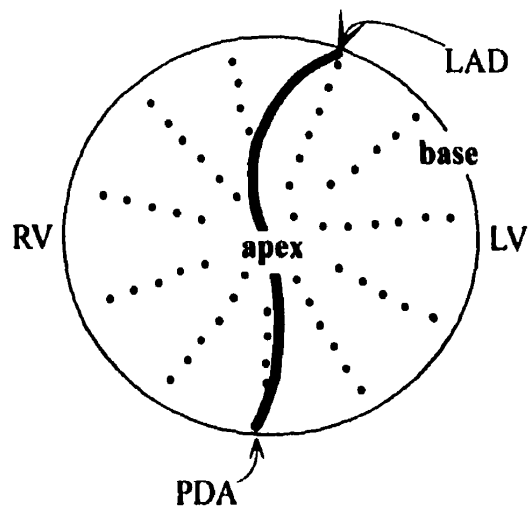

Sinus rhythm

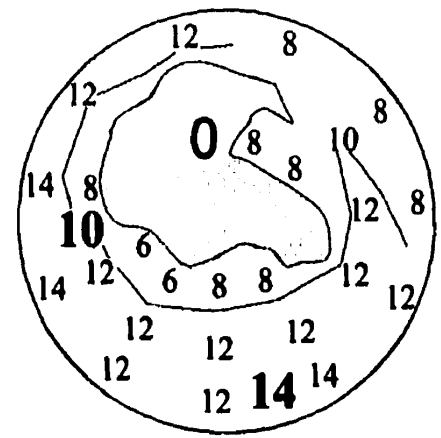

Idioventricular rhythms

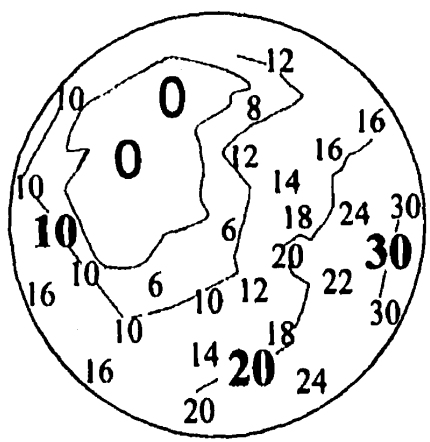

RV

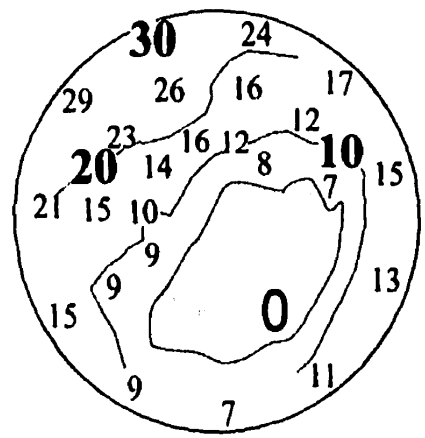

post. apical LV

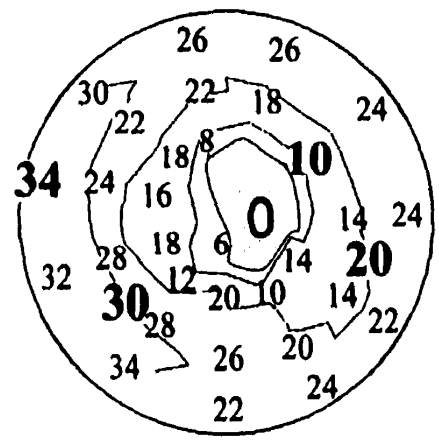

ant. apical LV

Figure 1. Isochronal activation maps during sinus rhythm and IDV rhythms under control conditions. The upper left diagram shows a schematic representation of the rabbit heart with the sock electrode array on its epicardial surface. The upper middle diagram shows the position of unipolar contacts (dots) on the ventricular epicardial surface as a polar representation in which the base is along the circumference and the center is at the apex. The upper right hand isochronal map was obtained during sinus rhythm. Localization of its epicardial breakthrough occurred on the anterior RV and the anterior apical LV. The total activation time was short, 14 msec. The bottom panels are isochronal maps of beats obtained during IDV rhythms. The localization of the epicardial breakthrough during IDV rhythms was either, on the anterior RV, posterior apical LV, or anterior apical LV, which was consistent with an origin in the right and left bundle branches after AV dissociation. Total activation times were between 28 and 34 msec. Isochronal lines are drawn at 10 msec intervals. The breakthrough area of this figure and subsequent figures comprises epicardial sites which activated in the first 5 msec (shaded area).

activation time (16 ± 2 msec, n=9, mean ± S.D, $p \leq 0.05$) than in IDV, in accordance with the fact that in sinus rhythm the impulses propagate along both the right and left bundle branches.

Cycle length dependent effect of *d*-sotalol on activation recovery intervals

ARI were determined at a short BCL (0.5 sec) at which TdP did not occur as well as at a much longer CL (5.5 sec) which was associated with the spontaneous occurrence of TdP. Under control conditions (fig. 2, A) the minimum and maximum ARI were 142 ± 10 and 196 ± 10, respectively, at the short CL, and 140 ± 10 and 211 ± 28, respectively, at the long CL, which were not statistically different between the short and long CL. Under *d*-sotalol (fig. 2, B) there was a significant increase in ARI in comparison with control at the short CL (minimum and maximum of 203 ± 45 and 278 ± 40 msec). At the long CL, ARI prolongation was significantly greater (409 ± 126 and 658 ± 128 msec, $p \leq 0.05$) and in all experiments greater prolongation occurred in the LV than RV (fig. 2, B, right hand map: shading). The LV location of the maximum ARI occurring at long CL under sotalol varied between experiments, occurring either at the apex (fig. 2), in the posterior wall or in the anterior wall (see below).

Activation-Recovery Intervals

A. Control

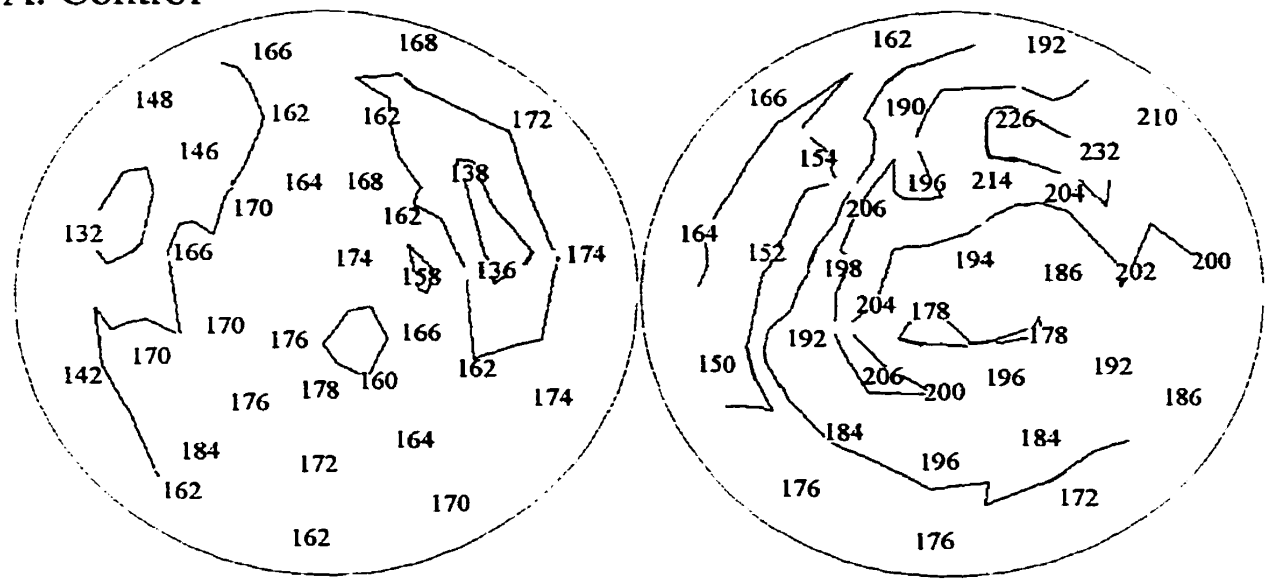

0. 5 sec

5.5 sec

B. *d*-Sotalol

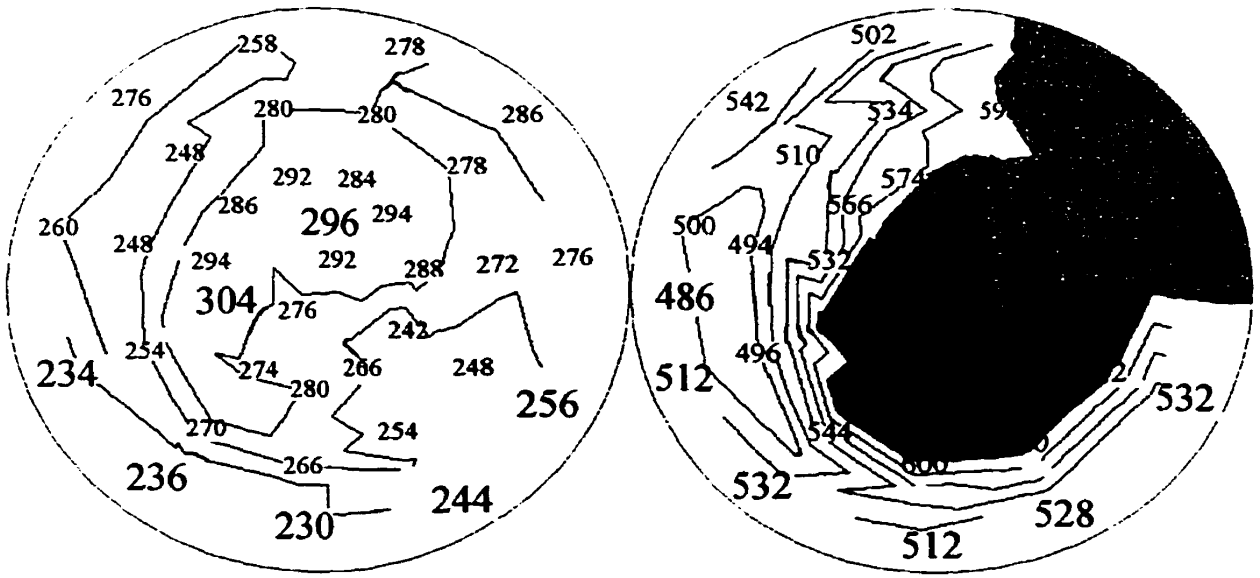

0. 5 sec

5.5 sec

Figure 2. Cycle length dependence of the ARIs under control condition and in presence of *d*-sotalol (40 μM). The upper left and right diagram show the ARIs measured under control conditions at a short (0.5 sec) and long CL (5.5 sec), respectively. The ARI was slightly prolonged at the long CL. The bottom left and right hand diagrams show the ARIs measured in the presence of *d*-sotalol (40 μM) at a short (0.5 sec) and long CL (5.5 sec), respectively. At the long CL prominent prolongation of ARIs was observed on the posterior apical LV epicardial surface. The isochronal ARI lines of this figure and subsequent figures were drawn at 20 msec.

In the presence of *d*-sotalol, many TdPs occurred spontaneously in each of the 7 hearts. A total of 50 TdPs (7 ± 5 per heart) were randomly selected and stored on disk. Thirty of these were subsequently analyzed and form the basis of this report. In all TdPs, no bridging activity was detected between the latest activation in the stimulated beat and the earliest activation in the first TdP beat as shown in the typical example in fig. 3A, where the total activation time of the stimulated beat was 40 msec and the interval between beat was 810 msec between the stimulated beat and the first beat of the TdP. This coupling interval (CI) was of similar duration to the longest ARI value (812 msec). The early epicardial breakthrough area in the first beat extended over the anterior RV wall (fig. 3, B), suggesting a focal origin in the conduction system and the total activation time was short (42 msec). Focal beats without delay are defined has focal (F). Fig. 3 is representative of 7 other TdP induced in different preparations. The total epicardial activation time in the majority of these TdP did not exceed 100 msec and the early epicardial breakthrough location changed between the anterior RV, anterior LV and posterior LV. In the remaining beats total activation time did not exceed 54 msec. In all TdP the CI between the stimulated beat and the first TdP beat was long, (averaging 747 ± 95 msec, n=7) and its total activation time was short (45 ± 7 msec). The activation patterns of the first TdP beats were similar to those of the IDV beats (see above, fig. 1).

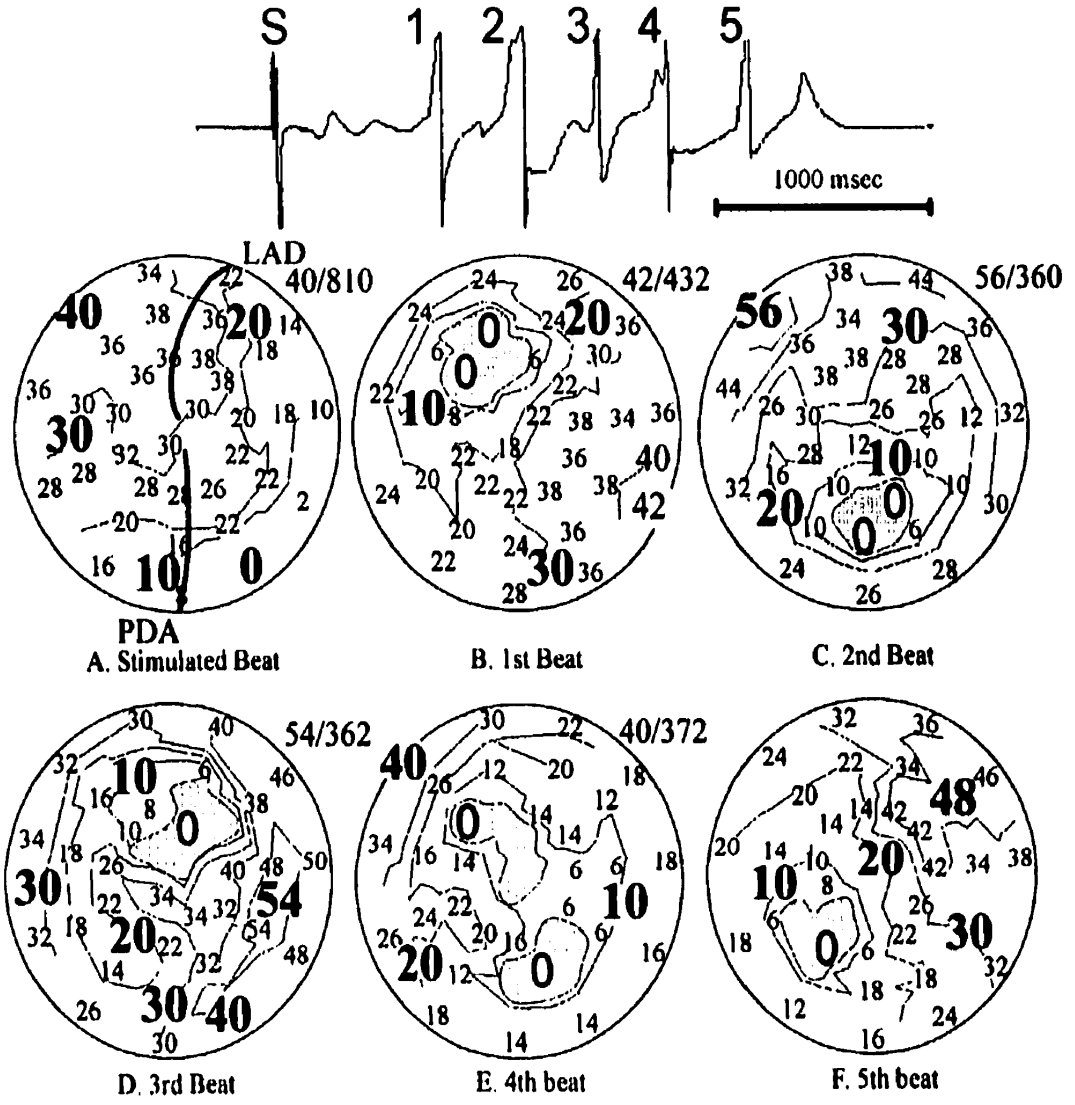
S 1 2 3 4 5
1000 msec
LAD
PDA
40/810
42/432
56/360
54/362
40/372
A. Stimulated Beat
B. 1st Beat
C. 2nd Beat
D. 3rd Beat
E. 4th beat
F. 5th beat

Figure 3. Typical example of a TdP showing a focal pattern. The top diagram shows the ECG trace of a 5 beat TdP. The first beat of the TdP was observed after an interval of 810 msec. Panel A shows the isochronal activation map of the paced beat (S) showing spread of activation from the stimulated site in the posterior LV to the anterior RV. The epicardial activation pattern of all beats (1-5) were consistent with an origin in the right (beats 1 and 5) and the left (beats 2 and 3) bundle branches showing large breakthrough areas similar to IDV beats together with a short total activation time which ranged from 40 to 56 msec. The activation pattern of beat 4 shows two simultaneous breakthrough areas, one on the anterior RV and the other on the posterior LV. The isochronal activation lines were drawn at every 10 msec.

In some beats generated through a focal mechanism (fig 4, TdP beat 1), the total epicardial activation time exceeded 100 msec, averaging 181 ± 30 msec (n=13). Among the beats which generated a "focal pattern with delay" (FD), those occurring as the first TdP beat had a shorter CI (575 ± 140 msec) than the focal beats without delay (747 ± 95 msec), with reference to the preceding stimulated beat. In beats displaying a focal pattern with delay, the early breakthrough area was located in the apical LV and extended over a smaller region than in the first type. The breakthrough areas were, in fact, located in the region of short ARI, at the periphery of the region of considerably more pronounced ARI prolongation (fig. 4, ARI map), which was the region where the activation times were delayed. This delay could lead to the reentrant generation of subsequent beats.

Reentrant mechanism

A second type of TdP was one in which all beats, with the exception of the first one, were generated by a reentrant mechanism (fig. 4, beats 2-24). The TdP illustrated in fig. 4 is representative of a total of 13 in which only reentrant patterns occurred in the body of the arrhythmia (fig. 4). In the first beat of the arrhythmia, the breakthrough area (first 5 msec) was located on the apical portion of the LV in proximity to sites with prominent conduction slowing (bunched up isochronal lines) (fig. 4, beat 1). The activation was rapid on the RV and part of

the posterior LV, whereas on the anterior LV the conduction was greatly slowed (sites with bunched isochronal lines). These sites forced the propagating wave front to travel around certain areas in a "figure-of- 8" configuration (arrows). On the next beat, beat 2, the earliest epicardial activation occurred in close proximity to the previous beat (beat 1) latest epicardial activation (178 msec). This type of epicardial activation is consistent with a reentry mechanism. Similar isochronal activation maps were observed in the subsequent beats (fig. 4, beats 3-24) and this activity was consistent with a "figure-of- 8" reentry (arrows). This figure also shows that the breakthrough area (0 msec) drifted from an initially apical location (beat 2) to the posterior LV (beat 4-12), posterolateral LV (14) and lateral LV (beats 16-24). The breakthroughs were associated with marked activation delay occurring at nearby sites which, under the assumption of reentry, would be part of the return pathway causing reexcitation in the following beat (breakthrough). Accordingly, the location of the regions of slow conduction (bunching of isochronal lines) changed as the breakthrough location shifted. We noted a change of 180^0 in the orientation of the activation pathway, which may explain the change in the polarity of the QRS complex observed in the ECG.

The magnitude of the activation delay displayed variations, decreasing from the first beat (178 msec) to beat 4 (142 msec), then increasing again and peaking in beat 10 (166 msec), then decreasing to 126 msec in beat 16, and increasing once more to reach a peak in beat 18 (164 msec) and then decreasing to reach a minimum in the last beat (78, 98 msec). Activation delay was significantly

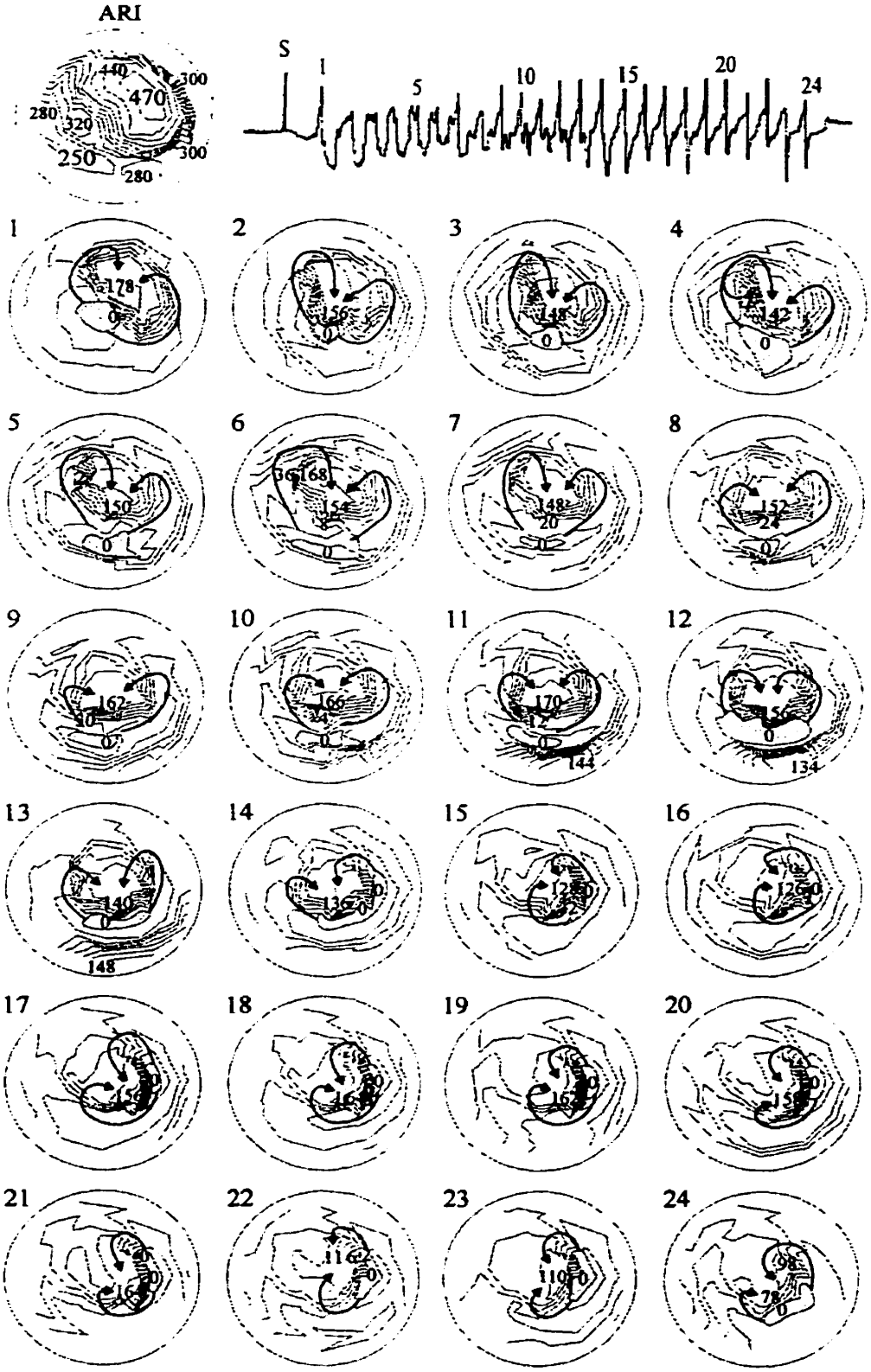
ARI
440
300
470
280
320
250
300
280
S
1
5
10
15
20
24
1
2
3
4
5
6
7
8
9
10
11
12
13
14
15
16
17
18
19
20
21
22
23
24

Figure 4. Typical example of a TdP showing reentrant isochronal activation patterns. The top panel shows the ECG trace of a 24 beat PVT with typical twisting pattern of a TdP. Note that the first beat is inscribed at the end of the T-wave with a CI of 426 msec to the previous stimulated beat. The isochronal ARI map of a stimulated beat prior to TdP is illustrated (ARI) It shows that the regions of prolonged repolarization intervals (ARI_{max}: 470 msec) are located mostly in the LV apical area, whereas the basal areas are least prolonged (ARI_{min}: 250 msec) . The isochronal activation map of all 24 beats of the TdP are shown. The breakthrough of the first beats is in the apical LV with a long total activation time (178) typical of a focal delay beat (FD). The impulse travels around the sites of slow conduction (bunched isochronal activation line) in a "figure-of-8" configuration. This beat is followed by the second beat (beat 2) which emerges (0 msec) close to the site of latest activation of beat 1 and the impulse follows a similar path around the sites of slowed conduction (arrows), consistent with a reentry mechanism. A similar pattern is maintained in all of beats. This figure also shows that the breakthrough area (0 msec) drifted from an initially apical location (beat 2) to the posterior LV (beat 4-12), posterolateral LV (14) and lateral LV (beats 16-22), a 180° rotation. Throughout all the beats of the TdP, the breakthrough and the sites with delayed activation are located proximal to one another and separated by sites with slowed conduction (bunched isochronal activation lines). The location and size of the sites of slow conduction progressively changes from beat to beat and decreases in size as the TdP progresses (beat 2 compared to beat 23 and 24). The isochronal activation lines in this and subsequent figures were drawn at every 20 msec

reduced in the last beats of all reentrant TdP to 106 ± 44 msec, from a peak of 186 ± 43 msec: Fig. 5A, in which the activation delays are plotted against beat number, illustrates that the variations in activation delay were associated with changes in the immediately preceding CL. In contrast, a TdP displaying only focal patterns (fig. 5, B) displayed little variation in activation delay although the CL showed marked variations. The TdP displaying reentrant patters were significantly faster (227 ± 27 msec) than those with focal patterns (428 ± 70 msec). The average length of TdP displaying reentrant patterns was 11 ± 7 (range 6-26)

Torsade de pointes arrhythmias with mixed focal and reentrant beats

Nine TdP included focal patterns as well as reentrant patterns intermixed in beats that followed the first one (fig. 6). The first beat of the TdP shown in fig. 6 (as well as beats 2,4,7) displayed a focal pattern with block (FB) occurring in regions with markedly prolonged ARI (shading). Among the beats which generated a focal pattern with block, those occurring as the first TdP beat had an even significantly shorter CI (328 ± 30 msec, n=10, $p \leq 0.05$) than those displaying a focal pattern with (575 ± 140, n=13) or without delay (747 ± 95 msec, n=7), with reference to the preceding stimulated beat.

Fig. 6 shows that the activation patterns of beats 2-4, 6-7, 9 and 13 were of the focal type (either focal with block or focal with delay) whereas the remaining

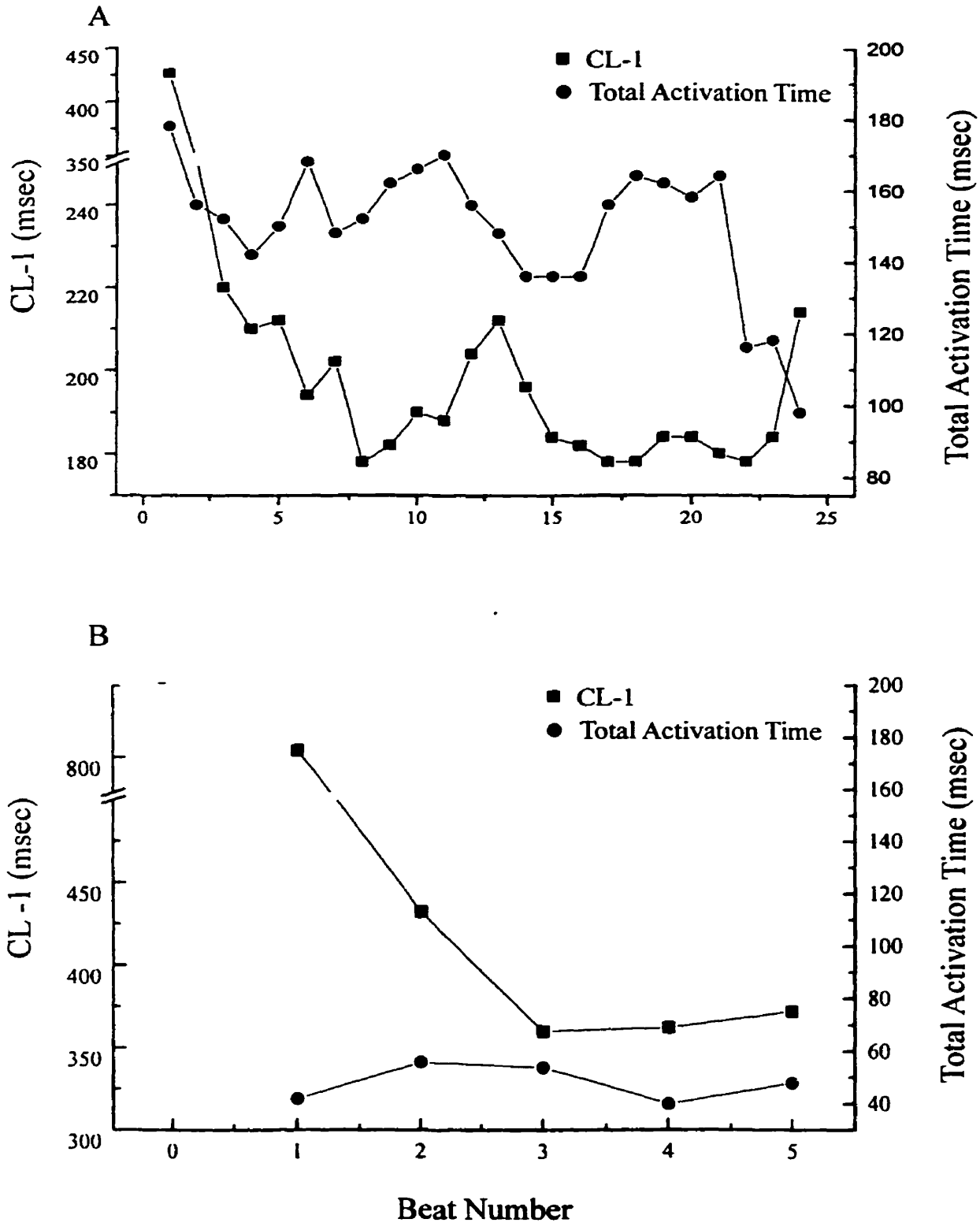

Figure 5. Relationship between total activation time and the immediately preceding CL (CL - 1) for each beat of a typical TdP in which the isochronal activation maps are consistent with either a reentry mechanism (A) or a focal mechanism (B).

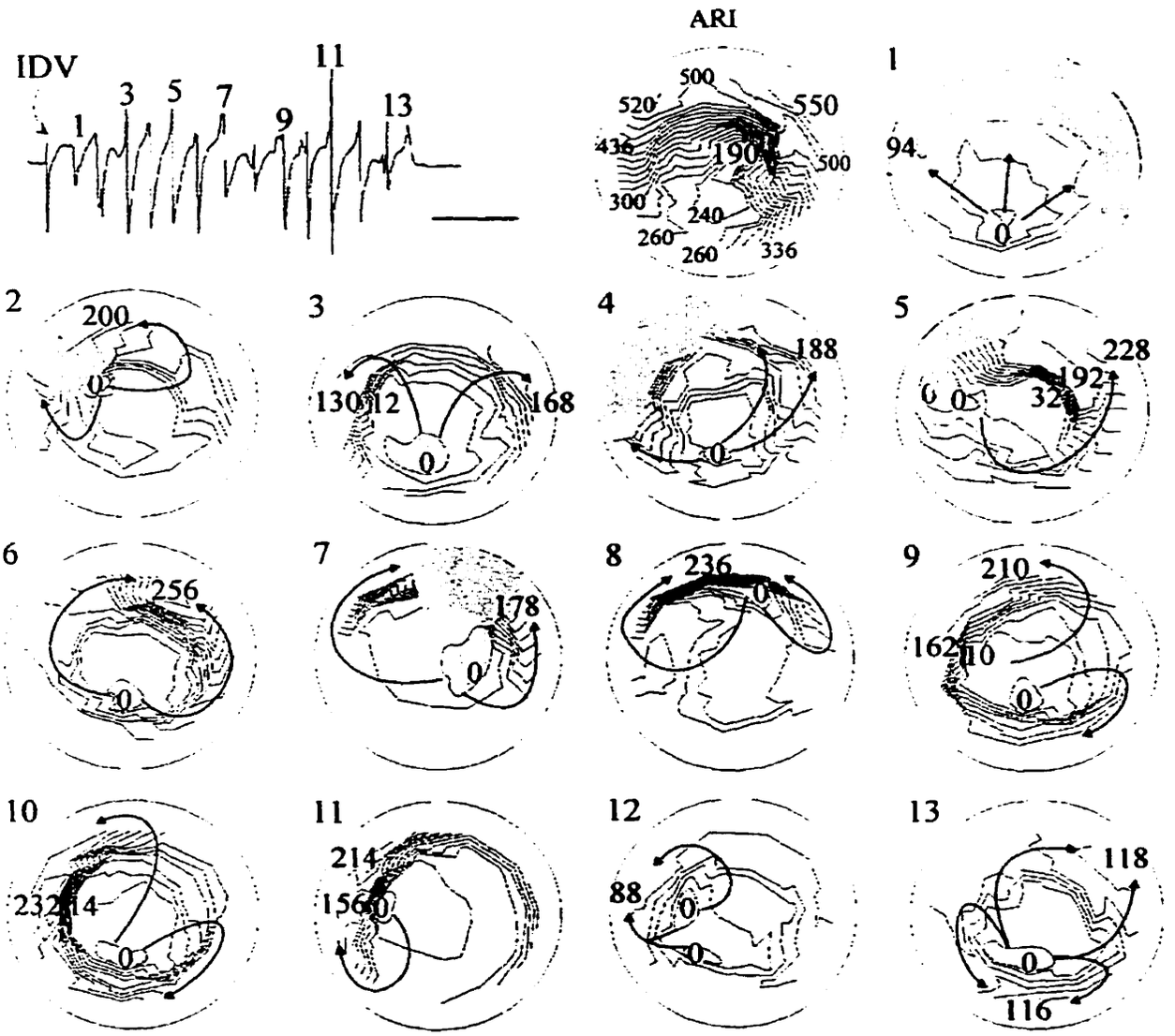
IDV
1
3
5
7
9
11
13
ARI
500
520
550
436
190
500
300
240
260
260
336
1
94
0
2
200
0
3
130
12
168
0
4
188
0
5
228
192
0
0
32
6
256
0
7
178
0
8
236
0
9
210
162
10
0
10
232
14
0
11
214
156
0
12
88
0
0
13
118
0
116

Figure 6. Typical example of a TdP showing isochronal activation patterns consistent with both reentrant and focal beats. Top left panel shows the ECG of a typical 13 beat TdP. ARI panel shows the isochronal ARI map of a beat preceding this TdP. It shows very prolonged ARI on the apical and anterior LV and RV (ARI_{max}: 550 msec) and shorter ARI values located on the posterior RV and LV (ARI_{min}: 190 msec). The breakthrough of the first beat of the TdP is located at a site where the ARI values were short. Within the 13 beat TdP there are isochronal activation patterns consistent with either a reentrant mechanism or a focal mechanism of initiation. The isochronal activation pattern of beats 1, 2, 4 and 7 are consistent with a focal block activation pattern. The isochronal activation pattern of beats 3, 6, and 9 are consistent with a focal delay pattern; in that it shows a breakthrough area in the same region of the IDV beats (not shown) together with a long total activation time which is greater then 100 msec. Beats 5, 8, 10-13 show epicardial activation maps which are more consistent with reentry. Their breakthrough area and the maximal increase in activation times of their preceding beats are in close proximity to one another. Beat 1 showed a FB isochronal activation pattern. The breakthrough area was located at a variety of epicardial sites in different beats of the TdP; on the posterior apical LV in 9 beats (beats 1, 3, 4, 6, 7, 9, 10, and 13) , on the anterior LV in three beats (beats 2, 5 and 11), on the anterior RV (beat 8) and on posterior and anterior RV (beat 12). The dashed area in the isochronal activation maps of beats 1, 2, 4, 5, and 7 represent area of block.

beats (5,8,10-12) were of the reentrant type. The mean CL of these TdP (324 ± 20 msec) was significantly longer than that of TdP consisting of reentrant patterns only (227 ± 27 msec, $p \leq 0.05$) but shorter than the mean CL of completely focal TdP (428 ± 7 msec). The length of the mixed type TdP averaged 10 ± 4 beats (range 8-16).

Summary of the TdP analyzed

Fig. 7 shows, for 21 of the 30 TdP analyzed, the relationship between the total activation time and the immediately preceding CL (CL - 1) displaying a reentrant activation pattern or a focal pattern (with or without delay/block). As stated above, the first beats of all TdP (A) displaying focal patterns, were always preceded by a CL-1 of at least 300 msec. Hence, we arbitrarily chose a value of 300 msec to separate beats which were the result of a reentry from focal mechanism. Activation delays varied depending on whether they were focal with or without delay and/or block. In the subsequent beats (B), the majority of those displaying a reentrant pattern are seen to be closely-coupled and to be associated with marked delay (quadrant III) whereas most of the beats displaying focal patterns have CIs of 300 msec or longer (quadrants I and IV). This suggests that beats with an immediately preceding CL of less than 300 msec and a total activation time of more the 100 msec are more likely to be reentrant. A total activation time of 100 msec was chosen (which define our focal beat, see vida supra) to separate focal beats without activation delay/block from those with delay.

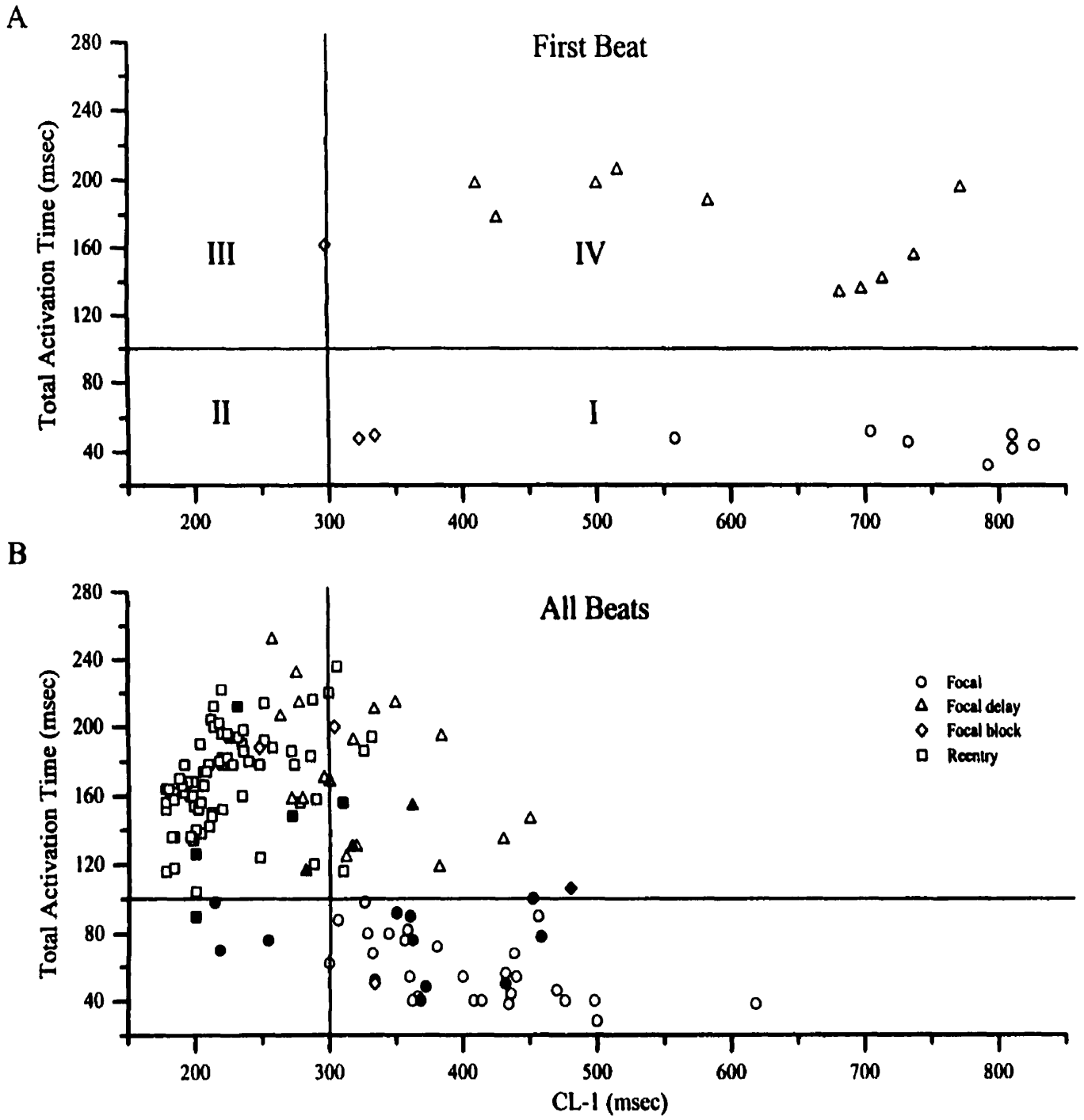
A
First Beat
Total Activation Time (msec)
280
240
200
160
120
80
40
III
IV
II
I
200
300
400
500
600
700
800
B
All Beats
Total Activation Time (msec)
CL-1 (msec)
Focal
Focal delay
Focal block
Reentry

Figure 7. Summary of the relationship between total activation time (TAT) with the immediately preceding CL (CL - 1) for each beat of the tachycardia in 21 of the TdP mapped. Each panel shows this relationship for beats whose pattern has been identified as either focal (F), focal with block (FB) focal with delay (FD) or reentrant (R). Each graphs is divided into quadrants labeled I to IV divided by a vertical line at a CL-1 of 300 msec and a horizontal line at a TAT of 100 msec. Panel A shows this relationship for the first beat. Beats which displayed a focal isochronal activation pattern are in quadrant I; and those with a FD isochronal activation pattern are in quadrant IV. Note that beats with a longer CL-1 (700-800 msec) have total activation times generally shorter those with a shorter CL-1 (300-600 msec). Panel B shows this relationship for all TdP beats of each TdP for remaining beats. Like the previous graph the beats which displayed a focal isochronal activation pattern cluster in the first quadrant. The beats with FD isochronal activation pattern cluster in quadrant IV. Beats which have a reentrant isochronal activation pattern cluster mostly in quadrant III. The last beat of the arrhythmia is represented by filled symbols.

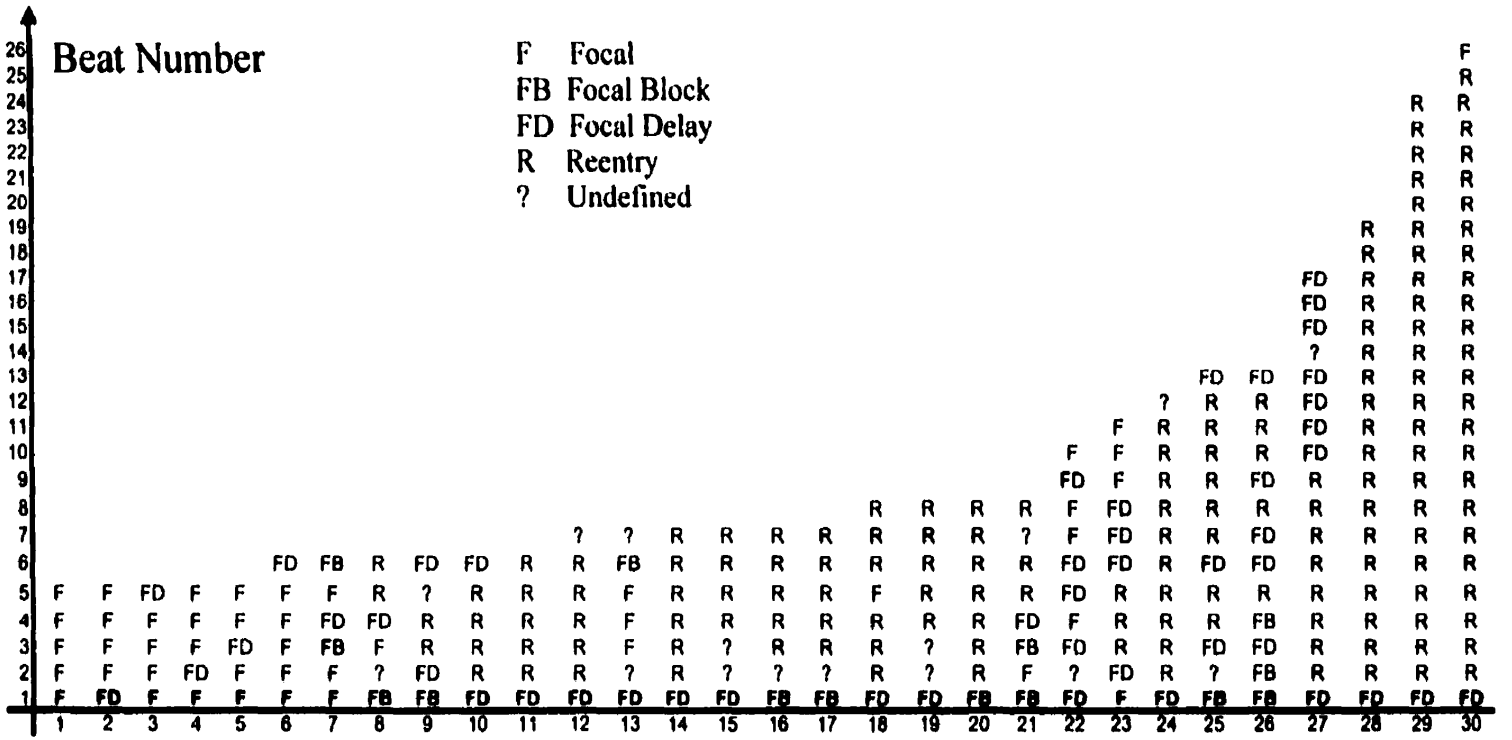
Beat Number
F Focal
FB Focal Block
FD Focal Delay
R Reentry
? Undefined
1 2 3 4 5 6 7 8 9 10 11 12 13 14 15 16 17 18 19 20 21 22 23 24 25 26 27 28 29 30

Figure 8. Summary of all TdP analyzed indicating the mechanism of each beat of each TdP. The number of beats in each TdPs episode ranged from 5 to 27 beats. Note that first beat of each TdP is due to a focal mechanism accompanied by no delay (F), significant delay (FD) or block of activation (FB). The last beat of each TdP may be either a focal (F), focal with delay (FD), or reentrant (R). The shorter TdP episodes were usually due entirely to a focal mechanism whereas the longer episodes were either totally reentrant or a mixture of reentrant and focal beats.

In a beat to beat summary of all TdP mapped shown in fig. 8, it is seen that short TdP are predominantly focal whereas longer ones are predominantly reentrant. This figure also shows the characterization and distribution of all the individual beats of all the TdP analyzed.

Discussion

This study is a further evaluation of the mechanism of *d*-sotalol induced TdP in our isolated Langendorf rabbit model. In the present study, TdP was induced by high therapeutic concentrations of *d*-sotalol under conditions of hypokalemia and extreme bradycardia. Under these conditions, TdP occurred spontaneously with an extremely high frequency (hundreds of episodes). Fifty of these episodes were recorded for analysis. The present report comprises a detailed analysis of 30 of them.

Unlike our previous study in the dog heart [5], TdP was generated without the necessity for alpha adrenergic agonists and was highly reproducible from one heart to the next permitting a detailed analysis of its characteristics.

A major advantage of the present study in determining tachycardia mechanism in contrast to our previous two studies in this model was the capability to monitor epicardial activation sequences and ARIs simultaneously which allowed us to correlate the two parameters and to follow the activation wave front of the impulse into regions with prolonged repolarization. This method produces consistent signatures which allowed us to interpret activity occurring in deeper structures as well, in particular the endocardial surface.

This study comprises for the first time a detailed analysis of the characteristics of every beat of each TdP and their relationship to one another. We divided this analysis into a consideration of the first beat which initiated the arrhythmia, characteristics of the body of the arrhythmia and the last beat resulting in its termination.

Beats initiating torsade de pointes

The results suggest that all beats initiating TdP are the result of EAD-induced triggered activity originating from the VSCS. Several findings support this conclusion.

We categorized these first beats into three types based on their epicardial breakthrough signatures and their CIs to the preceding stimulated beats.

The first type were focal characterized by isochronal activation patterns exhibiting a wide breakthrough region and a short total activation time similar to the activation patterns exhibited by beats of sinus origin and IDV beats known to originate in Purkinje fibers in VSCS. A second feature of focal beats was that their CI to the previous stimulated beat was long and no bridging activity could be detected. Whenever endocardial records were recorded with plunge wire electrodes endocardial potentials always preceded or were simultaneous with epicardial breakthrough signals.

In the second and third type of first beats the epicardial breakthrough area was large and usually occurred at the periphery of a region with prolonged ARIs. Such beats either exhibited large total activation times (and thus classed as focal delay) or exhibited areas of epicardium with no activation (and thus classified as focal block). We believe that first beats with focal delay or focal block signatures still arise from Purkinje fibers in the VSCS and that these signatures can be accounted for by propagation of the wave front in tissues with prolonged refractoriness.

Such a result can occur only if the impulse being initiated in the conducting system is encountering refractory tissue during its propagation to the epicardial surface in which it produces the various signatures observed which we have referred to as focal, focal delay or focal block. This could occur for one or both of two reasons, viz., either the ARIs are extremely prolonged in those situations in which we see focal delay or focal block beats versus focal beats or the CIs of the first beats occur at progressively shorter values which results in impingement of the propagating wave front upon a refractory barrier somewhere in the ventricles. Our results suggest that the major factor defining this first beat (which initiates TdP) is its CI to the previous stimulated beat. First beats showing a purely focal signature occurred at significantly longer CIs to the stimulated beat (which exceeded the ARI values) than first beats showing either a focal delay or a focal block signature (which impinged upon the ARI values). First beats showing

a focal delay occurred at CIs which were significantly longer from those showing focal block. On the other hand, the ARIs did not differ significantly from one heart to the next. Furthermore, first beats with either a focal, focal delay or focal block signature occurred in the same heart with the same ARI values further confirming that the defining feature of the signature of each first beat was largely the CI to the previous beat. Thus, beats with a focal delay or focal block signature still arose from an endocardial site but were forced to emerge at the periphery of sites with prolonged ARIs. This breakthrough region was at the periphery of the wide breakthrough region of IDV beats.

Further corroborative evidence for these first beats being of endocardial origin comes from our previous studies in rabbit endocardial preparations in which we have shown that the exact same conditions which lead to TdP in the present study produce EAD-induced triggered activity in rabbit Purkinje fibers [6]. We have shown as well in the same model and under the same conditions using monophasic action potential (MAP) recordings from selected endocardial and epicardial sites that initiation of TdP is accompanied by "EAD like deflections" at endocardial sites only in the beat initiating TdP [8]

Mechanism of perpetuation of torsade de pointes

Our findings indicate that the mechanism of perpetuation of TdP observed under the conditions in the present model may be either focal (fig 3), reentrant (fig 4) or a mixture of the two (fig 6).

The majority of TdPs beginning with a very long CI to the stimulated beat (a focal first beat) were due to a focal type of mechanism, ie., each beat of the TdP showed a focal type of signature (wide breakthrough areas and short activation times) with no bridging activity between beats. Such TdPs were usually of short duration (6 beats or less) and had a mean CL longer than the reentrant or the mixed type. In the focal type of TdPs, the total activation time of each beat usually showed only slight variation and bore no relationship to the immediately preceding CL.

These characteristics are in keeping with sustained triggered activity originating in Purkinje fibers on the endocardial surface as the mechanism of this type of TdP. We have shown previously that the same concentration of *d*-sotalol and under similar conditions with the exception of CL, can induce sustained triggered activity in rabbit Purkinje fibers [6]. Much longer cycle lengths were necessary to induce sustained triggered activity under *in vitro* conditions. This may have been related to the lack of an adrenergic component under *in vitro* and superfused conditions since addition of adrenaline to the superfusate allowed

multiple triggered activity to develop at rates comparable to that in the present study. Thus, the evidence is overwhelmingly in favor of EAD-induced triggered activity as the mechanism of the short duration TdPs under the conditions occurring in the present model.

The second major mechanism of perpetuation of TdP was reentry. Forty percent of TdPs were sustained solely by a reentrant mechanism. First beats initiated at short CI so the stimulated beat in a substrate with regions of prolonged refractoriness were found to emerge on the periphery of such regions at sites with shorter refractoriness and to propagate around the areas of either slowed conduction or block (often in a "figure-of-8" configuration) and emerging again at sites in close proximity to the previous beat suggesting involvement of the VSCS on the endocardial surface in the reentrant pathway with bridging of activity from beat to beat. Sites of earliest epicardial activation were in close proximity to the sites of delayed activation of the each previous beat. Seventy to 95% of the reentrant cycle could be detected on the epicardial surface.

TdPs sustained by a reentrant mechanism were of variable length and were much faster than those with a focal mechanism. Reentry was the mechanism of the longest duration TdPs. During the TdP there was an inverse relationship between the total epicardial activation time and the immediately preceding CL, a behaviour in keeping with a reentrant mechanism. These TdPs usually terminated

with an abrupt decrease in total activation time, a factor which would terminate reentry.

In one-third of the TdPs clearly reentrant beats were intermixed with beats showing a focal delay or a focal block signature. Such focal signatures likely reflect a return reentrant pathway involving the VSCS thus resulting in a part of the cycle being missed on the epicardial surface. The reentrant pathway must also circulate via a more tortuous route or break apart into several pathways resulting in longer cycle lengths than TdPs with purely reentrant signatures. To confirm the involvement of the VSCS in the reentrant pathway one would have to map the endocardial surface as well.

TdPs with a purely focal mechanism were too short to exhibit the typical twisting pattern. In those in keeping with a reentrant mechanism twisting may be the result of a slowly shifting reentrant wave front as observed by the slowly shifting position of the lines of functional dissociation and the earliest epicardial breakthrough of each reentrant beat around the area of refractory barriers (ie., prolonged ARIs). In mixed signature TdPs, beats with similar epicardial breakthrough patterns showed similar QRS morphologies suggesting that twisting may also be related to the gradual shift in the sites of emergence of the impulse from the conducting system again implicating the involvement of the VSCS in the reentrant mechanism.

As in the present study, El-Sherif et al. [3] showed in a dog model administered anthopleurin A that short PVTs were mostly focal. In their study the majority of nonsustained VTs were focal while the remainder were both focal and reentrant. As in our study, the beats initiating TdP were consistently focal. Their conclusion was revised in a subsequent manuscript in which they showed that all fast VTs were due to a reentrant mechanism. [14] A focal mechanism is more likely to have occurred in their model since the mechanism of Anthopleurin A involves inhibition of Na inactivation resulting in plateau type oscillations.

Contrary to our study the site of initiation was localized to a subendocardial origin either on the base (RVOT) or the apex of the ventricle. To our knowledge there are no PF termination at the base of the ventricle. It is noteworthy that a drug with a similar mode of action have been shown to induce multiple triggered activity in VM although at higher drug concentration. [15] Since the distribution of this drug *in vivo* is not known we cannot completely eliminate this effect after bolus injection. Also in this model, Anthopleurin A may have exherted a central effect which may have modulated the hearts electrical properties. [16]

Also, similarly to our study in an other isolated heart model, Jalife et al. [17] have observed almost exclusively an all focal mechanism of perpetuation for TdP arrhythmias. Similarly to us, the conditions used here were extreme -high drug

concentration, long CL (> 2 sec, and hypokalemia) which likely lead to multiple triggered activity. The site of origin is not clear from their recording technique even with their MAP probe on the endocardial surface. One major limitation of their study is that only a portion (RV LAD LV junction) of the epicardium was mapped to suggest either a focal or reentry mechanism as a mechanism of impulse formation. Also the need for optically sensitive dyes may have modified the effect of the drug used in this model.

In this model the absence of the influence of the sympathetic nervous system is another positive aspect to this model in that the effect of drug and rate could be investigated. We are not denying the importance of the sympathetic nervous system in the initiation of TdP clinically. There is clinical and experimental evidence that a high adrenergic tone can trigger TdP episodes (patient with the long QT syndrome, startle induction) This simple model could be easily modified to study the influence of both alpha and beta adrenergic stimulation and other facilitators.

Limitations of the study

Although we think the VSCS is implicated in both the initiation and maintenance of TdP in the present model no attempt was made to record from this region.

The extreme levels of bradycardia used in the present study were certainly not physiological for the rabbit heart. These extreme CLs were used only because we wanted to ensure that TdP would occur in these hearts. This did not preclude that TdP can occur at much more physiological CLs.

There is a possibility that FD is really in which we are missing reentry surface at the epicardial surface. This explains how a focal beat in the middle of an arrhythmia at a fast rate. This suggest that in the middle or the end of a reentry suggest that a focal epicardial signature may not necessarily mean a focal mechanism.

Conclusion

In a simple isolated Langendorf-perfused rabbit heart model, TdP was induced by high concentrations of *d*-sotalol in the presence of extreme bradycardia and hypokalemia. Using epicardial activation mapping and measurement of ARIs, we were able to show that under these specific conditions, TdP is likely initiated by a focal dependent mechanism originating from the VSCS in the context of an increased dispersion of repolarization. Subsequent beats are due to a reentrant mechanism or a combination of reentry and focal delay or block. The present study further supports our hypothesis that TdPs initiated by first beats with short CIs and thus exhibiting either focal delay (usually with marked delays) or focal

block signatures displayed mechanisms which were either entirely reentrant in nature or of a mixed nature. TdPs which were of very long duration showed almost entirely reentrant signatures. Such TdPs were initiated by first beats with CIs which were much shorter than the average ARI of the preparation . The ones in which all beats of the TdP showed a focal signature were shorter. Such TdP were initiated by beats occurring at extremely prolonged CIs.

Acknowledgments

The authors wish to thank Ms. Suzanne Seto for expert technical assistance and Bristol-Myers Squibb Canada for supplying *d*-sotalol.

References

1. Surawicz B: Electrophysiologic substrate of torsade de pointes: dispersion of repolarization or early afterdepolarizations?. [Review]. *Journal of the American College of Cardiology* 1989;14:172-184

2. Weissenburger J, Davy JM, Chezalviel F: Experimental models of torsades de pointes. [Review]. *Fundamental & Clinical Pharmacology* 1993;7:29-38

3. el-Sherif N, Caref EB, Yin H, Restivo M: The electrophysiological mechanism of ventricular arrhythmias in the long QT syndrome. Tridimensional mapping of activation and recovery patterns. *Circulation Research* 1996;79:474-492

4. Carlsson L, Almgren O, Duker G: QTU-prolongation and torsades de pointes induced by putative class III antiarrhythmic agents in the rabbit: etiology and interventions. *Journal of Cardiovascular Pharmacology* 1990;16:276-285

5. Derakhchan K, Cardinal R, Brunet S, Klug D, Pharand C, Kus T, Sasyniuk BI: Polymorphic ventricular tachycardia induced by *d*-sotalol in canine preparations of atrio-ventricular block: initiation in the conduction system followed by spatially unstable reentry. *Cardiovascular Research* 1998;(in press)

6. Sasyniuk BI, Brunet S: Proarrhythmic effects of *d*-sotalol in the rabbit ventricle associated with differential effects on endocardial cells at slow heart rates. *Circulation* 1994;90:I-146(abstract)

7. Brunet S, Sasyniuk BI: Proarrhythmic effects of *d*-sotalol in rabbit ventricle associated with differential effects on repolarization in endocardial cells: *in vitro* and *in situ* correlations. Chapter I

8. Sasyniuk BI, Brunet S: Torsade de pointes induced by quinidine, *d*-sotalol & e-4031 in the isolated rabbit heart: importance of interval dependent dispersion of repolarization. *PACE* 1995;18:II-904(abstract)

9. Brunet S, Sasyniuk BI: *D*-sotalol induced torsade de pointes ventricular arrhythmias in the isolated rabbit heart - model and mechanism. Chapter II

10. Sasyniuk BI, Derakhchan K, Brunet S, Cardinal R: Epicardial mapping of sotalol-induced torsade de pointes in rabbit hearts. *Canadian Journal of Cardiology* 1996;12:85E(abstract)

11. Cardinal R, Scherlag BJ, Vermeulen M, Armour JA: Distinct activation patterns of idioventricular rhythms and sympathetically-induced ventricular tachycardias in dogs with atrioventricular block. *Pacing & Clinical Electrophysiology* 1992;15:1300-1316

12. Dessertenne F: [Ventricular tachycardia with 2 variable opposing foci]. [French]. *Archives des Maladies du Coeur et des Vaisseaux* 1966;59:263-272

13. Motte G, Coumel P, Dessertenne F, Bouvrain Y: [Wave burst. Clinical, etiological and therapeutic study]. [French]. *Annales de Medecine Interne* 1970;121:879-887

14. el-Sherif N, Chinushi M, Caref EB, Restivo M: Electrophysiological mechanism of the characteristic electrocardiographic morphology of torsade de pointes tachyarrhythmias in the long-QT syndrome: detailed analysis of ventricular tridimensional activation patterns. *Circulation* 1997;96:4392-4399

15. Boutjdir M, Restivo M, Wei Y, Stergiopoulos K, el-Sherif N: Early afterdepolarization formation in cardiac myocytes: analysis of phase plane patterns, action potential, and membrane currents. *Journal of Cardiovascular Electrophysiology* 1994;5:609-620

16. Pichon Y: Pharmacological induction of rhythmical activity and plateau action potentials in unmyelinated axons. *Journal of Physiology, Paris* 1995;89:171-180

17. Asano Y, Davidenko JM, Baxter WT, Gray RA, Jalife J: Optical mapping of drug-induced polymorphic arrhythmias and torsade de pointes in the isolated rabbit heart [see comments]. *Journal of the American College of Cardiology* 1997;29:831-842

"From the result of the previous mapping study, it became clear that in order to understand the initiation of TdP induced in this model we needed to understand the initiation of the lessor arrhythmias. When compared to the previous study we used condition which gave rise to repetitive arrhythmic sequences, we could therefore map the transitions to arrhythmia. As opposed to the previous mapping study, the hearts were exposed to clinical concentration of *d*-sotalol and slight bradycardia. We mapped both the activation and the rate dependent repolarization effect with both activation mapping and monophasic action potential technology to gain a further insight into the mechanism of drug-induced TdP."

CHAPTER IV

CHANGES IN DISPARITY OF REPOLARIZATION INTERVALS ACCOUNTS FOR INITIATION, PERPETUATION AND TERMINATION OF *D*-SOTALOL INDUCED ARRHYTHMIAS

Current Status: Brunet S., Cardinal R., Derakhchan K., Sasyniuk BI.

To be submitted to *Circulation*

Abstract

D-sotalol combined with bradycardia result in a typical pattern of ventricular arrhythmias in the isolated rabbit heart consisting of a sequence of multiple singlets evolving into couplets, triplets and torsade de pointes (TdP). We hypothesized that these arrhythmias are really part of an ongoing continuum in which the same mechanism is responsible for their initiation, perpetuation, and termination. To test this hypothesis, unipolar electrograms were recorded from 63 epicardial and 20 endocardial sites in 9 isolated rabbit hearts with AV dissociation exposed to *d*-sotalol (20μM). Isochronal maps were generated and activation-recovery intervals (ARI) and their disparity (ARID) were determined. Epicardial monophasic action potentials (MAP) were also recorded at selected epicardial sites. Arrhythmias occurred when pacing at critical cycle lengths (CL) of 1.0-1.5 sec. ARID significantly increased from 69±13 msec during pacing at the basal CL (0.5 sec) to 155±49* msec (n=33) in paced beats preceding singlets, and to 275 ± 72* msec (n=19) in paced beats preceding TdP. The long ARIs mostly occurred at apical epicardial sites. Isochronal maps of the first singlets in an arrhythmic sequence showed wide epicardial breakthrough, located in an apical area where ARI was maximum, with short maximum delays; consistent with an endocardial focal mechanism In all subsequent singlets, first beats of couplets, triplets, and TdP, the impulses emerged from basal sites which blocked at apical sites with previously prolonged ARI, leading to reentrant excitation and generation of couplets, triplets or TdP. At apical sites MAP recordings showed fusion of

response to paced beat and focal response presumably originating from endocardial sites which accounted for the long ARIs at these recording sites. ARID quickly dissipated to basal levels by the second or third beat of an arrhythmic episode. We conclude that all singlets, first beats of each arrhythmic episode (including TdP) begins with a focal response which propagates into a substrate with disparate repolarization due to drug-induced interval differences at selective ventricular sites to set up a reentrant mechanism. This reentry then self-terminates because the conditions which initiated it are now eliminated by the faster rate of the arrhythmia. * $P \leq 0.05$.

Introduction

We have shown previously in our isolated rabbit heart model that perfusion of the heart with a class III antiarrhythmic drug such as *d*-sotalol, produces a typical sequence of ventricular arrhythmias consisting of multiple singlets that evolve into couplets, triplets, quadruplet and eventually TdP, if the heart is stimulated at slow rates [1-4]. There was a typical pattern of evolution into TdP which depended greatly upon a critical disparity created between endocardial and epicardial MAP duration (MAPD). [1,4] Based on these results, we hypothesized that TdP was not a separate entity with a discrete mechanism of its own but was really part of a continuum and that we could more fully understand its mechanism by understanding the mechanism of initiation of singlets and their evolution into more severe arrhythmias and ultimately TdP.

In our previous study, we had analyzed the mechanism of TdP under a different set of conditions, viz., upon exposure to a much higher concentration of *d*-sotalol, in the presence of hypokalemia and extreme bradycardic rates. [2,3] In that study, we concluded that TdP was initiated by a beat originating in the ventricular specialized conducting system (VSCS) as a result of a focal mechanism and was either perpetuated by a purely focal mechanism, a purely reentrant mechanism, or a combination of both mechanisms. In the present study, we use much lower concentrations of drug (therapeutic), normal extracellular potassium concentrations, and only a mild bradycardia, conditions more akin to what one

might expect to be present under clinical conditions during therapy with *d*-sotalol. [1,4-6]. Under these conditions, arrhythmias occurred in a more predictable and reproducible pattern which facilitated its analysis. In order to assess the mechanism of initiation, perpetuation and termination of *d*-sotalol induced arrhythmias and their evolution into TdP under the present conditions, we recorded from the epicardial surface with a sock electrode array, from the endocardial surface with plunge wires and from select epicardial sites with contact type MAP recording electrodes. These techniques allowed us to simultaneously measure repolarization throughout the epicardial surface and at selected endocardial sites and to follow the evolution of the circulating wave front as represented on the epicardial surface and at selective endocardial sites. Thus, it was possible to obtain both a global pattern of activation and repolarization plus a higher degree of resolution of repolarization at selected sites with MAP recordings.

We concluded that under conditions more likely to occur during therapy with *d*-sotalol, generation of singlets or couplets or triplets is a forerunner of evolution into TdP. Generation of these minor arrhythmias provides a disruption of the immediately preceding CL/ARI or MAPD relationship and leads to the greater change in ARID required for the generation of TdP. This study further suggest that singlets, couplets, triplets and TdP polymorphic ventricular tachycardia (PVT) occurring spontaneously under condition of delayed repolarization originates from the VSCS. TdP was then perpetuated by a reentrant

mechanism. The fast rate of the TdP episode effectively abolishes the substrate of the arrhythmia (dispersion of repolarization intervals). A preliminary report has been published in abstract form. [7]

Methods

All procedure for animal care and experimentation followed the guidelines of the Canadian Council for Animal Care and were monitored by an institutional committee. Nine New Zealand White rabbits (body weight, 2.0 - 2.5 Kg) were anaesthetized with xylazine (8 mg · Kg^{-1} i.m.) followed by ketamine hydrochloride (75 mg · Kg^{-1} i.m.). Heparin (400 IU · Kg^{-1}) was administered through the marginal ear vein. The hearts were excised and immediately immersed in a modified Krebs-Henseleit solution previously bubbled with 95 % O_2 and 5 % CO_2 (composition in mmol · $Liter^{-1}$: NaCl 122.0, KCl 25.8, $MgSO_4$ 0.5, $NaHCO_3$ 24.0, KH_2PO_4 1.2, $CaCl_2$ 1.8, Glucose 50). They were quickly mounted in a non-recirculating Langendorff apparatus and perfused at a constant pressure of 65 cm H_20 with oxygenated Krebs-Henseleit solution (composition in mmol · $Liter^{-1}$: NaCl 122.0, KCl 2.8, $MgSO_4$ 0.5, $NaHCO_3$ 24.0, KH_2PO_4 1.2, $CaCl_2$ 1.8, Glucose 5.0, Pyruvate 2.0).

To slow the down the intrinsic heart rate, the atrioventricular node was destroyed by injection of 0.1-0.2 ml of formaldehyde (37 %) into the AV nodal region. The resulting slow heart rate permitted us to stimulate the heart at variable CL. Bipolar stimulating electrodes were sutured on the mid wall of the right ventricle or left ventricle for pacing. The hearts were in a glass water-jacketed chamber filled with Krebs-Henseleit solution to keep a constant temperature of

approximately 37 °C. The hearts were paced at a basic cycle length (BCL) of 0.5 sec and then switched to a long CL of either 1.0 or 1.5 sec for at least 5 minutes. Between these rate changes the heart were paced at a BCL of 0.5 sec.

The nine hearts were equilibrated for 25 minutes at 0.5 sec BCL with *d*-sotalol (20 μM). After this time the hearts were paced alternately at either the BCL of 0.5 sec or CL of 1-1.5 sec. The longer CL were maintained for approximately 5 minutes and then changed back to 0.5 sec. The hearts were equilibrated between rate changes at 0.5 sec BCL for at least 2 minutes.

Epicardial activation mapping was performed as described previously. [8,9] Briefly, unipolar recording contacts (63 sites) of the sock electrode array and, in five of the hearts, endocardial plunge wires (20 sites), were connected to a multi-channel recording system and computer. Activation times were detected at the point of maximum slope deflections with dV/dt_{max} in excess of -0.5 $mV \cdot ms^{-1}$. All computer-selected events were verified by the operator on a videoscreen with an interactive program. Activation times were measured with reference to the earliest epicardial activation (zero time reference). Isochronal maps were computed automatically by linear interpolation and drawn at 10 ms intervals for selected beats. ARI, an index of local repolarization interval which is highly correlated with the refractory period measurements, [10] were measured from dV/dt_{max} in the activation complex to the maximum positive slope in the T wave of each of the unipolar electrograms.

In four different experiments MAP probes (4 French, model no 225, EP technologies inc.) were used for MAP recording from two epicardial sites. One probe was positioned apically and the other basally. The MAP signals were amplified by two DC amplifier (Isodam, WPI). These recordings were acquired simultaneously and digitized at 1Khz on an IBM compatible personal computer equipped with an A/D board (TL-125, Axon Instrument) and Axotape software (Version 2, Axon Instrument). The data was temporarily stored on the hard disk of the computer and then stored on digital audio tapes and on CD- ROM disk for later retrieval and analysis.

MAPD at 90 % repolarization level ($MAPD_{90\%}$) were measured by Data-Pac II software ((Data-Pac version 4.1) with the selection criteria and advanced spreadsheet module, Run Technologies). Only MAP signals with stable baseline were analyzed.

Drug

A concentrated drug stock solution (4×10^{-2} M) was made from powder in double distilled water each week. The stock solution was diluted in modified Krebs-Henseleit solution to the appropriate concentration of *d*-sotalol. *d*-Sotalol was kindly supplied by Bristol-Myers Squibb Canada.

Statistical analysis

Student's paired and unpaired *t*-test was used as an indicator of statistical significance ($P \leq 0.05$). Bonferroni's inequality was used when multiple student's *t*-test were needed. Data are presented as mean ± S.D.

Results

Perfusion of the isolated rabbit heart with therapeutic concentrations of *d*-sotalol resulted in the spontaneous occurrence of a typical sequence of arrhythmias. Typically, a series of multiple singlets evolved into couplets, triplets and quadruplets followed by episodes of TdP when the CL was increased to 2-3 times the basal value of 0.5 sec. [1,4]. TdP was always preceded by several instances of the lessor arrhythmias. In order to study the progression of these lessor arrhythmias to TdP we analyzed the activation and repolarization characteristics of beats at the BCL of 0.5 sec, paced beats immediately preceding generation of the first singlet, the first singlet, subsequent singlets, both beats of couplets, all beats of triplets or quadruplets, paced beats immediately preceding episodes of TdP, and all beats of TdP. A total of 168 beats of the forerunners of TdP and all beats of 37 TdP were analyzed and form the basis of this report.

Characteristics associated with initiation of the first and subsequent singlets

We had shown previously that generation of singlets was associated with a critical disparity between MAP recording sites on the endocardial and epicardial surfaces. [1,4] In this study, we evaluated the changes in ARI and its dispersion in association with singlets and ultimately TdP. Figs. 1 and 2 shows a typical example of an increase in ARI prolongation and dispersion on stimulated beats prior to singlets and on beats prior to TdP. The emergence of singlets was well

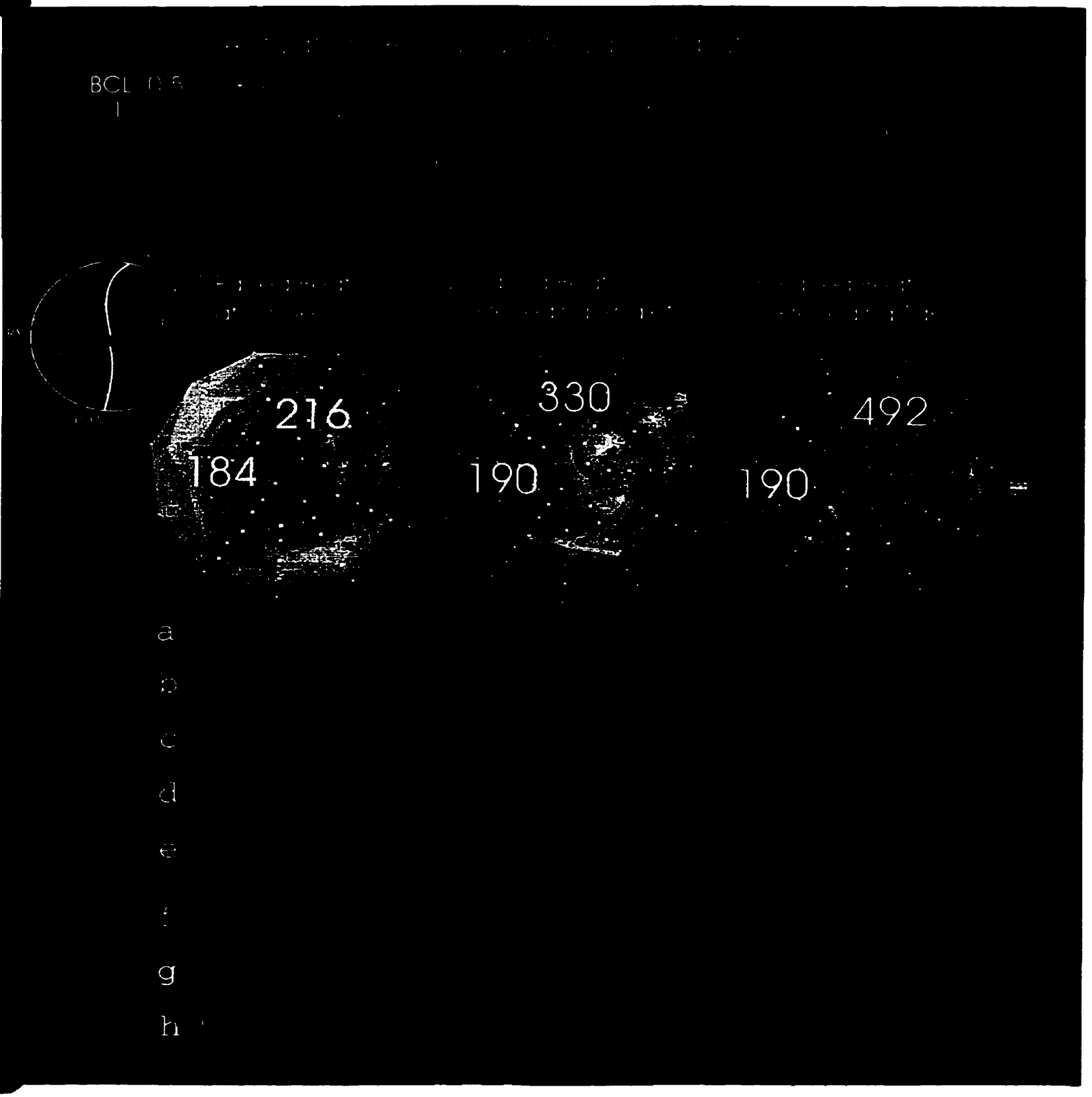
BCL
216
184
330
190
492
190
a
b
c
d
e
f
g
h

Figure 1. Comparison of the ARIs distribution of a paced beat at a short BCL (0.5 sec), during which no arrhythmia occurred, with that of a paced beat immediately preceding a singlet and one immediately preceding an episode of TdP. Top panel shows the electrogram of beats at the BCL of 0.5 sec and those generated at the longer CL of 1.5 sec. The upper left diagram shows the position of unipolar contacts (dots) on the ventricular epicardial surface as a polar representation in which the base is along the circumference and the center is at the apex. The three colored isochronal repolarization maps indicate this distribution on a polar representation of the epicardial surface. Below the three isochronal repolarization maps are selected epicardial (a-f) and endocardial (g and h) unipolar electrograms. The number above the electrograms is the ARI in msec. In this and all subsequent figures red indicates the minimal and violet the maximal values. Isochronal lines were drawn at 100 msec. PDA and LAD are the posterior descending artery and left anterior descending artery, respectively.

Figure 2. Typical example of unipolar electrograms showing the ARI_{min} and ARI_{max} of a paced beat at the short BCL (0.5 sec), the paced beat preceding a singlet and the one preceding an episode of TdP in the example shown in fig. 1. The vertical lines (yellow) on the unipolar electrogram indicate where the ARI measurement were taken.

correlated with an increase in ARI prolongation and ARID at the long when compared with the short CL. The ARI_{max} increased on the paced beats prior to singlets (216 vs 330 msec) while the ARI_{min} remained unchanged (184 vs 190) resulting in a 4 fold increase of ARID (32 to 140 msec). The ARI_{max} was further increased on the stimulated beat immediately preceding TdP (330 to 492 msec), while the ARI_{min} still remained unchanged. This resulted in a further 2 fold increase of ARID (140 to 302 msec). The changes in the ARI and ARID on the endocardial surface were qualitatively similar. Fig. 2 shows a prominent increase in the amplitude of the repolarization phase of selected electrograms in the beats prior to TdP. Most of the disparity was created by an increase in ARI toward the apex and midwall of LV of the heart whereas the basal portions show minimal intervals, similar to the values seen in beats generated at short cycle lengths and not associated with arrhythmia (190 vs 184 msec) (fig. 1). In all the experiments, ARID increased significantly by more then 2 fold prior to the first singlet (69±13 to 155±49, n=33, $P \leq 0.05$) and further increased another 2 fold on beats prior to TdP (275±72 msec, n=19, $P \leq 0.05$). All arrhythmias were eliminated when the hearts were paced at the BCL of 0.5 sec. The disparity was created largely as a result of prolonged repolarization at sites which normally show the earliest breakthrough activation in IDV beats originating from the left bundle branch. [3] These are the epicardial regions which have the greatest proximity to the termination of the underlying VSCS.

Fig. 3 shows an isochronal activation map of the earliest singlet. The total epicardial activation was short (42 msec) and the breakthrough area was wide and overlying the specialized conduction system breakthrough area as observed previously for IDV beats [3]. The endocardial unipolar recording (fig. 3, lower panel) located underneath the epicardial breakthrough area was activated before (site g: -4 msec) the earliest sites on the epicardial surface. Also, no bridging activity was detected between the stimulated beat and the subsequent beat. The evidence presented here is consistent with an impulse arising from the VSCS [3], and with an endocardial focal mechanism as being responsible for the generation of the first singlet. The isochronal activation pattern of the subsequent singlet (fig. 3, top right panel) was slightly different. The breakthrough area (red) was reduced and sites which showed lack of activation were located on the periphery of the breakthrough area. Note that the endocardial site which showed the earliest endocardial activation in the first singlet (lower right panel, (electrogram h)).

Fig. 4 shows a typical example of the pattern of activation of the first singlet and its evolution into multiple singlets. In this typical example taken from another preparation, pacing at the slow rate resulted in a series of singlets. Fig. 4 shows the isochronal map of the first 5 singlet of the series. The isochronal activation pattern of the first singlet was very similar to the one shown on the previous figure except that the breakthrough area was more posterior (posterior apical LV) (fig. 4, a). In the second and subsequent singlets the breakthrough area

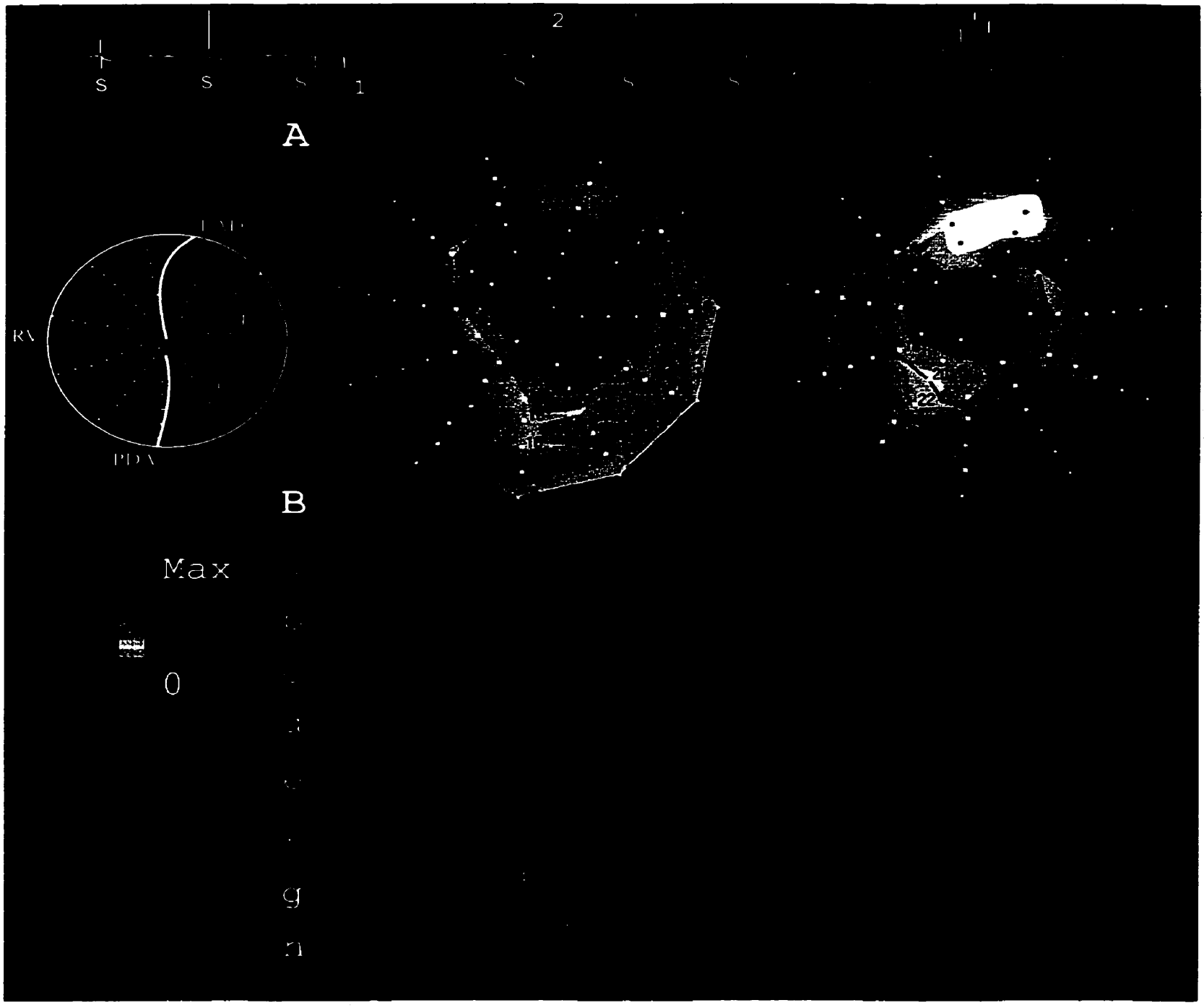
A
B
Max
0

Figure 3. Typical example of the isochronal activation map of the earliest singlet observed at the slow rate (1). The upper left diagram shows the position of unipolar contacts (dots) on the ventricular epicardial surface as a polar representation in which the base is along the circumference and the center is at the apex. The upper right map shows a large breakthrough area on the anterior apical LV together with a short total activation time (42 msec). The upper right map shows a smaller breakthrough area on the apical LV together with sites which show lack of an active response. The bottom panels shows the electrograms at selected epicardial sites (a-f) and endocardial sites (g-h). Number to the right of the electrograms indicate the activation time, in msec, in reference to earliest epicardial breakthrough. Activation at the endocardial recording site preceded activation at epicardial sites as observed in the unipolar recording at site g (* -4 msec). Note that the area of breakthrough was the same as that showing the greatest ARI of the stimulated beat immediately prior to TdP as illustrated in fig. 1. "S" in this figure and subsequent ones indicates the stimulated beat.

Figure 4. Comparison of isochronal activation maps of a series of 5 consecutive singlets. Below each isochronal activation map are shown unipolar records from the apical (A) and basal sites (B). These were the same sites for all the beats. The breakthrough of in beats (b-e) all occurred at the margins of a wide apical area in which no activation could be detected: i.e., this entire area did not generate a signal large enough for the computer to indicate an active response as shown in the unipolar record from the apical site.

was shifted to more basal sites: from the posterior and anterior paraseptal sites in the second singlet (b) to the anterior paraseptal sites in the third to fifth singlets (c-e); it occurred at the margins of a wide area in which no activation could be detected: i.e., on the apical area where the breakthrough area was located in the first singlet

What was the reason for a lack of activation in the apical area and why was the earliest epicardial breakthrough shifted to more basal sites in subsequent singlets? To try and answer this question, we placed MAP probes on both the apical area showing lack of activation and on the basal ventricular area showing breakthrough of activation (fig. 5). These MAP recordings were acquired simultaneously with the activation mapping. The MAP_{apical} recordings show progressive interference of the repolarization interference of the repolarization phase of the stimulated beat by the depolarization phase of the singlet (fig. 5, panel A). Initially, the activation phase of the first singlet (fig. 5, a) was very rapid in both MAP recordings. The isochronal activation pattern of this first singlet was focal (fig. 4, panel 1) . The coupling interval (CI) of the first singlet to the paced beat was always longer than that of subsequent singlets (412 versus 352 msec) The CI significantly decreased from the first singlet to the second singlet in all trials (312 ± 19 to 270 ± 30 msec, n=15, $P \leq 0.05$), and remained constant in subsequent singlets. In the second singlet (fig. 5, b) the duration of the response at the apical site to the paced beat is increased while the CI of the unstimulated response is decreased. Thus, the depolarization phase now interrupts the

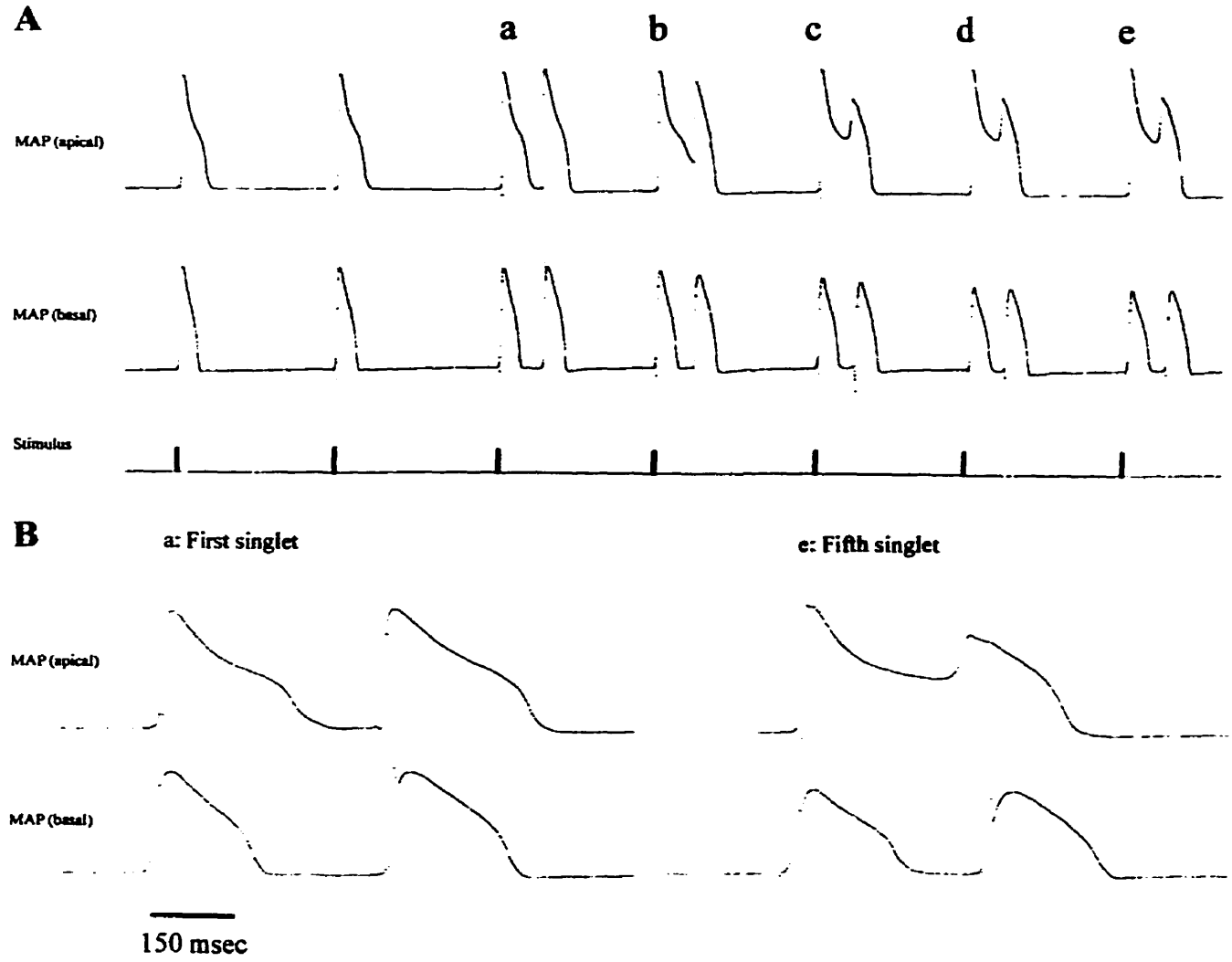

Figure 5. Panel A. MAP recordings from apical and basal epicardial sites during the series of singlet shown in fig. 4. Map recordings were acquired simultaneously with the activation mapping. Panel B. Expanded version of MAP recordings of first and fifth singlet. The $MAPD_{apical}$ are in msec: prior to coupling, 254; a: 256 and 272; b: not determined; c: 478; d: 478; and e: 480. The corresponding $MAPD_{apical}$ are in msec: prior to coupling, 187; a: 192 and 224; b:200 and 224; c: 208 and 224; d: 208 and 224; and e: 208 and 226. The CI measured from the MAP_{apical} are in msec: a, 392; b, 336; c, 288; d, 280; e, 280. The CI measured from the MAP_{basal} are in msec: a, 412; b, 352; c, 352; d, 352; e, 352.

repolarization phase of the MAP of the stimulated beat recorded from the apical site. Note that prior to and during the first singlet, the $MAPD_{90\%}$ at the apical recording site was slightly longer then the one recorded from the base (254 versus 187 msec). In the third and subsequent singlets, the MAP_{apical} looks as if there was only a very long MAP with a secondary deflection which is either an electrotonic early afterdepolarization (EAD) like "hump" or a local response which interrupts the repolarization phase of the stimulated beat (fig. 5, c-e). On the other hand, no interruption of the repolarization phase was observed in the MAP_{basal} recording which shows a full blown potential. The "fused potential" recorded at apical sites are those sites which showed lack of activation on the isochronal activation map (fig. 4, b-e). The "fused potential" gave rise to a prominent prolongation of the MAP_{apical} versus the MAP_{basal} (478 versus 224 msec) (fig. 5, panel B).

Evolution of singlet into couplet and TdP- part of a continuum

Fig. 6 shows the evolution of a singlet into a couplet and a TdP in another heart. This singlet (fig. 6, A. 1) shows an isochronal activation pattern which was similar to that seen in the second to the fifth singlet of fig. 4 (b-e), except that the breakthrough area of this impulse was shifted to the posterior paraseptal wall. The first beat of the couplet (fig. 6, B. 1) shows an isochronal activation pattern almost identical to that of the singlet, as would be expected. In the second beat of the couplet, the impulse emerges from those sites, which initially showed lack of an

Figure 6. Evolution of a singlet into a couplet and a TdP. Electrogram shows 3 successive singlets, a couplet and a TdP. Panels A, B (1-2) and C (1-2) show the isochronal activation maps of the singlet, the 2 beats of the couplet and the first two beats of the TdP. Numbers at the lower right of each activation map indicate the maximum activation time.

active response in the previous beat, but have now become available for activation and travel towards the basal ventricular areas.

Activation delays are observed between the border of the previously activated area and the sites which showed lack of an active response in the previous beat. Note that the minimal and maximal activation delays are in very close proximity to one another (red and violet are separated by bunched isochronal lines). A similar pattern was seen in the early beats of TdP (fig. 6, C. 1 and 2), except that the emergence of the impulse was located on the anterior RV and the degree of delay developing in the second beat (C. 2) was increased when compared to the couplet (162 versus 198 msec).

Fig. 7 shows the isochronal activation maps of all beats of the TdP shown in fig. 6. This figure also shows the isochronal activation map of the paced beat (S) immediately preceding the first beat of the TdP showing spread of activation from the stimulated site in the posterior LV to the anterior RV. In beats 2 and 3 of the TdP, we see isochronal map consistent with a complete reentry with a "figure-of-8" pattern. In beat 4 one of the limbs of the reentry was eliminated. Thus the impulse follows a single path (arrow). On the last beat, the "figure-of-8" pattern was also no longer present, the total activation time was considerably reduced (80 msec versus a peak of 198 msec) and TdP terminated. The isochronal activation pattern of the stimulated beat (S) following TdP (not shown) was identical to the one preceding it.

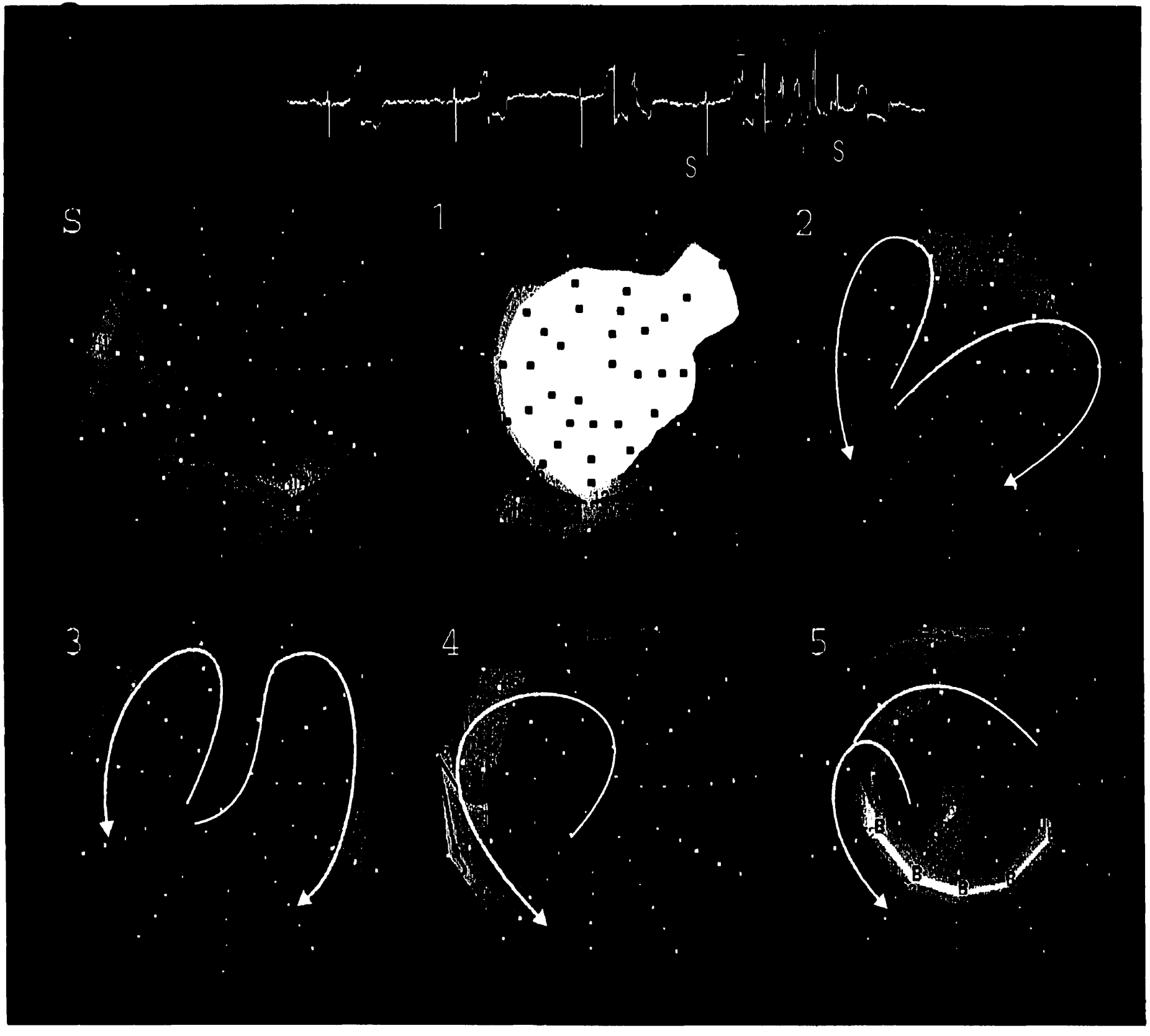
S
S
S
1
2
3
4
5
B
B
B
B

Figure 7. Isochronal activation maps of the stimulated beats (S) and all beats of the 5 beat TdP shown in fig. 6. Numbers at the lower right of each activation map indicate the maximum activation time.

Discrete areas of "fused potentials" on the apical epicardial surface were always observed in the first beat of couplets, triplets and TdPs. Fig. 8 is a typical example showing that the MAPs recorded from the apical site during a singlet, the first response of the couplet and TdP was always composed of a "fused potential" when compared to the basal site and corresponded to areas of lack of activation as observed in the typical example shown in fig. 6. This was observed in many episodes in the 4 hearts in which MAPs were recorded. Based on MAP recording from apical sites, we observed that areas of "fused potentials" were a necessary transition state to more severe arrhythmias including TdP.

Fig. 9 shows that each arrhythmic beat of the sequence, shown in fig. 8, began with a "fused potential" at the apical site. In the beats preceding TdP (fig. 9, A) TdP, the MAP_{apical} shows a "fused potential", and the MAP_{basal} shows what looks like an electrotonic "hump" following full repolarization. We interpret these records to mean that the beat preceding TdP was actually the beginning of a singlet which failed to propagate to the basal sites leaving part of the heart still refractory. The sites of "fused potentials" on the apical surface may be responsible for the very prolonged ARI observed prior to this TdP as shown in fig. 1 (panel 3). This is in contrast to the somewhat shorter ARI_{max} observed in the paced beat preceding a singlet (fig 1, panel 2) in which no fusion potential is present (fig. 5). In the singlet, (fig. 9, B) the MAP_{apical} similarly shows a "fused potential", but now the MAP_{basal} shows an active response. The secondary deflection at the apical

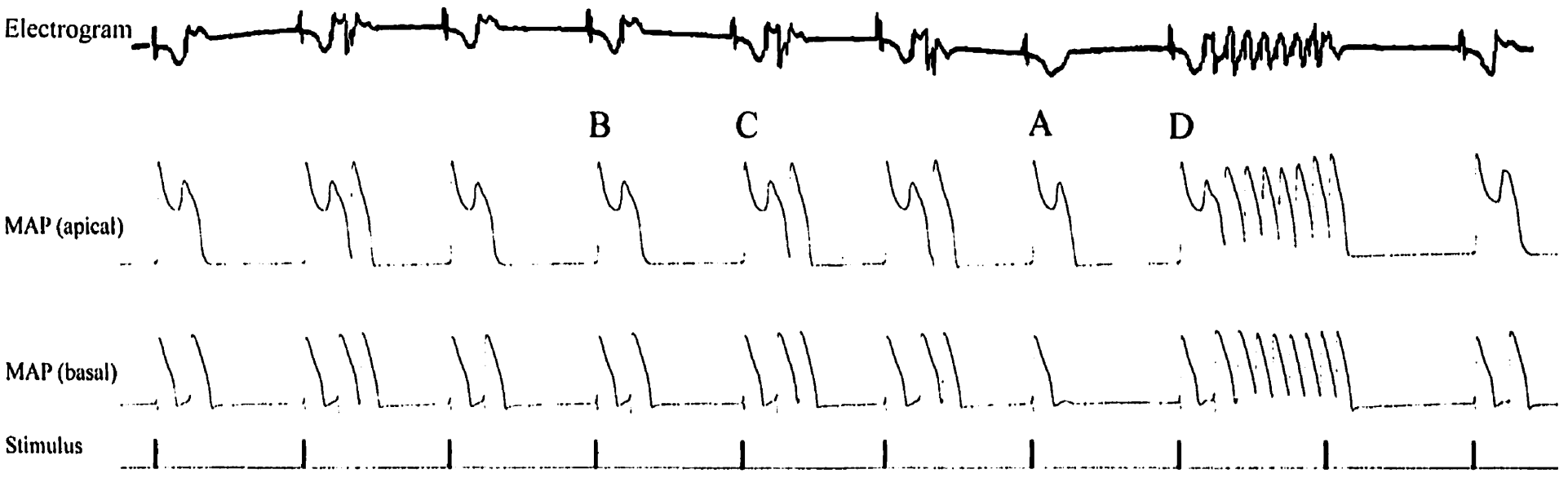
Electrogram
B
C
A
D
MAP (apical)
MAP (basal)
Stimulus

Figure 8. MAP recordings from apical and basal epicardial regions during an arrhythmic episode in which there were singlets, couplets, and TdP. Preparation was stimulated at a CL of 1.5 sec. A, stimulated beat immediately preceding TdP; B, singlet; C, couplet; D, TdP.

site occurred 88 msec prior to that at the basal site. The active response appears to be initiated at the peak of the electrotonic "hump" seen in fig. 9 (A). The active response at the basal site was accompanied by a prolongation of the MAP at the apical site, as compared to that seen in A, suggesting an electrotonic interaction between activity at these two sites. For the couplet (fig. 9, C), the MAP_{apical} shows initially a "fused potential" MAP which was followed by a full blown active response at the basal recording site. The first response occurred 92 msec after the secondary deflection at the apical site. The active full blown response at the apical site followed that at the basal site by 144 msec. The second basal response followed this apical response by 94 msec. We interpret this to mean that propagation had occurred from basal to apical recording sites and back to the basal site as a full reentry. This interpretation agrees with the isochronal activation map of the couplet shown in fig. 6 (B.1 and B.2). The start of the TdP was very similar to that of the singlet and couplet (fig. 9, D), except that the response at the basal site occurred later (100 msec) after the secondary deflection at the apical site. The first active response at the apical site occurred earlier than in the couplet (108 msec). The small difference in activation time appeared to be sufficient to setup a circulating wave front resulting in an 8 beat TdP. These results further support isochronal activation maps shown in fig. 6 and fig. 7; suggesting that the singlets, couplets, and TdP are all initiated in an identical way. Whether TdP occurs or not must depend upon an intimate relationship between the activation delay associated with the generation of the singlet and refractoriness at strategic sites in the ventricles here represented on the epicardial surface. Thus TdP is merely part of a

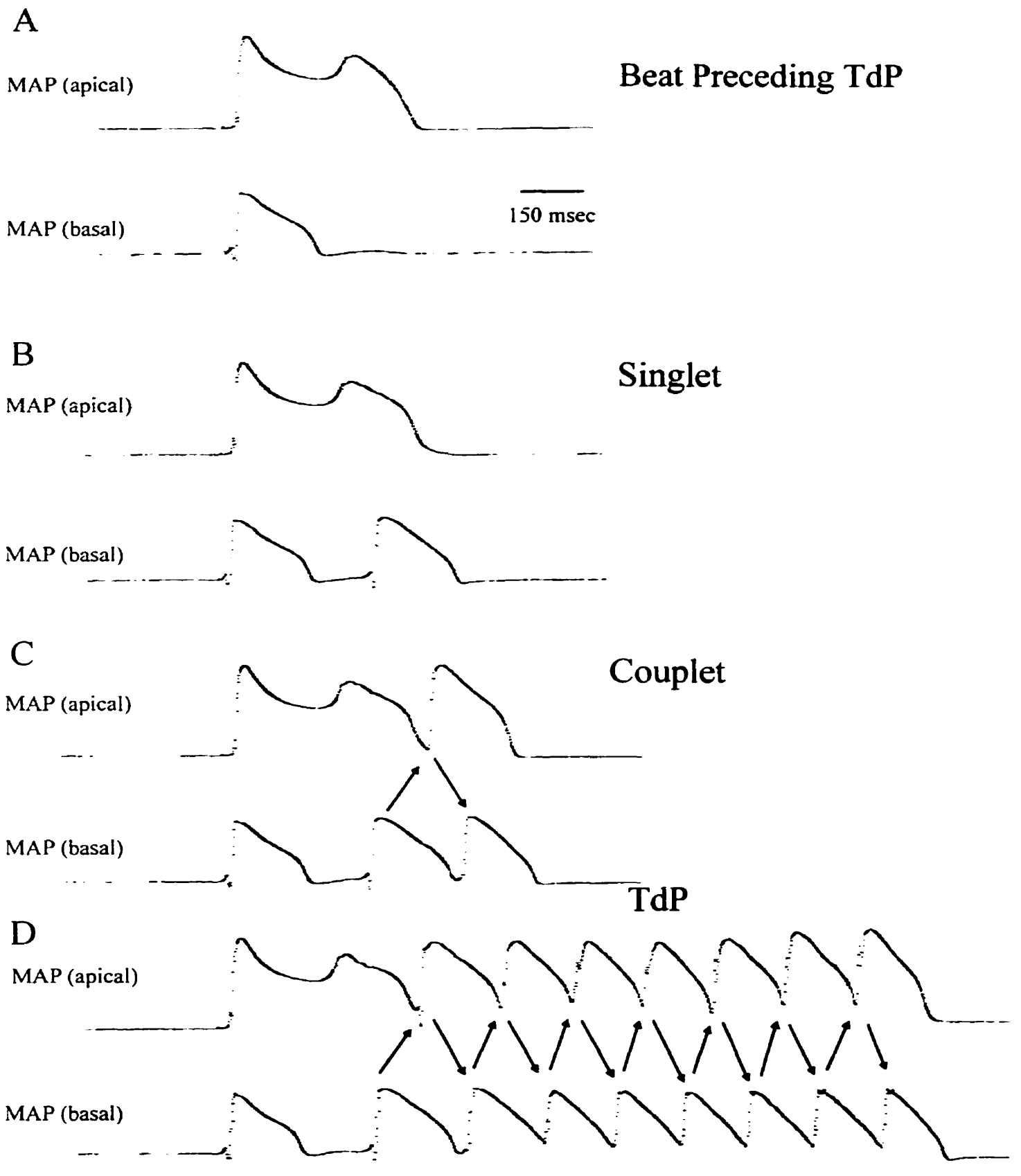
A
MAP (apical)
Beat Preceding TdP
150 msec
MAP (basal)
B
Singlet
MAP (apical)
MAP (basal)
C
Couplet
MAP (apical)
MAP (basal)
TdP
D
MAP (apical)
MAP (basal)

Figure 9. Comparison of the evolution of a singlet, couplet, and TdP. All panels show magnification of the MAP signals indicated in fig. 8.

continuum in which beats initiated in the VSCS conduct to the rest of the ventricle with variable delay depending upon the refractoriness and reenters one or more times.

Fig. 10 shows isochronal activation maps of the 17 beat TdP illustrated in fig. 1. This TdP shows the typical twisting pattern of the QRS complex. Beat 1 shows the typical activation pattern of other first beats. A "figure-of-8" activation pattern could be observed on beats 2 to 14. Note that prominent activation delays were established early and the sites with maximal delays (violet) were in close proximity to sites with earliest activation (red and violet) which was necessary to maintain a reentrant mechanism. On beats 15 and 16 the anterior component of the reentry path was eliminated. On the last beat a focal pattern was observed and there were a lessor number of sites showing activation delay suggesting that the reentrant impulse was propagated through the LV VSCS. The sites of slows conduction (bunched isochronal lines) varied location and this seems to have changed the direction of the activation wave front. In the initial beats the "figure-of-8" activation wave front was initially directed towards the posterior side of the both ventricles, then traveled around the sites of slow conduction (bunched isochronal lines) towards the basal anterior side of the LV to complete the cycle (beats 2-12). In the subsequent beats (beat 13-16) the activation wave front was emerging from the lateral LV and was propagated towards the lateral RV, going around the sites with slow conduction and finally going back to the apical LV. This gradual change in the orientation of the activation wave front by more then

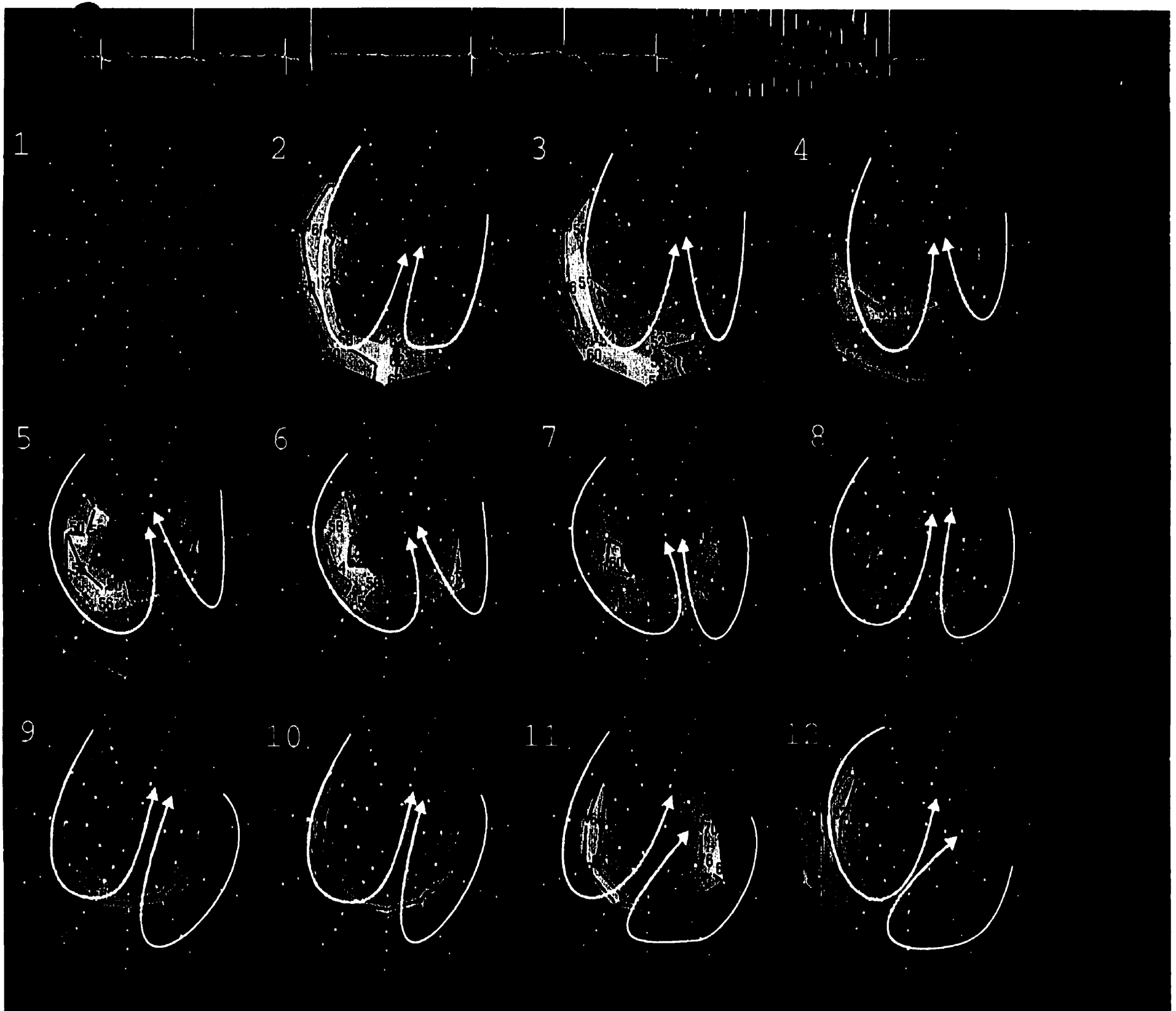
1
2
3
4
5
6
7
8
9
10
11
12

Figure 10. Isochronal activation maps of the 17 beat TdP shown in fig. 1.

90^0 may have been responsible for the apparent twisting of the QRS complex. The twisting pattern was only observed in longer TdPs, such as in this typical example.

ARID with respect to initiation and termination of TdP

Fig. 11 compares the ARI isochronal map and ARID in stimulated beats prior to TdP with that of the last beat of TdP. The maximal ARIs are observed on the apical LV area with shorter ARIs towards the base of both ventricles. The ARIs and ARID are greatly reduced on the last beat of the arrhythmia and their distribution is variable. This results in a more uniform repolarization pattern on both ventricular surfaces. This critical dispersion of repolarization was associated with the initiation of the TdP arrhythmias and the dissipation of that dispersion was associated with its' self-termination.

Fig. 12 shows that ARID was very quickly dissipated to basal levels by the second or third beat of an arrhythmic episode. This figure compares the ARID of stimulated beat at the basal CL (0.5 sec) with the ARID of stimulated beats immediately preceding TdP (from fig. 11), beats prior to singlet, in the last beat of couplet, triplet, and TdP. The. ARID is greatest in those stimulated beats immediately preceding TdP (c) thus, establishing the conditions for TdP initiation. A lessor degree of disparity was associated with initiation of singlets (b). It seems clear that by the second beat of couplets (e) or third beat of triplet (f), the ARID is already decreased to values present in the stimulated beats at the short BCL during

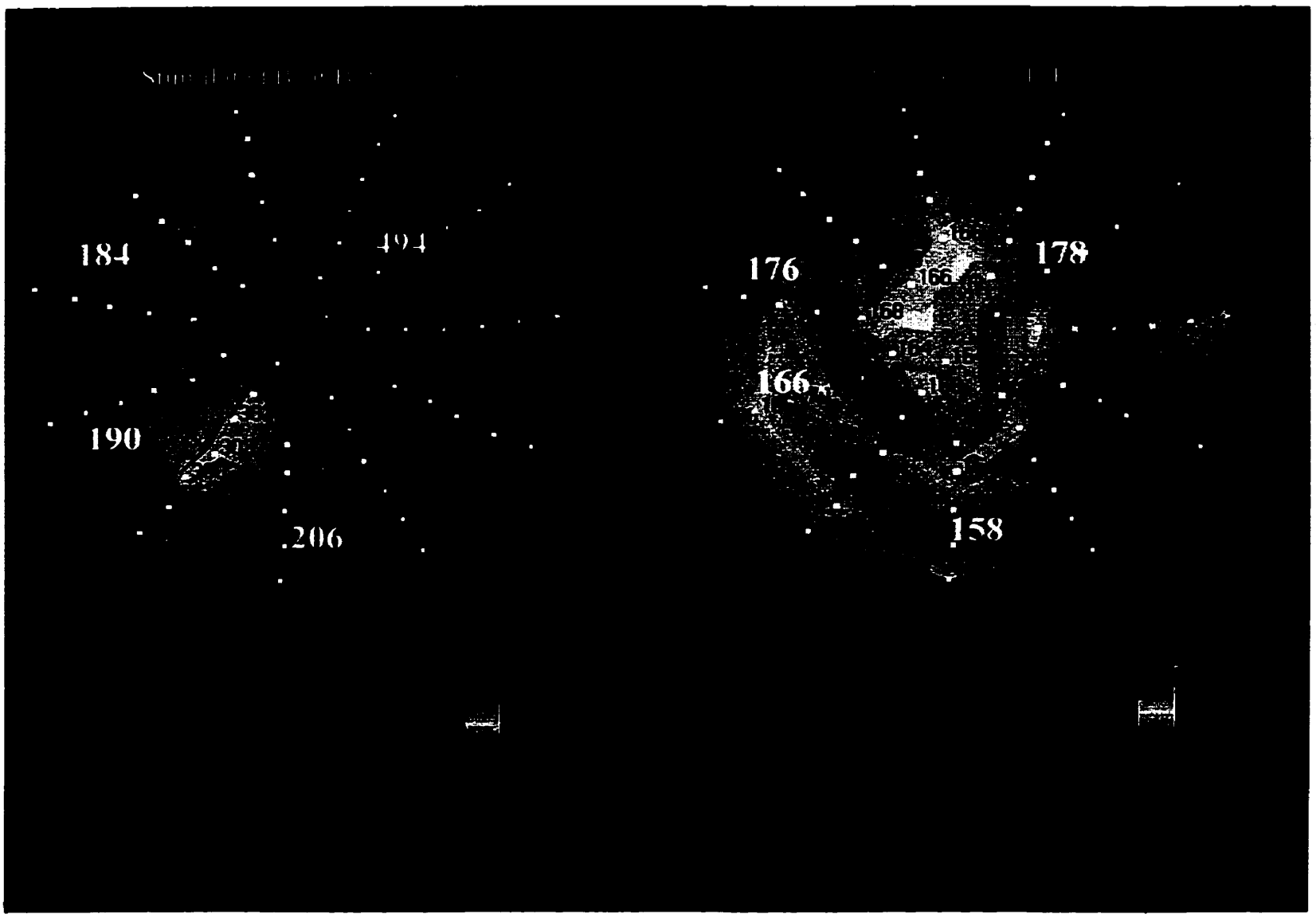
184
494
190
206
176
178
166
158

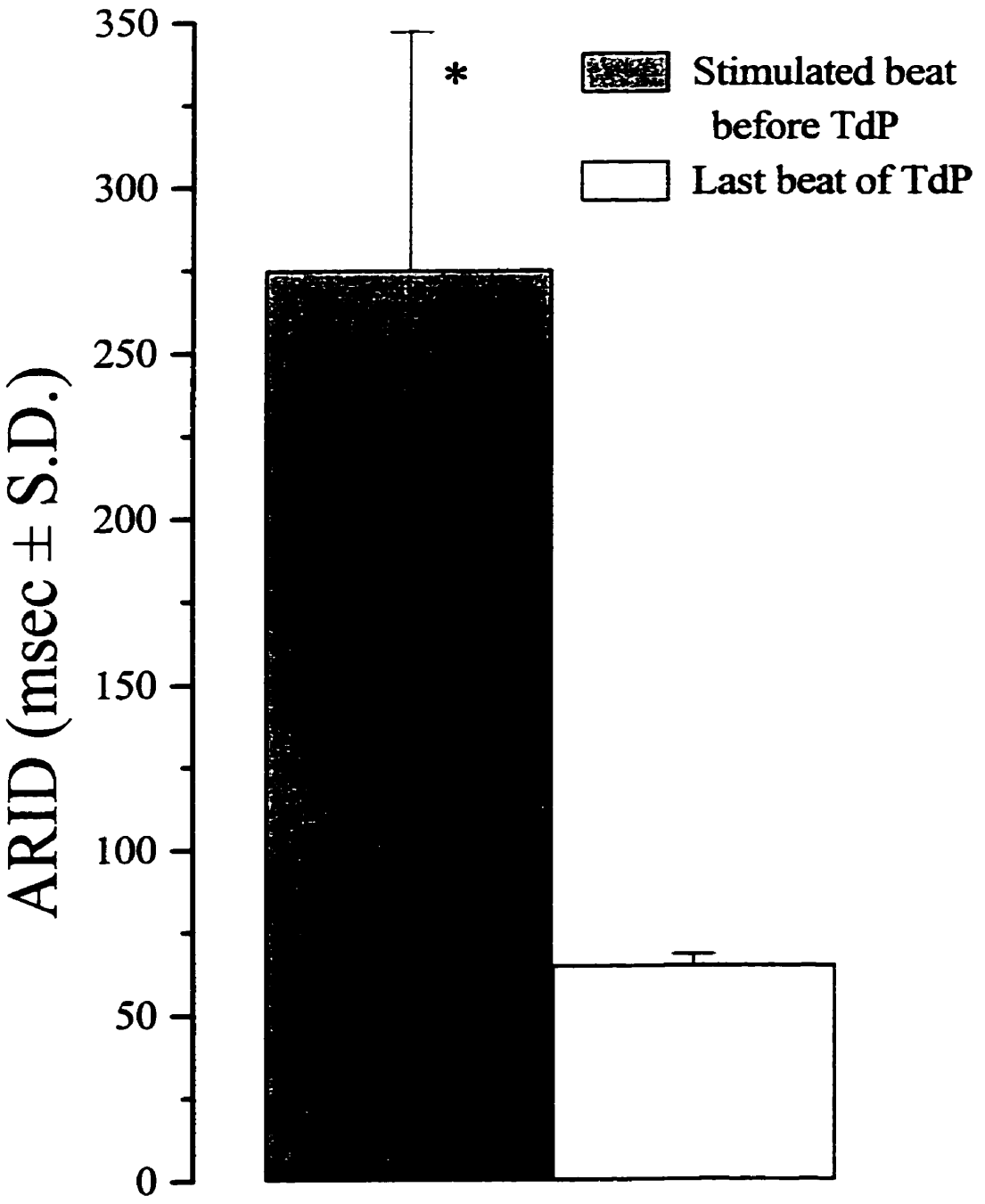
350
300
250
200
150
100
50
0
ARID (msec ± S.D.)
*
Stimulated beat before TdP
Last beat of TdP

Figure 11. Comparison of the ARI maps of the stimulated beat prior to TdP and the last beat of the TdP. Note the prominent ARI prolongation in the apical area of the LV and the prominent ARID in the beat prior to TdP. The ARI values together with the ARID are much reduced in the last beat of the TdP compared to the values observed before TdP. Bar graph shows ARID observed in all the stimulated beats prior to TdP (n=19) and the last beats of TdP analyzed (n=19).* $P \leq 0.05$. Isochronal lines were drawn at 40 msec.

which no arrhythmias is present (a). Note that the ARID observed on of TdP (g) is comparable to the ARID level observed at 0.5 sec BCL. We would interpret this result to mean that by the second beat of couplet or the third beat of triplet whether TdP occurs or not is no longer dependent upon the difference in repolarization intervals, but rather upon subtle changes in the propagation of the wave front around lines of functional dissociation leading to reentry.

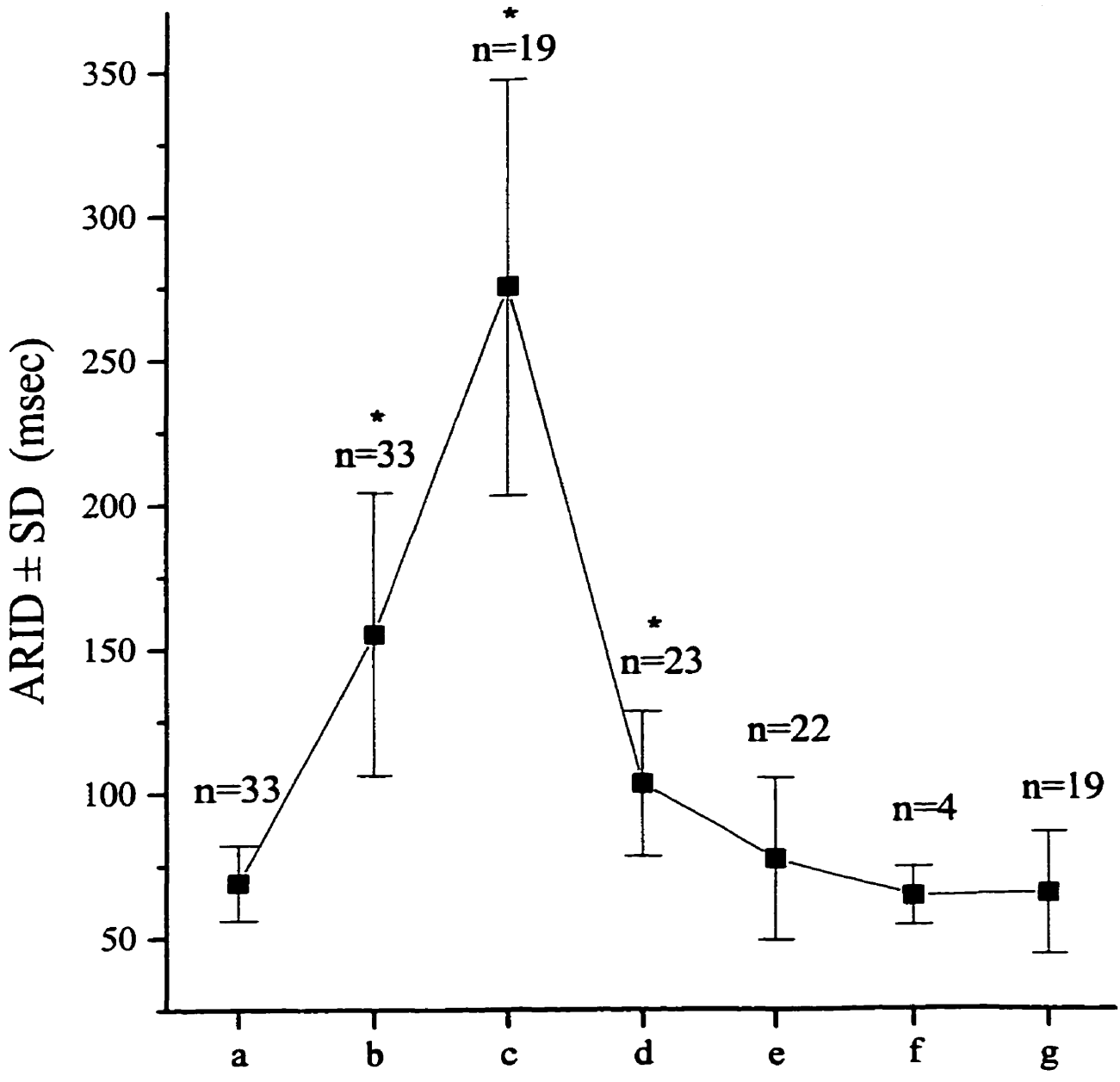

Figure 12. Plot of the ARID of stimulated beats at 0.5 sec BCL (a), stimulated beats prior to singlet (b),"fused potential" at apical sites (c), singlet (d), last beat of couplets (e), last beat of triplet (f), and last beat of TdP (g). * $P \leq 0.05$

Discussion

In this model, singlets, couplets, triplets, quadruplets, and TdP occur spontaneously in the isolated Langendorff perfused rabbit heart in the presence of a therapeutically high concentration of *d*-sotalol and a moderately slow heart rate. [4] These are conditions that have been associated with occurrence of TdP clinically. [6] In our model of drug-induced TdP, singlets, couplets, triplets, quadruplets, and TdP were consistently observed and therefore their underlying mechanism was amenable to analysis.

In our study we showed several novel findings on the mechanism of initiation, perpetuation and termination of experimentally drug-induced TdP. First of all, the occurrence of singlets are associated with an increase in ARID and further increase in ARID is associated with the initiation of TdP. The presence of sites of excessive ARI prolongation observed in isochronal maps are possibly owing to the presence of "fused potentials" that were recorded by MAP probes. In addition, the first singlet occurs as a result of a focal mechanism and that the subsequent singlets show areas, of varying sizes, of lack of activation recorded by unipolar electrodes as seen in the isochronal maps. With the help of MAP electrodes we were able to detect "fused potentials" in these areas of lack of activation. The appearance of these sites of lack of activation was necessary in the transition to more severe arrhythmias. The initiation of singlets, and the first beat of couplet, triplet, and TdP are the result of a focal mechanism and the subsequent

beats are the result of a reentrant mechanism. Therefore we suggest that TdP is the end results of a continuum. In this study we have shown for the first time that TdP - induced by clinically acceptable concentration of *d*-sotalol with a moderately slow heart rate - is perpetuated solely by a reentrant mechanism but not by a focal mechanism. Moreover, a decreased dispersion of repolarization causes self-termination of the TdP. This can be due to the fact that the rate of the TdP is acting as a negative feedback to decrease the repolarization intervals leading to the self-termination.

Characteristics associated with the initiation of the first and subsequent singlets

In the presence of *d*-sotalol and a moderately slow heart rate prominent ARI potential prolongation and dispersion were observed prior to singlets. Further prolongations were observed prior to TdPs (fig. 1). Prior to singlets, the ARI prolongation is likely to be related to the class III effect of *d*-sotalol on the epicardial myocardium. But since unipolar electrodes have a large recording field, this prolongation can be related to the electrical activity of cells located far from the recording sites, for example, Purkinje cells and/or "M cells". M cells have not yet been described in the rabbit heart. [11,12] Prior to TdP, areas of prominent ARI prolongation were observed on the LV apical surface in the proximity of the breakthrough area of IDV beats. We have shown that these sites with very prolonged ARI are the result of "fused potentials".

The beat associated with the first singlet in a series of singlet is consistent with a focal mechanism implicating the VSCS. Several observations support this concept. First of all, the beat of this singlet occurred after a long CI in which no bridging activity could be detected. We cannot completely discard the possibility that this beat may be generated by a reentrant impulse using a return pathway located outside of the recording field of the epicardial sock array. In addition the reentrant impulse can be out of the recording area of plunge wire electrodes. Secondly, the isochronal activation maps showed a wide breakthrough and a short total activation time similar to breakthrough area of IDV beats originating from the VSCS. [3] Moreover, when unipolar electrodes were placed in the region of earliest epicardial breakthrough they were activated before epicardial sites. This is to be expected if the impulse arose from the VSCS. Finally, the CI decreased from the first singlet to subsequent singlets. This later behavior is consistent with that of a pause-dependent EAD triggered activity (Valois M. and Sasyniuk B.I., unpublished observations).

Another finding was that after the first singlet, breakthrough area was replaced, either partially or completely, by sites without activation in isochronal activation maps (fig. 4). When MAP electrodes were placed in these sites without activation "fused potentials" were recorded. The reason why the unipolar electrode did not record any activation can be due to the slow depolarization and small amplitude of the secondary deflection observed at these

sites. In addition, premature action potential, at critical premature interval, have been shown to be undetectable by unipolar recordings. [13] This is an advantage of MAP recording over unipolar recording that even very small depolarization can be detected. [14] The appearance of "fused potential" at these sites provided a functional refractory barrier required for the initiation of a reentrant mechanism.

Although the epicardial activation pattern of the subsequent singlets, and first beats of couplet, triplet and TdP differed from the usual activation pattern of focal beats originating from the VSCS, we showed with the combination of activation mapping and MAP techniques that these beats similarly originated from a focal mechanism in the VSCS. The main reason why the isochronal activation map of these first beats were different is because of the emergence of fused potential in the area of earliest breakthrough sites. Similarly to the first singlet, no bridging activity to the stimulated beat could be detected. The CI of these beats were shorter and the impulse may have blocked at sites which were either more prolonged or "functionally more prolonged", the sites of "fused potential". This likely explains the isochronal map signatures of the first beat of TdP, focal block (FB) and focal delay (FD), observed in a previous study. [3] In another model of drug-induced PVT were profound ARI prolongation and dispersion were similarly observed prior to TdP, they showed in 40 % of the first beat of PVT a FD isochronal activation pattern; this may suggest that a similar initiation mechanism was operative in this model as well. [9]

Progression of singlet into couplet and TdP- as part of a continuum

We have demonstrated that TdP is the last element in a continuum that begins with a singlet (fig. 5 and 9). Singlets, couplets and TdP are all initiated by a focal mechanism and the following beats are the result of a reentrant mechanism.

In the presence of clinically relevant concentration of *d*-sotalol and moderately slow heart rate the perpetuation of TdP is the result of a reentrant mechanism. This is different then what we have shown at more extreme conditions -high drug concentration, hypokalemia and extremely slow heart rate- that the perpetuation of the arrhythmia were perpetuated by either a focal, reentrant or both mechanisms. We have shown previously that these more extreme conditions favor more EAD-dependent triggered activity originating from Purkinje fibers (PF). [15] Others, *in vivo* dog model witch similarly combined multiple predisposing factors -high plasma *d*-sotalol, slow heart rates, and an α_1-agonist (phenylephrine)- similarly showed that: short TdP are perpetuated mostly by a focal mechanism whereas longer ones are perpetuated mostly by a reentrant mechanism. [9] We therefore suggest that the combination of multiple predisposing factors seem to favor the generation of EAD-dependent triggered activity.

In another animal model which did not use an antiarrhythmic drug (anthopleurin A) have implicated a subendocardial focus for the initiation of the arrhythmia which is then perpetuated by a reentrant mechanism. The have

implicated a transmural reentry has a important contributor to the reentry process. In addition we could have observed a transmural dispersion if we would have recorded from the wall. Also, in this model the observed PVT were perpetuated by either a focal mechanism or a reentrant mechanism. [16] In a recent study this group failed to observe the all focal PVT and have attributed it to the lower sensitivity of the recording grid that was used in the previous study. [17]

In another isolated heart model of drug-induced TdP, although they were able to induce TdPs, they failed to identify the site of initiation of TdP. [18] We propose that the failure may have been related with the placement of their epicardial MAP recording electrodes. Their epicardial MAP recording electrode may have been recording from site of "fused potential". They interpreted these recording as triggered activity originating from the epicardial surface. Also, the sites of fused potential may have lead to the decrease in MAP disparity following the initial prominent increase in MAP disparity observed prior to TdP in their experiments. In their experiments they have not paid attention to the first triggered activity, like we did in these and previous experiments in order to implicate the VSCS in the initiation of the first beats of arrhythmias (including TdP). The appearance of "fused potential in the first arrhythmias beats appearing preferentially on the breakthrough area would have complicated the interpretation of these recordings. The placement of the MAP recording electrode were crucial for a correct interpretation. It would be interesting to see if a reevaluation of these data would give rise to a different interpretation by these authors. On the other

hand, the other interpretation is that since the condition used in their model were more extreme -much higher drug concentration, and other predisposing factors- these may have lead to triggered activity in both PF and ventricular muscles cells.

Under our experimental conditions, the twisting of the arrhythmia is likely the result of the movement of sites of slow conduction (bunched isochronal lines) which was generated early in the arrhythmia (fig. 10). The gradual change of these sites translated into the gradual change in the orientation of the activation wave front by more then 90^0. Whereas others [9,16,17] have suggested that the twisting of the QRS complex may have also been attributed to either changing focal sites, or one focal site from which impulses was propagated differently from beat to beat owing to the change in repolarization from beat to beat. We are the first to implicate one mechanism to more clinical conditions.

ARID with respect to initiation and termination of TdP

We have showed that the dispersion of repolarization is important for the initiation of TdP arrhythmias and that its elimination is related to the self-termination of the arrhythmia (fig. 11). The ARIs of the last beat of TdP were significantly shorter and more homogenous then the ARIs observed on beats prior to TdP. The rate of the TdP acted as a negative feedback to eliminate the arrhythmic substrate (dispersion of repolarization). This rate dependent effect is

related to the reverse rate-dependence property of *d*-sotalol and other selective class III antiarrhythmic drugs.

Based on the measurement of ARID of the last beats of couplet, triplet and TdP suggest that the initial dispersion of repolarization is quickly eliminated and that whether a TdP is observed beyond couplet is more dependent on the sites of unidirectional block within the ventricle.

Limitations

We have interpreted the potentials recorded from MAP probes to be related to local events, even though it is not well known what is the recording field of these probes. We are fully aware that these probes may have recorded activity which may have been localized in the subepicardial ventricular muscle layers. [14] With the limited number of endocardial recording sites we could not determine the activation and repolarization pattern of the endocardium. A more complex tridimentional activation pattern, like the one recently proposed by El-Sherif et al. [17], may account for the change in the QRS morphology. Further investigation, which were out off the scope of this investigation are necessary to establish if a meandering scroll wave is responsible for the morphology changes of the QRS complex.

Conclusion

This study suggest that singlets, couplets, triplets and TdP polymorphic VT occurring spontaneously under condition of delayed repolarization originates from the VSCS. This is likely related to an EAD and triggered activity in the PF system. "Fused potentials" are likely related to the effect of an EAD originating from the VSCS. The emergence of "fused potentials" is the necessary transition from singlets to more severe arrhythmias (couplets, triplets, and TdP). In the reentrant mechanism the sites of "fused potential" provide the functional refractory barrier which leads to the initiation of a reentrant mechanism. Reentrant activity slowly drifting between various regions of the ventricle may occur in later beats of TdP accounting for the twisting pattern. TdP is the end point of the reentrant continuum of which singlets are at the other pole. The fast rate of the TdP episode effectively abolishes the substrate of the arrhythmia (dispersion of repolarization intervals).

Acknowledgments

The authors wish to thank Mr. Gaétan Tremblay for cardiomap III and for experstert technical assistance, Debra Chan for expert technical assistance, and Bristol-Myers Squibb Canada for supplying *d*-sotalol.

References

1. Sasyniuk BI, Brunet S: Torsade de pointes induced by quinidine, *d*-sotalol & e-4031 in the isolated rabbit heart: importance of interval dependent dispersion of repolarization. *PACE* 1995;18:II-904(abstract)

2. Sasyniuk BI, Derakhchan K, Brunet S, Cardinal R: Epicardial mapping of sotalol-induced torsade de pointes in rabbit hearts. *Canadian Journal of Cardiology* 1996;12:85E(abstract)

3. Brunet S, Derakhchan K, Cardinal R, Sasyniuk BI: Mechanism of *d*-Sotalol induced torsade de pointes in an isolated heart model - a mapping study. Chapter III

4. Brunet S, Sasyniuk BI: *D*-sotalol induced torsade de pointes ventricular arrhythmias in the isolated rabbit heart - model and mechanism. Chapter II

5. Advani SV, Singh BN: Pharmacodynamic, pharmacokinetic and antiarrhythmic properties of d-sotalol, the dextro-isomer of sotalol. [Review]. *Drugs* 1995;49:664-679

6. Link MS, Foote CB, Sloan SB, Homoud MK, Wang PJ, Estes NA, 3rd. Torsade de pointes and prolonged QT interval from surreptitious use of sotalol: use of drug levels in diagnosis. *Chest* 1997;112:556-557

7. Brunet S, Derakhchan K, Cardinal R, Sasyniuk BI: Changes in activation-recovery interval disparity (ARID) accounts for initiation and termination of *d*-sotalol induced arrhythmias. *Canadian Journal of Cardiology* 1997;13:113C(abstract)

8. Cardinal R, Scherlag BJ, Vermeulen M, Armour JA: Distinct activation patterns of idioventricular rhythms and sympathetically-induced ventricular tachycardias in dogs with atrioventricular block. *Pacing & Clinical Electrophysiology* 1992;15:1300-1316

9. Derakhchan K, Cardinal R, Brunet S, Klug D, Pharand C, Kus T, Sasyniuk BI: Polymorphic ventricular tachycardia induced by *d*-sotalol in canine preparations of atrio-ventricular block: initiation in the conduction system followed by spatially unstable reentry. *Cardiovascular Research* 1998 (in press)

10. Millar CK, Kralios FA, Lux RL: Correlation between refractory periods and activation-recovery intervals from electrograms: effects of rate and adrenergic interventions. *Circulation* 1985;72:1372-1379

11. Sicouri S, Antzelevitch C: A subpopulation of cells with unique electrophysiological properties in the deep subepicardium of the canine ventricle. The M cell. *Circulation Research* 1991;68:1729-1741

12. Sicouri S, Quist M, Antzelevitch C: Evidence for the presence of M cells in the guinea pig ventricle. *Journal of Cardiovascular Electrophysiology* 1996;7:503-511

13. Myerburg RJ, Nilsson K, Zoble RG: Relationship of surface electrogram recordings to activity in the underlying specialized conducting tissue. *Circulation* 1972;45:420-432

14. Franz MR: Method and theory of Monophasic Action Potential Recording. *progress in cardiovascular diseases* 1991;XXXIII:347-368

15. Brunet S, Sasyniuk BI: Proarrhythmic effects of *d*-sotalol in rabbit ventricle associated with differential effects on repolarization in endocardial cells: *in vitro* and *in situ* correlations. Chapter I

16. el-Sherif N, Caref EB, Yin H, Restivo M: The electrophysiological mechanism of ventricular arrhythmias in the long QT syndrome. Tridimensional mapping of activation and recovery patterns. *Circulation Research* 1996;79:474-492

17. el-Sherif N, Chinushi M, Caref EB, Restivo M: Electrophysiological mechanism of the characteristic electrocardiographic morphology of torsade de pointes tachyarrhythmias in the long-QT syndrome: detailed analysis of ventricular tridimensional activation patterns. *Circulation* 1997;96:4392-4399

18. Zabel M, Hohnloser SH, Behrens S, Li YG, Woosley RL, Franz MR: Electrophysiologic features of torsades de pointes: Insight from a new isolated rabbit heart model. *Journal of Cardiovascular Electrophysiology* 1997;8:1148-1158

GENERAL DISCUSSION

Purpose

One of the major proarrhythmic side effects of class III antiarrhythmic drugs is an increase in the QT interval and associated Torsade de Pointe polymorphic ventricular tachycardia (reviews [1, 2]). Acquired-TdPs are usually observed clinically in the presence of drugs which delay the action potential repolarization phase (e.g. class III antiarrhythmic drugs) concomitantly with other facilitatory factors: slow heart rate, hypokalemia, hypomagnesemia, cardiac hypertrophy, etc. Typically, the cessation of the administration of the repolarization delaying drug (e.g. class III antiarrhythmic drug) and/or pacing of the heart at a faster rate, and/or infusion of a bolus of magnesium sulfate are usually effective in preventing the recurrence of TdP arrhythmias. The exact mechanism of this drug-induced arrhythmia remains elusive, primarily because of the lack of an appropriate experimental model.

The main purpose of this thesis was to examine the mechanism of drug-induced TdP. This major proarrhythmic side effect of more-selective class III drugs has impeded their clinical use and further development. We used *d*-sotalol as a prototypical class III antiarrhythmic drug to investigate the mechanism of this drug-induced ventricular tachycardia. Understanding the mechanism could lead to the development of a new generation of class III drugs, or the design of more effective ways of preventing its occurrence, and may lead to novel therapies for the treatment of the congenital form of the long QT syndrome and associated TdPs. Overall, our results suggest that TdP is initiated by a triggered beat, which likely originates in the ventricular specialized conduction system, most probably

from Purkinje fibers, in the presence of prominent dispersion of ventricular repolarization. TdP is then maintained by a reentry mechanism and spontaneously terminates, likely because of a prominent decrease of the initially present dispersion of ventricular repolarization.

Model

We have created a model of drug-induced TdP which is very different from other models which have been used in the past. In this model, TdP occurred spontaneously when the heart was exposed to clinically relevant concentrations of *d*-sotalol and a slight bradycardia (chapter II). The TdP that were induced strongly resembled the TdP which are observed clinically. Overall our animal model mainly differs from other models with respect to incidence, predictability, and the need for facilitatory factors. Another major difference and positive characteristic lies in the fact that this model is in an isolated heart and not in the whole animal (*in vivo*).

Our model is highly reproducible (≅ 100 %), with a very high incidence rate (as high as 100 TdPs / heart), and it was very predictable. TdP was shown to be well correlated with an increase in dispersion of repolarization.

Although the reproducibility of TdP in previous *in vivo* models was high (≤ 80%) their TdP incidence was very low. Weissenberger et al. [3], for example, showed reproducible TdP in conscious dogs with chronic AV block (5 out of 6 dogs exhibited TdP), but the incidence of TdP in these dogs was limited to, on average, 2 or 3 TdPs per dog. Similarly, Carlsson et al. [4] in the rabbit showed a

reproducibility as high as 90% (9 out of 10 rabbits), when a fast infusion rate of almokalant was used, but the incidence of TdP was very low (one TdP / rabbit). When the arrhythmia was observed, the rabbit was sacrificed in order to eliminate any neurological effect because of the decrease in arterial blood pressure which is associated with the arrhythmia. The low incidence observed in these models prevented these authors from investigating the mechanism of drug-induced TdP.

In a recent isolated rabbit heart model the reproducibility (TdP in 10 out 11 hearts) and incidence have been reported to be very high [5].The incidence may have been artificially high because these authors have defined TdP as short as 3 consecutive ventricular beats. The exact interpretation of their incidence was a problem.

In contrast to our model, the predictability of TdP in these previously mentioned models was very low. In most of these models it was suggested that TdP may have been related to an increased in QT interval dispersion or ARI dispersion but the correlation was not clearly established [3-7]. Zabel et al. [5], for instance, showed that the predictability in their model is related to both the change in the normal Tyrode's solution to one with much lower extracellular K^+ and Mg^{2+} (2.0 and 0.35 mM, respectively) and an increase in disparity of repolarization. The predictability of the increased dispersion of repolarization in this model was not very strong, since, although the dispersion of repolarization remained elevated, arrhythmias are only observed in the first 2 minutes of a 5 minutes infusion period with the modified Tyrode solution. These observations suggest that the dispersion

of repolarization is not the only predictive factor in this isolated heart model of drug-induced TdP. One major limitation of this model is that Zabel et al. [5] have not investigated the effect of low K^+ and Mg^{2+} solution in the absence of *d*-sotalol. This is important because low extracellular K^+ and Mg^{2+} are two facilitatory factors associated with TdP incidence clinically (general introduction, table 3).

The major difference between our and other models lies in the use of a drug which delays the repolarization phase of the action potential combined with other facilitatory factors: i.e., low extracellular K [3], acute [5,8,9] or chronic AV block [3,10], low extracellular K^+ and Mg^{2+} [5], α_1-adrenergic agonist [9,11], stimulation [12], consciousness [3,11]. We have included consciousness as a facilitatory factor because the incidence of TdP is much more elevated in the awake animal than it is in the anesthetized one; this suggests that an intact sympathetic system may predispose to drug-induced TdP. Most of these facilitatory factors have been associated clinically with TdP arrhythmia. For example, Weissenberger et al. [3] have used a combination of consciousness, chronic AV block and diuretic-induced hypokalemia. In this model, lowering plasma K^+ alone was associated with an increased number of arrhythmias and even TdP (from 50 arrhythmic episodes for 24 dogs to 139 arrhythmic episodes for 28 dogs). Cardiac failure (3 of 28 dogs) and sudden cardiac death (3 of 28 dogs) was also observed in this model [3,10].

Zabel et al. [5] have developed an isolated heart model in which they needed to combine a high drug concentration of *d*-sotalol (100 μM), slow heart rates and the transient perfusion with a low K^+ and Mg^{2+} containing solution (2.0 and 0.35

mM, respectively). *D*-sotalol at very high concentration has been shown to block the fast sodium current [13].

Also it was shown recently in both the rabbit and the dog *in vivo* models that the addition of an α_1-adrenergic agonist was required for the induction of class III drug-induced arrhythmia (almokalant and *d*-sotalol) [9,11]. The effect of the α-adrenergic stimulation is not clear. It could be the result of either a stretch-induced triggered activity related to the prominent increase in arterial blood pressure (review [14]) or a direct effect on membrane K^+ channels (I_{K1} [15]or I_{Kr} [16]) leading to a decreased conductance.

Others have used stimulation in the context of increased dispersion of repolarization to induced TdP in the *in vivo* and *in vitro* conditions. Vos et al. [12], in the dog *in vivo*, have used epicardial pacing (short-long-short stimulation sequence) in the presence of *d*-sotalol and slow heart rate. Antzelevitch et al. [7], in an *in vitro* canine model, have initiated a transmural reentry in the presence of erythromycin by epicardial stimulation. Neither of these model suggest a mechanism for the spontaneously occurring drug-induced TdP, they only suggest that, when both studies are combined, a premature stimulation in the context of an increased dispersion of repolarization, including a transmural gradient, can induce a ventricular tachycardia resembling TdP.

The concentration of drug which was required to induce TdP by sotalol was very different between experimental models. The concentration was either clinical or toxic. This can be explained in the following way. The use of many facilitatory factors may have decreased the requirement for a high drug

concentration. For example, Weissenberger et al. [3] have combined 4 facilitatory factors to induce the arrhythmia in his model and have reported the lowest plasma concentration of sotalol (approximately 12 μM) . On the other hand, Zabel et al. [5] have only used 3 facilitatory factors and have reported the need for the highest concentration of sotalol (100 μM). The need for these different drug concentration may have been due to a species difference between dog and rabbit.

If this previous explanation were valid, then our model would have required the need for the highest drug concentration since we did not need other facilitatory factors. On the contrary, our model needed clinically relevant concentration of *d*-sotalol (20μM) [8]. We propose the following explanations to explain the need for the lower drug concentration of *d*-sotalol in our model. First of all, in our model, an abrupt slowing in the stimulation rate was used, whereas in previous models the stimulation rate was maintained slow and then drug was infused with or without other interventions (infusion of low K^+ and Mg^{2+} modified Tyrode solution). The abrupt rate variation is associated with a profound increase in dispersion of repolarization. At a fixed rate, the dispersion of repolarization will increase more slowly and the APD of a cell may adapt more to the effect of the drug and therefore be less arrhythmic. At a fixed rate, it was shown that a higher infusion rate of almokalant was more proarrhythmic. This was suggested to be associated with the development of a higher dispersion of repolarization between PF and VM at the faster infusion rate than at a slower one. We suggest that this is related to the rate of change of the PF action potential when compared to the VM at the faster infusion rate. The other explanation is that

lower drug concentration were not investigated since the clinical belief is that high and toxic drug concentration are associated with TdP.

Previous models have mostly used *in vivo* preparations. There are a few factors which make an isolated heart model more advantageous to study the mechanism of drug-induced TdP. First of all, there is constant concern to maintain these animal alive in conditions where the cardiac output is greatly compromised. For example, the very slow intrinsic rate in models of acute and chronic AV block compromises the arterial blood pressure and cardiac output [3,10]. In the isolated heart we could stimulate the heart at a variety of cycle lengths without any concern for the rest of the animal. Secondly, a long period is required to induce the chronic AV block and hypokalemia. In addition, to determine the concentration of the drug which leads to the cardiac effect, the plasma drug concentration needs to be measured. This often requires very expensive equipment and techniques. Furthermore, the accessibility to the heart surface for recording is easier in the isolated hearts; both ventricular endocardial and epicardial surfaces are easily accessible. *In vivo*, the endocardial surface can be reached with intravenous catheters with fluoroscopic guidance. The epicardial surface can be reached with catheters only if the thorax of the animal is opened. These very invasive interventions greatly compromise the well being of the animals. Also, the extracardiac effect of the drug can never be completely eliminated. Finally, the need for anesthetic drugs may modify the effect of the drug which is under investigation. Most anesthetics have been shown to block ion channels [17,18]. By

the use of such models it is still not clear what is the implication of the drug itself in the mechanism of drug-induced TdP.

With this model in which TdP could be induced, spontaneously, reproducibly, at a high incidence and very predictably, the mechanism of initiation, perpetuation and termination could be investigated [19]. A variety of techniques have been used to investigate these mechanism: Intracellular recordings were used on endocardial superfused pieces of tissue [20]; MAP with and without activation mapping were used with the isolated rabbit heart [19,21,22].

Initiation

Dispersion of repolarization intervals

We have shown that generation of spontaneously occurring arrhythmias (singlet, couplet, triplet and TdP) was consistently observed at a slow stimulation rate at a peak dispersion of repolarization between some endocardial sites and epicardial sites [19]. The longer MAPD recorded at some endocardial sites reflects the electrical activity of both PF cells and VM cells, whereas the MAP recorded from the epicardium reflects activity of VM alone. This observation *in situ* is consistent with our finding *in vitro* which showed that PF cells and T cells action potential duration are more profoundly affected in the presence of *d*-sotalol at the slow stimulation rate when compared to the action potential duration of VM [20].

We also showed that the MAP located at these endocardial sites had "EAD like deflections" at the slow stimulation rate prior to arrhythmia. These "EAD like

deflection" may have been the result of local dispersion of repolarization, the reflection of a local EAD in the cells underneath the MAP probe, likely the PF cells, or both these phenomena. This is because that MAPD from contact MAP signal is the result of an average of the action potential duration of the cells located underneath the tip of the probe [23]. Since MAP probes can also record from deeper structures, we could not eliminate the contribution of other cells types to the MAPD and "EAD like deflection" (e.g. "M cell" [24]). Although M cells have not been shown in the rabbit heart; they have been identified in the dog [24] and the guinea pig heart ventricles [25]. Overall we have associated arrhythmia, including TdP incidence, with an increase in ventricular dispersion of repolarization between some endocardial sites and endocardial and epicardial VM [19].

When investigating the mechanism of drug-induced arrhythmia with the use of activation mapping by the use of ARI measurements, we observed yet another dimension to the dispersion of repolarization intervals. We have clearly shown a prominent dispersion of ARI on the epicardial surface prior to singlets [22] and that further prolongation was present prior to TdP [21,22]. We have now demonstrated an endocardial to endocardial, endocardial to epicardial, and epicardial- apical to base dispersion of repolarization interval prior to arrhythmia.

From the epicardial mapping we have shown that the first singlet sites which were located on the apex were more prolonged than the ones located at the base of the ventricle. This differential ARI prolongation may have been related to the greater action potential prolongation at these sites at the slow stimulation rate and may reflect a difference in the repolarization current from the base to the apex

of the ventricle of the rabbit heart. Because of the proximity of these apical sites to the sites of earliest activation breakthrough of IDV beats, the involvement of an electrotonic influence of deeper structures cannot be ruled out. The cells of the VSCS may have influenced the signal that is recorded by these unipolar electrodes and MAP probes.

Prior to TdP further ARI prolongation and dispersion were observed [21,22]. The sites which gave rise to further prolongation prior to TdP were sites where fused potentials were observed as recorded by contact MAP probes [22]. It is interesting that these sites are observed on or close to the sites of earliest breakthrough area of IVD beats. These sites developed fused potentials because of the combination of two factors: the ARI and MAPD at these more apical sites is slightly longer than at more basal sites, and the CI interval of the subsequent arrhythmic beats is shorter than the first singlet. We also suggest that the excessive ARI prolongation and dispersion which was observed under more extreme conditions -higher drug concentration, hypokalemia, and much slower stimulation rates- were the fused potentials and not the result of action potential prolongation at the slow rates, since the sites which gave rise to very prolonged activation recovery interval were similar between the two studies [21,22].

Similar patterns of ARI prolongation were also observed prior to TdP arrhythmias induced in the dog heart in the presence of *d*-sotalol and α_1-adrenergic stimulation [9]. It is our understanding that a similar phenomena may have been involved in this *in vivo* preparation as well, although the contribution of "M-cells" to the generation of the ARI epicardial distribution may have been

involved. Therefore direct MAP recordings from the apical-epicardial surfaces are required to determine if fused potential were indeed responsible for these very prolonged apical ARIs in this model. This may be more difficult to obtain in this model since it is required to see the transition from no arrhythmia to, ideally, a series of singlets followed by more severe arrhythmias. If the transitions are not seen, and these types of transition are seldomly seen in this model under the conditions used, it is very difficult to suggest that the MAP recorded from an epicardial apical recording site with an "EAD like deflection" is indeed a fused potential.

Two studies have shown a transmural dispersion of repolarization in the presence of drugs and toxin which prolong the action potential duration. El-Sherif et al. [6] have shown that anthopleurin A, a toxin which prevents the recovery from inactivation of the fast sodium channel, leads to prominent ventricular transmural dispersion of repolarization. The ARI prolongation is more prominent in the middle of the ventricular wall and was attributed to the effect of anthopleurin A on action potential duration of "M-cells". Similarly, Antzelevitch et al. [7] have shown that a high concentration of a drug which blocks I_{Kr} current (erythromycin) leads to prominent prolongation of the action potential duration of "M-cells" and to prominent dispersion of repolarization within the ventricular wall.

The involvement of the transmural dispersion of repolarization is being debated by certain investigators [7,26,27]. Rosen et al. [26,27] have shown that a low concentration of quinidine does not lead to prominent prolongation of the M-cell

layer in *in vivo* dog heart. Low concentration of quinidine have been previously shown to preferentially prolong the APD of M-cells [27] (review [28]). The *in vivo* ARI duration reflects the AP duration of M-cells rather than the duration of the epicardial or endocardial cell layers as was observed *in vitro* . These authors mainly explain this effect based on the difference in the cellular coupling between these two experimental preparations (*in vitro* slices and *in vivo*), the cells *in vitro* being more uncoupled than *in vivo*. This also suggests that the effect observed by Antzelevitch et al. [7] may also be the result of cellular uncoupling since the cells recorded are from a cut surface.

Triggered activity from the VSCS

We have shown *in vitro*, that when superfused with *d*-sotalol, PF and T cells were differentially affected compared to ventricular muscle [20]. At slow stimulation rates very prolonged action potentials were observed in PF cells. This lead to greater dispersion of repolarization. Furthermore, "EAD like deflections" were observed in PF cells at these slow stimulation rates. These "EAD like deflections" were either the result of multiple membrane oscillations (true EADs) in PF cells or the result of electrotonic interaction from a prolonged repolarization-dependent reexcitation mechanism [29]. This latter mechanism would implicate the electrotonic interaction between the PF, T and VM as the site of initiation. The prolongation of the APD in PF cell would lead to an electrotonic interaction in the T cell which would eventually reach threshold from the difference in voltage between itself and the adjacent PF cell. The triggered activity

is then reflected back to the PF cell which can be further prolonged and may lead to a second triggered activity in T-cell by a similar mechanism, that is, if the condition of drug concentration and stimulation rate are extreme enough. A similar mechanism has been proposed at the PF junction of the guinea pig exposed to EDTA [30,31]. It was suggested by these authors that the decrease in extracellular Ca^{2+} concentration would lead to the blockade of the delayed rectifier (I_K). This has not yet been directly investigated. Interestingly, also in support of such a mechanism at the PF-VM junction are the experiements of Joyner et al. [32]; they showed that when guinea pig ventricular VM cells are exposed to a low concentration of quinidine, they do not observe EADs, but when they couple these cells to model cells at a depolarized membrane potential they observe EADs in these cells. This result is very interesting since EADs are not easily induced in guinea pig cells even at very high concentrations of selective I_{Kr} blockers (5 μM E-4031) [33].

From the endocardial sites with most prolonged MAPD, "EAD like deflection", and *in vitro* results we have implicated the VSCS in the induction of the first beats of arrhythmias (singlets, couplets, triplets, quadruplets, and TdP). We needed more direct evidence that this was really the situation. Therefore to further clarify the involvement of the VSCS in the initiation of arrhythmias (singlets, couplets, triplets, quadruplets, and TdP), we have performed activation mapping of arrhythmias at two different drug conditions: one condition in which the combination of high drug concentration, hypokalemia, and slow stimulation rate were used [21], whereas in the other one a more clinically relevant condition of

drug concentration and rate was used [22]. The rational was that the more extreme condition would favor more the EAD-dependent triggered activity. These studies suggest that the first beat of the TdP is related to a triggered beat originating from the VSCS under both conditions.

Isochronal activation mapping of the first singlet in a series of singlets, arising after an increased dispersion of repolarization intervals, was likely related to a triggered beat arising from the specialized conduction system because of the following evidence. First, the isochronal activation pattern was similar to the IDV beats; in that, it had a wide breakthrough area and a short total activation time. Similarly, the breakthrough area of the first singlet was overlying the same epicardial area of the ventricular epicardial surface of corresponding IDV beats. The endocardial sites were activated prior to the earliest activated epicardial sites. This is to be expected if the impulse arises from the VSCS. From the stimulated beat to the premature ventricular activation, no bridging activity could be detected by both epicardial and endocardial unipolar recording electrodes. A local reentry could of been missed but this is very unlikely. In addition, the CI of the first singlet to subsequent singlets, in a series of singlets, was initially decreasing and then gradually increasing which is in keeping with triggered activity (Valois M. and Sasyniuk B.I., unpublished observations).

Our results support the fact that the subsequent singlets, the first beat of couplets, triplets, quadruplets, and TdPs originate, similarly to the first singlet, from a focal beat of endocardial origin from the VSCS. Although subsequent

singlets showed reduced breakthrough area and allthough some or most of the sites where earliest activation of the first singlet showed sites which lack activation, the evidence presented here supports a focal mechanism of initiation for the initiation of these beats as well. Similar to the first singlet, no bridging activity to the paced beat could be detected. The sites which showed lack of an active response, located in the earliest breakthrough area, have been shown to be sites from which fused potential were recorded by contact MAPs. In addition, premature AP, at critical premature interval, have been shown to be undetectable by unipolar recordings [34]. Therefore techniques which have relied on the use of unipolar or bipolar electrograms are likely miss the activation of closely coupled events. This may explain why under different conditions, in another model, the earliest activation of the first beat of polymorphic VT induced by anthopleurin A could only be detected in the subendocardial muscle and not in the endocardium where the PF are located. This behavior on electrocardiogram could be misinterpreted as a site of block conduction. When the activation from the MAP and the unipolar recordings are combined, the activation is in the same sequence as the first singlet.

The "EAD like deflection" of the fused MAP is related to the propagation of an active response, likely the result of a triggered action potential originating from the VSCS. The more prolonged MAPD or ARI prolongation at these apical sites, prior to fusion, is likely related to a difference in the repolarization current in these cells or the influence of electrotonic interaction of other cells with longer

action potentials. The similarity of the sites of earliest breakthrough area and the sites of fused potential suggest a possible electrotonic interaction from VSCS cells onto epicardial cells.

In the model of Zabel et al. [5] "EAD like deflections" have been observed on both the endocardial and epicardial surfaces; because of this observation these authors could not identify the origin of the triggered beat. We suggest that the "EAD like deflection" in the epicardial MAP are fused potentials. It would be interesting to see if reevaluation of Zabel et al's [5] data, in the light of our study, would lead to similar results, if attention was paid to the transition to arrhythmia and the positioning of the epicardial MAP. Excessive MAPD prolongation may have been responsible for these very prolonged MAPD and EAD like deflections because of the higher drug concentration and other facilitatory factors used in this study when compared to ours.

Perpetuation

We found distinctive evidence which supports either a focal or a reentrant mechanism for perpetuation of TdP [21]. We further showed that in conditions which were less extreme (clinically relevant drug concentration and mild bradycardia) that the TdPs are solely perpetuated by a reentrant mechanism [22].

Focal TdPs have a very long CL. This is in agreement with the CL of triggered activity which has been reported in *in vitro* preparations [35]. Also, the isochronal activation maps of their individual beats are similar to IDV beats [21].

Isochronal activation maps of IDV beats have a wide breakthrough area and short total activation times. Furthermore, they are of small number of beats (≤ 6 beats). This may be related to the fact that triggered activity associated with EADs is rate dependent; slow rates are needed for their manifestation. Then, the faster rate of these TdP beats may have eliminated the EAD and terminated the arrhythmia. Moreover, we have shown that there is no relationship between the immediately preceeding CL (CL-1) and the total activation time. This is to be expected for an arrhythmia which is maintained by a focal mechanism. And finally, we have shown previously, that under the condition of high drug concentration and long CL, multiple EADs can be observed in PF [36].

Different models of polymorphic VT which are maintained solely by a focal mechanism have been reported. In a dog model of acute AV block, *d*-sotalol infusion and bolus injection of PE, investigators observed all focal arrhythmias as long as 22 beats [9]. We suggest that, if these authors had evaluated the CL of the arrhythmia and total activation of the individual beats their conclusions would have been more similar to ours. In another model in which Anthopleurin A has been used to initiate TdP these investigators also observed all focal arrhythmias [6]. However, these investigators, in a subsequent study, failed to observe these arrhythmias and suggested that all focal type of arrhythmias were the result of a reentrant mechanism and that they have misinterpreted the mechanism of perpetuation in their previous study because of the reduced density of their 3D recording array [37].

On the other hand, the reentrant TdP beats were significantly faster than the focal TdP beats [21]. Reentrant activity is commonly associated with faster rates. Also, we have shown that there is a relationship between the CL-1 and the total activation time. As the arrhythmia accelerates the impulse slows down, which is reflected by a longer total activation time, and when the arrhythmias slows down the impulse subsequently accelerates; this is the behavior which is expected of a reentry circuit. In addition, the isochronal activation maps are consistent with a reentry mechanism. Sites of functional conduction block and "figure-of-8" reentry activation pattern were observed. The sites of earliest epicardial activation were in close proximity to the sites of delayed activation of the previous beat. A large proportion of the CL (70-95 %) could be detected in all reentrant beats. This suggests that the epicardial surface was intimately involved in the reentry circuit and not just reflecting activity as an epi-phenomenon. Finally, the length of these TdP can be longer than TdPs which are all focal. This suggests that the rate of these arrhythmias had less of an effect in contrast to the focal TdPs.

In some TdP, both focal and reentrant beats were observed in the body and on the last beat of the TdP. The focal activity observed here may be due to the termination of a reentry which retrogradely activated the VSCS. This longer reentry path may explain the intermediate CL of these arrhythmias. To determine whether the VSCS is implicated in the reentry path, recordings from the VSCS are required. It would be very unlikely that a focal beat due to triggered activity be observed after a few beats of short CL, especially on the last beat of the TdP.

We showed that the arrhythmia may be polymorphic in all focal, reentrant or mixed arrhythmias. In all focal arrhythmia, the sites of earliest breakthrough alternated between different epicardial areas. This alternating focus may have effectively changed the QRS morphology. On the endocardial surface there are a lot of PF which can generate triggered activity and therefore compete for the control of the heart's electrical activity. In contrast in a reentrant arrhythmia we showed that it may be the result of a slowly drifting reentrant path. This drift led in long reentrant type TdP to the change in polarity of the QRS complex. The drifting is likely to be related to the change in duration of the action potential at a fast rate. In the mixed arrhythmia, the alternation between a reentrant and a focal mechanism of perpetuation led to the changing orientation of the QRS morphology and polarity because of the changing impulse orientation.

Torsade de pointes: part of a continuum.

Under clinically relevant conditions we have demonstrated that TdP is the end part of a continuum of which the singlet is the starting point [22]. The spectrum is from singlet, couplet, triplet, short TdP, to longer TdP. This notion is extremely important because this suggests that when dispersion of repolarization is observed, subsequent singlets mean that the patient is at very high risk of TdP. This also suggests that preventing singlets would effectively eliminate the occurrence of TdP. What then makes a couplet become a TdP? The most likely factor is the pattern of the functional conduction block which develops on the second beat of

TdP. Experimentally and clinically TdP can degenerate into ventricular fibrillation, but in our novel model, degeneration into ventricular fibrillation was seldomly observed. We believe that when degeneration into ventricular fibrillation is observed, other facilitatory factors are present (ventricular damage, ventricular ischemia etc.) [6,9].

Termination

Decreased dispersion of repolarization was associated with the self-termination of TdP. The last beats of TdP were consistently more homogeneous with respect to the activation patterns and ARIs. The sites with functional conduction block were either less prominent or absent, which is reflected by the decrease in the total activation time on the last beat of the TdP when compared to a peak total activation times observed within the TdPs. The level of dispersion of repolarization was similar to the level observed at the fast rate of stimulation which was never associated with TdP arrhythmia. We therefore believe that the fast rate of activation of the TdPs effectively terminated the arrhythmia by eliminating the substrate: the increased dispersion of repolarization, sites of functional conduction block. This effect is possibly due to the result of the reverse-use dependence of the selective Ik_r blockers (review [38]).

Reconstructing the dispersion of repolarization at the end of different length arrhythmias shows that ARI dispersion is very quickly dissipated by the second or third beat of the arrhythmia, and that whether or not, a TdP is observed beyond a couplet is dependent on the sites of unidirectional block within the

ventricle. This conclusion is valid if such reconstruction can be extrapolated to all TdP beats and also if the recording sites located on the epicardial surface are representative of the whole heart.

Drug combination and possible therapy

From the proposed mechanism it is clear that, under clinically relevant drug concentration and rate, the proarrhythmic side effect of class III drugs can be eliminated by preventing the increased dispersion of repolarization and associated triggered activity. We will propose three novel interventions to eliminate TdP in this model. The proposed interventions may help the fate of Class III antiarrhythmic drugs and other drugs which have been associated with this proarrhythmic side effect. We further suggest that the knowledge acquired here on the mechanism of drug-induced arrhythmias and the novel mode of abolishment of these TdPs will help to further test and design new drugs which lack this proarrhythmic side effect. Furthermore the knowledge of this mechanism could be tested and used in patients who have the congenital long QT syndrome to design more effective therapy.

4-amino pyridine

We have shown that dispersion of repolarization is important in the initiation of this drug-induced arrhythmias. Therefore we hypothesized that if we

decreased the dispersion of repolarization we could prevent the arrhythmias including TdPs. To achieve this desired effect we used different strategies.

We first hypothesized that we could decrease the dispersion of repolarization by prolonging the action potential of VM. This effect would reduce the dispersion of repolarization between PF and VM if the effect is more prominent on the VM action potential. This will prevent the coupled beat if a "prolonged repolarization-dependent reexcitation" mechanism is responsible for the triggered activity, or it could make an EAD originating from PF ineffective; the increase action potential duration in VM could prevent the propagation of EAD dependent triggered activity originating from PF. To achieved this desired effect, we use a low concentration of 4-amino pyridine, because it was shown to increase the action potential duration in rabbit VM [39]. This effect is achieved mainly by the blockade of the second component of the transient outward current (I_{to2}) [39]. Our preliminary result suggests that this may be a useful approach to be used in the future. In this context the dispersion of repolarization between the endocardium and epicardium is eliminated (fig. 1). The EAD on the endocardial surface is no longer present, and the triggered activity is eliminated (fig. 2). The effect of this drug is likely due to the prolongation of VM action potential as reflected by the prolongation of the $MAPD_{epi}$. By combining these two drugs (*d*-sotalol and 4-aminopyridine) we have made the action potential more homogeneous and therefore we decreased the very prominent dispersion of repolarization that was associated with arrhythmias and TdPs in the presence of *d*-sotalol. The effect was present even at very long CL. The effect was fully

reversible. A different effect may have been seen with higher drug concentration of 4-AP or if 4-AP was used alone, since 4-AP has been shown to prolong the action potential duration of the PF [40].The effectiveness of this intervention in the prevention of triggered activity and TdP further supports the critical role of dispersion of ventricular repolarization in the initiation of TdP arrhythmias in this model.

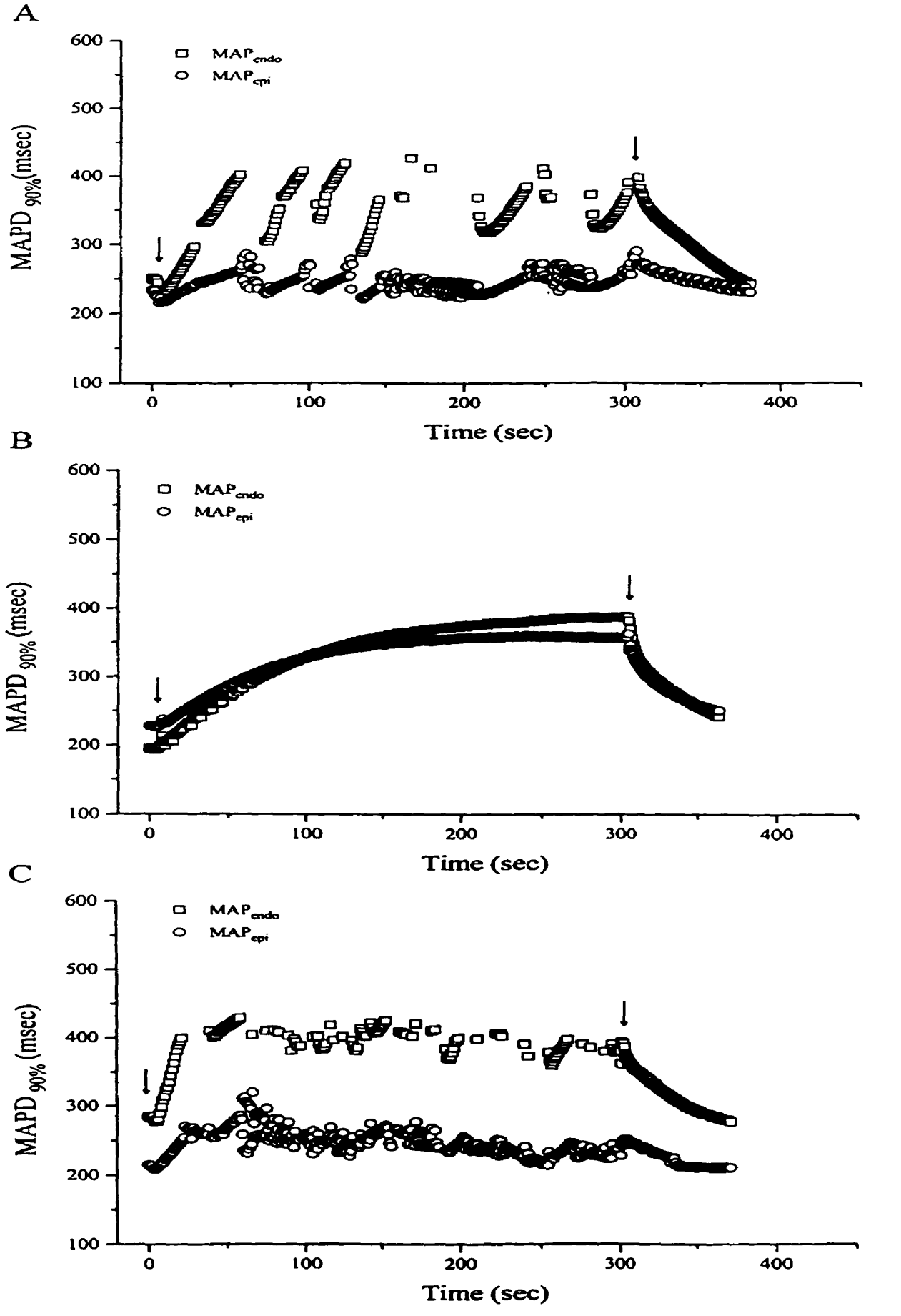
A
MAP$_{endo}$
MAP$_{epi}$
MAPD$_{90\%}$(msec)
600
500
400
300
200
100
0
100
200
300
400
Time (sec)
B
MAP$_{endo}$
MAP$_{epi}$
MAPD$_{90\%}$ (msec)
600
500
400
300
200
100
0
100
200
300
400
Time (sec)
C
MAP$_{endo}$
MAP$_{epi}$
MAPD$_{90\%}$ (msec)
600
500
400
300
200
100
0
100
200
300
400
Time (sec)

Figure 1. Typical effect of 4-AP in the presence of *d*-sotalol. Graphs of MAPD versus time in the presence of *d*-sotalol, *d*-sotalol with 4-aminopyridine, and after the washout of 4-aminopyridine. Top panel. Graph of MAPD versus time in the presence of *d*-sotalol (20 μM) at 1.0 CL. At 1.0 sec BCL, note the repetitive increased and decreases in $MAPD_{endo}$ and associated triggered activity and TdP. Arrhythmias including TdP occurred at peak MAP disparity. Three TdPs were observed under these conditions. Middle panels. Graph of MAPD versus time in the presence of *d*-sotalol (20 μM) and 4-aminopyridine (0.5mM) at 1.0. Note that the $MAPD_{endo}$ and $MAPD_{epi}$ follow a similar time dependent effect at the different CL. We did not observe any arrhythmia in the presence of this drug combination. Lower Panels. Graph of MAPD versus time after the washout of 4-aminopyridine at 1.0 CL. Note the different time dependent effect and the much pronounce $MAPD_{endo}$ prolongation at 1.0 sec CL; this is similar to the condition before the infusion of 4-AP. We observed 1 TdP at 1.0 sec CL. In this figure and other four figures, the endocardial MAP probe was located in the left ventricle close to the apex and the epicardial probe was located on the base of the right ventricle. MAPD was measured at the 90% repolarization level. The vertical arrows point to the time when the CL was changed from 0.5 sec BCL to a longer BCL (left arrow) and from the longer CL back to the BCL of 0.5 sec (right arrow). The heart was exposed to 4-AP (0.5 mM) for 1 hour. The washout period was 20 minutes. This effect was observed in 3 hearts.

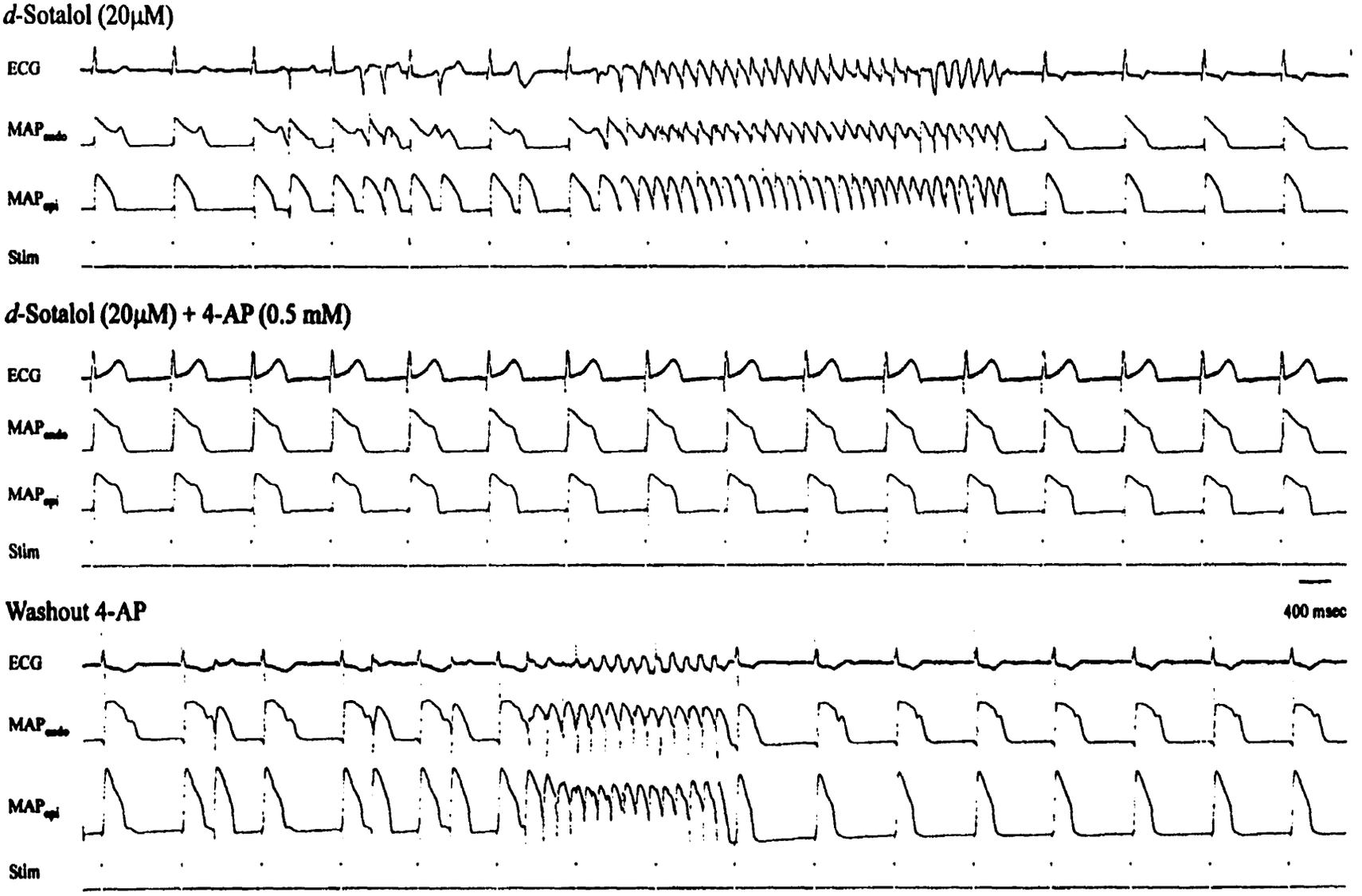
d-Sotalol (20μM)
ECG
MAP_{endo}
MAP_{epi}
Stim
d-Sotalol (20μM) + 4-AP (0.5 mM)
ECG
MAP_{endo}
MAP_{epi}
Stim
Washout 4-AP
400 msec
ECG
MAP_{endo}
MAP_{epi}
Stim

Figure 2. Typical example of the effect of 4-AP on the ECG, MAP_{endo}, MAP_{epi}. Top panel. Singlets, couplets, and TdP in the presence of *d*-sotalol. Note the prominent "EAD like deflection" on the MAP_{endo} and the big dispersion of repolarization prior to the first singlet and TdP. After the TdP arrhythmia the "EAD like deflection" and dispersion of repolarization is greatly reduced. Middle panel. Effect of 4-aminopyridine in the presence of *d*-sotalol. These traces were taken 4 min after the rate was changed to 1.0 sec CL. Note that the absolute prolongation of the MAP_{endo} is very similar to the one observed on the top panel and also the $MAPD_{epi}$ is much more prolonged here when compared to the top panel. Note the absence of an "EAD like deflection" on the MAP_{endo}, absence of dispersion of repolarization, and absence of triggered activity and TdP. Lower panel. Multiple singlet and TdP after the washout of 4-aminopyridine. Note again the prominent "EAD like deflection" on the MAP_{endo} and dispersion of repolarization prior to the first singlet and TdP. Note that after the TdP the "EAD like deflection" on the MAP_{endo} and the dispersion of repolarization is greatly reduced. The "EAD like deflection" and the dispersion of repolarization is quickly reestablished one stimulated beat later.

The effect of this drug combination may have increased the therapeutic index of *d*-sotalol. Furthermore, the further VM MAPD prolongation by this approach most likely increased the antiarrhythmic profile of *d*-sotalol. If ventricular ischemia is present then the drug used to increase the ventricular action potential should also prolong the action potential in the ischemic myocardium. Is this combination effective at the faster stimulation rate? The rate dependent profile of this drug combination needs to be tested. In the rabbit the blockade of the I_{To1} is not expected to be very effective at fast stimulation rate because the current is mostly inactivated at the faster rate, but in humans this effect may be different, since the current is less rate dependent and would lead to the same degree of block irrespective of the stimulation rate [41]. Therefore in humans, to achieve a positive rate-dependent effect, we require a drug which blocks this current in a use-dependent fashion. The effect of 4-AP is reverse use-dependent on I_{to1}, therefore another drug should be used [42].

Heptanol

We investigated the importance of cellular electrical coupling in the generation of arrhythmia in this model. We uncoupled the cells with a low concentration of heptanol [43,44]. We used low concentration of heptanol since high concentrations have been associated with arrhythmia [45,46]. The exposure to low concentration of heptanol reversibly blocked the occurrence of TdP arrhythmias in this model. Exposure to heptanol lead to a great decreased in the $MAPD_{endo}$,

whereas very little decrease in the $MAPD_{epi}$ was seen (fig. 3). Similarly to the treatment with Lugol's solution, exposure to heptanol produced a prominent decrease in dispersion of repolarization and elimination of all arrhythmias, including TdPs. This result suggest that the MAP_{endo} signal is very dependent on cellular coupling for its generation. This is likely the result of the uncoupling the PF cell, T cell and VM cells. From the higher resistance between the PF VM junction, we suggest that the low concentration of heptanol would have affected these sites more than other VM-VM junctions [47]. We showed that the effect of heptanol on PF leads to a slight decrease in action potential duration, which suggest that the effect of heptanol may not be selective to the gap junctions. The decrease seen *in vitro* is never as prominent as the one seen *in situ* on the $MAPD_{endo}$ and therefore may not explain this effect.

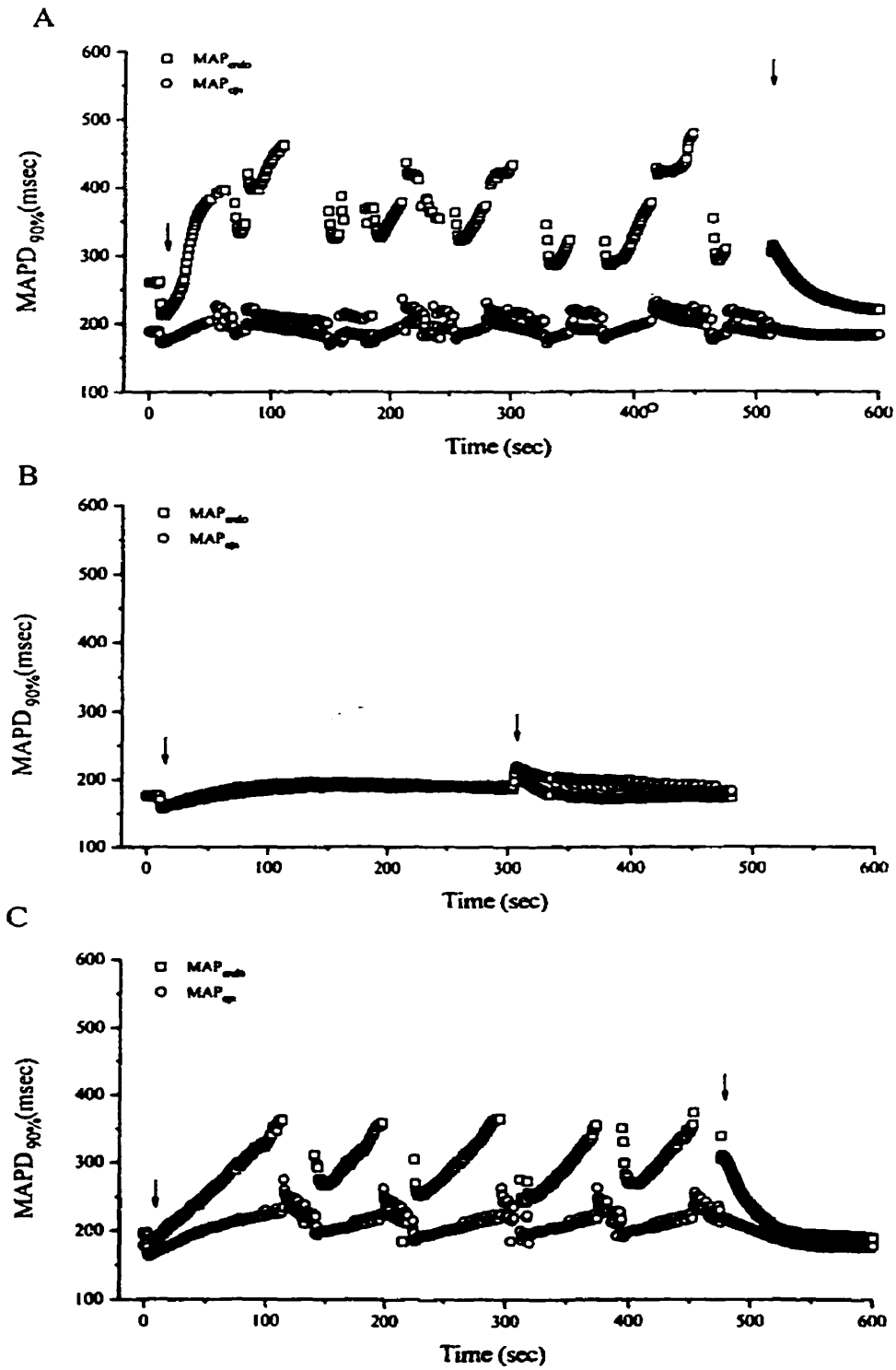
A
B
C
MAP
MAP
MAPD90%(msec)
Time (sec)
100
200
300
400
500
600
0
100
200
300
400
500
600

Figure 3. Typical example of the effect of heptanol in the presence of *d*-sotalol. Graphs of $MAPD_{endo}$ and $MAPD_{epi}$ versus time at 1.0 sec BCL in the presence of *d*-sotalol (20 μM), *d*-sotalol (20μM) with heptanol (0.4 mM) and after washout of heptanol. Top panel typical effect of *d*-sotalol (20μM). Similarly to figure 1, note the more prominent time dependent effect on the $MAPD_{endo}$ when compared to the $MAPD_{epi}$ at this CL. Note the repetitive increasing and decreasing $MAPD_{endo}$ and associated triggered activity and TdPs. We observed 5 TdPs at this CL in this trial. Middle panel. Effect of heptanol (0.4 mM) in the presence of *d*-sotalol (20μM). Note the very pronounce decrease of the $MAPD_{endo}$ and great reduction of the CL dependent MAPD prolongation of the $MAPD_{endo}$. The $MAPD_{endo}$ and the $MAPD_{epi}$ are of very similar duration at this BCL of 1 sec therefore greatly decrease the dispersion of repolarization. We did not observed any triggered activity or TdP under this condition. Lower Panel. Washout of heptanol (0.4 mM). The MAPD versus time at 1.0 sec CL relationship is very similar to what is observed on the top panel. We observed 3 TdPs under this condition. Heart were exposed to heptanol for 30 minutes. The washout period was approximately 20 minutes. This effect was observed in 2 of 3 hearts.

Lugol's solution

Another intervention that has been used experimentally to implicate the endocardium as part of the substrate of an arrhythmia is the use of Lugol's solution. Lugol's solution is commonly used to stain the VSCS. It does so by staining the collagen, which is more abundant in these cells, blue. When applied to the endocardium it kills a layer of about 3-4 VM cell layer including the cells of the VSCS cells [48]. When hearts were treated with Lugol's solution the arrhythmia was not observed. The effect was most prominent on the $MAPD_{endo}$ when compared to the $MAPD_{epi}$ (fig 4 and 5). The effect of Lugol's further supports the involvement of the endocardium (the SVSC) in the generation of dispersion of repolarization and triggered activity. The effect of Lugol's solution suggests that the involvement of "M-cells" in the increased dispersion of repolarization and initiation of arrhythmias, including TdP, may not be important in this model.

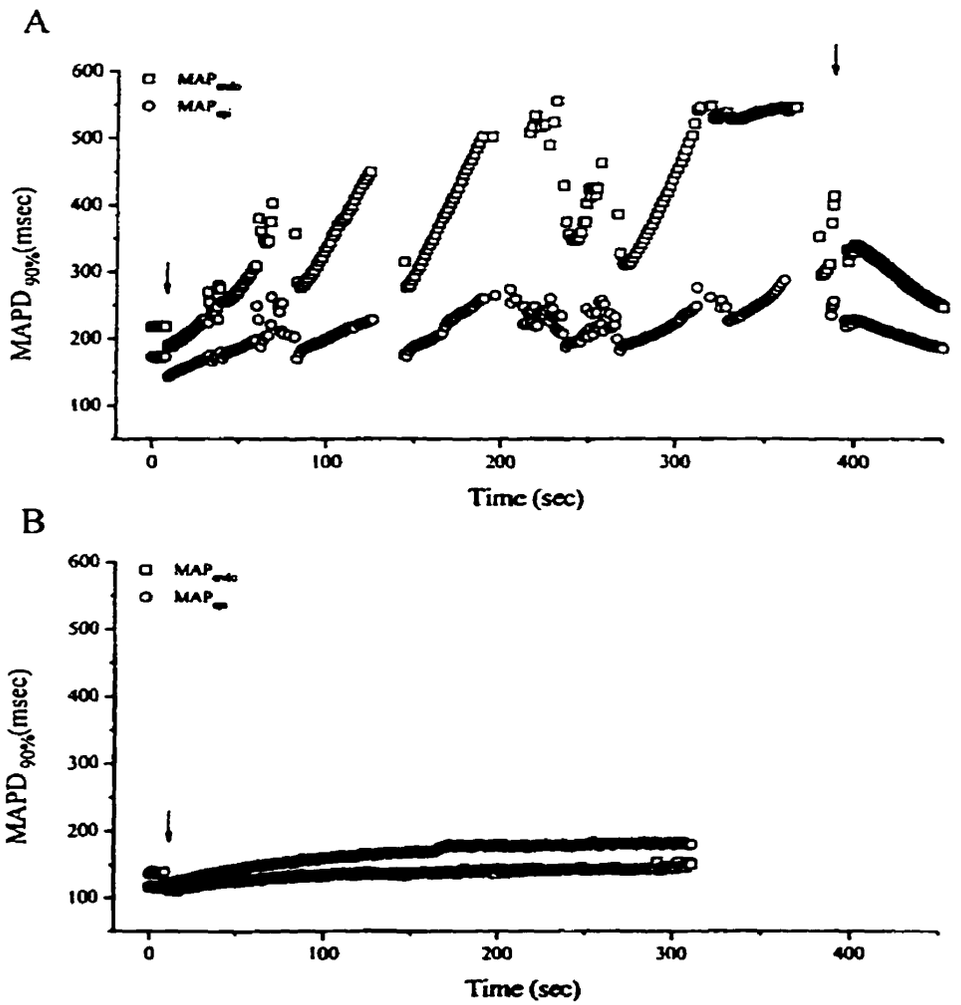
A
600
500
400
300
200
100
MAPD90%(msec)
0
100
200
300
400
Time (sec)
B
600
500
400
300
200
100
MAPD90%(msec)
0
100
200
300
400
Time (sec)

Figure 4. Typical example of the effect of Lugol's solution in the presence of a selective class III drug. Graphs of $MAPD_{endo}$ and $MAPD_{epi}$ versus time at 1.5 sec CL in the presence of *d*-sotalol (20 μM) and after the endocardial exposure to Lugol's solution still in the presence of *d*-sotalol. Top panel. Typical MAPD versus time at 1.5 sec BCL relationship. Note the similarity of this graph with those of figures 1 and 3. We observed 9 TdPs during at this longer CL during this trial. Lower panel. Effect observed after the exposure of the endocardial surface of both ventricles to Lugol's solution in the presence of *d*-sotalol (20μM). Note the very pronounce decrease of the $MAPD_{endo}$ and the greatly reduced BCL dependent MAPD prolongation. The $MAPD_{endo}$ and the $MAPD_{epi}$ are very similar; therefore this intervention greatly decreased the dispersion of repolarization. We did not observed any triggered activity or TdP in this condition. A small volume, less then 1 ml, was applied with a syringe sequentially to both ventricular endocardial cavity. Lugol's solution was then washed with modified Krebs-Henseleit solutions. This effect was observed in 3 hearts.

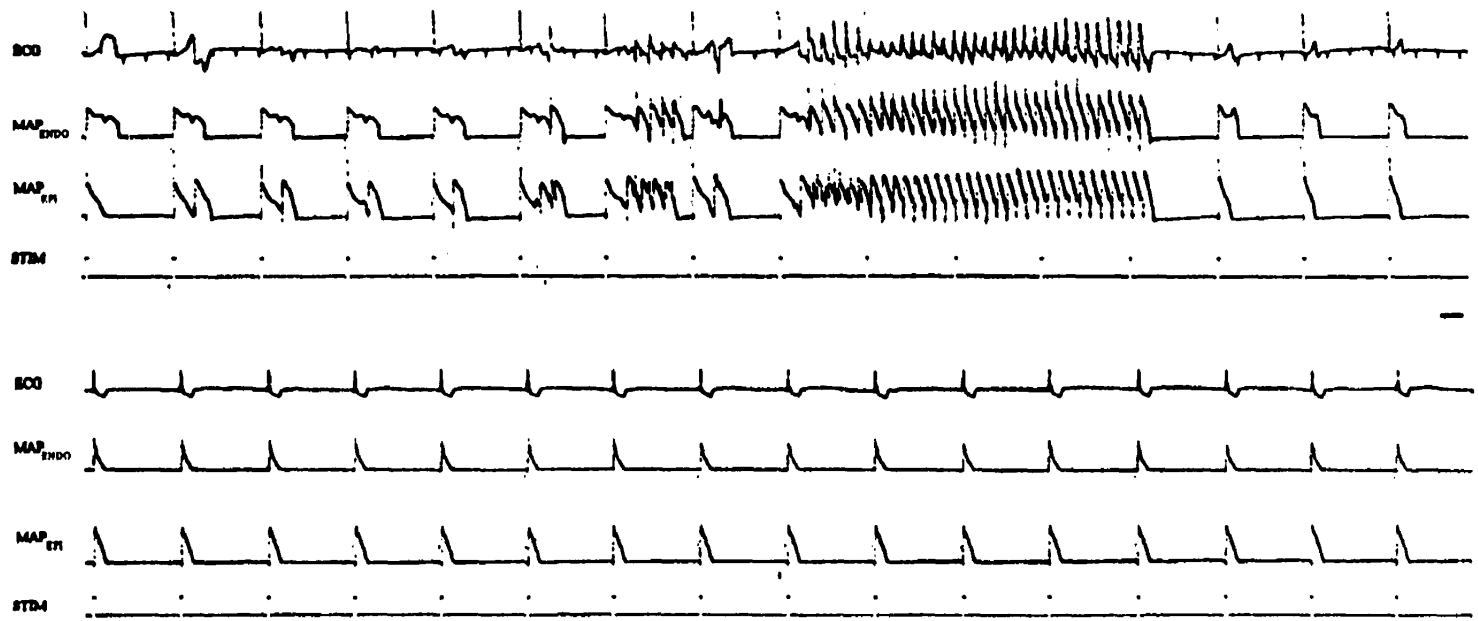
ECG
MAP ENDO
MAP EPI
STIM
ECG
MAP ENDO
MAP EPI
STIM

Figure 5. Typical example of the effect of Lugol's solution in the presence of a selective class III drug on the ECG, MAP_{endo}, and MAP_{epi}. Top panel. Singlets, couplets, and TdP in the presence of *d*-sotalol (20μM). Note the prominent "EAD like deflection" on the MAP_{endo} and the big dispersion of repolarization prior to the first singlet and TdP. Lower panel. Effect of Lugol's solution in the presence of *d*-sotalol. These traces were taken 4 min after the rate was changed to 1.5 sec BCL. The $MAPD_{endo}$ is very much reduced and its morphology is very triangular. The $MAPD_{epi}$ is slightly reduced and its morphology is not greatly affected. Note the absence of an "EAD like deflection" on the MAP_{endo}, absence of dispersion of repolarization and absence of triggered activity and TdP. Scale bar is 400 msec.

The effect of all these interventions is in agreement with the proposed initiation mechanism of drug-induced TdP. All these intervention decreased the dispersion of ventricular repolarization and were effective in preventing singlet, couplets, triplets, and TdPs.

The one strategy which has the most promising clinical benefit is the one which utilizes 4-AP. This is because it increases the VM action potential duration and this will likely increase the antiarrhythmic properties of class III antiarrhythmic drugs. The other two approach were used mostly as investigational tools. The 4-aminopyridine approach could be used as an antiarrhythmic approach in patients at high risk for sudden cardiac death and in patients with long QT syndrome. Patients with the long QT syndrome (LQT 3) with the Na channel mutation (SCN5A) are treated with low concentration of class I antiarrhythmic drugs (mexiletine). The use of mexiletine in these patients may expose these patients to the proarrhythmic side effect of this class of drug. These other proposed interventions may provide another antiarrhythmic strategy for these patients as well.

Conclusion

The experimental evidence from these diverse investigational systems indicate that, under a clinically relevant condition of antiarrhythmic drug concentration and of rate, the first beat of TdP is the result of a triggered beat

originating from the specialized conducting system, by a mechanism of either "prolonged repolarization-dependent reexcitation mechanism" or EAD-dependent triggered activity in the presence of very prominent dispersion of ventricular repolarization. The prominent dispersion of repolarization observed prior to TdP is the result of a fused potential. The dispersion of repolarization is essential for the initiation of the reentry mechanism. The termination of the TdP is likely the result of a rate dependent decrease of the dispersion of repolarization intervals. This novel model of drug-induced TdP can be used to screen existing, new antiarrhythmic drugs, or groups of drugs which have been associated with TdP arrhythmia clinically (e.g., antihistamines) and thus would lead to the generation of new drugs which lack this proarrhythmic side effect.

References

1. Hohnloser SH, Singh BN: Proarrhythmia with class III antiarrhythmic drugs: definition, electrophysiologic mechanisms, incidence, predisposing factors, and clinical implications. [Review]. *Journal of Cardiovascular Electrophysiology* 1995;6:920-936

2. Lazzara R: Antiarrhythmic drugs and torsade de pointes. [Review]. *European Heart Journal* 1993;14 Suppl H:88-92

3. Weissenburger J, Davy JM, Chezalviel F, Ertzbischoff O, Poirier JM, Engel F, Lainee P, Penin E, Motte G, Cheymol G: Arrhythmogenic activities of antiarrhythmic drugs in conscious hypokalemic dogs with atrioventricular block: comparison between quinidine, lidocaine, flecainide, propranolol and sotalol. *Journal of Pharmacology & Experimental Therapeutics* 1991;259:871-883

4. Carlsson L, Abrahamsson C, Andersson B, Duker G, Schiller-Linhardt G: Proarrhythmic effects of the class III agent almokalant: importance of infusion rate, QT dispersion, and early afterdepolarisations [see comments]. *Cardiovascular Research* 1993;27:2186-2193

5. Zabel M, Hohnloser SH, Behrens S, Li YG, Woosley RL, Franz MR: Electrophysiologic Features of Torsades de Pointes: Insight from a New Isolated Rabbit Heart Model. *Journal of Cardiovascular Electrophysiology* 1997;8:1148-1158

6. el-Sherif N, Caref EB, Yin H, Restivo M: The electrophysiological mechanism of ventricular arrhythmias in the long QT syndrome. Tridimensional mapping of activation and recovery patterns. *Circulation Research* 1996;79:474-492

7. Antzelevitch C, Sun ZQ, Zhang ZQ, Yan GX: Cellular and ionic mechanisms underlying erythromycin-induced long QT intervals and torsade de pointes. *Journal of the American College of Cardiology* 1996;28:1836-1848

8. Sasyniuk BI, Brunet S: Torsade de pointes induced by quinidine, *d*-sotalol & e-4031 in the isolated rabbit heart: importance of interval dependent dispersion of repolarization. *PACE* 1995;18:II-904(abstract)

9. Derakhchan K, Cardinal R, Brunet S, Klug D, Pharand C, Kus T, Sasyniuk BI: Polymorphic ventricular tachycardia induced by *d*-sotalol in canine preparations of atrio-ventricular block: initiation in the conduction system followed by spatially unstable reentry. *Cardiovascular Research* 1998;(in press)

10. Weissenburger J, Chezalviel F, Davy JM, Lainee P, Guhennec C, Penin, E, Engel F, Cynober L, Motte G, Cheymol G: Methods and limitations of an experimental model of long QT syndrome. *Journal of Pharmacological Methods* 1991;26:23-42

11. Carlsson L, Almgren O, Duker G: QTU-prolongation and torsades de pointes induced by putative class III antiarrhythmic agents in the rabbit: etiology and interventions. *Journal of Cardiovascular Pharmacology* 1990;16:276-285

12. Vos MA, Verduyn SC, Gorgels AP, Lipcsei GC, Wellens HJ: Reproducible induction of early afterdepolarizations and torsade de pointes arrhythmias by d-sotalol and pacing in dogs with chronic atrioventricular block. *Circulation* 1995;91:864-872

13. Carmeliet E: Electrophysiologic and voltage clamp analysis of the effects of sotalol on isolated cardiac muscle and Purkinje fibers. *Journal of Pharmacology & Experimental Therapeutics* 1985;232:817-825

14. Lab MJ: Mechanoelectric feedback (transduction) in heart: concepts and implications. [Review] *Cardiovascular Research* 1996;32:3-14

15. Braun AP, Fedida D, Giles WR: Activation of alpha 1-adrenoceptors modulates the inwardly rectifying potassium currents of mammalian atrial myocytes. *Pflugers Archiv - European Journal of Physiology* 1992;421:431-439

16. Lee JH, Rosen MR: Alpha 1-adrenergic receptor modulation of repolarization in canine Purkinje fibers. *Journal of Cardiovascular Electrophysiology* 1994;5:232-240

17. Gallagher JD: Effects of isoflurane on ouabain toxicity in canine Purkinje fibers. Comparison with halothane. *Anesthesiology* 1994;81:1500-1510

18. Weigt HU, Kwok WM, Rehmert GC, Turner LA, Bosnjak ZJ: Voltage-dependent effects of volatile anesthetics on cardiac sodium current. *Anesthesia & Analgesia* 1997;84:285-293

19. Brunet S, Sasyniuk BI: *D*-sotalol induced torsade de pointes ventricular arrhythmias in the isolated rabbit heart - model and mechanism. Chapter II

20. Brunet S, Sasyniuk BI: Proarrhythmic effects of *d*-sotalol in rabbit ventricle associated with differential effects on repolarization in endocardial cells: *in vitro* and *in situ* correlations. Chapter I

21. Brunet S, Derakhchan K, Cardinal R, Sasyniuk BI: Mechanism of *d*-Sotalol induced torsade de pointes in an isolated heart model - a mapping study. Chapter III

22. Brunet S, Derakhchan K, Cardinal R, Sasyniuk BI: Changes in disparity of repolarization intervals accounts for initiation, perpetuation and termination of *d*-Sotalol induced arrhythmias. Chapter IV

23. Ino T, Karagueuzian HS, Hong K, Meesmann M, Mandel WJ, Peter T: Relation of monophasic action potential recorded with contact electrode to underlying transmembrane action potential properties in isolated cardiac tissues: a systematic microelectrode validation study. *Cardiovascular Research* 1988;22:255-264

24. Sicouri S, Antzelevitch C: A subpopulation of cells with unique electrophysiological properties in the deep subepicardium of the canine ventricle. The M cell. *Circulation Research* 1991;68:1729-1741

25. Sicouri S, Quist M, Antzelevitch C: Evidence for the presence of M cells in the guinea pig ventricle. *Journal of Cardiovascular Electrophysiology* 1996;7:503-511

26. Anyukhovsky EP, Sosunov EA, Feinmark SJ, Rosen MR: Effects of quinidine on repolarization in canine epicardium, midmyocardium, and endocardium: II. In vivo study. *Circulation* 1997;96:4019-4026

27. Sosunov EA, Anyukhovsky EP, Rosen MR: Effects of quinidine on repolarization in canine epicardium, midmyocardium, and endocardium: I. In vitro study. *Circulation* 1997;96:4011-4018

28. Antzelevitch C, Sicouri S: Clinical relevance of cardiac arrhythmias generated by afterdepolarizations. Role of M cells in the generation of U waves, triggered activity and torsade de pointes. [Review]. *Journal of the American College of Cardiology* 1994;23:259-277

29. Brugada P, Wellens HJ: Early afterdepolarizations: role in conduction block, "prolonged repolarization-dependent reexcitation," and tachyarrhythmias in the human heart. [Review]. *Pacing & Clinical Electrophysiology* 1985;8:889-896

30. Li ZY, Wang YH, Maldonado C, Kupersmith J: Role of junctional zone cells between Purkinje fibres and ventricular muscle in arrhythmogenesis. *Cardiovascular Research* 1994;28:1277-1284

31. Li ZY, Maldonado C, Zee-Cheng C, Hiromasa S, Kupersmith J: Purkinje fibre-papillary muscle interaction in the genesis of triggered activity in a guinea pig model. *Cardiovascular Research* 1992;26:543-548

32. Kumar R, Joyner RW: An experimental model of the production of early after depolarizations by injury current from an ischemic region. *Pflugers Archiv - European Journal of Physiology* 1994;428:425-432

33. Sanguinetti MC, Jurkiewicz NK: Two components of cardiac delayed rectifier K+ current. Differential sensitivity to block by class III antiarrhythmic agents. *Journal of General Physiology* 1990;96:195-215

34. Myerburg RJ, Nilsson K, Zoble RG: Relationship of surface electrogram recordings to activity in the underlying specialized conducting tissue. *Circulation* 1972;45:420-432

35. Roden DM, Hoffman BF: Action potential prolongation and induction of abnormal automaticity by low quinidine concentrations in canine Purkinje fibers. Relationship to potassium and cycle length. *Circulation Research* 1985;56:857-867

36. Sasyniuk BI, Brunet S: Proarrhythmic effects of *d*-sotalol in the rabbit ventricle associated with differential effects on endocardial cells at slow heart rates. *Circulation* 1994;90:I-146(abstract)

37. el-Sherif N, Chinushi M, Caref EB, Restivo M: Electrophysiological mechanism of the characteristic electrocardiographic morphology of torsade de pointes tachyarrhythmias in the long-QT syndrome: detailed analysis of ventricular tridimensional activation patterns. *Circulation* 1997;96:4392-4399

38. Singh BN, Ahmed R: Class III antiarrhythmic drugs. [Review]. *Current Opinion in Cardiology* 1994;9:12-22

39. Hiraoka M, Kawano S: Mechanism of increased amplitude and duration of the plateau with sudden shorthening of diastolic intervals in rabbit ventricular cells. *Circulation Research* 1987;60:14-26

40. Graham B, Gilmour RF, Jr., Stanton MS, Zipes DP: OPC-88117 suppresses early and delayed afterdepolarizations and arrhythmias induced by cesium, 4-aminopyridine and digitalis in canine Purkinje fibers and in the canine heart in situ. *American Heart Journal* 1989;118:708-716

41. Fermini B, Wang Z, Duan D, Nattel S: Differences in rate dependence of transient outward current in rabbit and human atrium. *American Journal of Physiology* 1992;263:H1747-54

42. Wang Z, Fermini B, Nattel S: Effects of flecainide, quinidine, and 4-aminopyridine on transient outward and ultrarapid delayed rectifier currents in human atrial myocytes. *Journal of Pharmacology & Experimental Therapeutics* 1995;272:184-196

43. Bastide B, Herve JC, Cronier L, Deleze J: Rapid onset and calcium independence of the gap junction uncoupling induced by heptanol in cultured heart cells. *Pflugers Archiv - European Journal of Physiology* 1995;429:386-393

44. Takens-Kwak BR, Jongsma HJ, Rook MB, Van Ginneken AC: Mechanism of heptanol-induced uncoupling of cardiac gap junctions: a perforated patch-clamp study. *American Journal of Physiology* 1992;262:C1531-8

45. Boersma L, Brugada J, Abdollah H, Kirchhof C, Allessie M: Effects of heptanol, class Ic, and class III drugs on reentrant ventricular tachycardia. Importance of the excitable gap for the inducibility of double-wave reentry. *Circulation* 1994;90:1012-1022

46. Callans DJ, Kieval RS, Hook BG, Moore EN, Spear JF: Effect of coronary perfusion of heptanol or potassium on conduction and ventricular arrhythmias. *American Journal of Physiology* 1992;263:H1382-9

47. Rawling DA, Joyner RW: Characteristics of junctional regions between Purkinje and ventricular muscle cells of canine ventricular subendocardium. *Circulation Research* 1987;60:580-585

48. Damiano RJ, Jr., Smith PK, Tripp HF, Jr., Asano T, Small KW, Lowe JE, Ideker RE, Cox JL: The effect of chemical ablation of the endocardium on ventricular fibrillation threshold. *Circulation* 1986;74:645-652

ORIGINAL CONTRIBUTIONS

The following comprise the original contributions of this thesis to the field of antiarrhythmic drugs and proarrhythmia:

1. We showed that marked heterogeneity of action potentials exists on the endocardial surface of the rabbit ventricle and that adjustment of endocardial action potential durations to abrupt changes in cycle length is a two fold process consisting of an instantaneous effect and a delayed effect, both of which importantly contribute in determining the effects of class III drugs on repolarization.

2. We showed that in the presence of d-sotalol, the same conditions which led to generation of ;gered activity in Purkinje fibers in vitro led to the generation of coupled beats in the intact isolated heart. Only Purkinje fibers uniquely displayed prolonged action potential durations and were the site of origin of triggered activations. Both triggered activations in vitro and coupled beats in situ were associated with the attainment of critical disparities in repolarization on the endocardial surface and were highly dependent upon critical cycle lengths.

3. This study provides compelling evidence that the mechanism of initiation of coupled beats in the intact rabbit heart is triggered activity originating in Purkinje fibers on the endocardial surface.

4. We developed a unique isolated heart model of TdP ventricular arrhythmias in which initiation of TdP is predictable, reproducible and easily amenable to analysis of arrhythmic mechanisms displaying all of the features of the clinical arrhythmia. No other similar model has been developed.

5. Using this model we were able to determine for the first time the mechanism not only of the initiation, but also of the perpetuation and termination of drug induced TdP arrhythmias. We showed that under conditions unlikely to occur clinically, ie., very high concentrations of drug in the presence of extremely long cycle lengths, some TdP arrhythmias can be due to a focal mechanism as a result of sustained triggered activity arising from the endocardial surface, most likely in Purkinje fibers. However, under clinically relevant concentrations and cycle lengths, this mechanism does not occur.

6. We showed that under clinically relevant conditions, TdP arrhythmias are consistently initiated by a focal beat arising on the endocardial surface but are perpetuated by a reentrant mechanism as a result of a critical disparity in repolarization occurring both on the endocardial and epicardial surface. It is the elimination of this dispersion which results in termination of the arrhythmia and explains why this arrhythmia is notably self-terminating. Initiation of the arrhythmia is associated with attainment of a critical disparity in repolarization which is unique for the arrhythmia and independent of cycle length or drug concentration. Longer cycle lengths or higher drug concentrations merely increase the likelihood that the critical disparity is attained.

7. We have shown that dispersion in repolarization on the epicardial surface which may be manifested as dispersion in epicardial MAP potentials is really the result of abortive triggered action potentials arising from the endocardial surface and producing fusion potentials on the epicardial surface as a result of conduction block. Thus, what others have called prolonged repolarization may really be failure of activation.

8. We have clearly demonstrated that TdP arrhythmia is not an isolated entity with a unique mechanism of action but is really part of a continuum ranging from singlets to couplets, triplets, quadruplets and eventually TdP. The first beat of each of these is due to triggered activity originating on the endocardial surface, most probably in Purkinje fibers. All subsequent beats are due to a reentry mechanism. Whether a couplet or TdP is the result of the ensuing reentrant mechanism is dependent upon the degree of disparity immediately preceding the first beat of each episode. Greater disparities result in TdP.

9. We have for the first time clearly demonstrated the important role that the Purkinje system plays in the proarrhythmic effects of class III antiarrhythmic drugs and shown that it is this system which should be targeted for prevention or elimination of this arrhythmia.

10. Our results have important implications for the use of Class III antiarrhythmic drugs in the treatment of cardiac arrhythmias.

11. The model we have developed may be an important one for testing the proarrhythmic effects of both existing and novel antiarrhythmic as well as noncardiac drugs.